

# PRELIMINARY GUIDELINES ON THE DESIGN OF CABLE-NET STABILIZED HIGH-RISE TOWERS

- APPLICATION TO THE ROTTERDAM MOUNTAIN PROJECT -



Alexandru Ion Onițiu  
MSc Thesis, October 2021

 **TU Delft**

**& SUMMUM**

**RD**

# Preliminary guidelines on the design of cable- net stabilized high-rise towers

Application to the Rotterdam Mountain Project

by

Alexandru Ion Onițiu

- Master Thesis Building Engineering -

to obtain the degree of Master of Science

at the Delft University of Technology

to be defended publicly on Thursday October 28<sup>th</sup>, 2021 at 4:00 PM

**Student number:** 5033861

**Project Duration:** January 2021 - October 2021

**Thesis Committee:**

Dr. Ir. M.A.N Hendriks,	TU Delft, chair
Ir. L.P.L van der Linden,	TU Delft
Ir. H. Alkisaiei,	TU Delft
Dr. D. Veenendaal,	Summum Engineering

An electronic version of this thesis is available at <http://repository.tudelft.nl>.



# Preface

---

This thesis marks the end of my MSc studies at the Delft University of Technology, where I have been following the Building Engineering–Structural Design Track of the Faculty of Civil Engineering and Geosciences. This research has been conducted in collaboration with the Summum Engineering Firm and the Rotterdam Dreamers Group.

Even before starting my studies at TU Delft, I have been fascinated about big structural engineering projects and their feasibility and challenges. Further, during my MSc studies I have developed a passion towards parametric engineering and parametric design. With these two ideas in mind, I was thrilled to be able to work on the ambitious project that the Dreamers have envisioned – the Rotterdam Mountain, and to bring it one step further towards its completion. Such, I would like to thank Summum Engineering and the whole community of the Rotterdam Dreamers for granting me the opportunity to work on this fascinating project.

Conducting this thesis would not have been possible without the help of the amazing people that I have had the chance to work with. I would like to thank all of my committee members for their continuous guidance throughout the last ten months. Their critical reviews, comments and suggestions have made every meeting a fruitful and pleasant one, shaping the progress of the thesis towards its final outcome.

I would like to thank Max Hendriks for agreeing to chair my graduation committee. His fast and relevant replies to any questions that I have had during the thesis were an extremely valuable contribution.

I would also like to thank Diederik Veenendaal of Summum Engineering for his constant guidance throughout this thesis. Without him sharing his expertise in parametric engineering and form finding, and without his comments on the progress of the thesis, this research would have not have been possible. After every meeting with Diederik, I knew where I should focus my attention next.

I would also like to thank Lennert van der Linden for his continuous feedback throughout this research. His comments during our meetings and on the written part have always been clear, consistent and extremely valuable.

I would also like to thank Hoessein Alkisaiei for his regular advice during my work. His help, especially in the early stages of this research when developing the methodology, and during the middle part of this thesis when I was lost in too much information, has kept me on track.

My sincere thanks go towards my girlfriend, Maria, who has always been supportive of my work, being considerate towards my busy schedule. I would also like to gratefully thank my family, especially my father, Ion, for his unconditional support and mentorship. Lastly, I would like to thank all of my friends that have kept me motivated during this period, despite the COVID-19 pandemic.

*Alexandru Ion Onițiu,  
Delft, October 2021*

# Summary

---

The starting point of the thesis relates to the “Rotterdam Mountain” Project, envisioned by the Rotterdam Dreamers, which proposes an artificial mountain in the otherwise flat landscape of the Netherlands, supported by a cable network that is spanning between multiple high-rise towers, to cover highway and railway stations. This network has the double function of supporting the weight of the green roof of the mountain and connecting and stabilizing the towers, while transferring wind forces towards the foundation more efficiently. The unique, yet ambitious project, can be simply seen as a large tent-like structure, where the towers act as tent masts and the cable-net acts as the tensile canopy. The project is relevant due to the current housing shortage in the Netherlands, creating a large number of residential and office spaces in otherwise unusable areas. Below the mountain surface, large data centers and other logistic functions are placed and taken from view. The project further addresses the current climate challenges, by proposing a system that converts the large heat generated by these functions and converting it to energy to be used for the residential and office spaces.

With the “Rotterdam Mountain” Project as a starting point, the thesis aims to investigate the structural feasibility and performance of a new typology for the design of high-rise towers, where a cable-net interconnects and stabilizes them. The final goal of the thesis is to form preliminary guidelines on the design of such a system, with respect to relevant parameters, such as the relative position of the connection of the cable-net and the spacing between towers. Such a core system to which the cable-net is connected is proposed to be used throughout the thesis.

Due to the inclusion of the cable-nets in the large category of form active structures, which among others includes grid shells, air-supported membranes, cable-nets or tensegrity structures, a form finding process is required to reach the equilibrium shape of the net to be analysed together with the core. This is required because, as no bending moment occurs, the shape of the form active structures is determined by the force and vice versa. Further, due to the large occurring deformations of the cable elements, a geometric non-linear analysis is required in order to obtain reliable results on the behaviour of the system.

To understand the relative influence of the different parameters on the stiffness and strength of the system, a parametric approach is used, developing a script using the Grasshopper plug-in for Rhino, that allows for a rapid change of the initial properties of the system. The parametric approach also allows for a rapid modelling of the complex shape of the cable-net, that would otherwise be time consuming in a conventional FEM package. After the form finding process is conducted in the Grasshopper environment, using the Kangaroo 2 plug-in, the geometry of the system to be analysed (composed of the core(s) of the tower(s) and the form found geometry of the cable-net) is exported to the Robot Structural Analysis (RSA) software, where the non-linear analysis is performed. Throughout the thesis, a systematic approach is used, from firstly analysing a simplified version of the system by modelling the cable-net as a 2D cable with an equivalent diameter, to finally performing a more complex 3D analysis of the system.

To develop conclusions on the behaviour of the system based on the variability of the initial parameters multiple iterations are performed, by ranging the spacing between towers from 30 to 140 meters and the relative position of the cable-net from 0.2 to 0.7 of the height of the tower(s). The outputs of the RSA analysis refer to both the serviceability limit state and the ultimate limit state, as both the cable-net and the core are designed to meet the stability and strength requirements imposed by the Eurocode. These outputs show that the relative position of the cable-net is the parameter with the highest influence on the stability of the system, while the spacing between towers is the parameter with the highest influence on the strength of the system.

Based on the Eurocode checks, conclusions are drawn on the preliminary design of the system, by identifying multiple design zones with respect to the two relevant initial parameters, as Figure 1 shows: a zone where the stability of the core is governing (zone 1), a zone where the strength of the core is governing due to the big load imposed by the mountain (zone 2), a zone where the influence of the cable-net is negligible (zone 3), and a zone where the design of the cable-net becomes impractical (zone 4). Zone 1, in which the range of slenderness of  $1/8.3 \rightarrow 1/23$  is achievable without the need of over dimensioning the core is considered optimal, as the highest weight reduction is expected. Based on the proposed preliminary design zones, a feasible design configuration is proposed and analysed for the Rotterdam Mountain, to cover the Terbregseplein highway node in Rotterdam, validating the approach. This further leads to the conclusion that, if designed accordingly, the project is feasible from a technical point of view.

Design Zones based on Relative Cable Position and Spacing Between Towers

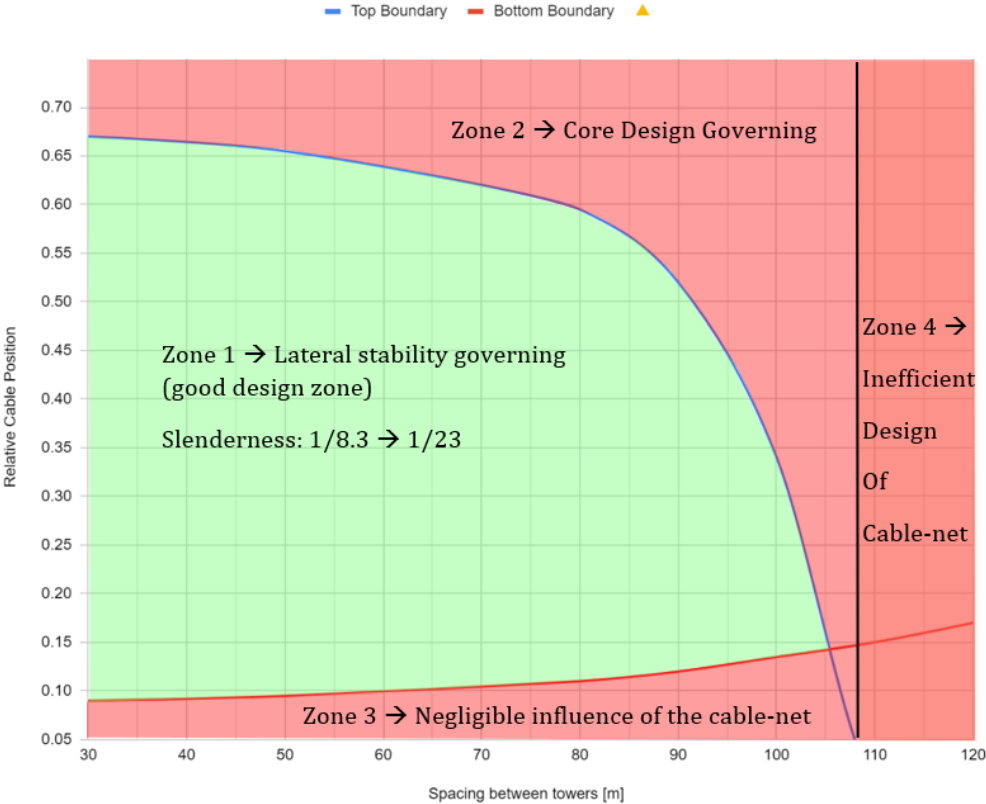


Figure 1 Design zones based on the two relevant parameters

Conclusions are further drawn on the performance of the system, by comparing it to the simple core and outrigger system. It is observed that the proposed core + cable-net system performs (at least) as good in terms of stability and strength with less material usage. A concrete weight reduction of the core of up to 50% is observed when compared to the simple core system and a steel weight reduction of up to 20% is observed when compared to the outrigger system, concluding that the system is a feasible design alternative for the design of high-rise towers.

From an economic point of view, preliminary calculations have shown a reduction of the total weight of the structure of up to 13%, due to the increase in slenderness when the cable-net is placed. This is equivalent to a number of up to 5 extra floors that can be constructed with the same amount of material, leading to the conclusion that the proposed system could lead to a more economic design, using less material and decreasing the ratio of cost to built area.

Lastly, it is noted that this research has provided *preliminary* insight on the design of the proposed system, by respecting a strict set of initial assumptions. The results are based on a constant geometry of the analyzed tower, a set concrete class of C45/55 and using the minimum possible strength of the cable-net. Using a stiffer cable-net, increasing the concrete class, or using a lower in-plane dimension of the tower, will lead to an even higher range of achievable slenderness. A more in-depth study, considering the variability of these parameters, as well as considering a full economic evaluation of the system, would provide valuable insight on the design of this new high-rise typology, and push the “Rotterdam Mountain” one step closer towards its completeness.

# Table of Contents

---

Preface.....	
Summary.....	
Table of Contents.....	
1. Introduction.....	1
1.1. Research Background.....	1
1.2. Research Description.....	4
Phase 1: Context.....	9
2. Literature Review.....	10
2.1. Strength and stability of high-rise towers.....	10
2.2. Guyed mast systems.....	14
2.3. Cable elements-properties and analysis.....	15
2.4. Cable-nets (Cable roofs) - properties and analysis.....	18
2.5. Form finding process for form active structures.....	22
3. Starting assumptions for the modelling and analysis.....	27
3.1. Assumptions for the tower.....	27
3.2. Assumptions for the cable elements.....	28
3.3. Assumptions for the cable-net system.....	29
3.4. Form finding process.....	30
3.5. Parametric model.....	30
3.6. Loads on the structure.....	33
3.7. Analysis assumptions for the cable-net.....	42
3.8. Geometrical nonlinear analysis - Robot Structural Analysis.....	43
Phase 2: Exploration.....	45
4. Parametric study of relevant parameters.....	47
4.1. Influence of the cable stiffness.....	48
4.2. Influence of the relative position of the cable-net.....	49
4.3. Influence of the cable angle.....	49
4.4. Conclusions of the parametric study.....	50

5.	2D Study of a single tower.....	52
5.1.	Not prestressed and not loaded cables .....	53
5.2.	Prestressed and not loaded cables.....	54
5.3.	Prestressed and loaded cables.....	56
5.4.	Conclusions of the 2D study.....	61
6.	3D Study of a rectangular grid of towers .....	63
6.1.	Initial remarks on the geometry and analysis of the system .....	63
6.2.	Design of the cable-net for the 3D case .....	71
6.3.	Range of Slenderness for the 3D case .....	75
7.	Overall design of the system.....	77
7.1.	Design of the core.....	77
7.2.	Temporary stabilizing elements .....	88
7.3.	Lowest relevant position.....	90
Phase 3: Elaboration .....		91
8.	Results .....	92
8.1.	Preliminary design of the system .....	92
8.2.	Comparison to the 2D case .....	100
8.3.	Comparison to existing systems.....	102
8.4.	Simplified economic evaluation .....	104
9.	The Rotterdam Mountain Project.....	106
10.	Discussion .....	108
10.1.	Discussion on the high-rise tower system .....	108
10.2.	Discussion on the cables and cable-net.....	109
10.3.	Discussion on the imposed loads.....	111
10.4.	Discussion on the proposed methodology .....	112
10.5.	Discussion on the 2D and 3D representation of the cable-net .....	113
10.6.	Discussion on the economic evaluation and comparison to existing systems.....	113
11.	Conclusion.....	114
12.	Recommendations for future research .....	118
12.1.	Weight optimization of the system components.....	118
12.2.	Typology of the towers.....	118

12.3.	In depth study of the cable-net .....	119
12.4.	Other research opportunities .....	119
	References .....	120
	Appendix A – Structural elements of the tower .....	123
	Appendix B – Loads on the structure .....	125
	Appendix C – Trial models .....	132
	Appendix D – Linear and Nonlinear analysis for the 2D case .....	134
	Appendix E – Parametric study .....	136
	Appendix F – 2D study of a single tower .....	140
	Appendix G – 3D study of a rectangular grid of towers .....	149
	Appendix H – Design of the core .....	158
	Appendix I – Simplified economic evaluation .....	171
	Appendix J – The Rotterdam Mountain design .....	173
	Appendix K – Parametric script .....	178

# 1.Introduction

---

## 1.1. Research Background

---

The plan for creating an “urban mountain” was first introduced by journalist and cyclist Thijs Zooneveld in 2011 but, at the time, the project was deemed unfeasible both from financial and technical points of view. Years later, the Rotterdam Dreamers revived the idea, creating a new set-up for the project, and proposing the “Rotterdam Mountain” (Figure 2). The vision is to create a mountain surface in the otherwise flat Dutch landscape, covering the infrastructure node of Terbregseplein, and thus transforming it into a link rather than a barrier between otherwise disjoint areas of the city. By building the mountain in layers, with various functions within, the project becomes a solution to the dullness that threatens the cultural landscape.

The project proposes the connection of the mountain to a number of high-rise towers, by using a network of cables to interconnect them, while providing support for the mountain’s surface. In a simplified view, the Rotterdam Mountain can be regarded as a tent-like structure (Figure 3), where the towers act as tent masts, while the mountain and cable-net act as the tensile canopy. The project exploits the usable space by joining built and green areas: just as a tent provides shelter for people, the mountain can accommodate a large part of the city underneath it. At the same time, above it, the large green area equals six times the current municipal ambition for green spaces, offering significant space for recreational activities, such as cycling, hiking or even skiing in the cold season (Summum Engineering, 2020).



Figure 2 The Rotterdam Mountain Project (Rotterdam Dreamers, 2020)

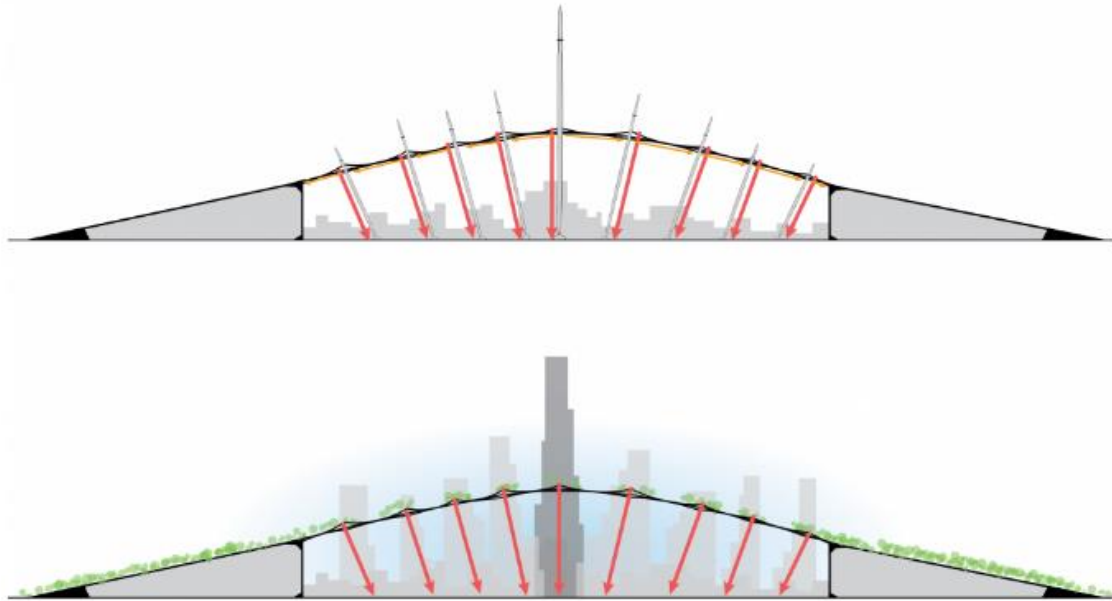


**Figure 3 The Rotterdam Mountain as a tent-like structure (Summum Engineering, 2020)**

In terms of structural design, the project addresses two relevant topics. Firstly, the design of high-rise towers, as the trend of building tall structures becomes prevalent as cities are becoming denser and denser. Secondly, the design of cable-net structures, included in the broad category of special structures which, often, due to the efficient use of materials lead to lighter, more efficient designs. Such, the innovative structural approach of the project, proposing the mutual interaction between the high-rise towers and the cable-net, becomes apparent.

It is known that cables have proven efficient in the design of tall, slender towers as guy mast systems, that are commonly used for TV or broadcast antennas. Nowadays, such system reaching heights of over 600 meters are not uncommon. On the other hand, the usual high-rise towers are constrained to lower, less slender designs. For example, the Maastoren in Rotterdam (now the highest completed high-rise in the Netherlands) rises up to 165 meters. However, the tallest structure is the guyed tower Gerbrandytoren, measuring 372 meters. Cables have further proven successful in the design of more functional structures, as the Torre de Collserolla or the Sydney Tower. A more extreme example is the Dubai Creek Tower, which uses a series of cables to provide its stability, that aims to surpass the now tallest building in the world.

This creates the opportunity to explore a new typology for the design of high-rise towers, that can lead to a higher range of achievable slenderness. If the guy masts are stabilized by large cables running to the ground, the proposed typology uses a network of cable to connect multiple towers that stabilize each other, transferring lateral loads towards the foundation more effectively. A higher range of achievable slenderness further translates to a reduction in the weight of the structure, with a positive influence on the foundation design and resulting in a range of benefits such as the reduction of the total embodied energy of the project, and possibly leading to a more economical solution for high-rise buildings.

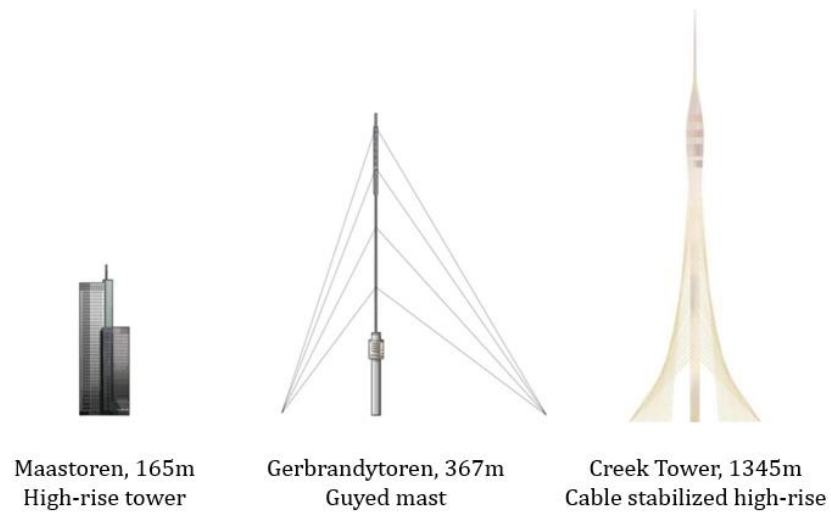


**Figure 4 The Maastoren, the Gerbrandytoren (Summum Engineering, 2020), the Creek Tower (Calatrava, 2016)**

It is suitable to discuss the further impact of the project in order to understand why such innovations in structural design are of relevance. First of all, the project addresses the housing challenge that the Netherlands currently faces, by providing a significant number of residential and office spaces in an otherwise unusable area. According to the estimation of Primos (2020), the housing shortage will reach a peak of nearly 415 000 homes in 2024. This issue leads to a continuous rise in house prices, with a concerning average increase of 7.8% in 2020 (de Groot et al., 2021). This problem is increasingly alarming among youth, as in 2020 approximately 22 000 students were left without accommodation at the start of their studies. Jolan de Bie, the chief on Kences, estimates that this figure will have risen to at least 50 000 by 2025. As most of the projections show a continuous growth in the population of the Netherlands in the following years, the housing shortage will continue to increase if little to no action is taken. To tackle this issue, in 2020 the Dutch Minister of Home Affairs Kasja Ollongre presented a report on the state of the housing market, explaining that nearly 850 000 homes need to be built by 2030. Addressing the projections of the Ministry, the large complex of the Rotterdam Mountain would allow for a number of residential spaces equivalent to the downtown of Rotterdam.

At the same time, the ambitions of the Paris Agreement of reaching net-zero emissions and climate resilience by 2050 pose a challenge to the building sector. In the Netherlands, the built environment has a crucial role in the transition towards the net-zero goals, according to the vision of the National Climate Agreement in the Netherlands. With the slogan "Save Energy Now!", the Dutch government encourages the building sector to direct its attention towards more environmentally friendly constructions. The vision of energy-efficient buildings, with performant insulation materials, that use renewable heating and in which clean electricity is adopted or even generated stands as a guideline for the future.

If above the mountain, the space is used for recreational activities, beneath it a more functional reason is proposed. It would combine distribution centers with the already existing highways and railways, and hide large distribution centers or other industrial functions from view. To tackle the

climate challenges, the project envisions a capturing system of the large heat produced by the data and distribution center, to be converted to energy used for the apartments and offices above.

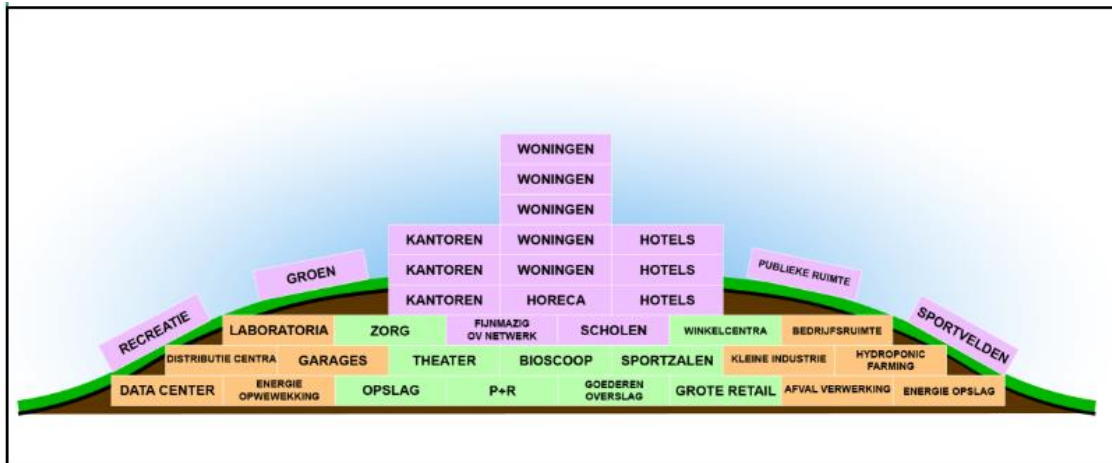


Figure 5 Functional distribution of the Rotterdam Mountain (Rotterdam Dreamers, 2020)

To conclude, the project envisioned by the Dreamers is relevant from an architectural, social (housing and recreational spaces), climate (energy efficiency) and possibly economic point of view. To achieve these goals, the structural feasibility of the system, which is addressed in this research, is of great importance.

## 1.2. Research Description

### 1.2.1. Research Aim

With the Rotterdam Mountain project forming the background of the thesis, the writer aims to develop the understanding of the structural behavior of a system composed of multiple high-rise towers, which are interconnected by a network of cables. The proposed system does not only apply to the mentioned project, but can form further basis towards a more economic design for towers, as higher slenderness is expected to be achievable.

Further, in the progressing field of constructions, this thesis aims to explore a new typology for the design of high-rise, contributing to the ever-growing knowledge regarding a structurally sound, economic and aesthetic built environment. If the guyed mast towers are stabilized by huge cables running to the ground, the proposed typology uses the cable-net to connect multiple towers that mutually stabilize each other. Such a system has not yet been widely reported.

With the proposed concept in mind, the feasibility of the system is explored from a structural point of view and a simplified economic evaluation is proposed. As the cable-net has the double function of both stabilizing the tower and providing support for the mountain's weight, the thesis aims to provide preliminary design guidelines on the configuration of the system with respect to relevant parameters. These parameters, as the relative position of the cable-net or the spacing between towers are expected to have an influence on the stability and strength of the tower. Such a range is searched for these parameters under which the system poses a feasible design alternative to other commonly used systems in the design of high-rise towers.

Lastly, the thesis aims to provide a feasible design alternative for the Rotterdam Mountain, to cover the Terbregseplein highway node in Rotterdam.

### **1.2.2. Research Questions**

Considering the thesis aim, two main research questions arise, as follows:

**Question 1:** “What are the most relevant parameters that influence the design of the cable-net stabilized high-rise towers and what is their influence on the overall performance of the system?”

**Question 2:** “Are cable-net stabilized high-rise towers feasible design alternatives to the existing stability systems for high-rise towers?”

### **1.2.3. Research Objectives and Sub questions**

To be able to answer the main research question, the thesis is divided into three main objectives (1-3) and a secondary objective (4), each addressing specific sub-questions on the behavior of the system, as follows:

1. Provide a thorough study on the starting assumptions used through the thesis, based on a literature review, focusing on the design and analysis of high-rise towers and the design and analysis of cables and cable-nets.
2. Study the influence on the *stability* of a single high-rise, when the tower is stabilized by cables connected to the ground.
  - What is the relative influence of the relevant parameters (relative position of the cable connection, cable stiffness and cable angle) of the cable system on the stability of the single tower?
  - What is the range of slenderness in which the cables + tower system falls, based on the geometry of the system?
  - What differences appear in the cases of clamped and pinned connections of the base of the tower to the foundation?
  - What is the influence of prestressing the cables and of the gravitational loads applied on the cables?
3. Study the influence on the *overall design* of a high-rise, when multiple towers placed in a rectangular grid are interconnected by a network of cables.
  - What is a suitable geometry of the cable-net for connecting the multiple towers?
  - How do the relevant parameters influence the overall design of the high-rise and which are the governing design criteria for different geometrical configurations of the system?
  - Based on the previous sub-question, what design guidelines can be concluded for the proposed system?
  - How does the system compare to the existing stability systems commonly used for the high-rise towers, both from a technical point of view, and from a simplified economical point of view?

4. Provide a system configuration for the Rotterdam Mountain, based on the outcome of the first three thesis objectives.

#### **1.2.4. Research Approach & Methodology**

##### **Research Approach**

To address the proposed objectives, the thesis is divided in three phases. In the *Context* phase, information is gained, analyzed and synthesized to form starting assumptions on the design of the system. In the *Exploration* phase, multiple analyses are conducted to obtain results on the behavior of the system. The *Exploration* phase follows a systematic approach, starting from a simplified 2D model to a more complex 3D model, to gradually increase the complexity of the problem. In the *Elaboration* part, the main results are presented, and the used approach is reviewed and discussed. Below, the main steps conducted in each of the phases are explained.

##### **Research Methodology**

###### ***Phase 1: Context***

The relevant literature is investigated to gain a comprehensive view on both the design of high-rise towers and cable-net systems (Chapter 2).

Based on the knowledge gained through the literature review, engineering assumptions are imposed to keep the design variables and space within defined boundaries (Chapter 3).

###### ***Phase 2: Exploration***

A systematic approach is followed to understand the behaviour of the system, starting from a highly simplified system to a complex one. At the end of each steps, the outcomes are reviewed and, at specific points, assumptions are made.

The systematic approach is divided in steps, each with individual end goals. The first three steps can be viewed as preliminary steps to reach sufficient knowledge to perform a more complex analysis of the systems.

In the first three steps the goal is to find a range of slenderness based on the top deflection of the system and to understand the influence of different components, such as the stiffness of the cable-net, the prestress and the form-finding process. It is expected, however, that the high load of the mountain will have an influence on the design of the tower according to the strength requirements, so that not only the deflection criterion is governing. Such, this overall behavior of the system is checked in the fourth step of the study, where more accurate results are expected, due to the complexity of the analysis.

- Step 1 (Chapter 4): 2D parametric study & assumptions → the goal of the first step is to understand the relative influence of different parameters (cable stiffness, relative height of the connection of the cable, cable angle, cable stiffness); the parametric study compares different configurations of the system by setting the top deflection as the comparison criterion;

- Step 2 (Chapter 5): 2D analysis of a single tower stabilized by cables connected to the ground on each side → the goal of the second step is to find a range of slenderness under which the system falls, based on the relevant parameters chosen in step 1, by setting the top deflection as the comparison criterion; in this step, the influence of the prestress and of the gravitational loads on the cables is treated, by analyzing three cases:
  - Unloaded and unstressed cables
  - Unloaded and prestressed cables
  - Loaded and prestressed cables
- Step 3 (Chapter 6): 3D analysis of a rectangular infinite grid of multiple towers interconnected by a network of cables → the goal of the third step is to find a range of slenderness under which the system falls, based on the relevant parameters; in this step, the design of the cable-net becomes a point of interest;
- Step 4 (Chapter 7): Overall design of the system → the goal of the fifth step is to gain a comprehensive understanding on the overall behaviour of the system; in this step, the top deflection does not remain the only comparison parameter, as the strength of the tower is also addressed;

Throughout the exploration phase a fully parametric model is used, to allow ease in changing the relevant parameters. Such, performing multiple iterations of different variants of the system becomes less of a time-consuming issue.

### ***Phase 3: Elaboration***

In the *Elaboration* phase the results of the *Exploration* phase are condensed and analyzed, by:

- Providing preliminary design recommendations for the configuration of the proposed system based on the overall design requirements of the system (Chapter 8.1).
- Reviewing the differences between the 2D and 3D analysis (Chapter 8.2).
- Providing a comparison to other existing systems commonly used for the design of high rise towers (simple core system and outrigger system), both from a performance and economic point of view (Chapter 8.3).
- Providing a simplified economic evaluation of the system, by means of a “total weight cumulation” (Chapter 8.4).
- Providing a design alternative for the Rotterdam Mountain (Chapter 9).

Lastly, the obtained results are discussed (Chapter 10) with respect to the initial assumptions that have been imposed throughout the research, and conclusions (Chapter 11) with respect to the completeness of the thesis objectives and answering the research questions are presented.

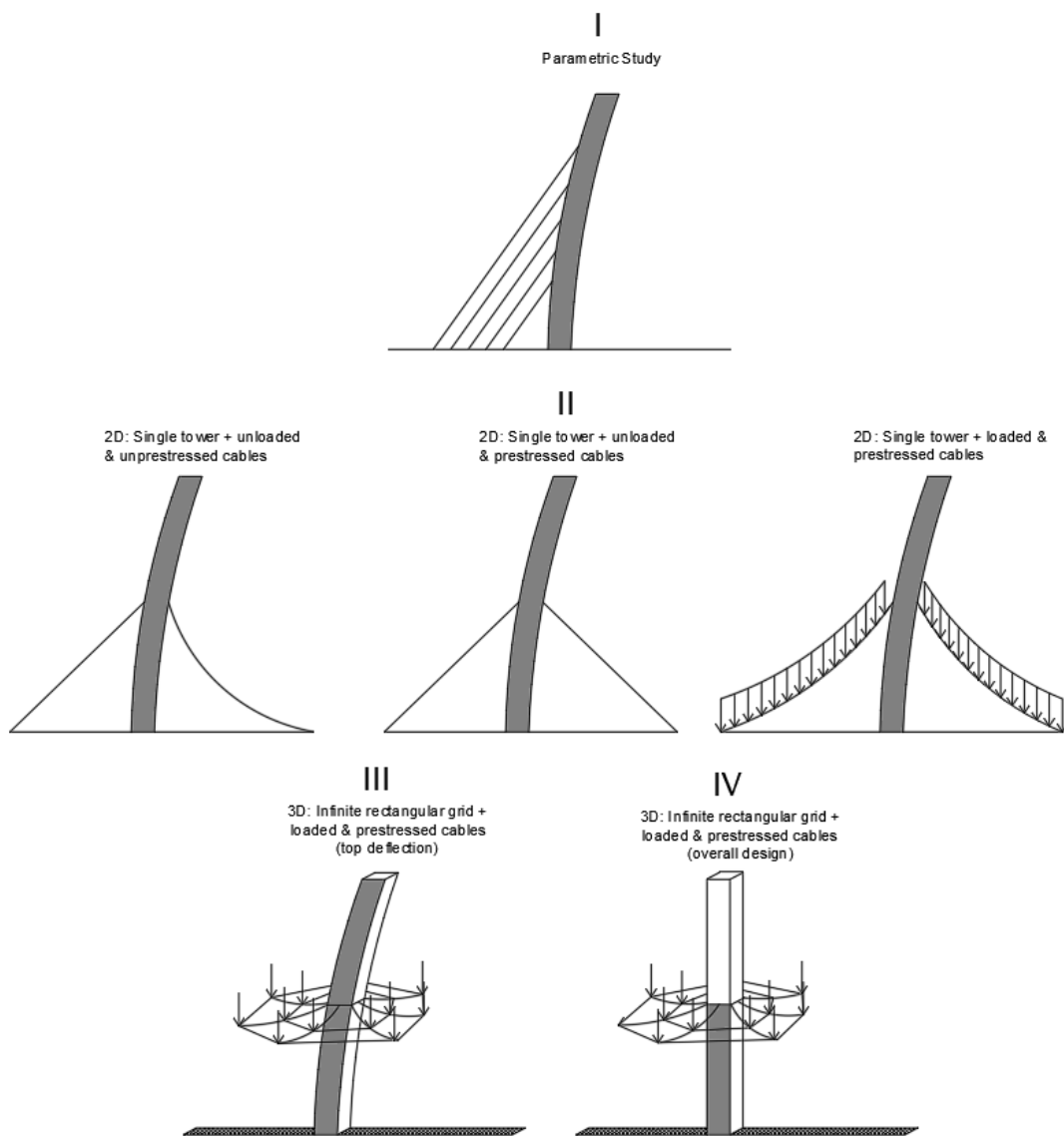
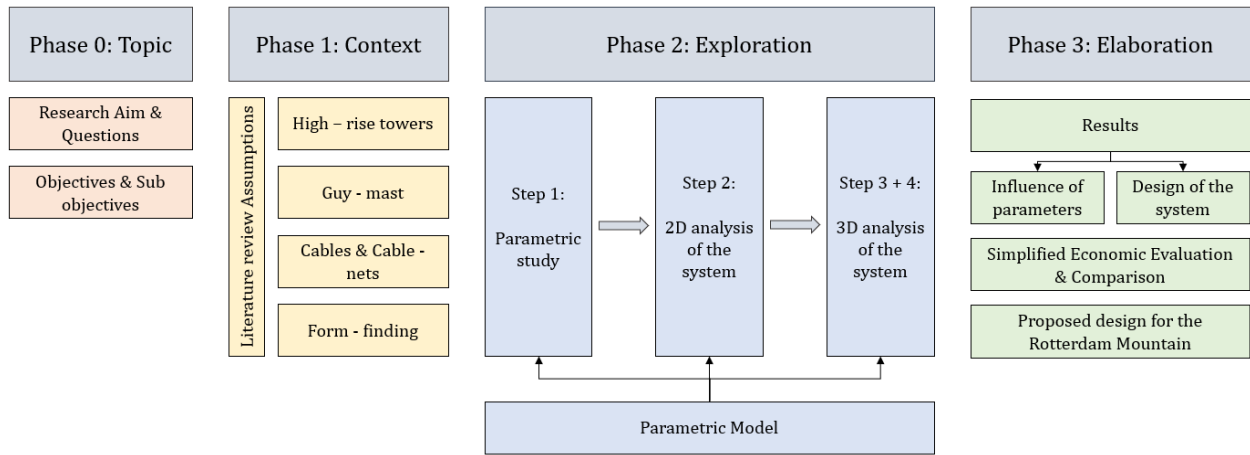


Figure 6 Research Scheme (Top) & Exploration Phase Visualization (Bottom)

# **Phase 1: Context**

## 2. Literature Review

---

As the Rotterdam Mountain proposes a system in which multiple high-rise towers are interconnected by a network of cables, a number of relevant topics are reviewed. The aim of the literature study is to provide sufficient knowledge to understand the most important design and analysis criterions for the proposed system, and to provide sufficient knowledge to impose sound starting assumptions for the design of the system. Such, the following topics are reviewed:

- The strength and stability of high-rise towers → as the system proposes functional high-rise towers to be analyzed together with the cable-net, it is sensible that a review on the typology of such towers, as well as their design and analysis is relevant.
- Guyed mast systems → the guyed mast systems are examples in which cables are successfully used to stabilize high, slender structures. Although usually used for functions as TV antennas, such systems provide a first insight in the benefit of cables on the stability of tall structures.
- Cables and cable-nets → as the towers are interconnected by the network of cables, attention must be directed towards understanding the types of individual cables used in practice and their properties, as well as the typologies, design and analysis of cable-net structures.
- Form finding of form active structures → due to the inclusion of the cable-nets in the category of form active structures, a form finding process is required to reach their initial equilibrium shape. Such, a review on the form finding theory, available methods and available software to perform it is conducted.

In the following sub chapters, each of the reviewed topics is presented, outlining the most critical findings. Further, in Chapter 3, the starting assumptions of the research, that are based on this literature review are outlined and explained.

### 2.1. Strength and stability of high-rise towers

---

Tall structures have, since the beginning of civilization, been a fascinating topic for mankind, with the first tall constructions having served for defense and ecclesiastical purposes. In modern times the growth in the number of tall buildings began in the 1880s, serving mostly for commercial and residential purposes (Smith et al., 1991).

The design of high-rise towers is based on both strength and stability criterions. For the ultimate limit state, the prime design criterion is that all structural members should have adequate strength to resist and remain stable under the worst probable load combination that might occur during the lifetime of the building. An analysis of the forces and stresses that will occur in the members must be conducted - this analysis should include the augmented moments that may arise from second-order effects, such as the additional moments due to the deformed shaped of the structure.

Additionally, checks must be made on the governing load combination to establish that the lateral forces will not cause the entire building to topple as a rigid body with respect to one edge of the base. Such, the resisting moment caused by the dead weights must be greater than the overturning moment caused by lateral loads.

Moreover, lateral stiffness is one of the major design considerations of tall buildings. This lateral stiffness is achieved by means of a lateral load resisting stability system (LLRSS), which provides the system the needed stiffness to withstand lateral forces. The system has to ensure the global stability of the buildings, to provide sufficient stiffness to prevent collapse due to the P-delta effect and to prevent excessive building motion (Hoogendoorn, 2009). Wind loads, seismic loads and eccentric gravity loads are part of the category of lateral forces to be expected to act on high-rise buildings (Sandelin, 2013).

In common practice, different alternatives for the lateral load resisting stability systems of (high-rise) towers exist - some of the commonly used ones are presented in the following paragraphs. The main parameter that judges the efficiency of the proposed LLRSS is the drift index, defined as the ratio between the maximum deflection at the top of the building under the governing load combination and the total height of the high-rise. The drift limits are not specified in code requirements, so a sound engineering judgement is required when deciding on the imposed limit. Conventional values range from  $H/600$  to  $H/400$  (Smith et al., 2019). In this research a traditionally accepted value of  $H/500$  (maximum value for the drift index) will be used to judge the effectiveness of the proposed LLRS.

### **2.1.1. Frame system**

#### **a. Rigid frame system**

A rigid frame system is composed of beams and columns that are linked together with fully moment resistant connections. Usually, they are not used for buildings with more than 10 stories. However, due to their good performance under seismic loads, higher structures using the rigid frame system can be found in earthquake prone areas. An important advantage of the system is the possibility to design wide, open rectangular spaces. (Smith et al., 2019)

#### **b. Braced frame system**

In braced frames the lateral resistance is provided by diagonal members (braces) that, together with the girders form the “webs” of vertical trusses. The columns are, consequently, working as the “chords” of the vertical trusses. Braced systems are conventionally regarded as steel-only systems, due to the fact that the diagonals are inevitably subjected to tension (due to the lateral load acting from either direction). Their main advantage is the possibility of erecting very stiff structures with a minimum amount of additional material (Smith et al., 1991).

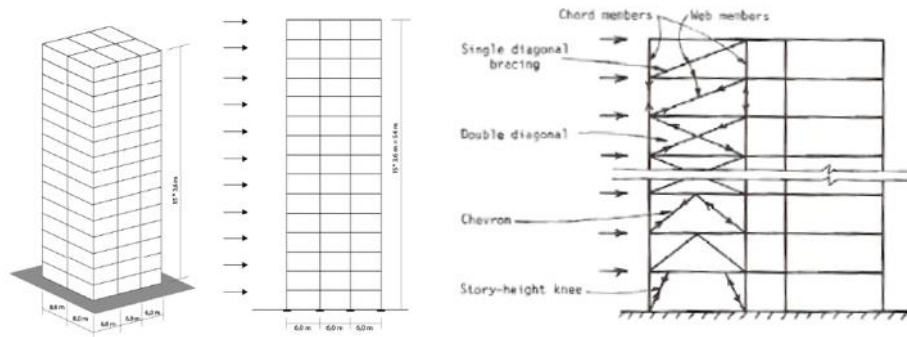


Figure 7 Left: Rigid Frame System (Terwel et al., 2017); Right: Braced Frame System (Smith et al., 1991)

### 2.1.2. Core system

The simple core system is a commonly used structural system for high-rise towers, generally used for buildings up to 100-120 meters tall. The core, which usually has a slenderness (width over height ration) of approximately 1/8, and with a width usually not exceeding 15 meters, acts as stiff cantilever. To take into account the cracking of the concrete and the openings in the core, a reduced modulus of elasticity of the concrete must be assumed (Terwel et al., 2017).

### 2.1.3. Outrigger system

Outrigger systems are used when the simple core system does not provide sufficient stiffness to the building. The outrigger is usually a truss system placed at one or more heights of the core, connecting it to exterior columns. These columns participate as stabilizing members, decreasing the deflections and imposing a shift in the bending moment diagram (Terwel et al., 2017).

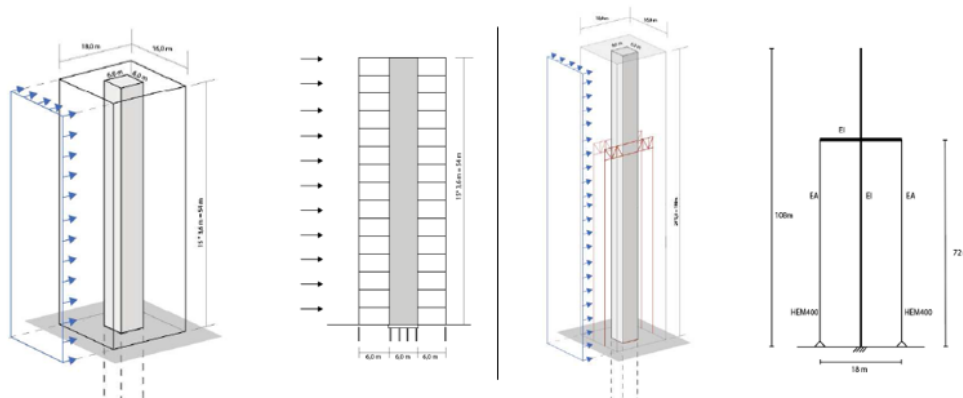


Figure 8 Left: Core System; Right: Outrigger System (Terwel et al., 2017)

### 2.1.4. Tube system

In a tubular system the façade of the building acts as the primary lateral load resisting stability system. Such, the exterior columns and beams are designed as strong structural members, usually of steel or concrete, forming a large tube with many openings for windows. The connections between the members are fully rigid, such that the tube acts as a sway frame (Terwel et al., 2017).

### 2.1.5. Mega frame system (Braced-tube system)

A way of increasing the efficiency of tube systems is to add diagonal bracings on the faces of the tube. This leads to potentially bigger achievable heights and allows for greater spacing between the columns. The bracings further contribute to the overall performance of the system by also carrying gravitational loads (Smith et al., 1991).

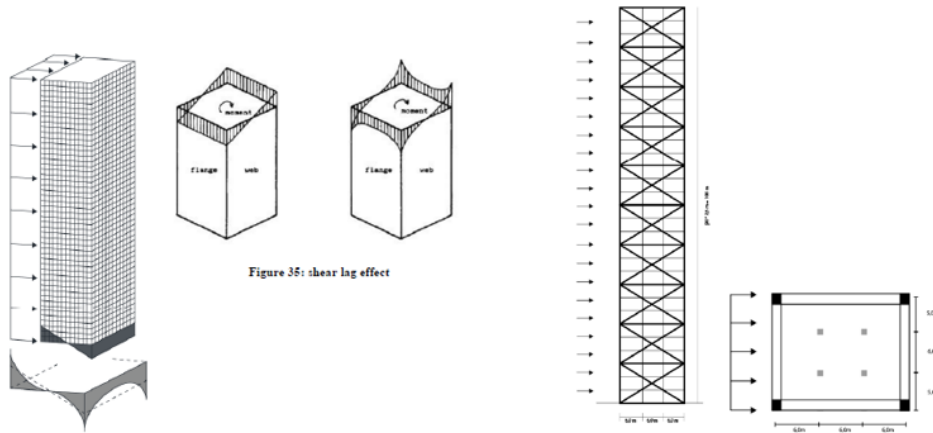


Figure 9 Left: Tube System; Right: Mega Frame System (Terwel et al., 2017)

Not to be omitted, other possible LLRS are used in practice, such as: shear wall structures, wall-framed structures, suspended structures or hybrid structures.

Ching et al. (2009) provides a graph relating the different stability systems with reasonable achievable building heights based on common building practices and studied existing high-rise towers. For this comparison, the heights are expressed in stories.

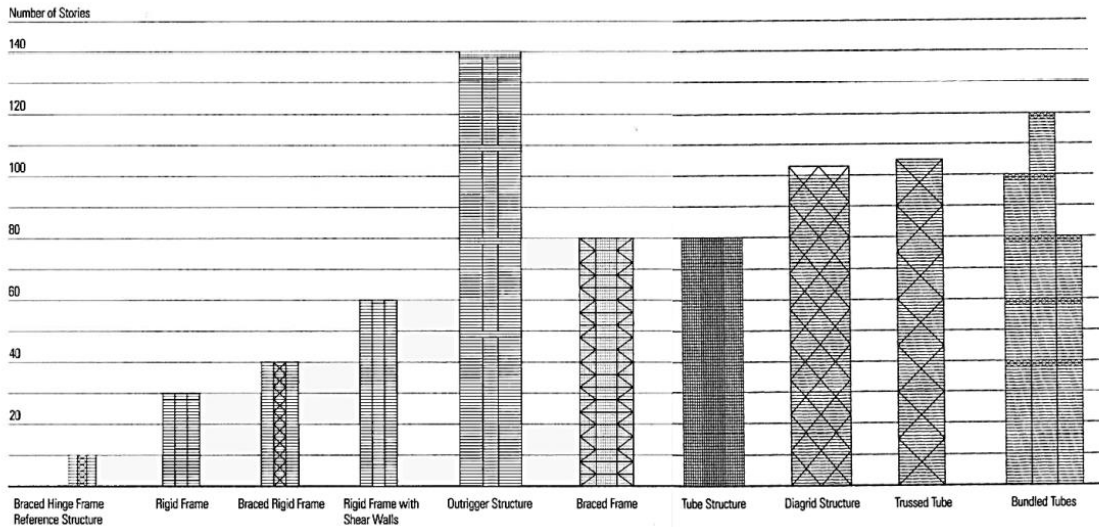


Figure 10 High-rise stability systems related to their achievable heights (Ching et al., 2009)

## 2.2. Guyed mast systems

---

Mostly used as support systems for tall slender towers, such as TV or broadcast antennas, the guy-mast towers are among the tallest structures in the world. Nowadays, such towers measuring more than 600 meters in height are not uncommon. Their stability efficiency leads to economical material usage. Comparing earlier design of towers with recent structures proves this statement. The Eiffel tower, measuring 300 meters weights about 7000 tons while, on the other hand, a modern TV mast of the same height, that is stabilized by guys weights over 20 times less (Strottrup, 2014).

Ulrik Strottrup, member of the IASS research group for Masts and Towers, argues that guyed masts are usually more cost effective than self-supporting towers. This applies for heights of over 60 meters. In practice, hybrid solutions where the guy-mast is placed on top of a concrete, self-supporting tower have been adopted, such as the Gerbrandy Tower.

Some of the main considerations to be taken into account for the design of guy mast systems are:

- They are mainly subjected to lateral wind loads (Stottrup, 2014);
- Their response to dynamic loads is increased compared to the response of buildings or bridges (Stottrup, 2014);
- The guys should be designed such that the working stress should be close to the allowable stress to take full advantage of the material usage (Gantes et al., 1992);
- The connection of the mast to the foundation can be either pinned or fixed. Storrup explains usually, especially for highly slender towers, a pinned foundation is preferred;
- The detailing of the connection of the guy to the mast and foundation should allow for the free pivoting of the guys to prevent fatigue damages (Nielsen, 2014);

The guyed mast systems are a clear example of the positive influence of the cables on the behavior of tall structures. An exact parallel cannot be drawn to high-rise towers, as due to their high flexibility, the guyed towers exhibit dynamic response under turbulent wind load (Gantes et al., 1992), which is not expected in the behavior of towers with larger in-plane dimensions.

Structures like Torre de Collserola in Barcelona or the Sydney Tower are examples of more functional towers that achieved high slenderness by using cables as stabilizing elements. The newly design Creek Tower in Dubai pushes the limits of such systems, with its proposed height of over 1000 meters.



**Figure 11 Left: Torre de Collserola (Foster & Partners); Right: Sydney Tower (Wikipedia);**

## 2.3. Cable elements-properties and analysis

---

### 2.3.1. Introduction

The cables can be defined as flexible steel tension members that could be a strand, multi-strand, or parallel wires acting as a unit member. They are protected by a uniform coating, usually made of pure zinc (Ossman, 2003). The basic component of the cables is the steel wire, drawn from high-strength steel rods. The wire is then galvanized by hot-dip or the electrolytic process (Krishna, 1978). Stainless steel wires are also used in practice, but to a far lesser extent than high tensile steel wires. The longitudinal direction of cables largely exceeds their transverse direction, thus having negligible buckling strength. Moreover, cables cannot sustain any bending or torsion moment and act only in tension.

### 2.3.2. Strands & Ropes

Modern cables that are used with structural purposes are made from steel wires, usually of cylindrical shape, with a diameter of up to 7mm. The combination of such wires results in **strands** or **ropes**, depending on their arrangement. These types of tensile elements are most commonly used in the design of tensile structures, such as cable nets, or textile constructions (Llorens, 2015).

#### A. Strands

The structural *strand* is composed of a set of wires rolled symmetrically into a spiral around a center wire. The number of wires depends on the required diameter and strength. As cables get larger, the number of strands increases. For instance, cables with a diameter of 19mm have 19 strands, while cables of 50mm have 91 strands.

The most traditional type of strand has been the spiral strand which consists in a number of concentric small size galvanized wires. Typically, spiral strands with diameters up to 300mm (having some 800 small wires) can be produced.

Alternatively, to the common spiral strands, locked coil strands can be produced - in this configuration, one or more outer layers of 'z' shaped wires are used.

Further, parallel wire strands are a different commonly used tension member. These are formed by twisting a number of small size galvanized wires in a single operation with a long lay. This solution is often employed in the cable stayed bridge design (Krishna, 1978).

#### B. Ropes

The structural *rope* is composed of multiple strands wound around a nucleus (core). The rope is usually larger in diameter and lower in stiffness than the structural strand or solid rods. The number of wires per strand depends on the required diameter and strength of the rope (Ossman, 2003). While the ropes offer an advantage in flexibility, the size has to be kept limited - a rope has more open form of construction and, consequently, a lower extensional modulus compared to the strands (Krishna, 1978).

A comparison between the main attributes of strands and ropes is presented below:

- Strands are stronger than ropes for the same nominal size;

- Strands have a greater value for the modulus of elasticity;
- Ropes are more flexible than strands;
- Ropes are easier to handle → where cables have to pass over saddles, smaller radii can be used for ropes;
- Strands have better strength/ weight ratio;

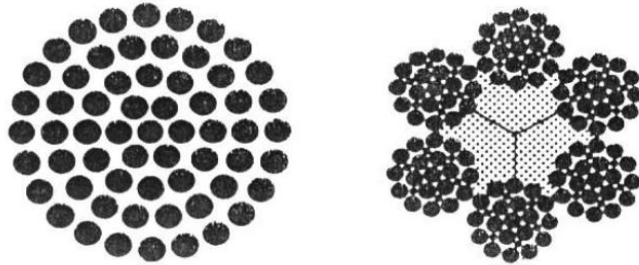


Figure 12 Spiral Strand (left) and Rope (right) (Krishna, 1978)

### 2.3.3. Strength

The steel wire strength is significantly higher than the strength of structural steel, due to higher carbon content in its composition, of 0.5%-0.8%. Thus, for typical round wires for structural strength of 1600-1800 MPa can be reached for the minimum expected ultimate tensile strength. Eurocode 1991-1-11 proposes 4 values for the wire tensile strength grade, ranging from 1570 MPa to 1960 MPa. Opposed to their high strength, the ductility of steel wires is six times lower than that of structural steel. The usual spiral strand ropes have lower elasticity modulus compared to structural steel, with values ranging from 150 to 200 GPa (Pipinato, 2016).

Up to and including wire tensile strength grade 1570 N/mm <sup>2</sup>	Up to and including wire tensile strength grade 1670 N/mm <sup>2</sup>	Up to and including wire tensile strength grade 1770 N/mm <sup>2</sup>	Up to and including wire tensile strength grade 1960 N/mm <sup>2</sup>
---	---	---	---

Figure 13 Wire Tensile Strength (EN 12385)

	High strength tension component	$E_Q$ [kN/mm <sup>2</sup> ]	
		steel wires	stainless steel wires
1	Spiral strand ropes	150 ± 10	130 ± 10
2	Fully locked coil ropes	160 ± 10	–
3	Strand wire ropes with CWR	100 ± 10	90 ± 10
4	Strand wire ropes with CF	80 ± 10	–
5	Bundle of parallel wires	205 ± 5	–
6	Bundle of parallel strands	195 ± 5	–

Figure 14 Wire E-value (EN 12385)

### 2.3.4. Eurocode Considerations and Requirements

Eurocode 3-Design of steel structures-Part 1- 11: Design of structures with tension components defines three groups of tension components, as shown in Figure 15.

Group	Main tension element	Component
A	rod (bar)	tension rod (bar) system, prestressing bar
B	circular wire	spiral strand rope
	circular and Z-wires	fully locked coil rope
	circular wire and stranded wire	strand rope
C	circular wire	parallel wire strand (PWS)
	circular wire	bundle of parallel wires
	seven wire (prestressing) strand	bundle of parallel strands

Figure 15 Tension element groups (EN 1993-1-11)

Group A generally have single solid round cross section connected to end terminations by threads. Their main applications are for the design of bracing systems, steel trusses or space frames.

Group B products are composed of wires which are anchored in sockets or other end terminations , fabricated in the diameter range of 5 to 160 mm. Spiral strands and ropes fall into this group.

Group C products need individual or collective anchoring and appropriate protection. Bundles of wire and strands fall into this group.

According to EN1993.1.11.2006, the minimum breaking force of a cable has to be calculated using the breaking force factor (K), which takes into account the fill factor for the rope (f) and the spinning loss factor (k). The rope grade (R<sub>r</sub>) does not necessarily correspond to the tensile strength grades of the wires in the ropes.

$$K = \frac{\pi f k}{4} \quad F_{\min} = \frac{d^2 R_r K}{1000} \text{ [kN]}$$

Figure 16 Minimum breaking force (EN 1993-1-11)

EN 12385: Steel Wire provides good insight into standard values of the K factors for common strands and ropes, and provides tables with the corresponding minimum breaking force. For spiral strands, usually the filling factor of 0.65 and the spinning loss factor of 1 are used.

In terms of requirements, the Eurocode states that the following limit states shall be considered:

- In ULS, the applied axial load shall not exceed the design tension resistance
- In SLS, the stress and strain levels in the component shall not exceed the limiting values
- Stress ranges from axial load fluctuations and wind and rain induced oscillations shall not exceed the limiting values

Moreover, to prevent the de-tensioning of a cable element (by the stress reaching a value below zero, making it become slack and pose stability or fatigue issues), the tension components are

preloaded by deformations imposed on the structure → prestressing. In this case, the permanent actions, respectively the gravitational loads (G) and the prestress (P) shall be considered as a singular permanent action G+P.

### 2.3.5. Protective Coating

Apart from the structural requirements, cables have to ensure sufficient resistance against corrosion. Such, additional protection by having galvanized or aluminized wires with protective metal sheaths is adopted as a usual practice. However, even when applying this extra measure, regular checks to ensure that the lubricants or dressings have not been removed by chemical reactions have to be performed. (Buchholdt, 1999).

## 2.4. Cable-nets (Cable roofs) - properties and analysis

---

### 2.4.1. Definition and Classification

A cable-net or a cable roof can be defined as a system in which a cable or a multitude of cables are used as a load-carrying structural element. A first classification of the cable roofs can arise from the manner in which the cables are used:

- Cable-supported roofs
- Cable-cum-air-supported roofs
- Cable-suspended roofs

*The cable-supported roofs* are similar to cable-stayed bridges. In such a system, the cables have the function of providing additional support for elements which inherently carry most of the loading. The cables system's purpose is doubled by their use in the erection process of the cladding, where they can be used as false work.

The cable-cum-air-supported roofs propose a system in which the roof is supported either by air pressure alone or by a combination between air pressure and cables. The air stretches the skin of the roof to form a tension membrane attached to cables.

These two systems, the cable-supported and the cable-cum-air-supported roofs are not part of this research.

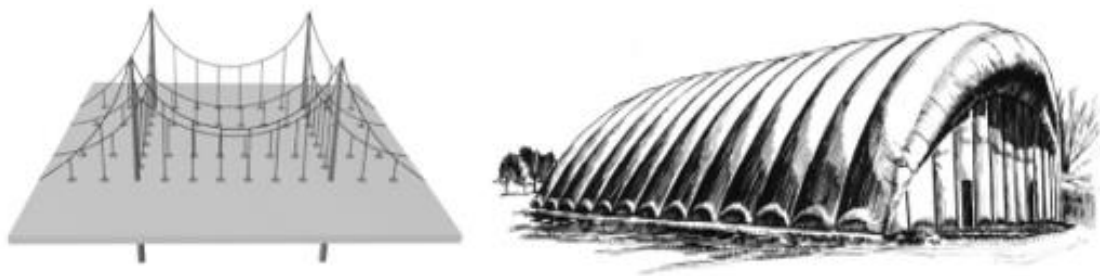


Figure 17 Left: Cable-supported roof (Krishna et al., 2013); Right: Cable-cum-air roof (Krishna, 1978)

*The cable-suspended roofs* propose a system in which the cables carry the gravitational load directly, acting as the primary load carrying structures. Based on multiple factors, this type of cable-nets can be further divided into subcategories.

Based on the geometry of the system:

#### **a. Simply suspended cable structures**

If the in-plane shape of the roof is rectangular or trapezoidal, the support system can be made of a series of simply suspended cables hanging in vertical planes (Figure 18 left-top). For in-plane circular or elliptical shapes, the cables are suspended radially and attached at the perimeter of the roof to a compression ring and, at the center of the roof, to a tension ring (Figure 18 left-bottom).

#### **b. Pretensioned cable-beam structures**

When connecting a second set of cables to the suspension cables of the simply suspended cable structures, lighter and stiffer systems can be obtained. The resulting system can be stiff if tensioned to a level at which all cables remain in tension under any given load combination. The cable-beams can be referred to as concave, convex or convex-concave beams, depending on the geometry and arrangement of the cables. Multi-span cable beam constructions are suitable for cases where large spans can be interconnected or where column-free interiors are not required.

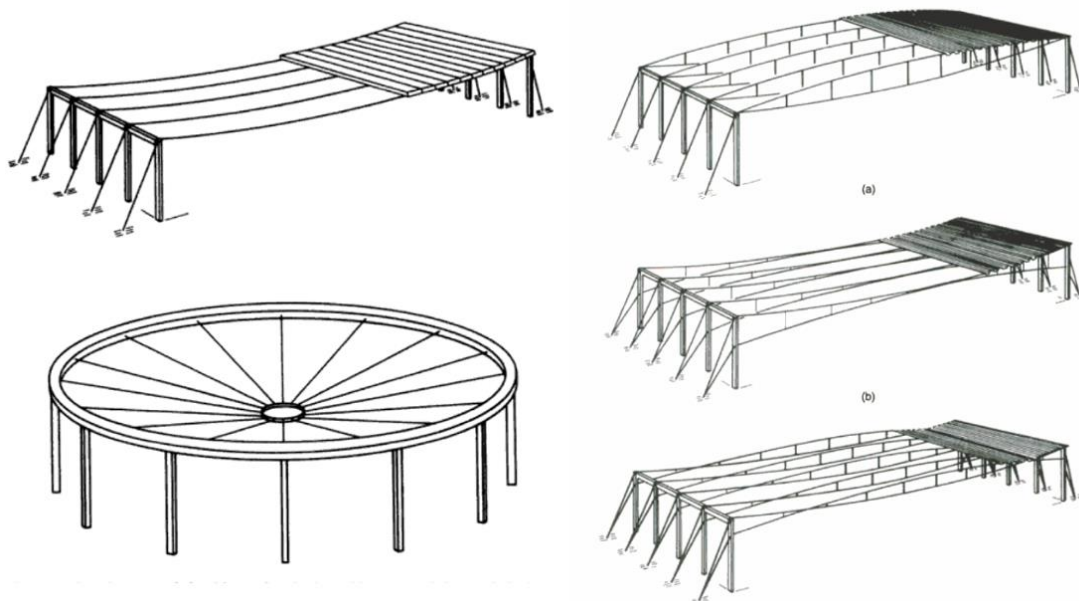


**Figure 18 Left: Simply suspended cable structures-left; Right: Pretensioned cable-beam structures (Buhholdt, 1991)**

#### **c. Pretensioned cable-net structures**

In the third type of cable roof structures, the pretensioned cable-net system imposes a structure in which the suspension (concave) and pretension (convex) cables lie in one surface, forming a large net. Similar to the previous category, the cables must be in tension at all times to provide the needed stiffness. Such, the shape of the surface must be anticlastic or saddle-shaped. Even flat surfaces should be avoided, especially when designing large-span roofs, to avoid flutter. Depending

on the support conditions and tension in the cables, the geometry of the cable net can be set. It can resemble tent-like structures, using masts and edge cables (Figure 19 Left), or use stiff boundaries such as beams or arches (Figure 19 Right). The tent-like structures, shown in Figure 19 can be extended to multi-net constructions, such as the ones in Figure 25.

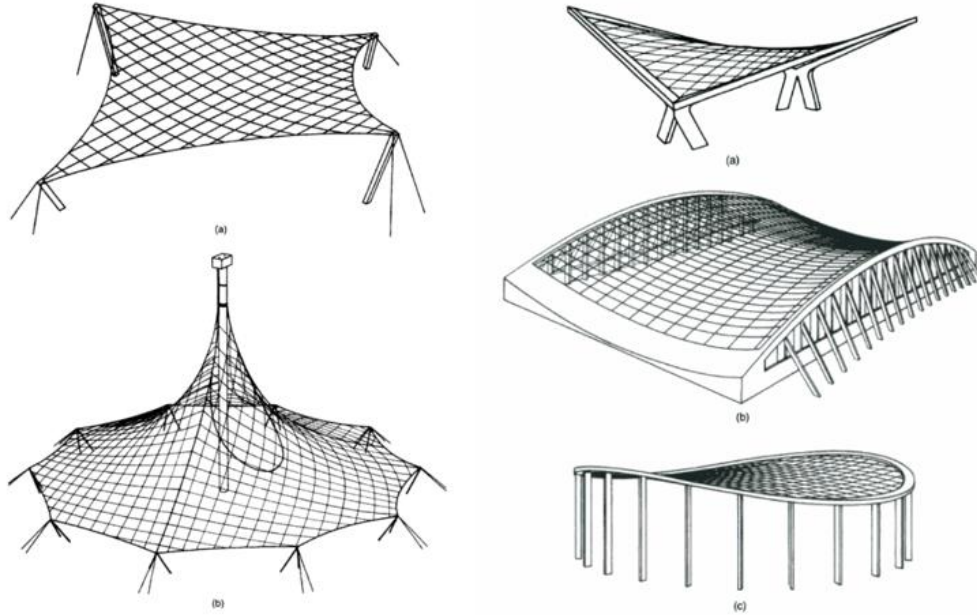


**Figure 19 Left: Pretensioned cable-net structures with edge cables;  
Right: Pretensioned cable-net structures with stiff boundaries (Buchholdt, 1991)**

In addition, Buchholdt proposes a set of notes for the design of pretensioned cable-net structures

- For large spans, the geometry must almost always be anticlastic or saddle shaped.
- The clamps connecting the cables must exert sufficient pressure on them to prevent slipping, as movement of the clamps will result in loss in tension and reduced stiffness.
- In the case of large nets, where “flat areas” cannot be avoided due to architectural considerations, additional stiffening measures must be used, as internal or external ties.

Generally, the spacing of the cables in a pretensioned cable roof ranges from 0.5 meters to 5 meters (Ossman, 2003). The pitch is dictated by the design and weight of the cladding. Secondary support structures for the cladding, such as purlins or rectangular frames may be adopted, but it usually leads to less economic solutions than a smaller inter cable pitch. The cladding will usually not significantly increase the stiffness of the roof but it is the major source of structural damping.

Usually, a sag between 4%-6% of the span of the cables will lead to satisfactory structural behavior, given that the cables are sufficiently tensioned so that they do not go slack under any given load combination (Buchholdt, 1991).

### 2.4.2. Analysis of cable nets

Due to the fact that most pretensioned cable structures are mechanisms, and due to the high-tensile forces that steel cables permit (nearly six times those allowed in usual steel constructions), cable roofs are classified as nonlinear structures. The stiffness of the system tends to increase with the increase in deformation, as long as all cables are maintained in tensions. A linear analysis method would tend to overestimate the occurring displacements and forces. (Buchholdt, 1991)

The degree of nonlinearity varies with the type of structure and with the loading conditions. To sustain the applied loads, the cables need to follow the funicular curve of the loads and thus, it experiences significant geometric adjustments (especially when loaded unsymmetrically or by concentrated loads) - this leads to the so-called geometric nonlinearity of the cables. This will occur irrespective of the linearity (or non-linearity) of the cable material. (Krishna, 1978)

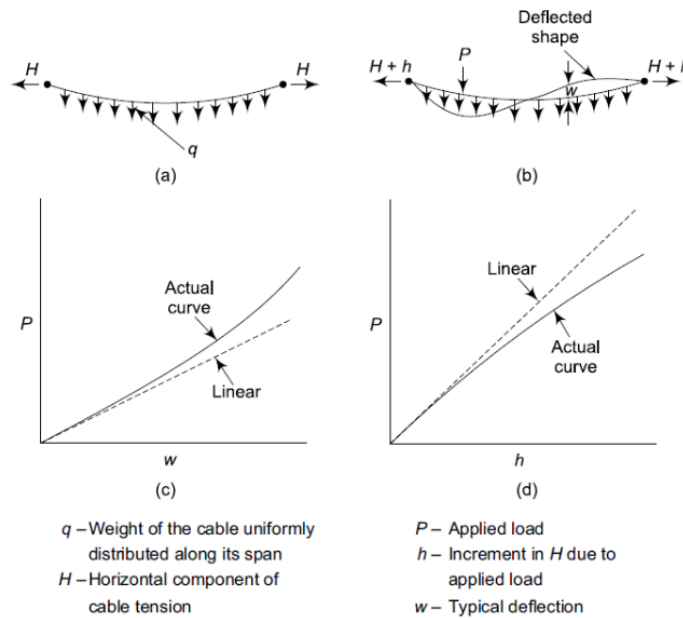


Figure 20 Analysis of cable elements (Krishna et al, 2013)

Analyzing cable systems tends to be a complex problem, but simplifying assumptions can be made to reduce the required effort, especially in the preliminary design work. The cable-roof analysis can be conducted under two different broad assumptions, depending if the network is treated as a: (a) discrete system or (b) continuous membrane.

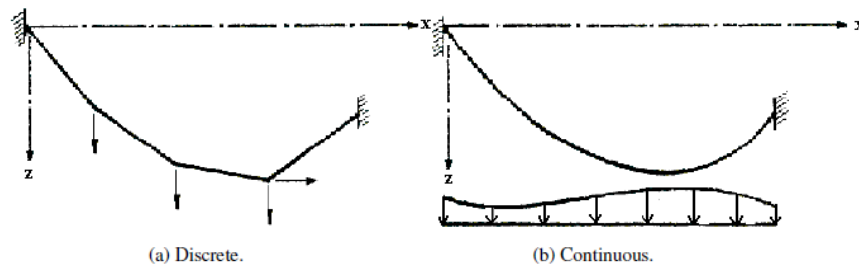


Figure 21 Discrete & Continuous System (Krishna, 1978)

A number of existing structures have been analyzed in order to get realistic values for the dimensions of the cables usually used in practice. As in the first part of the research, structural models and calculations are performed in 2D, this analysis gives good insight on how to approximate the dimensions of a whole cable net to a single equivalent cable.

**Table 1 Cable Dimensions for different structures**

Project Name [-]	Height [m]	Single Cable Dimensions	Single Cable Equivalent Diam. [mm]	Number of Cables [-]	Cable type [-]
Torre de Collserolla	288	180 wires x 15mm	200	3x3	Pre-tensioned high-strength steel
Sydney Tower	304	235 wires x 7mm	107	56	High-tensile wires
Hwamyung Bridge	-	-	200-280	72	Multi strand high-strength cables
1001 Tower Dubai	450	-	400	48	-
Munich Olympic Stadium	-	Net: 19 x 3.3mm Edge: 81 Main: 165	Net: 14.5 Edge: 81 Main: 165	75 x 75 cm mesh	Parallel strand bundles

### 2.4.3. Prestressing of the cable-nets

As Krishna (1978) mentions, prestressing is usually the responsibility of the cable manufacturer, with the most major strand or rope companies being able to provide an adequate cable length with good accuracy. Cable nets are particularly sensitive to errors in length, which may lead to high over or under stressing of the elements, with peak found errors of up to 60% of the force. As the execution and manufacturing of the cables and cable-net does not form a part of this research, the accuracy requirements and local overstressing are not introduced in the calculations.

However, it is commonly known that a tension member which is subject to repetitive stress can fail due to fatigue. The level and the amplitude of the fluctuating stress has, naturally, an influence on the fatigue resistance of the element. Gabriel (1974) has observed that the prestress load should be in the range of 10% to 40% of the ultimate strength of the cable, to account for fatigue issues.

## 2.5. Form finding process for form active structures

### 2.5.1. Introduction to Form Finding

In the case of structures which transfer the loads purely through axial forces or in-plane stresses, the principle of form finding becomes relevant. In these cases, where no bending occurs, the shape is determined by the force and vice versa. Cable-nets, together with shells, grid-shells, tensegrity structures or air-supported membrane structures fall in the broad category of form-active structures. The shapes of these structures are not known in advance, so a *form finding* process is required to obtain their initial geometry. (Veenendaal, 2017)

Such, the *form finding* can be defined, based on the proposed definition of Adrianenssens et al. (2014) as:

“A forward process in which parameters are explicitly/ directly controlled to find an ‘optimal’ geometry of a structure which is in static equilibrium with a design load”

Three main categories of form finding methods can be identified, namely: the stiffness matrix method (SM) or nonlinear finite element method (FEM), the force density method (FDM), and the dynamic relaxation method (DR) (Lewis 2003, Li&Chan, 2004). A fourth category, of minimization methods has been proposed based on the Buchholdt’s et al. (1968) description. Veenendaal (2017) proposes the following main families to categorize the existing form finding methods.

- **Stiffness matrix methods** - use the standard elastic and geometric stiffness matrices. These methods assume initial properties such as the initial geometry or use a fictitious material stiffness. If, in case, the effective material stiffness is used, these methods can be viewed as nonlinear large displacement FEM methods.
- **Geometric stiffness methods** - use only a geometric stiffness matrix, being independent of the material properties. In some cases (starting with the FD method) the ratio of force to length is a central parameter in the calculations.
- **Minimization methods** - use a Quasi-Newton or gradient descent solver to formulate a function or energy to be minimized. This avoids the need to construct or invert a stiffness matrix.
- **Dynamic equilibrium methods** - use an integration scheme to arrive at a steady-state solution (to solve the problem of dynamic equilibrium).

### **2.5.2. Form Finding Software**

For this thesis, the form finding process is performed using the Kangaroo 2 plug-in for Grasshopper. Kangaroo works by minimizing the total energy, proposing an iterative solver for finding an equilibrium solution where forces sum to zero at each defined node of the structure. Kangaroo 2 uses a new form of the classical Dynamic Relaxation method, by combining projections onto the zero-energy state of each goal, as described by Daniel Piker, the developer of Kangaroo 2.

For the proposed form finding process, the cable elements are treated as zero-length springs in the Kangaroo environment, which are proposed by Harding & Shepherd (2011). This is done by attributing each cable element a length goal with the target “zero”. Piker explains that defining such elements will lead to the same result as using a constant force density element, since the tension force is proportional to the length of the line. Veenendaal (2017) further explains that this method is identical to the linear force density method in terms of its elements.

Such, in the categorization proposed by Veenendaal (2017), a hybrid between geometric stiffness method and the dynamic equilibrium is used, as the force to length ratio (force density) is the central parameter in the calculations, and Kangaroo 2 uses a dynamic solver to reach equilibrium.

### **2.5.3. Force Density Method**

The force density method (FDM), also known as the “(Stuttgart) direct approach” is chosen due to its rapid generation of feasible shapes for prestressed hanging structures. It is especially relevant in

the early stages of the design due to the possibility of exploring numerous alternatives (Adriaenssens et al. 2014). The method was proposed at the beginning of the seventies by Schek. (Schek, 1974)

The method finds the geometry of (network) structures when the internal forces balance the external ones. The concept is based on the ratio of the force-length (or force densities), defined for each branch of the structure. The force densities are suitable parameters to find the equilibrium state of networks, as the coordinates of the nodes are obtained by only solving a system of linear equations (Schek, 1974). Through the Linear FDM, the method makes it possible to find all equilibrium configurations of a net with prescribed connectivity and boundary conditions on the nodes. Each found configuration correlates to an assumed force density distribution. The FDM is still one of the most widely applied tools for finding the initial geometry and prestressing of form-active structures (Malerba et al, 2012).

The FDM has the advantage of not needing any material information during the form find process. The materialization of the elements follows in a second step of the design, so no conditions with respect to material laws are imposed. Such, the materials can be later chosen for each independent member of the structure, without changing the found shape (Adriaenssens et al., 2014).

An explanation on how the method reaches equilibrium is thoroughly presented by Adriaenssens et al. and summarized in the following paragraphs. The explanation is simplified to gain a better understanding of the method. The simplification considers a single node (P0) connected to four elastic bars (a to d). If slacked, the four bars are shorter than the distance between the point P0 and points P1 to P4 respectively. Such, when connecting the bars tension forces Fa to Fd are generated.

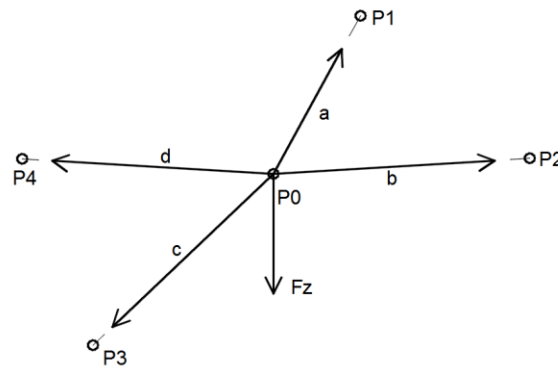


**Figure 22 Single Loaded Point-starting configuration**

To find the equilibrium state and the resulting geometry three relationships are first drawn:

1. Each bar is elongated due to the respective tension force acting on it. The change in length is described by Hook's law of elasticity. The tension in each bar is a function of the axial stiffness of the material (EA), the initial non-stretched length (l0) and the elastic elongation of the bar "e" (the difference between stretched and non-stretched lengths l and l0).

$$F_i = \left[ \frac{EA}{l_0} \cdot e \right] i \quad (\text{Eq 1.1})$$

2. The length of each extended bar is equal to the geometric distance between the nodes to which the bar is connected. For each bar, the length can be described based on the coordinate of the central point and the coordinate of each Pk (where k = 1,2,3,4).

$$l_i = \sqrt{(x_k - x_0)^2 + (y_k - y_0)^2 + (z_k - z_0)^2} \quad (\text{Eq 1.2})$$

3. The forces in the system are in equilibrium (tension forces Fi and self-weight applied to the central node) in each of the three dimensions x, y and z. The forces are decomposed in each direction based on the angles of each bar. For the x direction, the following relation holds:

$$\frac{x_1 - x_0}{l_a} \cdot F_a + \frac{x_2 - x_0}{l_b} \cdot F_b + \frac{x_3 - x_0}{l_c} \cdot F_c + \frac{x_4 - x_0}{l_d} \cdot F_d + F_x = 0 \quad (\text{Eq 1.3})$$

Equation 1.1 relates the internal forces and deformations formulating the *constitutive equations*. Equation 1.2 relates the deformations and translations formulating the *kinematic equations*. Finally, equation 1.3 relates the external and internal loads formulating the *equilibrium equations*. A number of substitutions are conducted to find a solvable system, resulting in the following final equation (for the x direction):

$$\frac{x_1 - x_0}{l_a} \cdot \frac{EA_a}{l_{0,a}} \cdot (l_a - l_{0,a}) + \dots + \frac{x_4 - x_0}{l_d} \cdot \frac{EA_d}{l_{0,d}} \cdot (l_d - l_{0,d}) + F_x = 0 \quad (\text{Eq 1.4})$$

The coordinates of the fixed points and the initial lengths of the elastic bars are known input parameters. To solve the system for the unknown coordinates x0, y0 and z0 requires a nonlinear calculation, as the coordinates are also contained in the final lengths la, lb, lc and ld.

The FDM proposes the linearization of the system, as the obtained system is nonlinear with respect to geometry and material properties. Such, the force densities or 'tension coefficients' are introduced as the ratio between the force in the bar and the stressed length of the bar. The ratios of F/l are declared as new variables qi (force densities) for each bar.

$$FD = \frac{F_i}{l_i} = q_i \quad (\text{Eq 1.5})$$

Rewriting and reordering equation 1.3 leads to a linear system of equations to find the equilibrium position, dependent on the chosen set of force densities qi (equations 1.6 to 1.8). For each such chosen set, a unique position of the unknown point P0 is found. The unique solutions are equivalent to the solutions of the nonlinear equations (1.4).

$$x_0 = \frac{F_x + x_1 \cdot q_a + x_2 \cdot q_b + x_3 \cdot q_c + x_4 \cdot q_d}{q_a + q_b + q_c + q_d} \quad (\text{Eq 1.6})$$

$$y_0 = \frac{F_y + y_1 \cdot q_a + y_2 \cdot q_b + y_3 \cdot q_c + y_4 \cdot q_d}{q_a + q_b + q_c + q_d} \quad (\text{Eq 1.7})$$

$$z_0 = \frac{F_z + z_1 \cdot q_a + z_2 \cdot q_b + z_3 \cdot q_c + z_4 \cdot q_d}{q_a + q_b + q_c + q_d} \quad (\text{Eq 1.8})$$

For a more complex system, as nets with arbitrary topology the mathematical tools need to be extended, introducing matrix formulations combined with graph theory. However, the principle of the “single three-dimensional” point in space, previously explained, still holds. In matrix form, provided given loading conditions and position of fixed points, each set of prescribed force densities leads to exactly one equilibrium shape (Adriaenssen et al., 2014).

The solution of the system leads to the geometry of the form found structure. This geometry is determined without any information about the materials and material properties, purely based on force densities. Such, each individual member can be defined with a different materialization. By imposing values to the axial stiffnesses EA of each element, the corresponding elastic elongations  $\epsilon$  and initial lengths  $l_0$  can be calculated, based on Hooke’s law and the assumed force density. Equation 1.6 mentions the relationship between the force densities Q and the loads F, while equations 1.7 and 1.8 shows the calculation of the initial strain and initial lengths.

$$Q = \frac{F}{L} \quad F = Q \cdot L \quad (\text{Eq 1.6})$$

$$\epsilon = \frac{F}{EA} = \frac{Q \cdot L}{EA} \quad (\text{Eq 1.7})$$

$$L_i = L \cdot (1 - \epsilon) \quad (\text{Eq 1.8})$$

# 3. Starting assumptions for the modelling and analysis

---

## 3.1. Assumptions for the tower

---

Of the multitude of structural systems commonly used for high-rise towers, the core system is chosen as starting and reference point throughout this thesis. A usual concrete class of C45/55 is used. The most important parameter in the stability assessment of a core system is its bending stiffness,  $EI$ .

Concrete structures subjected to bending have a physical nonlinear behavior, as the compressive zone becomes increasingly nonlinear after a certain stress and the tensile zone loses its linearity quickly as the concrete cracks. Further, the E-modulus value of concrete subjected to constant loads decreases in time, due to the so-called creep effect (van Ingen, 2021). The geometrical nonlinearity also plays an important role on the stability of the core structures, as the eccentricity of the gravitational loads relative to the center of gravity of the undeformed cross section increases with the increase in lateral deflection (van Ingen, 2021). Moreover, to account for openings in the core, it is common practice to further reduce the modulus of elasticity by 20-30%, thus resulting in the final fictitious E-value (Terwel et al., 2017).

To account for the above presented nonlinearities, two different fictitious E-modulus values are used in the calculations, depending on the loads on the core.

As bending moments, combined with small axial forces are expected at the top part of the core (the part above the cable-net position), tensile stresses are expected to occur. Usually, in such a case, a 1/3 value of the uncracked modulus of elasticity is a fair assumption, as agreed by both Terwel et al. (2017) and van Ingen (2021). Such, a value of 12000 MPa is imposed, to account for the nonlinearities. Further, this value is reduced by 25% to account for the openings in the core resulting to the final fictitious E-value for the part of the core above the cable-net of 9100 MPa.

Below the position where the cable-net is connected, the core is considered as always in compression, due to the high load imposed by the mountain and the prestress of the cable-net. This statement is further addressed and checked in Chapter 7.1. Such, as tensile forces are not expected to occur under any loading conditions and due to the stabilizing effect of the cable-net, both the physical and geometrical non-linearity is disregarded. Thus, for this part of the core, the value of the modulus of elasticity is only reduced by 25%, resulting in the fictitious E-value 27 000 MPa.

The geometric nonlinearities are accounted by performing nonlinear analyses of the system, that consider the P-delta effect.

Respecting the design considerations presented for high-rise towers, the strength and the stability of the core system will represent the design criterions of the core. The following checks are imposed:

- The strength of the core is sufficient to resist the loads under the worst possible load combination (ULS);
- The applied lateral forces do not cause an overturning moment at the base of the system;
- The system is sufficiently stiff to limit the drift at the top of the core to a value of  $H/500$ ;
- The core does not buckle under the big axial load imposed by the mountain;

The geometry of the tower is imposed as unchangeable parameters, by using conventional dimensions used in practice. A tower with the height of 100 meters and a rectangular in-plane cross-section of 30x30 meters is proposed. The tower uses a core stability system with the thickness of 0.35 meters. The in-plane widths of the core are, on the other hand, changeable variables used for finding the range of slenderness in which the proposed system falls. The 100 meters tall tower is assumed to have 27 floors, with a floor-to-floor height of 3.7 meters. For ease of the economical evaluation, presented in Chapter 8.4, the tower is considered to be fully built of reinforced concrete cast in-situ. Such, the load bearing elements are dimensioned by rules-of-thumb to conventional values based on their span. Appendix A provides an explanation of the structural elements of the tower.

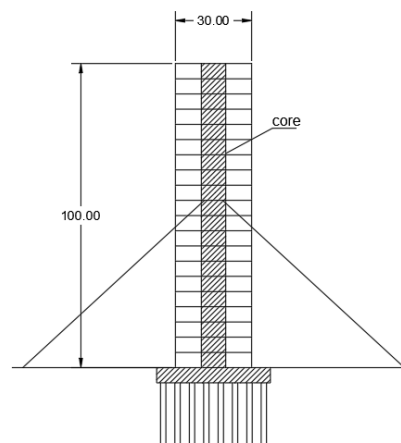


Figure 23 Tower Starting Geometry

### 3.2. Assumptions for the cable elements

The cables used throughout this research are galvanized spiral strand cables. This is a conventional solution for cable-roofs, due to their higher modulus of elasticity and better strength/weight ratio when compared to ropes. Wires with strength of 1570 MPa and a modulus of elasticity of 160 GPa are used. A spinning factor of 1 and a filling factor of 0.65 are assumed to calculate the individual minimum breaking force of the strands, according to the recommendations of EN 12385.

Respecting the design considerations for cable elements, the following checks are imposed:

- In ULS, the applied axial load shall not exceed the design tension resistance.
- In SLS, the stress and strain levels in the component shall not exceed the limiting values.
- Stress ranges from axial load fluctuations and wind and rain induced oscillations shall not exceed the limiting values → not included in the calculations, as it is assumed that the high

permanent load that the mountain imposes on the cable-net induces sufficient stiffness to the cable-net.

### 3.3. Assumptions for the cable-net system

Based on the conventional design classifications and recommendations of cable roofs and cable-net systems presented in Chapter 2.4, a number of preliminary assumptions for the design of the cable-net supporting the mountain are drawn.

The aim is to use a cable-net configuration that is in line with the usually designed cable systems for roof structures. This translates to a set of requirements to be considered when choosing the initial shape of the cable system:

- The cable-net surface should, at all locations, be doubly-curved;
- The average sag or rise of the cables should be in the limits of 4 to 6% of the span;
- The average cable spacing should be of ~ 4 meters;

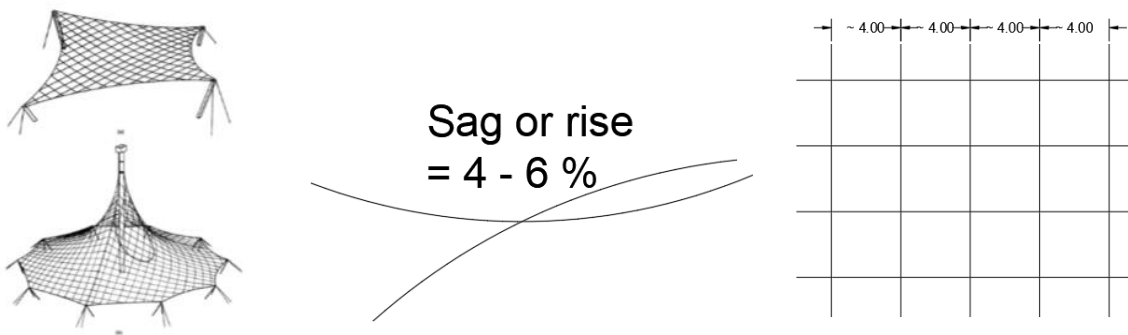


Figure 24 Imposed requirements for the cable-net design

Two suitable typologies are identified as starting points for the cable-net:

- A saddle shaped cable-net with rectangular grid and strong edge cables
- A mast supported cable-net with radial cables

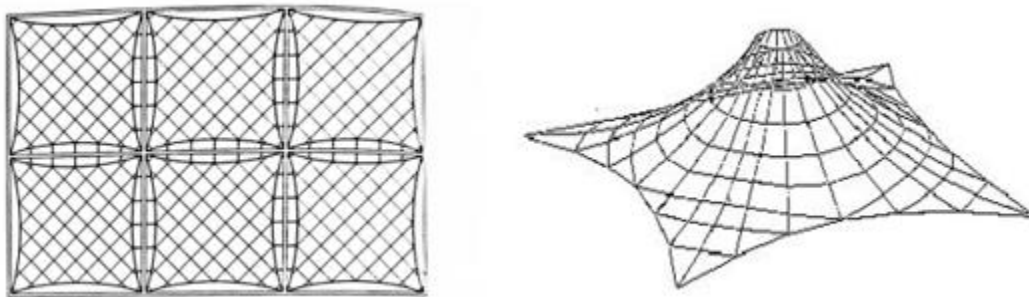


Figure 25 Left: Saddle Shaped cable-net; Right: Mast supported cable-net with radial cables Buchholdt (1999)

The saddle shaped configuration has the advantage of the equal spacing between cables resulting in equal cable lengths. However, due to the large spans between towers, large tensile forces are expected in the “edge cables” connecting the high-rise buildings. Moreover, a preliminary form finding analysis showed that the equilibrium form of the cable-net would be reached when significant sag or rises of the cables are attained, usually larger than 10%.

The most supported configuration, on the other hand has the advantage of a more even distribution of the forces in the cable-net. The preliminary form finding analysis showed satisfactory results in terms of the sag or rise of the net in its equilibrium state, with reachable sags or rise of the cables between 4 to 6%. As a disadvantage, the unequal length of the cables and the irregular grid are expected to pose challenges in the execution process and manufacturing of the connections.

Such, the most supported cable-net with radial cables system is chosen as the configuration of the cable-net. The admissible prestress level in the cable elements is set to a maximum limit of 40%, according to the observations of Gabriel, as described in Chapter 2.4.3.

Lastly, the cable-net shall be analyzed as a discrete system, in which the cables are assumed to form straight lines between the nodes. At these nodes, all loads are applied.

### **3.4. Form finding process**

---

Due to the inclusion of cables and cable-nets in the category of form-active structures, a form finding process is conducted to obtain the initial geometry of the system to be analyzed when the cables or cable-nets are loaded by gravitational load. This process is conducted for the cases of the loaded single cable in the 2D analysis (described in Chapter 5.3) and for the 3D analysis (described in Chapter 6). The form finding is conducted using the Kangaroo 2 plug-in for Grasshopper, as explained in Chapter 2.5.

### **3.5. Parametric model**

---

To create a workflow that allows for multiple iterations and different scenarios based on the configuration of the system, a parametric model is created using the plug-in for Rhino, Grasshopper. Although an initial effort is required to create a logic script, the benefits of building the geometry in Grasshopper for such research are undoubtable. Changing the geometry of the system takes merely minutes, compared to the effort of remodeling the whole system, as it would be the case for any conventional structural analysis software.

Two models are created to model the geometry of the system, each used for different steps of the research:

- A 2D model, representing the tower(s) and a 2D representation of the cable-net (as a single cable on each side of the tower);
- A 3D model, representing the tower(s) and a full 3D representation of the cable-net;

The structural analysis of the Grasshopper models is conducted either using the Karamba plug-in, within the Grasshopper environment or using the Robot Structural Analysis (RSA) FEM software. When using RSA, a plug-in is used to directly export the geometry, boundary conditions and loads/ load combinations from the Grasshopper environment to the RSA software.

Below, a description of each of the Grasshopper scripts, namely the 2D and the 3D script is presented. Appendix K shows a more in-depth description of the scripts, including figures of the relevant components used in Grasshopper, the full list of initial parameters, and figures of the geometry of the system based on these initial parameters.

## 2D Model

### Input

The 2D model allows for the change of multiple relevant input parameters, to provide a fast iterative process for the generation and analysis of the system. The input parameters are divided in:

- Geometry of the system input → height of the core, core dimensions, relative position of the cable, cable angle, cable type, cable diameter;
- Analysis input → Loads on the structure & Boundary Conditions;
- Physical Input → Material Properties;

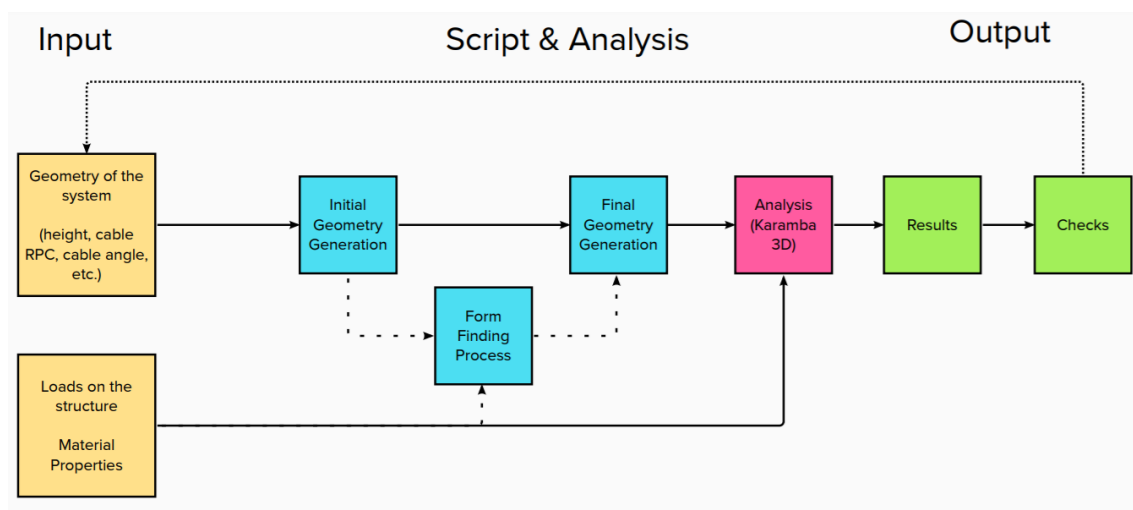


Figure 26 Script Logic 2D model

### Geometry Generation

Based on these input parameters, a large design space is created, which allows the rapid reconfiguration of the system based on the desired initial conditions. Depending on the studied case, the final geometry of the system is either generated directly after the definition of the input parameters or a form finding process precedes the final geometry generation:

- Straight (unloaded) cables work flow: Input Parameters → Initial Geometry Generation → Final Geometry Generation;

- Sagged (loaded) cables work flow: Input Parameters → Initial Geometry Generation → Form Finding of the Shape of the Cable → Curved Cable(s) Generation → Final Geometry Generation;

### Analysis

As the analysis is conducted in Karamba3D, using a linear approach, within the Grasshopper environment, all the defined elements are directly connected to the analysis component and attributed cross sectional and material properties accordingly. The loads on the system, as explained in Chapter 3.6, are defined and added to the analysis component.

### Results & Checks

The linear analysis provides results in terms of the displacement at the top of the core or at the connection of the cable position, tension forces in the cable, axial and bending moment forces on the core and the respective utilizations of the cross sections. These results are used when studying the influence on the different parameters on the design of the system in later chapters of this research. The script allows for a rapid visualization and check of these results, making the iterations of changing parameters a fast process.

### 3D Model

#### Input parameters

Similar, 3D model also allows for the change of the multiple input parameters. Additional to the previous model, as the whole cable net is now represented, the spacing between cable elements to form the geometry of the net and the spacing between towers are added as a parameter.

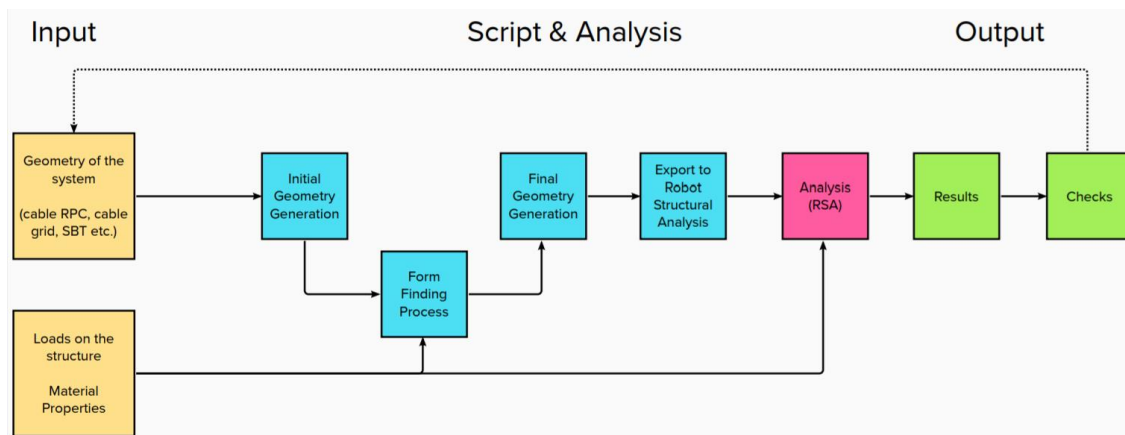


Figure 27 Script Logic 3D Model

#### Geometry Generation

Based on the input parameters, the initial geometry of the system is created. A form finding process is conducted to obtain the geometry of the cable-net, respecting the set requirements. Further, based on the initial geometry and the form found geometry, the final geometry is obtained:

- Input parameters → Initial Geometry Generation → Form Finding of the Shape of the Cable-net → Final Geometry Generation;

The script also outputs relevant information on the properties of the cable-net, such as the total amount of steel used, the total weight of the mountain or the total weight of the core structure.

### Export to RSA & Analysis

As the analysis of the system is, in the case of the 3D study, performed in Robot Structural Analysis, the geometry is exported using the plug-in for Rhino, Geometry Gym. This allows for a reasonably rapid interaction between the Grasshopper environment and the RSA software.

All the sectional properties of the elements, loading cases and combinations, and boundary conditions are defined within the Grasshopper environment, and exported to Robot together with the geometry. The prestress of each cable element is computed after the form finding process and attributed to the exported cable elements. Such, RSA directly runs the analysis after the information is transferred, without any additional steps being performed.

The loads acting on the net are assumed to act at the intersection nodes of the cable elements, as explained in Chapter 3.3. Using Karamba's component "Disassemble mesh load", the tributary area corresponding to each of the nodes is calculated, directly attributing the respective mountain load force to each node. This further allows for the rapid reconfiguration of the system, as no manual work in computing the tributary area must be conducted.

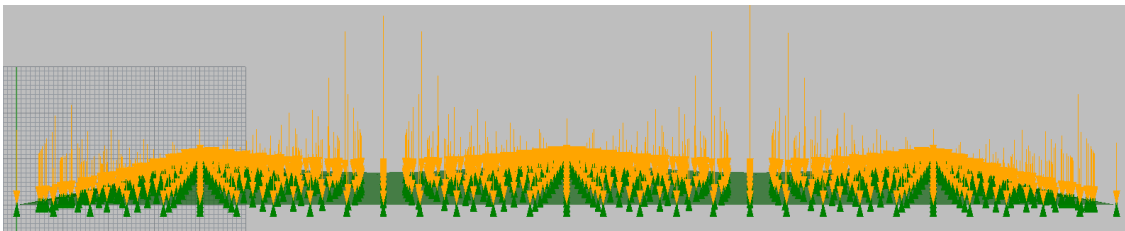


Figure 28 Mountain Loads on each node according to the tributary area

### Results & Checks

The relevant results in terms of top deflection, cable-net deflection and forces on the core are obtained from the Robot Structural Analysis program, and checked using a spreadsheet. This leads to a slower iterative process than in the 2D case, as, if input parameters need to be changed, the whole export process needs to be reiterated. This is further addressed in Chapter 10, when the proposed methodology is discussed.

## 3.6. Loads on the structure

---

The loads acting on the structure are calculated according to Eurocode 1: Actions on structures and the corresponding Dutch National Annexes, and are further detailed in Appendix 3. A summary of the loads is presented below. The loads are defined in the two main categories of:

- Permanent Loads: self-weight of elements (tower system → core & flooring system), cable-net (cable self-weight & mountain load);
- Variable Loads: lateral loads (wind load on the tower and on the cable-net), live loads according to EN 1990-1-1 (live loads on the tower, live loads on the cable-net);

According to NEN-EN 1990-1-1, every structure needs to comply with the two limit states, related to the strength and usability of the structure. The ultimate limit state (ULS) is used to check the structural safety, while the serviceability limit state (SLS) is used to check usability. The combination of the design values of permanent and variable loads with adequate partial factor coefficients leads to the values used in each of the limit states. Further, the Rotterdam Mountain project is assumed to fall in the consequence class 3, according to NEN-EN 1990-1-1, due to a major impact on loss of life and major economic implications. This further translates to an increase in the partial safety factors with a  $K_{FI}$  coefficient of 1.1.

The load factors in ULS are considered according to two design situations, as Table 2 presents, according to NEN-EN 1990-1-1 NB Table NB. 5, for consequence class 3. The load combinations are considered according to equation 3.1 and 3.2 in ultimate limit state (obtained from equation 6.10a and 6.10b in NEN-EN 1990-1-1) and according to equation 3.3 in serviceability limit state (obtained equation 6.14b in NEN-EN 1990-1-1).

**Table 2 Design situations according to NEN-EN 1990-1-1**

Design situation	Permanent loads unfavourable	Permanent loads favourable	Variable loads leading	Other
1	1.5	0.9	-	1.65
2	1.3	0.9	1.65	1.65

$$\sum_j \gamma_{G,j} \cdot G_{k,j} + \gamma_P \cdot P + \gamma_{Q,1} \cdot \psi_{0,1} \cdot Q_{k,1} + \sum_i \gamma_{Q,i} \cdot \psi_{0,i} \cdot Q_{k,i} \quad (\text{Eq 3.1})$$

$$\sum_j \xi_j \cdot \gamma_{G,j} \cdot G_{k,j} + \gamma_P \cdot P + \gamma_{Q,1} \cdot Q_{k,1} + \sum_i \gamma_{Q,i} \cdot \psi_{0,i} \cdot Q_{k,i} \quad (\text{Eq 3.2})$$

$$\sum_j G_{k,j} + P + Q_{k,1} + \sum_i \psi_{0,i} \cdot Q_{k,i} \quad (\text{Eq 3.3})$$

To check the serviceability limit state, the following combinations are used:

1. SLS-1: Permanent Loads + Wind Loads + Live loads (reduced)
2. SLS-2: Permanent Loads + Live Loads;

$$1 \cdot G_{k,j} (\text{permanent}) + 1 \cdot W (\text{wind}) + 0.5 \cdot LL (\text{live}) \quad (\text{SLS-1})$$

$$1 \cdot G_{k,j} (\text{permanent}) + 0 \cdot W (\text{wind}) + 1 \cdot LL (\text{live}) \quad (\text{SLS-2})$$

To check the ultimate limit state, the following combinations are used:

1. ULS-1: Unfavorable Permanent Loads Design Situation 1
2. ULS-2: Unfavorable Permanent Loads Design Situation 1 + Live Loads (reduced)
3. ULS-3: Unfavorable Permanent Loads Design Situation 2 + Live Loads Leading
4. ULS-4: Unfavorable Permanent Loads Design Situation 2 + Wind Leading + Live Loads (reduced)

$$1.5 \cdot G_{k,j}(\text{permanent}) + 0 \cdot W(\text{wind}) \quad (\text{ULS-1})$$

$$1.5 \cdot G_{k,j}(\text{permanent}) + 1.65 \cdot 0.5 \cdot LL(\text{live}) + 0 \cdot W(\text{wind}) \quad (\text{ULS-2})$$

$$1.3 \cdot G_{k,j}(\text{permanent}) + 1.65 \cdot LL(\text{live}) + 0 \cdot W(\text{wind}) \quad (\text{ULS-3})$$

$$1.3 \cdot G_{k,j}(\text{permanent}) + 1.65 \cdot W(\text{wind}) + 1.65 \cdot 0.5 \cdot LL(\text{live}) \quad (\text{ULS-4})$$

For ULS a partial factor of 1.3 or 1.5 is used for the permanent loads, depending on the design situation, and a partial factor of 1.65 is used for the variable loads. When the live load is not considered the leading variable load, it is reduced by the  $\psi$  factor of 0.5, according to the recommendations of NEN-EN 1990 -1-1 for office areas. When the wind load is not considered the leading variable load, it is neglected (using the  $\psi$  factor of 0), according to the NEN-EN 1990 -1-1 recommendations for wind load.

For SLS a partial factor of 1 is used for permanent loads. Similar, when the live load is not considered the leading variable load, the  $\psi$  factor of 0.5 is used.

### 3.6.1. Permanent Loads

Self-weight

The self-weight of the core and cable elements is automatically calculated by the analysis software's used. Additionally, the permanent load imposed by the floors of the tower is calculated using the tributary area around the core, as presented in Appendix B. For ease of an economical evaluation (Chapter 8.4), the tower is considered to be fully considered of in-situ cast reinforced concrete, as previously explained in the assumptions in Chapter 3. A normal finishing detail for floor system is used, with floor tiles, cement screed and sound insulation mineral wool.

**Table 3 Permanent load of floor system due to finishing detail**

Layer nr.	Layer Name	Thickness [mm]	Technical weight [kN/m <sup>3</sup> ]	Load value [kN/m <sup>2</sup> ]
1	floor tiles + adhesive layer	13	24	0.3
2	cement screed	50	21	1.1
3	concrete slab	200	25	5
4	sound insulation mineral wool	30	15	0.4
Total				6.8

The "Mountain"

The permanent load of the mountain is composed of a green roof system and a decking system spanning between the cables. The green roofs are commonly classified in two groups: extensive and intensive systems, based on the depth of the substrate layer, cost, irrigation and maintenance. The intensive systems are designed with a deeper substrate layer, of more than 150 mm to allow for a

wider variety of plants and recreational possibilities. The extensive system, although significantly lighter and less costly, can utilize only limited types of plants, as grasses or mosses. (Cascone, 2019)

Due to the ambition of the Rotterdam Dreamers of creating a usable mountain space, with recreational spaces and significant amount of vegetation, an intensive green roof is chosen. The usual weight of such a system is approximately 200 kg/m<sup>2</sup>. The SIG Design Technology Company (2020) proposes an intensive system with the weight of 175 kg/m<sup>2</sup> (~1.7 kN/m<sup>2</sup>), which is used throughout this research.

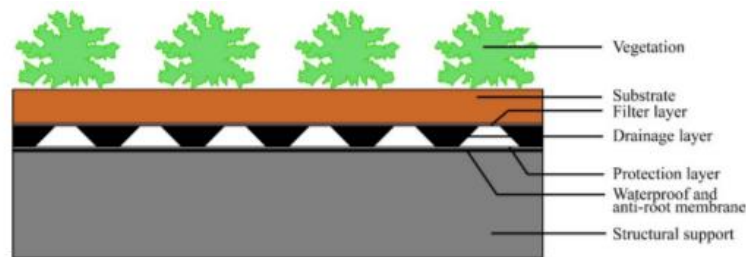


**Figure 29 Green Roof System configuration (Cascone, 2019)**

Krishna (1978) mentions that the decking of the cable roofs can be erected from numerous materials, from corrugated sheets of steel or aluminum to concrete or timber. The choice of the decking depends on the spacing between cables and functionality of the roof. Buchholdt (1999) adds that the choice of the cladding material will have significant impact on the form of the structure. Heavy roof claddings, as precast or sprayed concrete result in much stiffer structures than in the case of lightweight metal sheeting. Moreover, in the case of heavyweight structures, dynamic problems are unlikely to appear. To support the (already heavy) green roof system and to prevent dynamic issues from appearing, a concrete deck system, spanning an average of 4 meters between cable elements, with the self-weight of 2kN/m<sup>2</sup> is chosen, resulting in a total permanent load of 3.7 kN/m<sup>2</sup> together with the green roof system.

### **3.6.2. Variable Loads**

#### **Live Loads**

The live loads acting on the core are defined in accordance to the EN 1991-1-1 recommendation for variable loads for office areas-floors, with a value of 2.5 kN/m<sup>2</sup>.

The same value of the live loads is used for the mountain area. This assumption is made based on the large area of the mountain, thus excluding it from the category C of Congestion areas. A comparison could be made to category F, of light traffic areas, which specifies a load of 2 kN/m<sup>2</sup>. However, to maintain a safe assumption, 2.5 kN/m<sup>2</sup> is used.

#### **Wind Load**

The imposed wind loads are calculated according to Eurocode 1: Actions on structures - Part 1-4: General Actions: Wind Actions (EN 1991-1-4) and the Dutch National Annex NEN-EN-1991-1-4+A1+C2. Appendix B presents more information on the wind load, as only the basis of the calculations is outlined below.

### Wind Load on the tower

According to Soons et al. (2014), for buildings with a regular in-plan shape a simplified version of the code can be used for design purposes, to obtain the horizontal wind load as a function of the height of the structure. The proposed formula is presented below in equation 3.1:

$$F_i = c_{scd} \cdot c_f \cdot q_p(z_e) \cdot A_{ref} \quad (\text{Eq 3.1})$$

In equation 3.1  $F_i$  is the value of the wind force on the structure or structural component expressed in kN. The factor  $c_{scd}$  is the structural factor and, in this case is assumed to have a value of 1, which is a conservative approximation according to Vrouwenvelder et al. (2005). The factor  $c_f$  is the force coefficient for the structure and  $q_p(z_e)$  is the peak velocity pressure at the reference height.

The wind load acts as pressure on one side of the tower, and as suction on the other side of the tower, depending on its direction, according to the zone distribution of wind pressure for rectangular buildings with vertical facades. Based on the zone distribution, the force coefficient factor  $c_f$  can be obtained, based on the ratio of height to width of the tower, as presented in Appendix B. A final  $c_f$  coefficient with the value of +1.42 is assumed for the windward side, accounting for both pressure and suction.

The peak velocity pressure  $q_p(z_e)$  is obtained using Figure 108 and Table 40, found in Appendix B, as presented in the Dutch National Annex of NEN-EN 1991-1-4. Figure 108 presents the three wind areas in the Netherlands - as the Rotterdam Mountain is located in Rotterdam, the wind area II, for an urbanized area is chosen.

Using equation 3.1, instead of using the whole façade area as reference area, but using the width of the tower instead, the wind load on the core can be obtained as a distributed force along the height.

NEN-EN 1991-1-4 explains that a reduction in the wind force can be assumed for buildings with a height larger than twice the width as shown in Figure 30. A linear distribution should be assumed between the reference height  $z_e = b = 30$  meters and  $z_e = h - b = 70$  meters. However, as Karamba3D does not allow for trapezoidal load definition, a uniform distributed load with the value of 43.8 kN/m is assumed up to half of the height of the tower, and 62.9 kN/m above the half of the height, shown in Figure 31. This wind load distribution is assumed for all analyzed 2D cases (Chapter 4, 5).

**Table 4 Wind values as distributed load on tower**

Reference height [m]	$c_{scd}$	$c_f$	Peak Velocity Pressure [kN/m <sup>2</sup> ]	Width of the tower [m]	Wind Value as distributed load [kN/m]
30	1	1.42	1.03	30	43.8
100	1	1.42	1.48	30	62.9

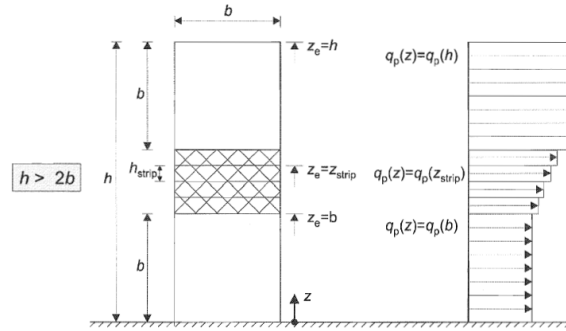


Figure 30 Wind Load as a function of height (EN 1991-1-4)

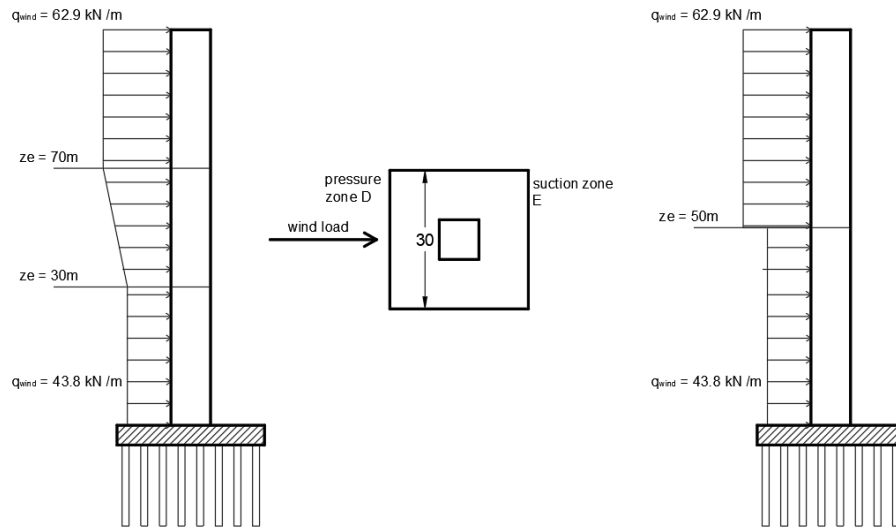


Figure 31 Wind Distribution for the chosen tower dimensions-2D cases; Left → actual distribution for 2D analysis  
*Wind load on the cable-net (3D case)*

It is difficult to predict the exact wind loads that will act on the mountain. Usually, a wind tunnel test would be advised in such a case. However, due to the lack of possibility to perform such a test, assumptions are made. Such, the shape of the cable-net is compared to a double pitched inclined roof, and the wind loads are calculated accordingly. As the assumptions of the previous chapter mention, an average sag or rise of the cables of 4-6% is imposed. This translates to an average angle of the cable net of approximately 5 degrees (and, consequently, simplified to a double pitched inclined roof with the angle of 5 degrees).

The wind load value is calculated according to the zones defined by EN 1991-1-4 (F, G, H, I and J), as seen in Figure 32. The pressure and suction wind forces acting on the mountain are assumed to act normal to its surface. Due to the green roof, the occurring friction forces need to be added, leading to the total wind force obtained by vectorial summation. A roughness coefficient of 0.02 is assumed for a rough surface, based on the EN 1991-1-4 guidelines.

The wind load is calculated for each zone, based on the  $e$  value, corresponding in the studied case to the spacing between towers. Moreover, the wind load is influenced by the reference height, which is a function of the relative position of the cable-net. As these values vary with the multitude of

studied cases (different spacings and different relative positions), the wind value changes its value for each iteration. Such, a script is developed in the Grasshopper environment to automatically calculate the wind pressure, suction and friction for each zone, for each iteration.

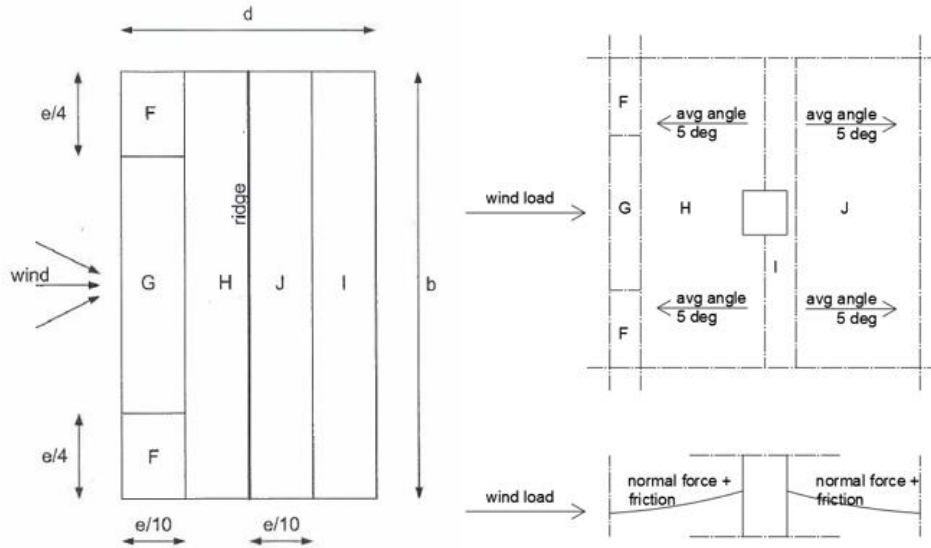


**Figure 32 Wind on Roof (EN 1991-1-4) (Left); Wind Roof on Cable-net (Right)**

The peak velocity pressure  $q_p(z_e)$  is no longer obtained from Figure 108 and Table 40, but calculated according to NEN-EN 1991-1-4 to account for the orography and roughness of the mountain surface. To obtain its value, few factors need to be determined.

First, the basic wind speed  $v_b$  is calculated as the scaled fundamental basic wind speed  $v_{b,0}$ , with the value obtained from the Dutch National Annex. For wind area II, the fundamental basic wind speed has a value of 27 m/s. The  $c_{dir}$  and  $c_{season}$  have a recommended value of 1.0.

$$v_b = c_{dir} \cdot c_{season} \cdot v_{b,0} \quad (\text{Eq 3.3})$$

Then, the mean wind velocity is calculated for the reference height, scaling the basic wind speed with the factors  $c_r(z)$  - to account for the surface roughness and  $c_0(z)$  - to account for the surface orography. The  $z_0 = 0.5$  meters,  $z_{min} = 7$  meters,  $z_{max} = 200$  meters and  $z_{0,II} = 0.2$  meters are chosen according to the Dutch National Annex recommendation for a terrain category III (built-up area). The  $s$  and  $\Phi$  factors in equation 3.7 are dependent on the geometry of the inclined surface.

$$v_m(z) = c_r(z) \cdot c_0(z) \cdot v_b \quad (\text{Eq 3.4})$$

$$c_r(z) = k_r \cdot \ln\left(\frac{z}{z_0}\right), z_{min} \leq z \leq z_{max} \quad (\text{Eq 3.5})$$

$$c_r(z) = c_r(z_{min}), z \leq z_{min}$$

$$k_r = 0.19 \cdot \left( \frac{z_0}{z_{0,II}} \right)^{0.07} \quad (\text{Eq 3.6})$$

$$c_0(z) = 1 + 2 \cdot s \cdot \phi \quad (\text{Eq 3.6})$$

Further, the turbulence intensity  $I_v(z)$  is calculated for the reference height and finally the peak velocity pressure  $q_p(z)$  is obtained according to the NEN-EN 1991-1-4 formulae. The density of air is assumed to have the recommended value of  $\rho = 1.25 \text{ kg/m}^3$ .

$$I_v(z) = \frac{k_f}{c_0(z) \cdot \ln\left(\frac{z}{z_0}\right)}, z_{min} \leq z \leq z_{max} \quad (\text{Eq 3.7})$$

$$I_v(z) = I_v(z_{min}), z \leq z_{min}$$

$$q_p(z) = (1 + 7 \cdot I_v(z)) \cdot \frac{1}{2} \cdot \rho \cdot v_m(z)^2 \quad (\text{Eq 3.8})$$

To exemplify, the results for the calculation of the wind force on the mountain for a 50 meters spacing case, with the cable-net placed at half of the tower's height, are presented below. The used mean wind velocity and turbulence intensity are calculated using eq 3.7. and 3.4, accounting for the terrain roughness and orography.

**Table 5 Peak velocity pressure calculation.**

Reference height z [m]	Turbulence intensity $I_v z$ [-]	Air density $\rho$ [kg/m <sup>3</sup> ]	Mean wind velocity $v_m(z)$ [m/s]	Peak velocity pressure $q_p(z)$ [kN/m <sup>2</sup> ]
50	0.194	1.25	31.1	1.42

The final calculated peak velocity pressure  $q_p(z=50 \text{ meters})$  has a value of 1.42 kN/m<sup>2</sup>. As expected, this is higher than the recommended value for simplified calculations of  $q_p(z=50 \text{ meters})$  of 1.21 kN/m<sup>2</sup>, found in Table 40, as the orography and roughness coefficients are included in the wind estimations. Further, using the calculated peak wind velocity, the wind pressure and suction acting normal on the mountains surface is distributed to each wind zone (F, G, H, I and J) accordingly, using the  $c_f$  coefficients recommended by EN 1991-1-4 (Table 8). Additionally, the friction force acting parallel to the wind direction is, as explained, calculated with a friction coefficient of 0.02.

**Table 6 Wind forces normal to the mountain surface**

Reference height z [m]	$c_s c_d$ [-]	Peak velocity pressure [kN/m <sup>2</sup> ]	Zone F $c_{f,i}$	Zone G $c_{f,g}$	Zone H $c_{f,h}$	Zone I $c_{f,i}$
50	1	1.42	-1.7	-1.2	-0.6	-0.6

**Table 7 Friction forces on the mountain surface, parallel to the wind direction**

Reference height z [m]	Friction coefficient $c_{fr}$ [-]	Peak velocity pressure [kN/m <sup>2</sup> ]	Friction force on all zones [kN/m <sup>2</sup> ]
50	0.02	1.42	0.03

**Wind load on the tower + cable-net (3D Case)**

Due to the cover that the mountain structure offers, there is no wind load below the level of the connection of the cable-net. However, due to the orography of the mountain, the wind that would theoretically act on the bottom of the tower is considered to act above the position of the cable connection. In this way, a point load, which is a function of the cable-net dimensions and the relative position of the cable-net (and the corresponding peak velocity pressure at that height) is considered as horizontal load on the tower, to account for the wind that would theoretically act below the mountain. In Appendix B the calculation of the equivalent point load wind value acting on the tower is presented. Similar to the wind load acting on the net, this equivalent point load is calculated automatically in the parametric script.

Such, the total wind force on the system is composed of the wind load on the tower above the cable-net, the normal pressure/ suction imposed on the cable system, the friction imposed on the cable system, and the equivalent point load acting at the position of the cable connection, as shown in Figure 33. This is the wind load distribution assumed for the studied 3D cases (Chapter 6, 7).

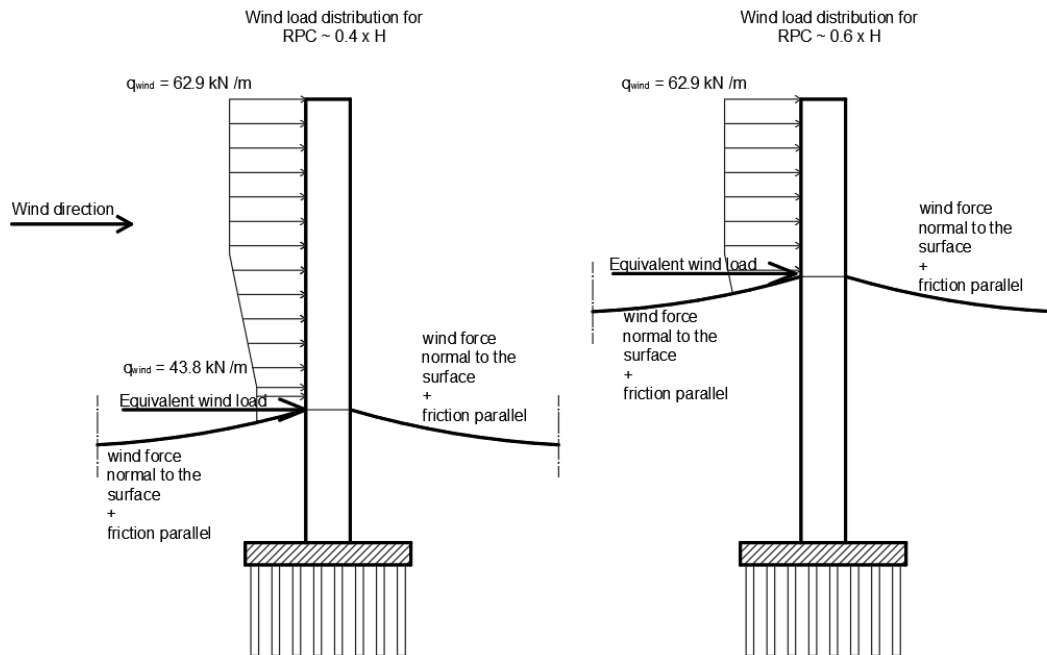


**Figure 33 Wind distribution for actual configuration for the 3D model**

### 3.6.3. Summary of the loads on the structure

#### Tower

The gravitational loads on the tower are imposed as a uniformly distributed load on the tower's height, by calculating the total vertical load and dividing it with the height of the tower. Based on the load combination, the gravitational load has different values. The full calculation is presented in Appendix B, and outlined in the table below. The wind load is also factored accordingly to each combination case, and expressed as a horizontal line load.

**Table 8 Load values on tower according to the load combinations**

	SLS 1	SLS 2	ULS 1	ULS 2	ULS 3	ULS 4
DL + LL equivalent line load [kN/m]	519	564	620	745	788	662
Wind Load top [kN/m]	62.9	-	-	-	-	103.8
Wind Load bottom [kN/m]	43.8	-	-	-	-	72.3

#### Cable-net

For the "mountain" surface, the live loads, dead loads and wind loads are imposed as surface area loads, and further distributed to the joints of the cable-net based on their surrounding tributary area. This process is done automatically in the parametric script.

**Table 9 Load values on the cable-net according to the load combinations**

	SLS 1	SLS 2	ULS 1	ULS 2	ULS 3	ULS 4
Dead Load [kN/m <sup>2</sup> ]	3.7	3.7	4.9	4.9	4.4	4.4
Live Load [kN/m <sup>2</sup> ]	1.75	2.5	1.75	2.6	3.7	2.6
Wind Load pressure / suction	Calculated for each zone	-	-	-	-	Calculated for each zone

### 3.7. Analysis assumptions for the cable-net

A general method of the analysis of cable systems is based on the tension coefficient approach that leads to a stiffness-matrix solution. Certain assumptions need to be imposed, in order to simplify the computational work, as follows (Krishna, 1978):

- The cable is treated as completely flexible, without being able to carry any bending moment;
- The cable is treated as a tension-only element, without being able to take any compressive force;

- The cladding does not contribute to the stiffness of the cable-structure; although this assumption is not fully correct, it can be justified based on the following grounds by the fact that the error caused is on the safe side, in the worst case leading to over-dimensioning;
- The intersection between more cables is treated as a joint;
- The cable elements lie along straight lines between joints; this means that all loads are acting at the intersection nodes, considering the system as a discrete one;

The numerical procedure used for the analysis is The Newton-Raphson Method. The computations in this method are based on *instantaneous* stiffnesses of the structure, which are derived at each iterative cycle.

### 3.8. Geometrical nonlinear analysis - Robot Structural Analysis

The geometrical non-linear analysis of the cable-net is conducted using Robot Structural Analysis, using the Newton-Raphson Method. In this chapter a description of the used models is given. The same analysis parameters are used for all nonlinearly analyzed models through this research.

For the modelling of the cables forming the cable-net two nodes cable elements are used. The cable element theory in Robot is based on the general theory of cables with a small value of cable sag. Such, the cable rigidity is defined as a function of the cable tension rigidity, cable tension, cable support displacement and loading (RSA User’s Guide, 2020). The cables are considered as tension-only elements, such that no shear or bending moments can occur. In all models a first “assembly load case” is included, case in which the initial tension forces are specified, by either inputting:

- The initial cable stress;
- The initial tension force;
- The initial cable length;
- The initial relative cable shortening/ elongation;

In all analyzed model, the initial tension (prestress force) is defined using an initial relative cable shortening.

For the modelling of the tower (core), two nodes line elements are used. The line elements are attributed hollow cross-sectional properties, representing the actual in-plane dimensions of the core system.

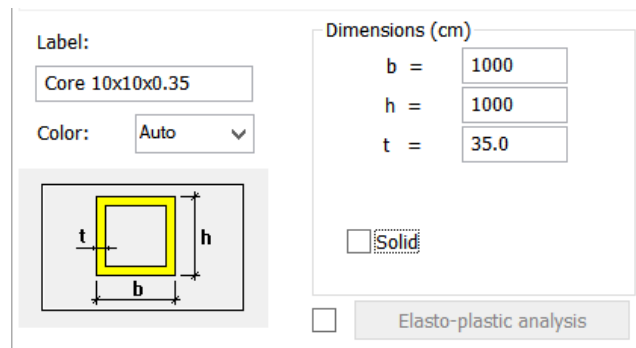


Figure 34 Core definition-RSA

For all models an iterative scheme is used. The characteristics of the iterative scheme are presented in Table 10. The load is applied using the force control method, in step sizes of 0.05, resulting in a total of 20 steps. Both force and displacement convergence norms are used, with a convergence tolerance of 0.0001. The “large displacements” non-linear analysis ensures that the changes in stiffness due to the deformed shaped are accounted for. Further, the “P-delta” effect considers the additional lateral rigidity and stresses resulting from the deformation of the structure is accounted for.

**Table 10 Properties of the iterative scheme**

Method	Geometric Nonlinearity	Load increment	Maximum nr. of iterations	Convergence norms	Convergence tolerance
Newton-Raphson	P-Delta	0.05 (20 steps)	40	Force	0.0001
	Large Displacements			Displacement	0.0001

### ***Trial models***

To check the validity of the approach two trial models were created and analyzed. The trial models aim to replicate conventional cable-net configurations that were studied by different researchers when proposing analysis methods for cable structures. Based on a comparison between the obtained results in RSA and the results obtained by the researchers, the proposed approach can be deemed accurate. Appendix C shows the comparison between the results of the analysis performed by Thai et al. (2010), Lewis (1984) and the results of the analysis performed with RSA.

A divergence between the results obtained from Robot and the studies between 0.26% to 2.99% is observed. These divergences are considered to fall in acceptable limits, confirming that the nonlinear analysis is correct and can be used for the analysis of the full cable-net.

## **Phase 2: Exploration**

The exploration phase is, according to the proposed methodology, divided into four steps. The first two steps propose a 2D simplification of the cable-net, by using equivalent single cables, while step 3 and 4 propose a full 3D representation of the cable-net. The first two steps refer to a core stabilized by cables connected to the ground. Step 3 and 4 refer to multiple cores in a rectangular grid which are interconnected by the cable-net, stabilizing each other.

For the first three steps the top deflection is the comparison parameter, and the aim is to find a range of slenderness under which the system falls. These can be regarded as steps that develop the understanding of the system, by exploring the influence of prestress, form density, mountain load and relevant cable-net parameters. Finally, step 4 aims to provide a more comprehensive representation of the system, as the strength of the core is also considered.

For the 2D cases a linear analysis is considered sufficient, performed with the Karamba software. This justification is further presented in Appendix D, where a comparison between linear and non-linear results for the 2D case is provided. For the 3D cases a non-linear analysis is conducted, using Robot Structural Analysis.

The four steps of the Exploration phaser are:

- Step 1: a parametric study of the different parameters relevant to the design of the system, with the top deflection as comparison parameter.
- Step 2: a 2D study of a single tower when the cables are connected to the ground on each side of the tower, with the top deflection as comparison parameter.
- Step 3: a 3D study of multiple towers placed in an infinite rectangular grid interconnected by a cable-net, with the top deflection as comparison parameter.
- Step 4: a 3D study of multiple towers placed in an infinite rectangular grid interconnected by a cable-net, studying the overall behavior of the system.

## 4. Parametric study of relevant parameters

---

In the first step, a parametric study of three relevant parameters is performed. These parameters are the cable stiffness, the relative position of the cable net and the cable angle. The parametric study is conducted on the most simplified case - 2D with unprestressed and unloaded cables. As no prestress is added, only one cable, on the windward side of the tower adds stiffness to the system. The cable on the leeward side, due to the horizontal deflection of the tower, is not in tension and goes slack, thus having no influence on the stability of the tower. The procedure used in this step is presented in Appendix E.

The parametric study further allows for the reduction of the changeable inputs by setting certain parameters to constant values, or restricting the variability of the parameters by imposing minimum and maximum boundaries for them. To judge the relative influence of the different parameters, for this step, the displacement at the top of the structure is considered as the comparison criterion. The top deflection of the proposed cable + core system is further compared to the top deflection of a simple core system. Under the applied lateral loads, a 100 meters high simple core system with the proposed dimensions has a top deflection of 302 mm. Below, the properties of the model are explained:

- The core has unchangeable dimensions of 10 x 10 x 0.35 meters;
- The core is considered fixed to the foundation;
- The cables are considered pinned to their foundation and to their connection to the core;
- The loads on the system are described in Chapter 3.6 → as the top deflection is the comparison parameters, only the load combination SLS-1 is considered;
- The reduced core E-modulus is considered over the height of the core, as the compressive stresses due to the axial load of the mountain are not considered;

The ranges for which the influence of the changeable relevant parameters is studied are:

- The cable stiffness → by ranging the cable diameter between 100 and 500 mm
- The relative position of the cable-net (abbreviated as RPC) → by ranging the relative position between 0.3 x H and 0.75 x H;
- The angle of the cable connection → by ranging the connection angle between 35 and 75 degrees;

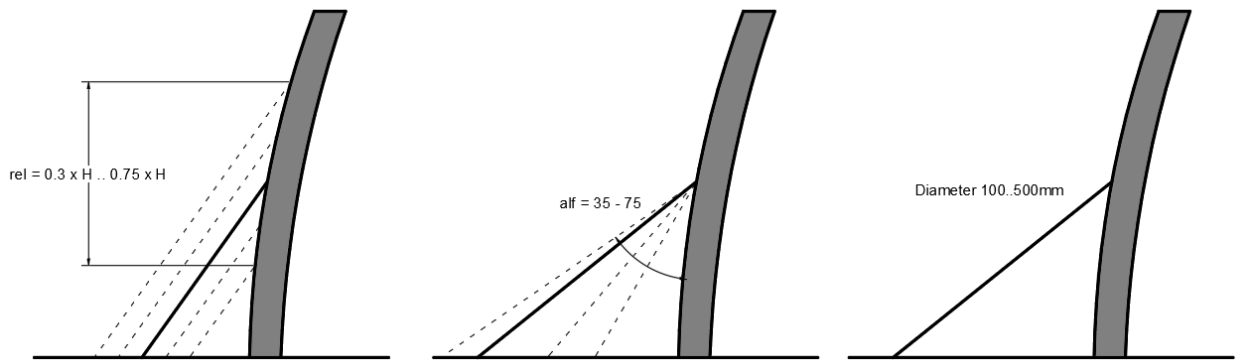


Figure 35 Changeable Parameters for Parametric Model

#### 4.1. Influence of the cable stiffness

It is sensible that when the cable stiffness increases, so does its influence on the overall stiffness of the system. In other words, a larger cable or network of cables will increase the stiffness of the system, reducing the top deflection of the core.

To check the relative influence of the cable stiffness, the two other parameters of the study are imposed fixed values. Such, the presented results are obtained by using:

- An angle of the cable connection between the cable and the tower of 55 degrees;
- A relative cable position of  $0.5 \times H$ ;

By maintaining the set constant modulus of elasticity of  $E = 160 \text{ GPa}$  for the spiral strands, the cable diameter is increased up to five times (from 100 mm to 500 mm). This translates to an increase in stiffness of 25 times. The influence of the cable stiffness rapidly increases up to  $\sim 300 \text{ mm}$ , after which the graph slightly flattens. As expected, for low stiffnesses of the cable, little influence is observed on the top displacement.

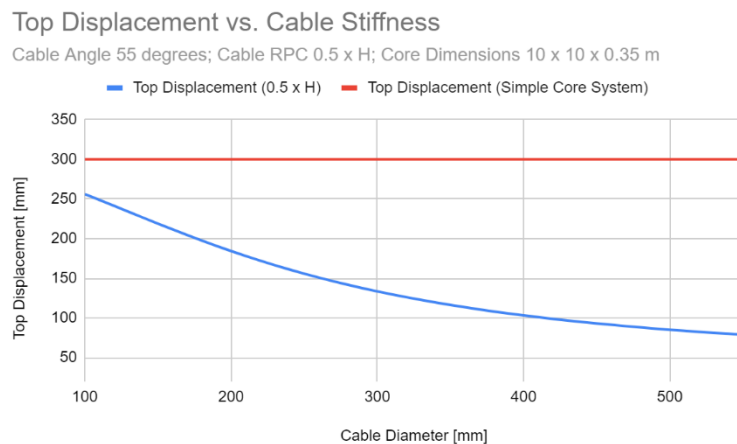


Figure 36 Top Displacement and Cable Stiffness

## 4.2. Influence of the relative position of the cable-net

---

It is also sensible that when the relative position of the connection of the cable-net to the core increases, so does its influence on the overall stability of the system. In other words, the higher the cable is connected, the bigger the reduction of the top deflection of the core.

To check the relative influence of the position of the cable-net, the two other parameters of the study are imposed fixed values. Such, the presented results are obtained by using:

- An angle of the cable connection between the cable and the tower of 55 degrees;
- A cable diameter of 300 millimeters;

The cable relative position was increased gradually from  $0.3 \times H$  to  $0.75 \times H$ .

A clear influence on the top deflection is visible as the higher the connection, the lower the deflection at the top of the core. Percentage wise, when compared to the simple core system, this translates to a reduction of 15-20% when the cable is connected as low as  $0.3 \times H$ , and up to 70-80 % when the cable is connected as high as  $0.75 \times H$ .

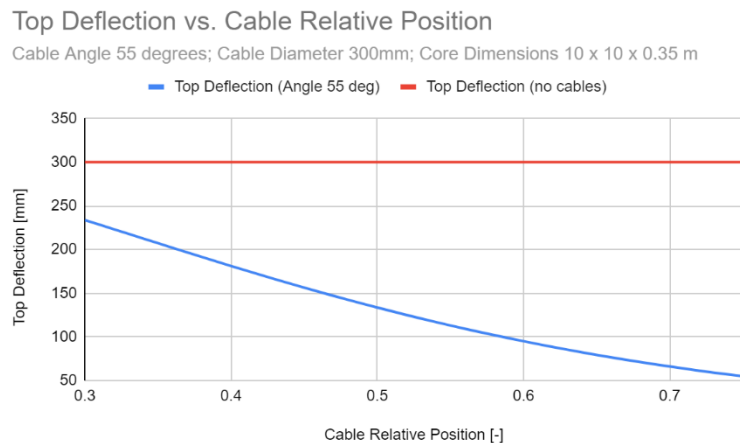


Figure 37 Top Deflection and Cable Relative Position

## 4.3. Influence of the cable angle

---

The influence of the cable angle is less sensible as the for the previously studied parameters. Such, a further study which analyzes the change in the angle from 35 degrees up to 75 the degrees is conducted.

To check the relative influence of the angle, the two other parameters of the study are imposed fixed values. Such, the presented results are obtained by using:

- A relative cable position of  $0.5 \times H$ ;
- A cable diameter of 300 millimeters;

The graphs show an optimum cable angle of  $\sim 55$  degrees. At this angle, the influence of the cable on the overall stiffness of the system is largest. Although an optimum is found, the relative difference in the reduction of the top deflection for different angle cases is not large  $\rightarrow$  a maximum

relative difference of up to 18% can be observed between an angle of 35 (or 75) degrees and the found optimum of 55 degrees.

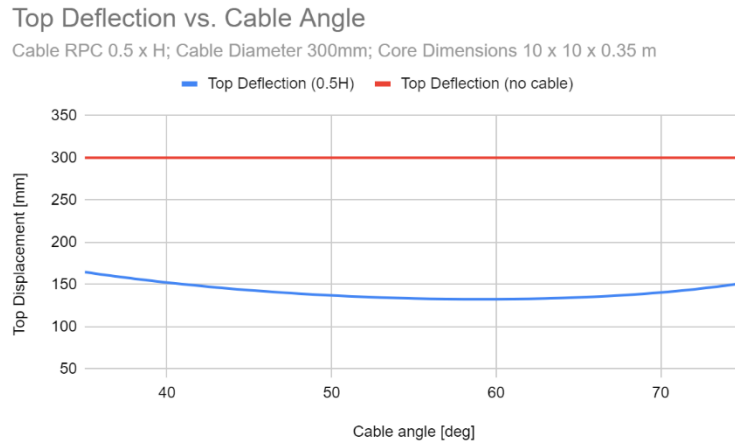


**Figure 38 Top Deflection and Cable Angle**

The optimum value of 55 degrees is explained in Appendix E. Simply put, the total deflection at the top of the core is influenced by the horizontal component of the tension in the cable. The tension in the cable varies with the length of the cable (which is influenced by the cable angle), the loads and cable and core stiffnesses. This tension function has a maximum horizontal component for an angle of ~ 55 degrees. This optimum remains valid as long as the cables are connected to the ground.

#### 4.4. Conclusions of the parametric study

1. The stiffness of the cable has a rapid increase up to a diameter of 300 mm then slightly flattens. Naturally, the larger the stiffness of the cable, the larger its influence, so a larger stiffness would be preferred. However, the diameter of the equivalent cable is restricted by feasible dimensions of cables used in practice for designing cable nets → such, an assumption shall be made on the equivalent diameter of the used cable, to respect a feasible design, as presented below.
2. The relative position of the connection has a large influence on the top deflection → a decrease of up to 80% when compared to the single core system is visible when the cables are connected at high positions. From this parametric study, this parameter results to be the most influential one, so more attention is directed towards it in further studies.
3. The cable angle further influences the length of the cable → if the cables are extending to ground level, an optimum angle of 55 degrees is found. However, the cable angle, as seen in Figure 38, has a rather small overall influence on the stiffness. It is such concluded that restricting this parameter to an unchangeable value does not significantly influence the final results, while narrowing the design space. Such, for the further 2D studies, imposing an unchangeable value for the cable angle to 55 degrees is considered a fair assumption.

Based on the presented conclusions, the following assumptions are imposed for the next part of the research - the 2D analysis of a single core:

- Set the cable angle to the found optimum of 55 degrees, as its influence is small when the cables are connected to the ground;
- Set the relative position of the cable connection at 5 heights (0.3 x H, 0.4 x H, 0.5 x H, 0.6 x H and 0.7 x H), as it is the most influential parameter;
- Set an equivalent cable stiffness with a diameter of 350 millimeters, based on conventional dimensions used for cable-net systems, as presented below;

The equivalent dimension is found using a spacing between cables at the connection to the core of 500mm, and using individual cables with a diameter of 80mm, based on the studied cases in Chapter 2.4. The cables are formed from high-strength steel with a tensile strength value of 1570 MPa. Each cable is formed as a strand rope, composed of 44 wires, each with a diameter of 9mm. Thus, by considering the area of each cable, and factoring it by its angle towards the wind direction, an equivalent dimension for the single cable of 350mm diameter (red cable in Figure 39) is imposed.

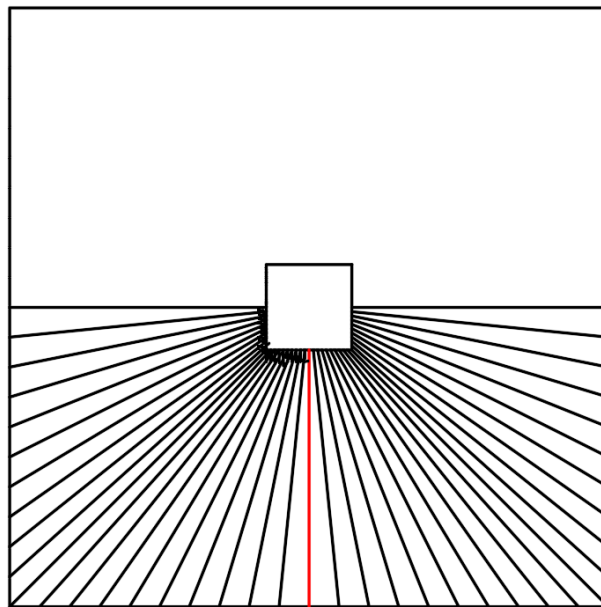


**Figure 39 Single Equivalent Cable**

## 5. 2D Study of a single tower

The 2D study of a single tower can be seen as a preliminary step towards the final 3D analysis of the system. The goal is to quantify the differences between the unloaded and loaded cables, to check the influence of prestress and of the force density, and to form preliminary conclusions on the achievable slenderness of the system. Such, three system configurations are proposed:

- System configuration 1: unloaded and unprestressed cables;
- System configuration 2: unloaded and prestressed cables;
- System configuration 3: loaded and prestressed cables.

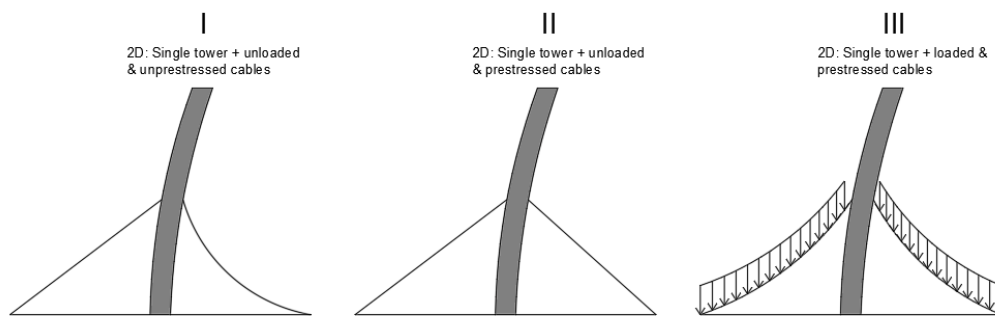


Figure 40 Sub Cases of 2D analysis of a single tower

The assumptions used for the analysis of the system are presented below. Appendix F shows the procedure used in this step, for the three studied cases.

Comparison criterion: The comparison parameter between cases is the deflection at the top of the core, set to the maximum admissible limit of  $H/500 \rightarrow$  this further leads to a feasible range of slenderness for the system, based on the required core width, under the proposed assumptions;

Properties of the model:

- The cables on both sides have a diameter of 350 millimeters, and a cable angle with respect to the tower of 55 degrees, based on the assumptions after the parametric study;
- The material properties are described in Chapter 3 (core) and Chapter 3.2 (cables);
- The cables are considered pinned to their foundation and to their connection to the core;
- The loads on the system are described in Chapter 3.6  $\rightarrow$  as the top deflection is the comparison parameters, only the load combination SLS-1 is considered;
  - For cases I and II the load imposed by the mountain is not considered;
  - For case III the load imposed by the mountain is considered;

Variable inputs:

- The core is changeable in width, in order to find the slenderness for which the maximum deflection limit is reached, under each of the system configurations.
- The relative position of the cable net ranged from an RPC of 0.3 to an RPC of 0.7.
- The cases of both pinned and fixed connection of the core to the foundation are considered;

For the first two cases the parametric script generates the geometry of the system based on the input parameters, followed by the analysis process and the output of the results. For the third case, as the cables are loaded gravitationally, to find the equilibrium shape of the cable under the imposed loads, a form finding process precedes the analysis step, as presented in Chapter 3.5. The workflow of this step is presented in the diagram in Figure 41.

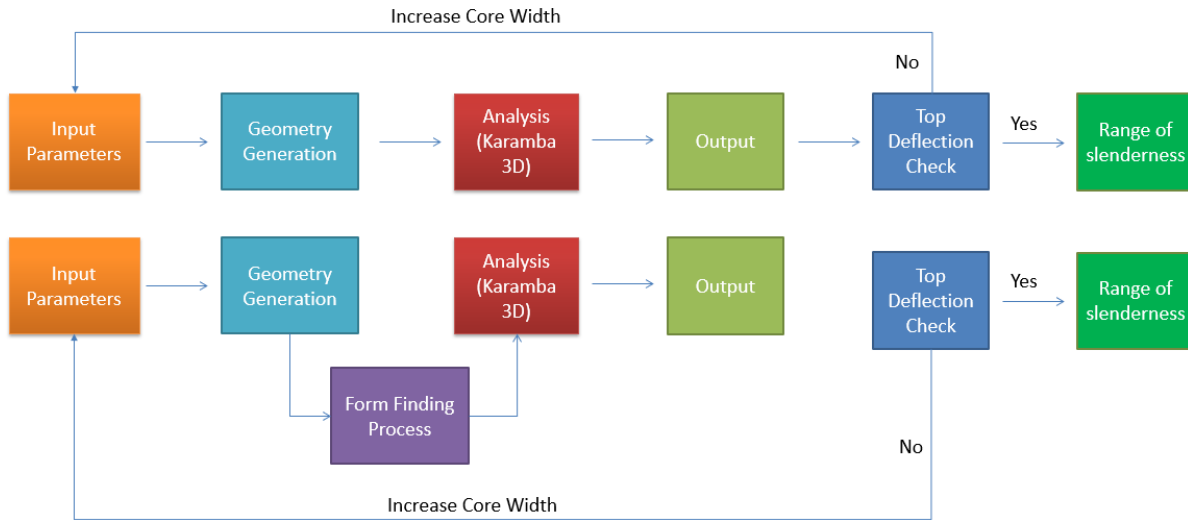


Figure 41 Script logic for the 2D analyses

## 5.1. Not prestressed and not loaded cables

In the first case, as no prestress is added, only one cable, on the windward side of the tower adds stiffness to the system. The cable on the leeward side, due to the horizontal deflection of the tower, is not in tension, thus having no influence on the stability of the tower. Cases may arise in which prestressing of the leeward cable to a sufficient level, so that it does not sag, is not possible. For example, if the required prestress induces too high forces in the core, then the prestress of the leeward cable to a sufficient level is not possible. Such, the system will act as the one presented in this chapter. The procedure used for this case, including further results is found in Appendix F.

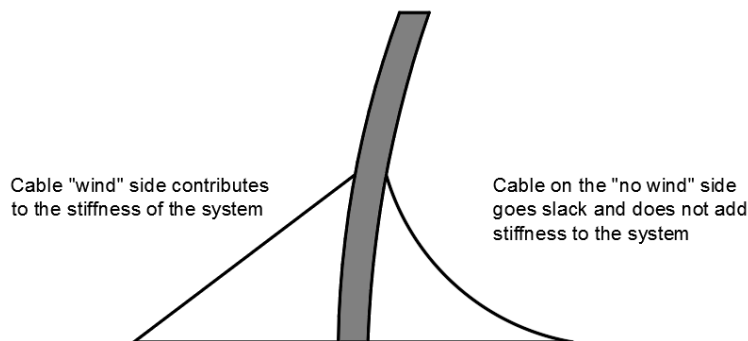


Figure 42 Case A-no load and no prestress

A range of slenderness between  $1/9.5$  and  $1/28.6$  is found, based on the RPC. As the RPC increases, the difference between the fixed and pinned connection to the foundation decreases. Above  $0.5 \times H$ , the same slenderness is achievable with both types of connection. This behavior happens due to the stiff cable that is used. Due to the high value of the horizontal component of the tension force in the cable, the bending moment at the foundation level in the fixed base case decreases significantly, thus making the behavior of the fixed and pinned connection similar. This issue is further addressed in Chapter 7.1.

### Range of Slenderness - Not Prestressed Cables

Fixed and Pinned Base Connection

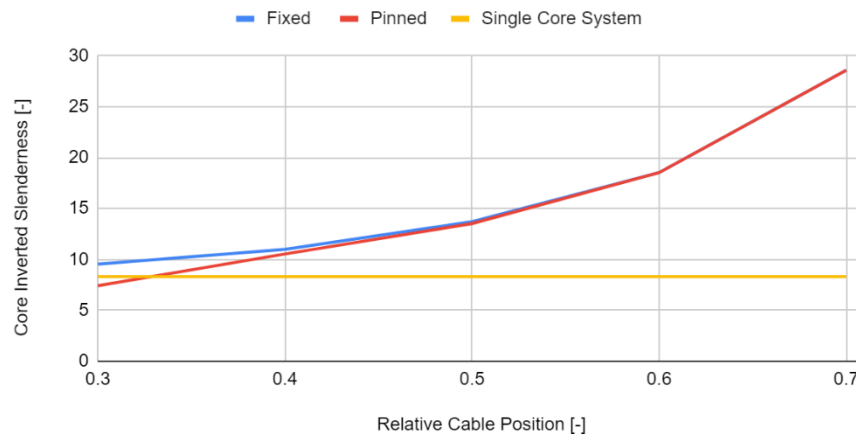


Figure 43 Range of slenderness → unprestressed cables (pinned and fixed connection)

## 5.2. Prestressed and not loaded cables

In the second case, as prestress is added, the cable on the leeward load side of the tower still remains in tensions, although the tower is horizontally deflecting at the position of its connection. Thus, it adds stiffness to the system irrespective of the wind loads direction, given that the imposed prestress is large enough to keep the cable in tension. Both cables are prestressed with the same value to account for wind loads in both directions. The procedure used for this case, including further results is found in Appendix F.

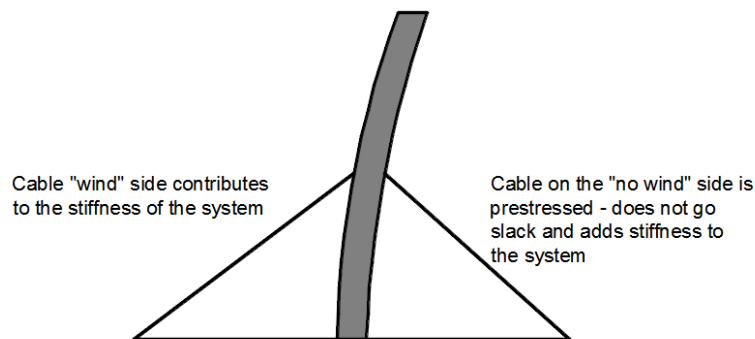


Figure 44 Case B-no load and prestress

A prestressing value of approximately 10% of the minimum breaking force of the 350 mm cable is needed to keep the cable on the leeward side in tension under the wind load. The exact values of the applied prestress are presented in Appendix 6, as difference appear based on the length of the cable. Applying a larger prestress does not add an additional benefit to the stiffness of the system (as Figure 45 shows), thus the minimum required values are used. A range of slenderness between 1/10.4 and 1/30.8 is found, based on the RPC. Due to the higher stiffness of the cases of the core base connection (fixed and pinned), lead to similar results, already starting from a low RPC, as Figure 46 presents.

Influence of the Prestress - 0.3 x H - fixed connection

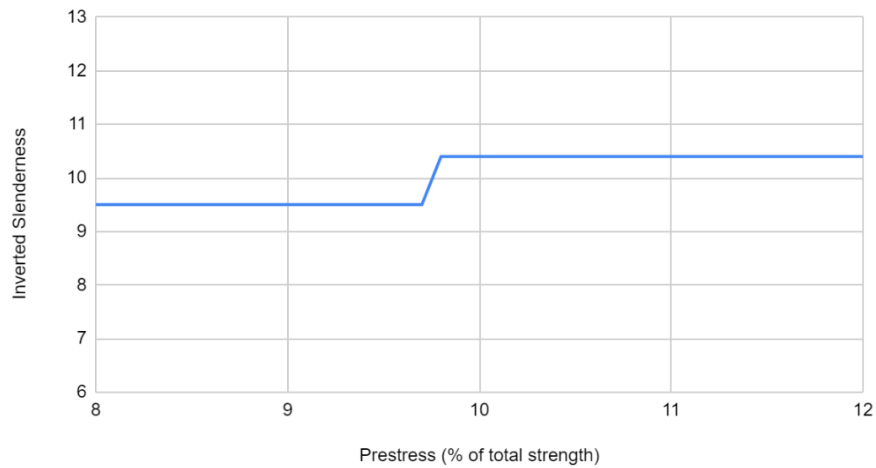


Figure 45 Influence of Prestress

Range of Slenderness - Prestressed Cables

Fixed and Pinned Base Connection

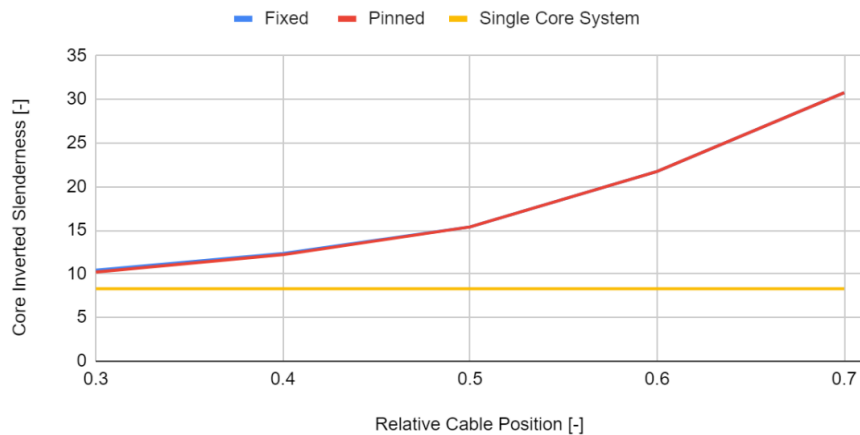


Figure 46 Range of slenderness → prestressed cables (pinned and fixed connection)

## Comparison between cases I and II

Compared to the unstressed cables case, an increase in slenderness is observed, now ranging from 1/10.2 to 1/30.8. When comparing the achievable slenderness between these first two cases, an average increase of approximately 10% is observed when the leeward cable remains in tension, as Figure 47 shows.

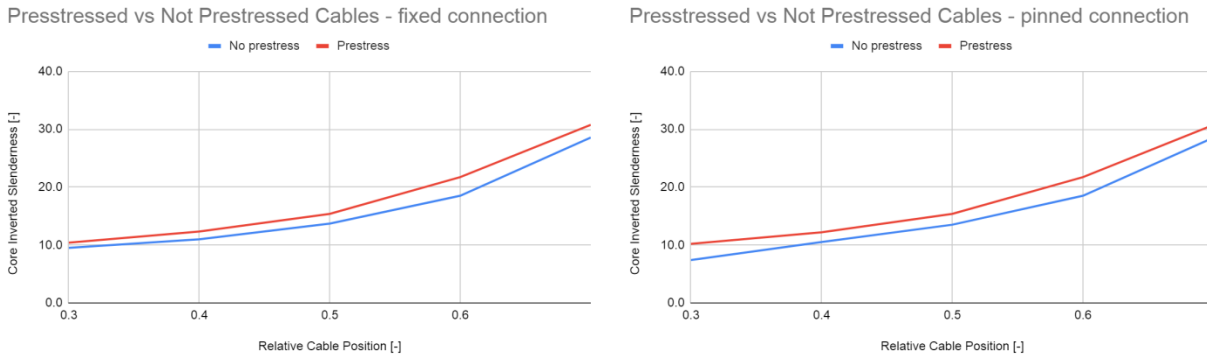


Figure 47 Comparison between Prestress and No Prestress Cables

## 5.3. Prestressed and loaded cables

In the third step, the vertical load and, consequently, the shape of the cable under the gravitational forces are parameters added to the analysis. The mountain load is imposed on the cables based on the tributary area corresponding to a single cable, representing the whole net. The procedure used for this case, including further results is found in Appendix F.

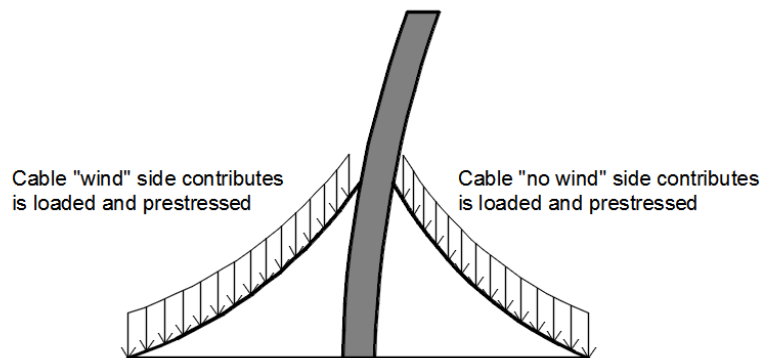
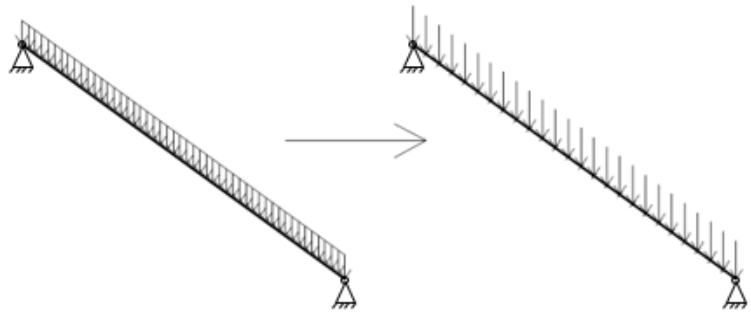


Figure 48 Case C-Loaded Cables

Starting with this step a form finding process is relevant, to find the equilibrium geometry of the cable under the applied loads. This process precedes the structural analysis of the system, to find the geometry of the cable to be connected to the tower. As explained in Chapter 2.5, the process is conducted using Kangaroo with the force density method. The shape of the cable is found under the unfactored dead loads.

Using the FDM, the geometry is found purely based on assumed force density and later the actual stiffness of the cable  $EA$  is used in the materialization step. To be able to use Kangaroo 2, a discrete system is used to define the cable and point loads are added at each node. Buchholdt (1999)

explains that a discretization with at least 20 elements suffices. In the studied case 25 elements are used. Starting from a system with a straight cable, an equilibrium solution is found. The dead load is imposed as a point load at each intersection node between two adjacent cable elements.



**Figure 49 Uniform Distributed Load --> Point Load in 26 nodes**

As shown in the theory of the FDM, there is not a single solution for the shape of the cable under the given load, but multiple independent solutions based on the initially assumed force density. Such, as the initially assumed ratio between forces and lengths changes, so does the geometrical output of the Kangaroo script. With a higher assumed FD value, a stiffer cable with less sag, but bigger initial strain values are found. Consequently, with a lower assumed FD value, a less stiff cable with higher sag and lower initial strain value is found. Figure 50 shows the difference in the geometrical output between a relatively low assumed FD and a relatively high assumed FD.

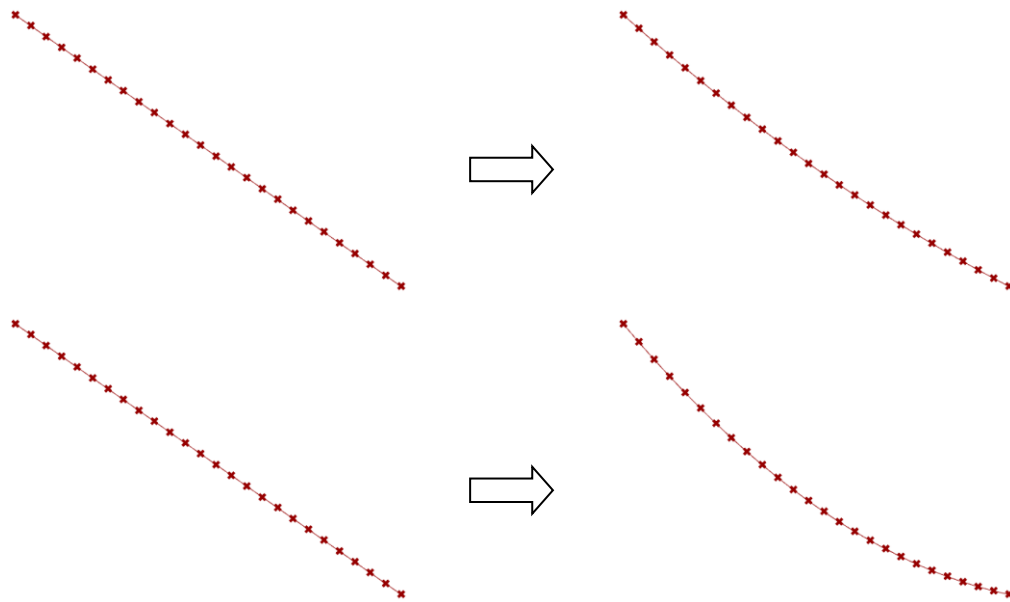


**Figure 50 Form Finding Process-Initial Straight Geometry (left) → Final Geometry High FD (top right)/ Low FD (bottom right)**

The output of the form finding process is the geometry of the cable under the dead loads, with the assumed FD and boundary conditions. To translate the output to a real cable, the materialization process needs to be conducted. The actual stiffness of the cable,  $EA$ , is defined and the initial strains and initial lengths can be calculated based on Hooke's law, as presented in Chapter 2.5.3.

The force in the found cable is, as expected, not constant. As for simple catenary cables, the tension increases as the angle relative to the horizontal axis increases. Such, the lowest forces and consequently initial strains appear at the lower part, where the angle relative to the horizontal axis approaches zero and the highest forces and initial strains appear at the top part. Figure 51 presents the average of the initial strains over the length of the cable (by averaging the initial strains for each of the 25 cable segments) compared to the initially assumed force density (defined as the “strength” of the individual cable segments in the Kangaroo 2 software). A linear increase is observed. The linear increase of the initial strain translates to a linear increase of the initial prestress value. The initial strain is dependent on the lengths of the cable segments, increasing with the increase in length. Contrary, as Figure 52 shows, the sag of the found geometry decreases exponentially as the force density increases, reaching a point where the cable is nearly straight. The sag is defined as the maximum deflection at the middle of the form found cable divided by the initial length of the straight cable, expressed in percentage.

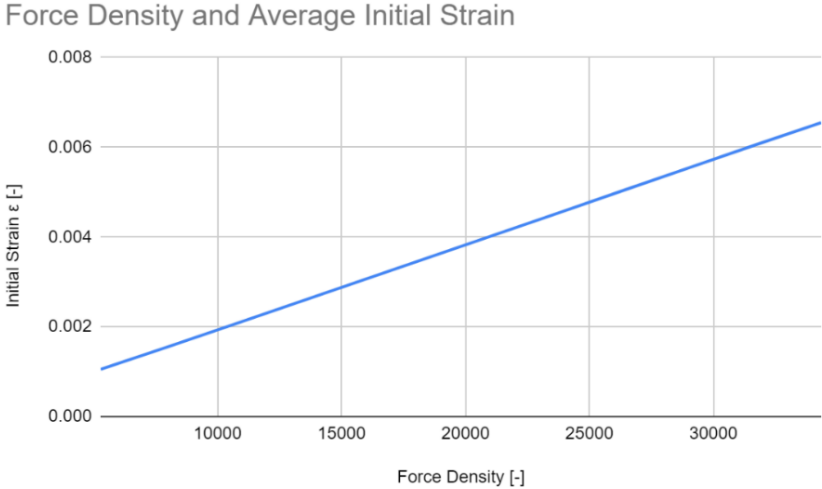


**Figure 51 FD Value and Average Initial Strain**

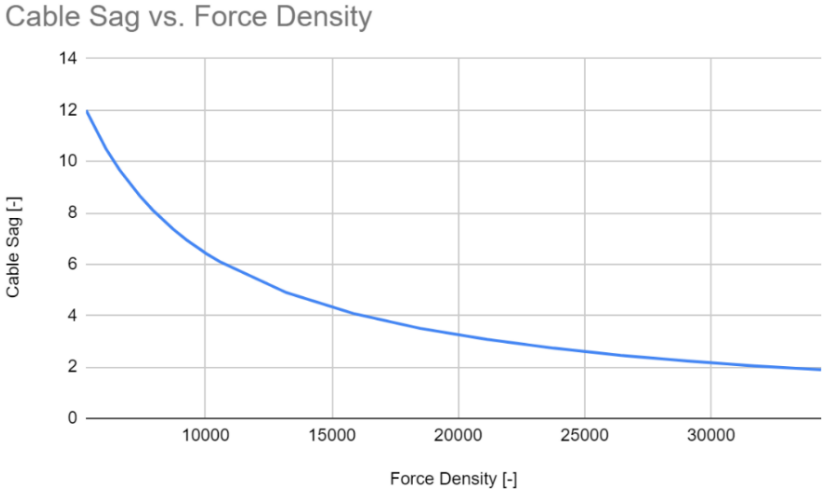


**Figure 52 Cable Sag and Force Density**

To check the influence of the loaded cables on the design of the towers, the form found output is added to the model of the core. The comparison criterion remains the top deflection, leading to a range of slenderness under which the system falls until it fails to meet the stability design criteria. As presented in the introduction chapter, it is expected that the high load of the mountain will have an influence on the design of the core according to the strength requirements → this is studied in the 3D calculations (Chapter 7), as more accurate results and definition of loads are possible.

Three force density values are chosen, leading to three geometries of the cable to be analyzed together with the core. Based on the three chosen force density values, different results are expected. The straighter, and consequently, more prestressed the cable, the higher its influence on the stiffness of the system. As the goal of this step is to find a range of slenderness, the three force density values are chosen to represent a highly sagged cable (low FD), an almost straight cable (high FD), and a cable with the sag between the two extremes.

- A low value of the force to length (FD) parameter →
  - in such a case, it is expected that the initial strain obtained from the form finding process is small, corresponding to a small initial prestress value;
  - on the other hand, it is expected the initial length of the cable to be high, leading to a cable with the sag of 10.5%
- A high value of the force to length (FD) parameter →
  - in such a case, it is expected that the initial strain obtained from the form finding process is high, corresponding to a high initial prestress value;
  - on the other hand, it is expected the initial length of the cable to be small, leading to an almost straight cable with the sag of 2.2%.
- A medium value of the force to length (FD) parameter →
  - the medium value is chosen to lead to an initial strain and consequently, sag of the cable, between the two presented extremes; this led to a sag of 4.9%
  -

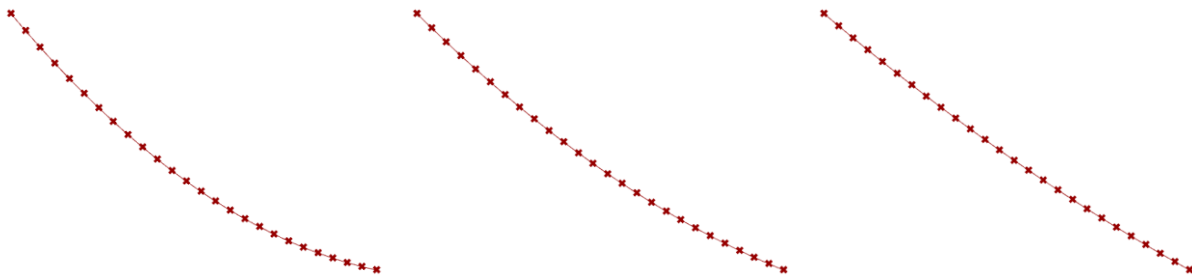


**Figure 53 Geometry Output for different FD values: left (low) → right (high)**

The initial strain values are dependent on the relative position of the cable connection, as the length of the cable elements are used in their mathematical formulation. Additionally, a higher position of the cable connection translates to a higher length of the cable and, consequently, higher load values. This means that the initial strain and initial prestress not only increases with the increase in the FD value, but also with the increase in the length of the cable, up to values higher than the prescribed limit of Gabriel of 40%, as shown in Appendix F.

## Results based on the influence of the chosen FD value

Figure 54 shows the results in terms of the achievable slenderness, based on the chosen FD value. A more extensive description of the results in tabular form can be found in Appendix F, where the prestress in the cable based on the form finding process and the final tension in the cable are also presented.

If a low FD value is used, the influence of the cable on the stiffness of the system is small. As seen in Figure 54, a range of slenderness of 1/8.8 to 1/10.2 is found, compared to the 1/8.1 slenderness of the simple core system. In this case, the pinned connection is not an option as the cables do not provide sufficient supporting at the connection position, and the tower deflection exceeds the allowable limits by up to 300%.

As the FD value is increased, the influence of the cables on the stability of the tower becomes larger. When a medium FD value is used, the range of slenderness increases to 1/9 up to 1/18.2, based on the RPC. In this case, only for higher positions of the cable connection (above  $0.6 \times H$ ), the pinned connection to the foundation becomes a feasible solution.

A high FD value further increases the range of slenderness to 1/9.6 to 1/25.6. As the cable is almost straight, this range is similar (slightly lower) to the case of the unloaded prestressed cables, as Figure 55 shows. For all relative positions of the cable, the pinned connection becomes a feasible alternative.

### Range of Slenderness - Loaded Cables

Fixed Base Connection

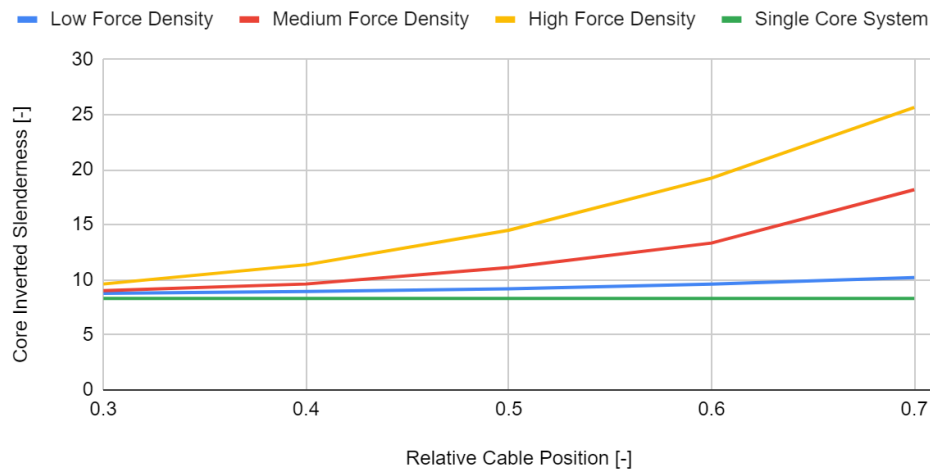


Figure 54 Range of slenderness → loaded cables

## 5.4. Conclusions of the 2D study

The range of slenderness under which the system falls is greatly influenced by the loading condition on the cable and the applied prestress → either computed through the form finding in the case of loaded cables, or assumed so that the cable on the leeward side doesn't go slack in the cases of unloaded cables. As mentioned, using a high FD value, imposing a nearly straight cable, will lead to a similar range as the unloaded prestressed cables. The forces in the cables and on the tower will, however, increase drastically in the case of the loaded cables, and will be discussed further in Chapter 7. A cable with a sag of more than 10% will lead to unsatisfactory results, adding little benefit to the stiffness of the system. Figure 55 shows the difference in results between the cases analyzed in step 2. The plotted slenderness curves presented in Figure 55 show the behavior of the system when:

- The cables are not loaded gravitationally and no prestress is added → Red line (“No Prestress Cables”), as presented in Chapter 5.1;
- The cables are not loaded gravitationally, but prestress is added → Blue line (“Prestressed Cables”), as presented in Chapter 5.2;
- The cables are loaded gravitationally, and different FD values are initially assumed:
  - Yellow line (High FD value), as presented in Chapter 5.3;
  - Green line (Medium FD value), as presented in Chapter 5.3;
  - Orange line (Low FD value), as presented in Chapter 5.3;

Table 11 presents the maximum achievable slenderness of the system, under the initially assumed cable stiffness EA (with the diameter of 350 mm, and the E-value of 160 GPa).

**Table 11 Maximum achievable slenderness based on studied Cases**

	No prestress cables	Prestressed cables	Loaded cables
Maximum achievable slenderness	1/28.6	1/30.8	1/25.6

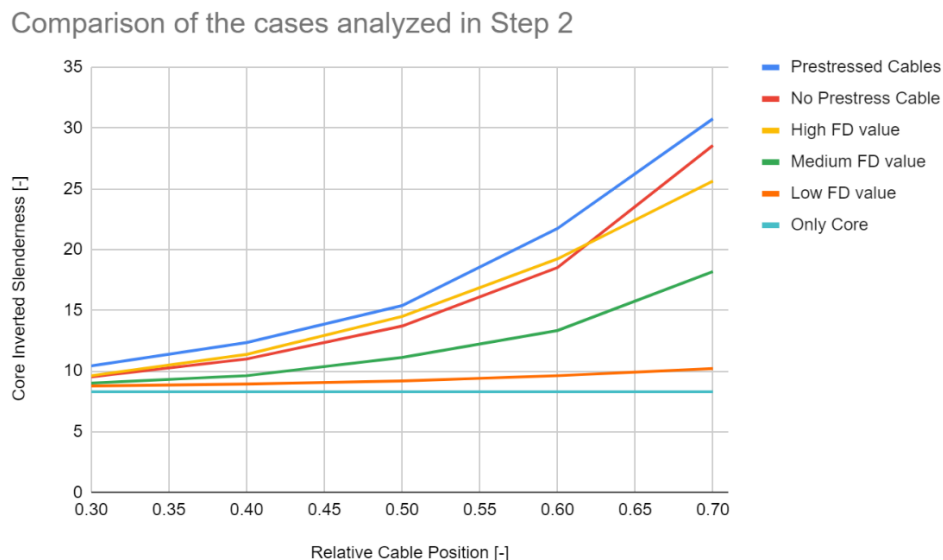


**Figure 55 Comparison between the cases analyzed in Step 2**

Based on the conclusions of the 2D study, a number of remarks to be further used in the more complex 3D study can be outlined:

- Due to the stiffness that the cable net adds to the system, especially in high relative cable position cases, the pinned and fixed connection of the core to the foundation lead to similar results → to further reduce the design space for the 3D analysis, only the *fixed* connection can be considered;
- The chosen force density value has a high influence on the initial prestress in the cable (and further, the overall stiffness of the system). As seen in Appendix F, for high FD values (that correspond to a little sag of the cables), the initial prestress exceeds the proposed limits of 40% used in this thesis. Such, for the following 3D cases, the FD value shall be chosen by an iterative process, to lead to a geometry with the proposed sag of 4-6 %, according to Chapter 3.3 (corresponding, in the 2D study to the so-called medium FD value);
- The relative position of the cable net has, as expected from the parametric study, a high influence on the achievable slenderness, and will continue to remain one of the main changeable parameters of the study;
- It is again noted that the 2D comparison is based on the influence on the top deflection. It is expected that the high slenderness cases will pose additional issues in terms of the strength of the core, due to the high mountain load, and will be further studied in Step 4 of the Exploration phase (Chapter 7).

# 6. 3D Study of a rectangular grid of towers

Step 3 and Step 4 propose the 3D study of a rectangular grid of multiple interconnected towers and aim to provide sufficient information to form preliminary recommendations on the design of the core + cable-net system. If in the 2D study the cable-net was modelled as a single equivalent cable, in the 3D study a full design of the cable-net is conducted. The analysis of the system is conducted in RSA, to account for the geometric non-linearity of the cable elements. In step 3, the top deflection is at first set as the comparison criterion to find a range of slenderness under which the system falls, under the starting assumptions, while step 4 addresses the overall design of the system, including the strength of the core. The workflow of Step 3 and Step 4 is presented in Figure 56. The procedure used for this case, including further results is found in Appendix G.

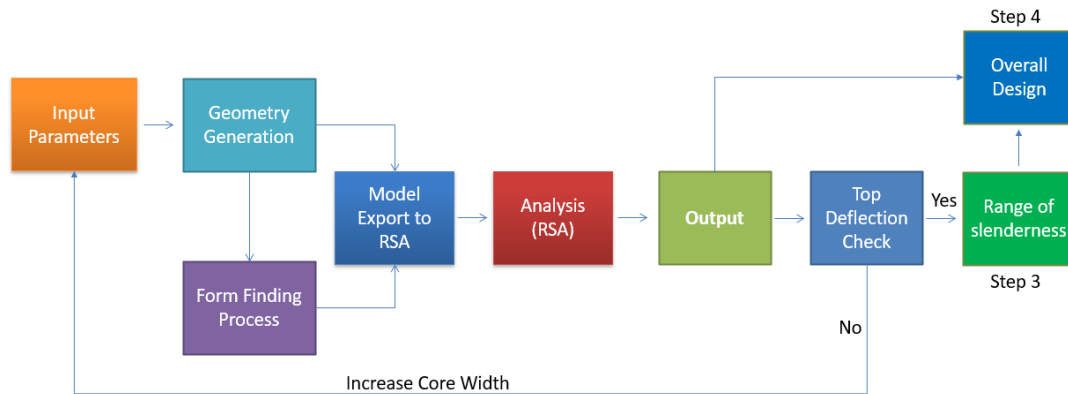


Figure 56 Script logic for 3D analyses (add ref in text)

## 6.1. Initial remarks on the geometry and analysis of the system

### 6.1.1. Geometry of the system

Based on the assumptions after the literature review, the design of the 3D cable-net has to meet the imposed requirements in terms of topology, sag/ rise and element lengths. The topology is chosen as a multi-span mast supported cable-net with radial and edge cables. The sags and rise must fit in the imposed boundary of 4-6 % of the span, and the average cable element must be of approximately 4 meters.

The proposed geometry of the cable-net is composed of a number of different types of cables, based on their location, shown in Figure 57 and Figure 58:

- edge cables → the cables that are not connected to the towers
- diagonal cables → the cables that are spanning between towers
- internal cables (vertical) → the cables connected between the towers and the edge cables
- internal cables (horizontal) → the radial cables

To simulate an infinite rectangular grid of towers, the geometry of the cable-net is reduced to a rectangular grid of 9 towers and the study is conducted for the middle tower.

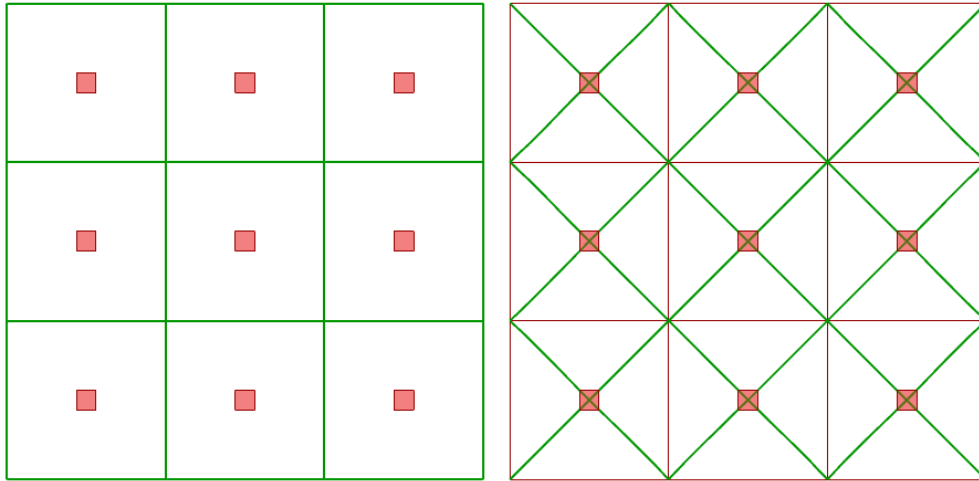


**Figure 57 Edge Cables (left) & Diagonal Cables (right)**

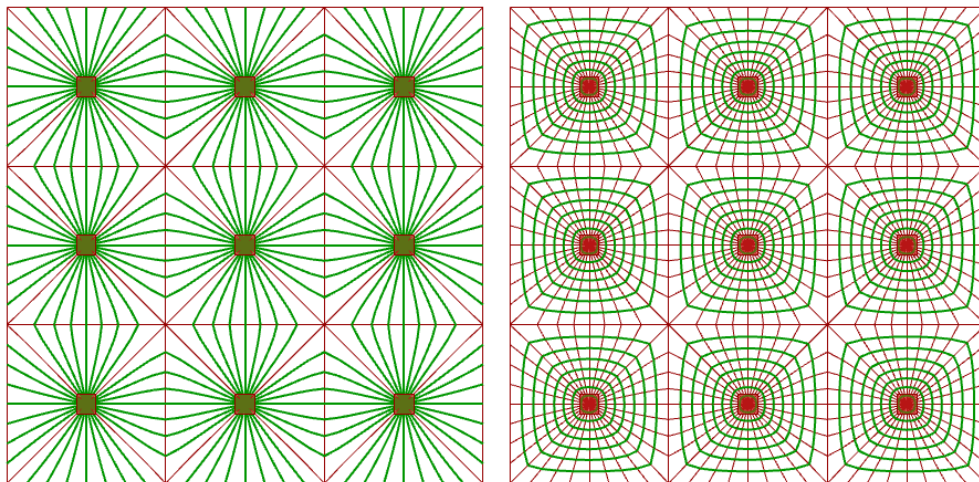


**Figure 58 Internal Cables Vertical (left) & Horizontal (right)**

The equilibrium geometry of the cable-net is generated using the form finding process, under the unfactored permanent loads, as follows. The procedure is further explained in Appendix G:

- At first creating the initial geometry of the cable-net, using straight cables, as a function of the spacing between towers and relative position of the cable-net (Figure 59 top). Define the number of cable elements so that, after the form finding process, an average cable length of 4 meters is obtained (Figure 61);
- Using Kangaroo, conduct the form finding process through an iterative approach, such that the imposed requirements in terms of sag (4-6%) are met. If a too big FD value is used, the resulting sag is smaller than the imposed one, and if a too low FD value is used, the reusing sag is higher than the imposed one.;
- Calculate the average initial strain and consequently initial prestress value as a function of the initial assumed FD value and the final form found length and material and cross-

sectional properties (EA), for each cable element type. Additionally, calculate the relative elongation of the cable element, as the prestress is added in RSA as such (using the equations 1.6, 1.7, 1.8 from Chapter 2.5.3);

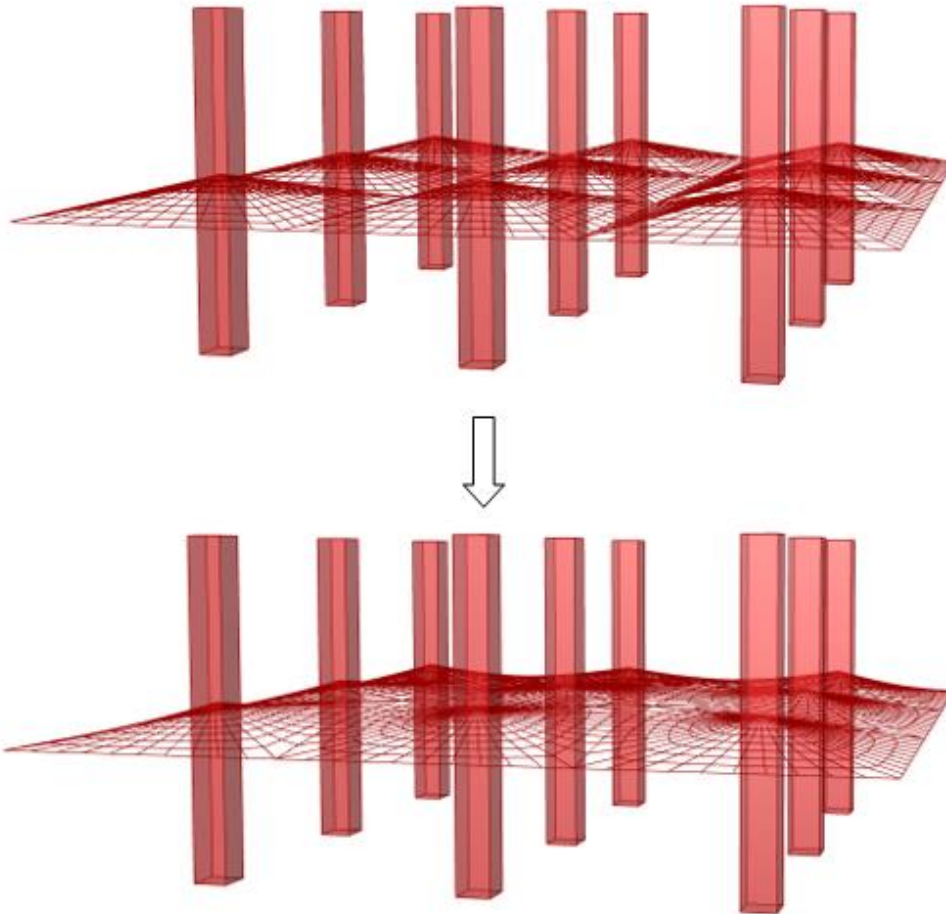


**Figure 59 Initial Geometry (top- before FF) and Final Double Curved Geometry (bottom-after FF) 3D view**

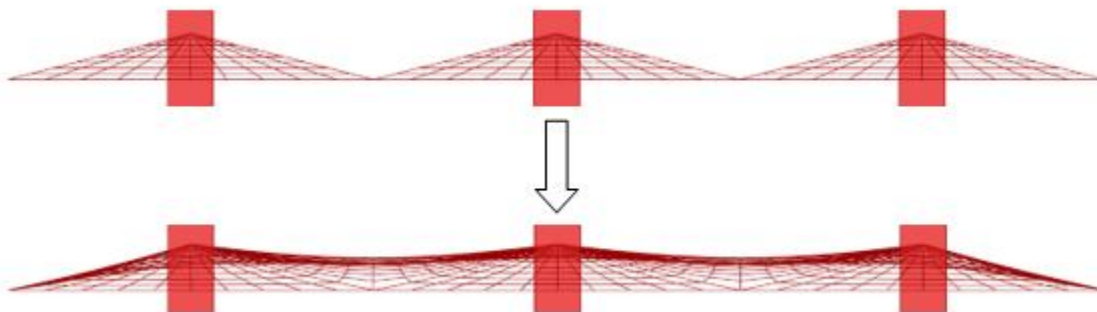


**Figure 60 Initial Geometry (top-before FF) and Final Double Curved Geometry (bottom-after FF) 2D view**

On average, an approximate prestress of 20-35% of the minimum breaking force is computed based on the results of the form finding process. The exact values depend on the spacing between the

towers, number of cable elements (grid) and cable type (edge, diagonal, etc.). These values are in line with the recommendations of Gabriel (1974), as the values do not surpass the set limit of 40%.

The weight of “the mountain” and the required number of cable elements (to attain the average length of 4 meters) are functions of the distance between the towers, as presented in Figure 61. For example, for a 30 meters spacing case, the grid to obtain an average cable length of 4 meters is 7 x 7 (seven divisions of the vertical cables and seven divisions of the horizontal cables), but to achieve the same cable length for an 80 meters spacing case, the grid needs to be of 10 x 10 (ten divisions of the vertical cables and ten divisions of the horizontal cables).

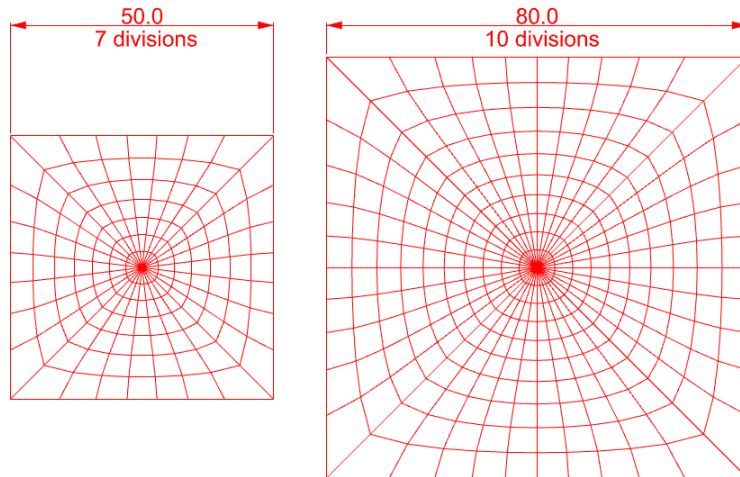


Figure 61 Cable-net geometry top view (different grid for different spacing)

### 6.1.2. Analysis of the system

As presented in Chapter 3.8, the analysis of the 3D system is performed with the help of Robot Structural Analysis. The geometry of the cable-net, together with the obtained initial prestress values are exported from Grasshopper to RSA, using the Geometry Gym Plug In.

A full analysis of the whole system is time consuming, as on average a full procedure (starting from generating the geometry in Grasshopper, exporting and analyzing it in Robot Structural Analysis) for a case lasts at least 15 minutes (depending on the number of elements, up to 25 minutes). This lengthy process makes the iterations of changing different values of the relevant parameters hard to conduct. Such, only the middle tower is exported to Robot and analyzed accordingly. This reduces the computational effort drastically, reducing the time needed for a single iteration by nearly 10 times. The results between a full analysis (9 towers + cable-net) and a simplified analysis (middle tower + adjacent cable-net) are similar, as explained below in this Chapter.

To mimic the behavior of the infinite grid, the end nodes of cable-net are imposed with the following boundary conditions:

- Nodes in the X direction → pinned in the X direction;
- Nodes in the Y direction → pinned in the Y direction;
- Corner nodes → pinned in both X and Y directions;

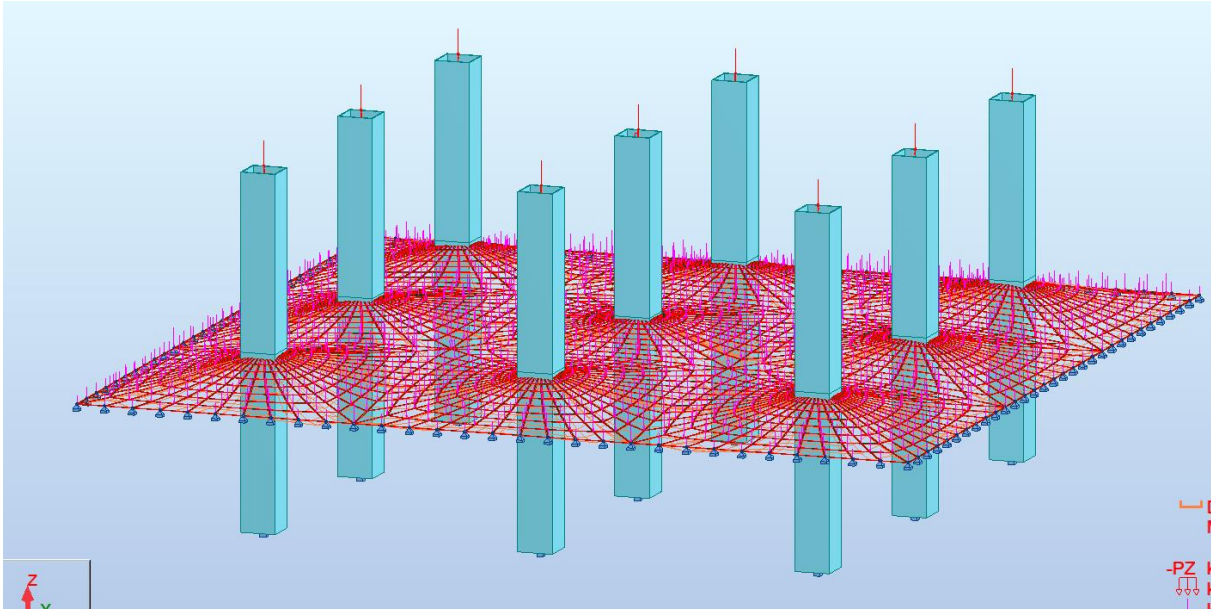


**Figure 62 RSA Full Model**

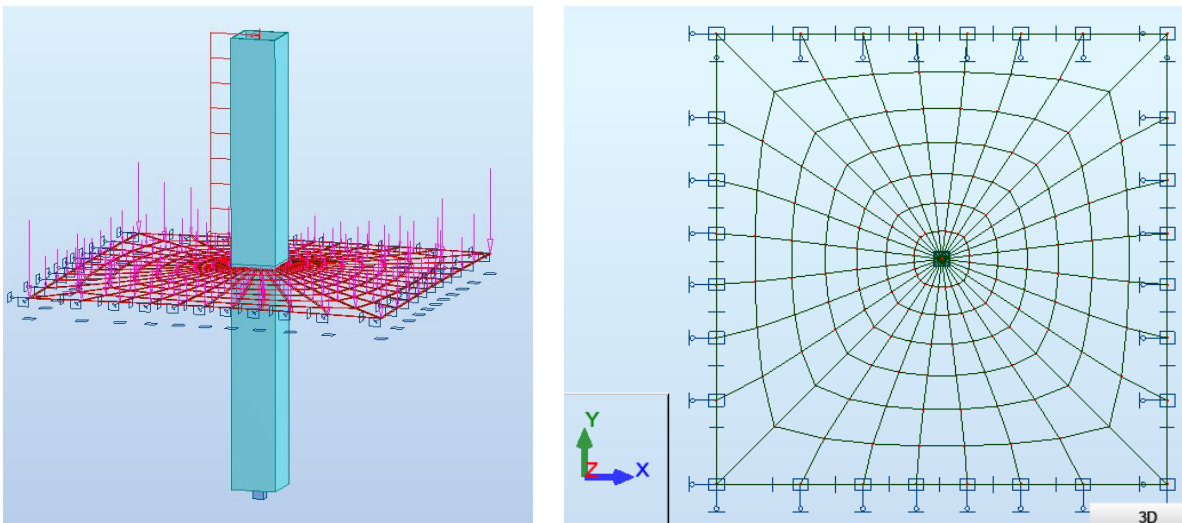


**Figure 63 RSA Simplified Model-3D view (left), Top View (right)**

By performing a full analysis of the system (including all the 9 towers) and comparing it to the simplified analysis of a single tower with boundary conditions, remarks can be concluded on the similarities of the results in the two cases. A comparison of these results is presented in Appendix G. The simplified model (single middle tower) slightly underestimates the stiffness of the cable-net. Such a difference of up to 8% is observed when comparing the top deflection, bending moment, axial force or cable-net deflection between the two models. These deviations are considered acceptable, as the computational time is drastically reduced.

Multiple load cases are assigned to the analysis model, and are summarized below. In the first load case, the permanent load and the prestress are applied, as the “assembly case”. The wind load and live loads are applied in subsequent steps. The imposed values for the loads were described in Chapter 3.6.

- LC1: permanent load + prestress in the cable elements, including:
  - The dead load of structural elements;
  - The prestress in the cable elements;
  - The permanent load imposed by the floors of the tower and by the mountain;
- LC2: wind load, including the wind load on the tower and on the mountain's surface;
- LC3: live load, including the live load on the floors of the tower and the live load on the mountain;

The load cases are combined in the load combinations described in Chapter 3.6: SLS-1, SLS-2, ULS-1, ULS-2, ULS-3, ULS-4, with the different factors depending on the considered leading variable load and the considered designed situation.

As explained in Chapter 3.8, the non-linear analysis is conducted using the Newton-Raphson method, considering geometric non-linearity. The loads are incremented in 20 steps with a maximum of 40 iterations per step.

The created models refer to the variability of the relevant parameters, to study the influence of the cable-net on the design of the system, by changing:

- The distance between the cores from 30 meters to 140 meters (considering spacings of 30, 50, 80, 110 and 140 meters);
- The relative position of the cable-net from 0.2 to 0.7 in steps of 0.1;

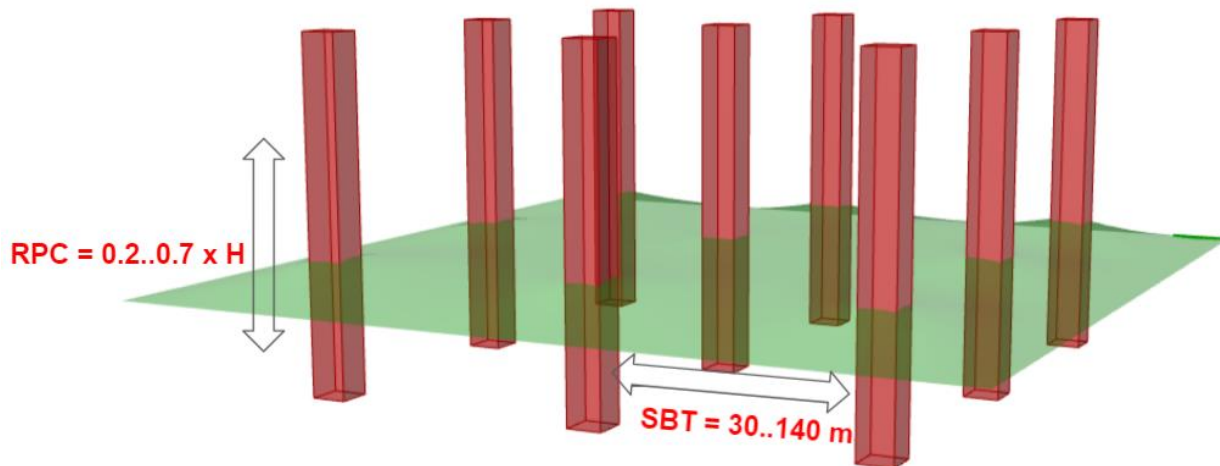


Figure 64 Variable parameters of the 3D analysis

### Properties of the analysis models

To be able to draw fair conclusions, the result of the form finding process for the different iterations (spacing between towers) is required to meet the following geometrical requirements. Table 12 shows the initial geometrical properties of the analyzed systems, including the average initial sag/rise of the cables and the initial average cable lengths.

- The sag/ rise of the cable-net to be similar between the models (approx. 4% of the span) → the initially assumed force density value of the form finding process is adjusted to meet this

criterion; this further leads to a similar angle of the connection of the cables to the core in all spacing cases;

- The cable length to be similar between the models (approx. 4 meters) → the grid (number of intersection points between vertical and horizontal cables) is adjusted to meet this criterion;

The modulus of elasticity used for the different elements in the iterations is the same, with the following values and remarks, as also explained in Chapter 3.1.

- E-value of the concrete above cable-net connection = 9100 MPa;
- E-value of the concrete below cable-net connection = 27000 MPa;
- E-value of the cable elements = 160 GPa;

The boundary conditions applied to the model are as follows:

- Core bottom connection → fixed connection
- Cable-net connection to the core → pinned connection
- Cable ends nodes in x direction → pinned in X direction (see Figure 63)
- Cable ends nodes in y direction → pinned in Y direction (see Figure 63)
- Cable ends corner nodes → pinned in X, Y direction (see Figure 63)

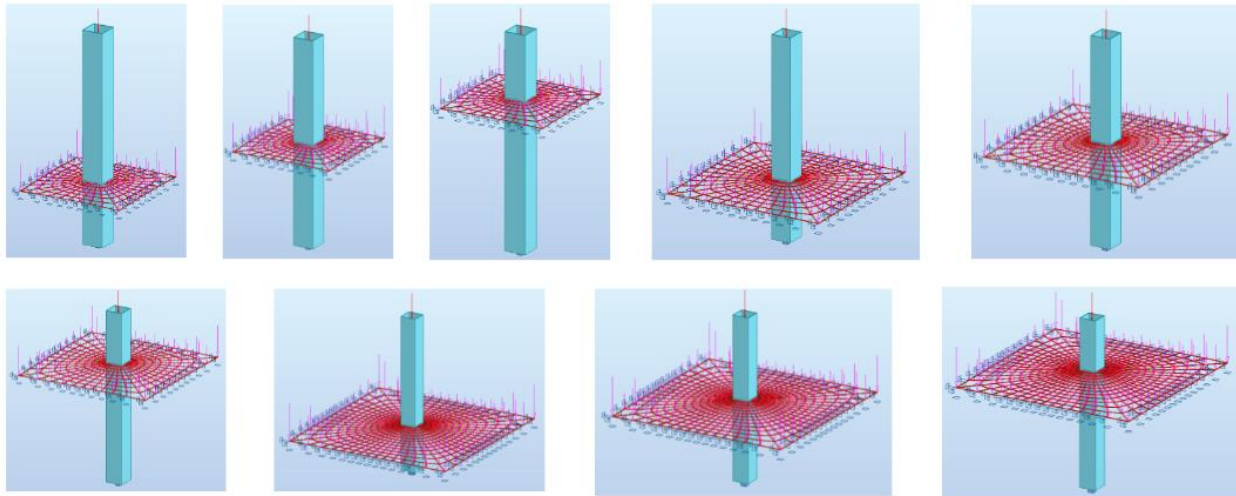


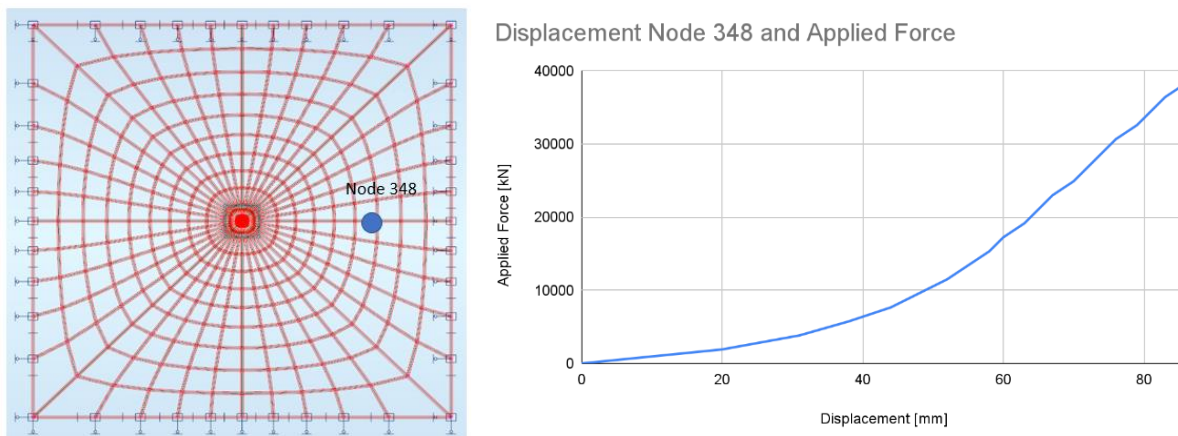
Figure 65 Different Configurations of the System

Table 12 Starting Geometrical Properties of the Models

Spacing between towers [m]	Height of the tower [m]	Cable Division [-]	Average sag/rise [-]	Average cable length [m]
30	100	5x5: 20 Internal Horizontal Cables 20 Internal Vertical Cables 4 Diagonal Cables 4 Edge Cables	4.2	3.85

50	100	7x7: 24 Internal Horizontal Cables 24 Internal Vertical Cables 4 Diagonal Cables 4 Edge Cables	4.2	4.08
80	100	10x10: 36 Internal Horizontal Cables 36 Internal Vertical Cables 4 Diagonal Cables 4 Edge Cables	4.1	4.05
110	100	14x14: 52 Internal Horizontal Cables 52 Internal Vertical Cables 4 Diagonal Cables 4 Edge Cables	4.1	3.95
140	100	16x16: 60 Internal Horizontal Cables 60 Internal Vertical Cables 4 Diagonal Cables 4 Edge Cables	4.1	3.98

The effects of the geometric non-linearity of the cable-net are shown in Figure 66. The graph shows the evolution of the displacement of a middle node of the cable net as a function of the applied vertical forces (considering dead loads for this case). An exponential increase in the stiffness of the cable-system is observed, in line with the expectations and theory presented by Kirshna (1978), described in Chapter 2.4.



**Figure 66 Force vs Displacement Graph for a middle node of the cable-net**

## 6.2. Design of the cable-net for the 3D case

---

In this sub chapter, the design process of the cable-net is presented. Extended results can be found in Appendix G.

### 6.2.1. Deflection of the cable-net (SLS Check)

The deflection of the cable-net is checked in the serviceability limit state, using the load combination SLS-2. This is the governing SLS combinations, as the live loads acting on the mountain are fully considered. In SLS-1, although the wind loads are present, the deflection of the net is found to be lower with approximately 15%.

According to Buchholdt (1999), due to the flexible nature of the cable structures, a less strict restriction on the deflection can be considered, opposed to traditional structures. Buchholdt (1999), in his design examples uses a limit deflection of 1/100-1/150 of the span. However, due to the functionality of the mountain, a more conservative limit of 1/200 of the span is considered, compared to the conventional limit of 1/250 of the span in traditional structures.

The prestress in the cable elements, combined with the cable dimensions are the two main factors influencing the deflection of the net under the applied loads.

### 6.2.2. Strength of the cable elements (ULS Check)

The cable elements are designed according to the maximum tensile force occurring in the element. The tensile force occurs due to the prestress in the cable and due to the applied loads at the intersection joints between multiple cables (the distributed mountain load based on the tributary area surrounding each joint). The maximum force occurs in the load combination ULS 3, when the permanent mountain load is combined with the full live loads. The axial force in the cable needs to be lower than the minimum breaking strength of each spiral strand, according to Chapter 2.3. As a filling factor of 0.65 is used, this is equivalent to the maximum tensile stress occurring in the element to be lower than the used design wire strength of 1570 MPa reduced by the filling factor. This leads to a maximum admissible stress of 1020 MPa, as equations 7.1 and 7.2 show.

$$\sigma_{max} = \frac{N}{A_{cable}} \quad (\text{Eq 7.1})$$

$$\sigma_{max} < 0.65 \cdot f_{t,d} \quad (\text{Eq 7.2})$$

The cable elements are designed for each spacing case, and for each cable type (diagonal cable, edge cable, internal cable vertical/ horizontal) based on the maximum occurring tensile force per element type. Although optimization could be conducted for each cable in particular, this would cause a difficult execution process. Such, all cables in a category (diagonal, edge, etc.) are designed based on the maximum tensile force occurring for an element in that category. As the spacing between the towers increases, so does to total load on the cables, leading to larger needed cables as the spacing increases.

Each cable element is design according to its minimum breaking force. Based on the geometry of the cable-net the different cable element types are designed, as follows:

- Edge cables and diagonal cables → diameter between 100 and 200 mm;
- Internal cables → diameter between 60 and 150 mm;

### 6.2.3. Design of the cable-net

An example of the design of the cable-net is presented in this chapter, for the 80 meters spacing case. The calculations for each spacing case can be found in Appendix G, and are only outlined at the end of this chapter.

Figure 67 shows the axial forces occurring in the cable elements under the load combination ULS 3. Table 13 Cable elements design for the 80 meters spacing case (ULS) shows the chosen diameters for each cable type and the final unity check. Using equations 7.1 and 7.2, a minimum required area for each cable type is calculated, and based on this area a cable diameter is chosen to respect the strength requirement. Based on the axial force in the cable and the area of the now found cable, the maximum stress is calculated and verified to be lower than the admissible stress.

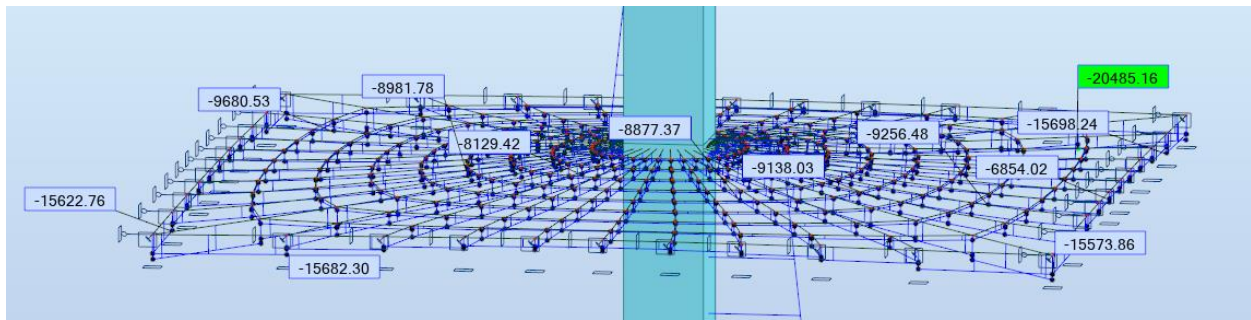


Figure 67 Axial Force in the cable elements → 80 meters spacing case

Table 13 Cable elements design for the 80 meters spacing case (ULS)

Case	Cable Type	Maximum Axial Force [kN]	Required Diameter [mm]	Chosen Diameter [mm]	Maximum Tensile Stress Cable [MPa]	Admissible Stress [MPa]
80 meters spacing	Edge Cable	15698	141	145	962.6	1020
	Diagonal Cable	20485	160	165	958.0	1020
	Internal Cable-Vertical	9680	110	115	922.4	1020
	Internal Cable-Horizontal	2714	58	80	539.9	1020

Further, the deflection is obtained under the load combination SLS-2, and verified to be lower than the maximum set value of span/200. The deflection is checked in two relevant positions: at the middle of the edge cables (Position 1) and at the intersection of the edge cables with the diagonal

cables (Position 2), as shown in Figure 68. The span is considered as the spacing between two adjacent towers for Position 1, and as the spacing between two diagonally placed towers for Position 2.

**Table 14 Cable elements design for the 80 meters spacing case (SLS)**

Case	Position	Span [m]	Maximum Deflection [mm]	Maximum Allowable Deflection [mm]	Unity Check [-]
80 meters spacing	Position 1	80	388	400	0.97
	Position 2	113	482	565	0.85

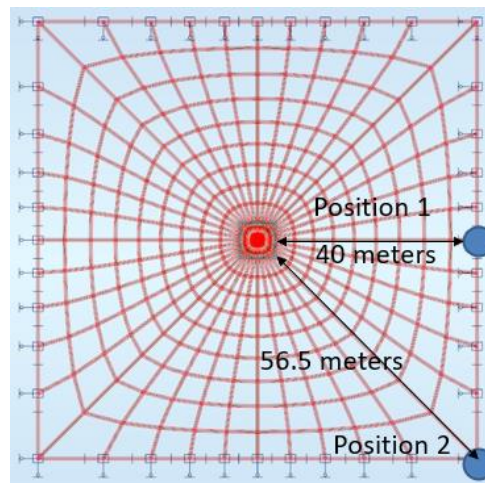


**Figure 68 Checked positions for displacement limit → 80 meters spacing case (Half of the span shown)**

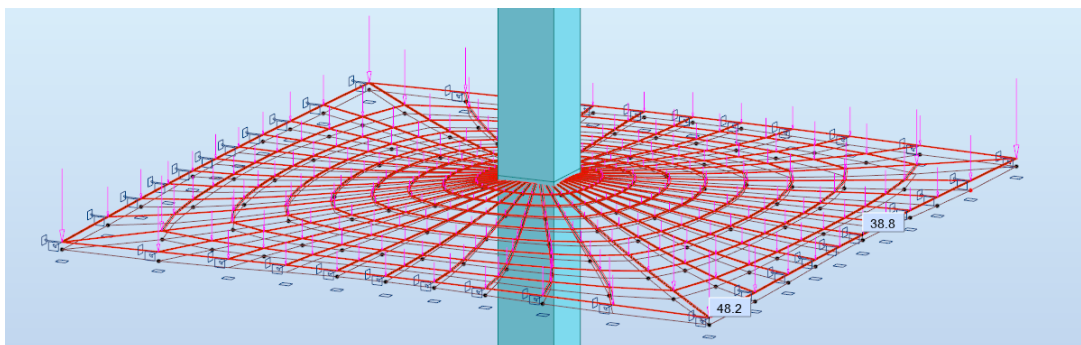


**Figure 69 Displacement values in SLS 2 → 80 meters spacing case**

Depending on the spacing case, the prestress in the cables obtained from the form finding process is adjusted, in order to meet the deflection requirements. For low spacing case (30-50 meters), the obtained prestress is sufficient, but for higher spacing cases (80-140 meters), the prestress value is slightly increased. This is due to the fact the form finding process is based on the permanent load only. As in the analysis model, the live loads are also added, the deflection of the net increases. In Table 15, the prestress for the presented 80 meters case, as percentage of the maximum strength of the cable elements is presented for each cable type.

**Table 15 Prestress values for the 80 meters spacing case**

Case	Cable Type	Maximum Stress	FF Prestress as % of Maximum Stress	Final Prestress as % of Maximum Stress
80 meters spacing	Edge Cable	1020	32.9%	36.8%
	Diagonal Cable		30.3%	36.5%
	Internal Cable-Vertical		32.9%	36.5%
	Internal Cable-Horizontal		19.1%	20.4%

By verifying both the serviceability limit state and ultimate limit state requirements, the final geometry of the cable-net, to be analysed together with the core is obtained. For the 80 meters spacing case, a plan view of the cable elements to be used is presented in Figure 71. The values of the cable diameters used for the other spacing cases are found in Table 16, and as mentioned, further explained in Appendix G. It is worth noting that the high spacing cases of 110- and 140-meters lead to unusually high diameters of the cable elements, thus may be leading to unfeasible designs. These high spacing cases also pose additional problems, that are described in the following Chapters. Further, as Figure 70 shows, due to the increased cable diameters for higher spacing, the weight of the cable-net increases exponentially with the increase in the spacing between cores.

It is further worth noting, that, due to the fact that the elements are designed for an optimal cross section (with a high unity check) the obtained net configurations have the minimum achievable stiffness of the cable net. A less stiff configuration than the used (with smaller cable diameters or smaller prestress) is not feasible. On the other hand, the designer might opt for a stiffer cable-net by over dimensioning the elements. This is further addressed in the discussion Chapter 10.

**Table 16 Cable diameters for all spacing cases**

	Edge cable [mm]	Diagonal Cable [mm]	Internal Cable-Vertical [mm]	Internal Cable-Horizontal [mm]
30 meters spacing	100	120	80	70
50 meters spacing	130	135	100	80
80 meters spacing	145	165	115	90
110 meters spacing	170	195	125	90
140 meters spacing	195	220	150	100

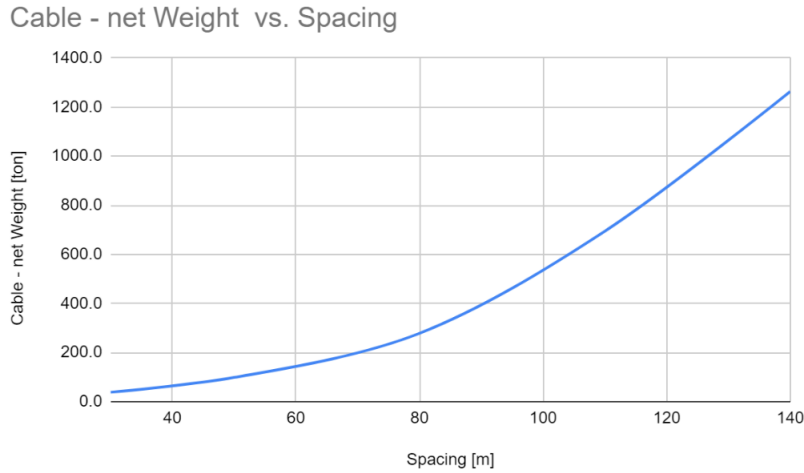


Figure 70 Cable-net weight vs spacing between towers

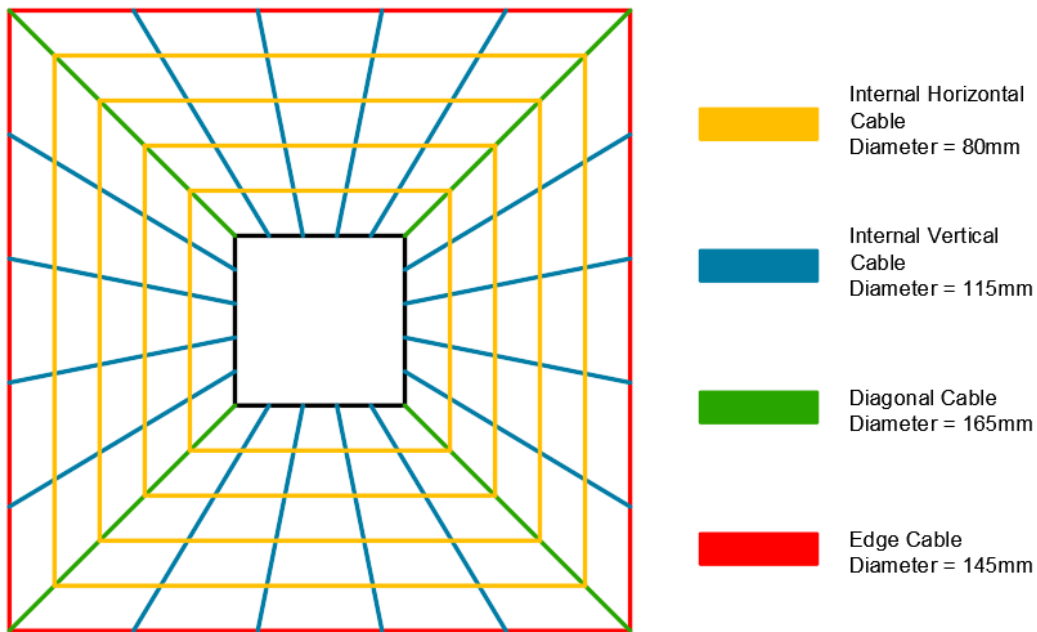


Figure 71 Cable-net final configuration → 80 meters spacing case

### 6.3. Range of Slenderness for the 3D case

Similar to the 2D study, by setting the limit of the top deflection to  $H/500$  a range of slenderness can be found. By only changing the width of the core, the maximum slenderness under which the system meets the imposed deflection requirement are found. The procedure and extended results of this case are found in Appendix G.

Figure 72 shows the achieved core slenderness with respect to the spacing between towers and to the relative position of the cable net. A slight benefit is observed when the towers are closer to each other, as the cable-net becomes stiffer with the decrease in span. The increase in slenderness based

on the reduction of the spacing between towers is approximately 10%, when comparing a 140 meters spacing case with a 30 meters spacing case, as Table 17 shows.

A more visible influence is observed, as expected based on the results of the previous preliminary studies when referring to the RPC. A big benefit, of approximately 150% is observed when comparing a low RPC of 0.3 to a high RPC of 0.7, as Table 18 shows.

A full table of the maximum achievable slenderness, with the corresponding core dimensions, based on which the graph in Figure 72 is obtained can be found in Appendix G for further clarification.

**Table 17 Maximum achievable slenderness based on spacing between towers**

Relative cable position	140 meters spacing	30 meters spacing	Benefit [%]
0.3 x H	9.2	10.1	10.9%
0.5 x H	12.9	15.5	12.0%
0.7 x H	22.2	25.6	11.5%

**Table 18 Maximum achievable slenderness based on relative cable position**

Spacing between towers	0.3 x H	0.7 x H	Benefit [%]
30 meters	10.1	25.6	153%
80 meters	9.4	24.4	159%
140 meters	9.1	22.2	143%

**Core Slenderness vs Relative Position of the Cable Net**

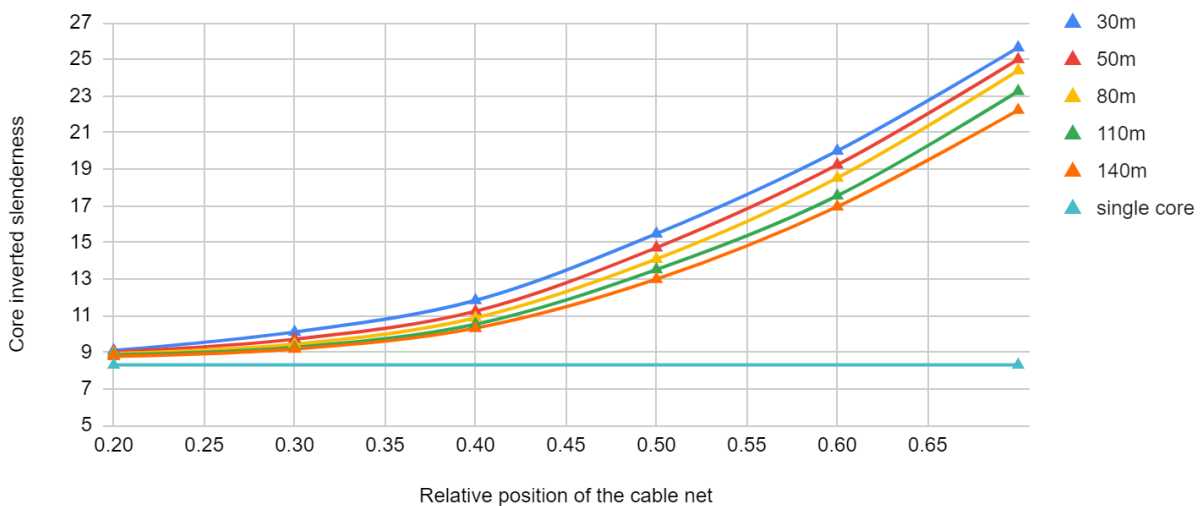


**Figure 72 Core Slenderness and Relative Position of the Cable-net**

# 7. Overall design of the system

---

Thus far, the top deflection has been set as the relevant parameter for the study. Step 4, the overall design of the system, on the other hand, aims to provide a more thorough study of the system, by checking the strength design requirements of the core and other possible occurring issues, such as the need of temporary stabilizing elements during the construction phase.

## 7.1. Design of the core

---

To find the forces on the core, the ULS combinations ULS 3 and ULS 4 were found to be governing. In ULS 3, the live loads are considered to be the leading variable action, so the wind force is not considered. In ULS 4, the wind load is considered to be the leading variable action, so the live loads are reduced by the factor of 0.5, according to the guidelines provided in NEN-EN 1990-1-1.

Attention must be directed towards the forces acting on the core, the axial force and bending moment. If the concrete crushes, buckles, or too high tensile stresses occur in the core, the presented range slenderness based on the top deflection can not be reached. In such cases, the strength of the core becomes governing, opposed to the stability.

### 7.1.1. Axial force

The axial force on the tower is imposed by the self weight of the concrete core, the loads transferred by the floors of the tower to the core, the weight and live loads on the mountain and the prestress in the cable net. The axial forces are biggest in the load combination ULS 3, and presented in this chapter. The axial forces in the load combination ULS 4 are lower with approximately 15%, due to the reduction in the live loads.

As expected, the axial force on the core increases with the increase of the spacing between towers, due to a bigger mountain load being transferred towards the core. Figure 73 shows the total axial force in ULS 3 at the bottom of the core, as a function of this increase. This results in an increase of up to 190% of the total load when increasing the spacing between the towers from 30 meters up to 140 meters, as Table 19 shows.

On the other hand the axial force on the core decreases with the increase of the relative position of the connection of the cable net, as seen in the different curves of Figure 73. This is due to the fact that with this increase, the slenderness of the core increases and, consequently, the self weight of the core decreases. As the self weight of the core is small compared to the weight of the floors or the mountain load, this decrease in the axial force is not significant, as a decrease of up to 24% is observed (see Table 19 → decrease between  $0.3 \times H$  and  $0.7 \times H$ ). This relation holds as the cable-net angle is maintained the same as the spacing between the towers increases.

Figure 74 shows the division on the axial force into the two main contributors: the tower (including the permanent loads and live loads) and the mountain (including the permanent loads, live loads and prestress force). The blue line shows the evolution of the axial force imposed by the mountain as the spacing between towers increases, while the red, yellow and green line show the axial force

imposed by the tower for different RPC cases. At each spacing case, if the mountain load and the tower load would be added, the resulting load value would be equal to the one presented in Figure 73. Naturally, depending on the spacing between towers, the percentage wise contribution of the two parts is different:

- For a low spacing between towers (30 meters), the distribution is: ~25-35 % of the axial load imposed by the mountain + prestress; ~65-75% of the axial load imposed by the tower;
- For a medium spacing between towers (90 meters), the distribution is: ~45-55 % of the axial load imposed by the mountain + prestress; ~45-55% of the axial load imposed by the tower;
- For a high spacing between towers (140 meters), the distribution is: ~70-80% of the axial force imposed by the mountain + prestress; ~20-30% of the axial load imposed by the tower;

**Table 19 Axial force on tower base on spacing between towers**

Relative position	30 meters spacing	140 meters spacing	Increase in Axial Force
0.3 x H	131519 kN	334508 kN	155%
0.5 x H	115894 kN	320221 kN	175%
0.7 x H	104723 kN	305935 kN	191%
Decrease due to RPC	24%	10%	

### Axial force on Tower vs Spacing Between Towers

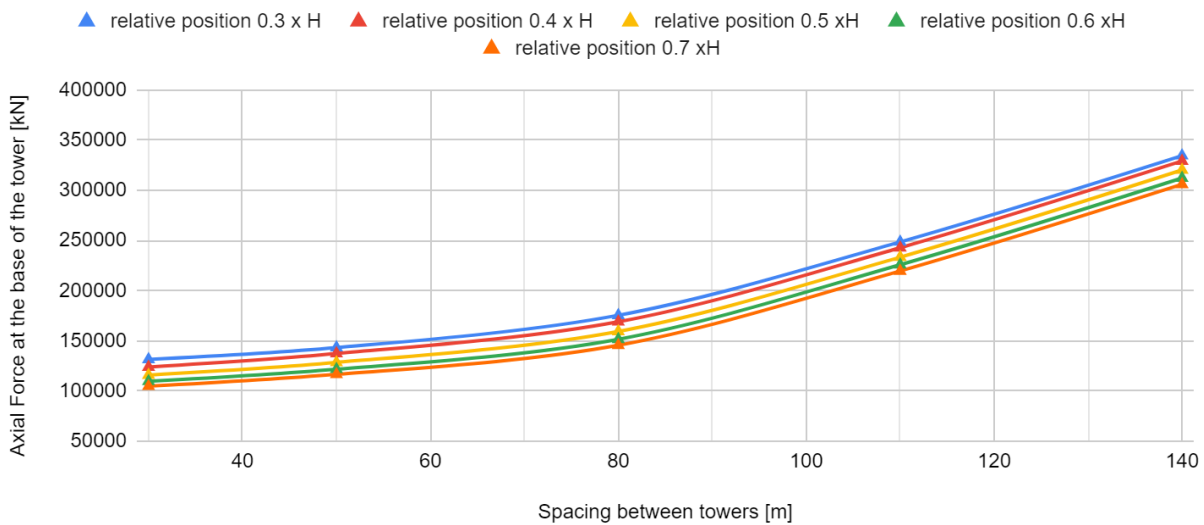


**Figure 73 Axial Force and Spacing Between Towers**

## Distributed Axial Load on the Tower

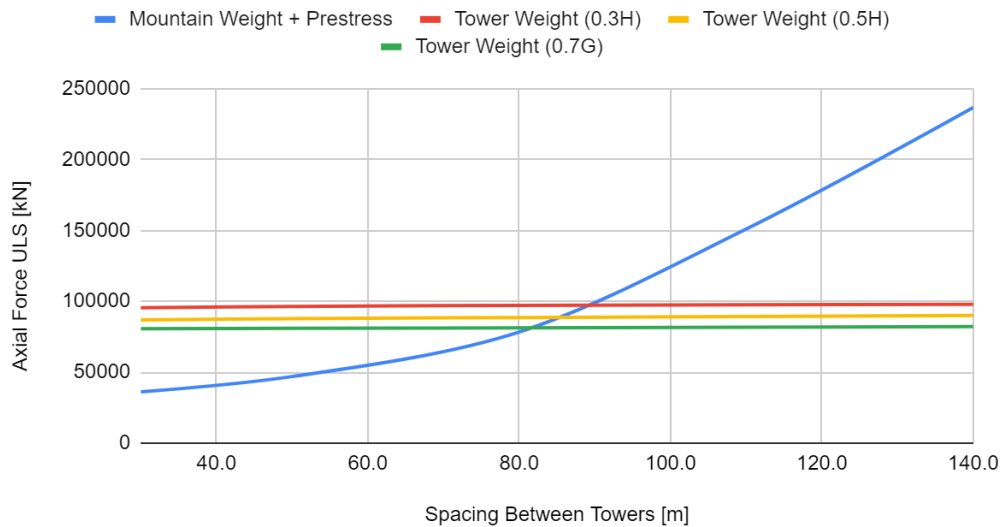


Figure 74 Distributed axial load on towers between tower weight and mountain weight

### 7.1.2. Bending moment

The bending moment is of interest due to its influence on the foundation design and due to its influence on possible tensile stresses. The two relevant positions at which the moment is checked are the bottom of the core and the cable connection position. At the position of the cable connection, the bending moment is only a function of the lateral wind load (further elaborated in Appendix H), while at the bottom the bending moment is a function of both the lateral wind load and the tension forces in the cables. The governing load combination for the bending moment is ULS 4, as the horizontal wind loads are considered.

Figure 75 shows the bending moment evolution at the bottom of the tower with respect to the relative position of the cable net and the spacing between towers. As the position of the connection increases, so does the lever arm of the horizontal component of the tensile forces in the cables. As the position increases, the tensile forces balance the wind load, resulting in significant reductions of the bending at the foundation level. Over a relative position of 0.5, for all spacing cases the bending at the bottom becomes insignificant.

### Bending Moment vs Relative position of the cable net

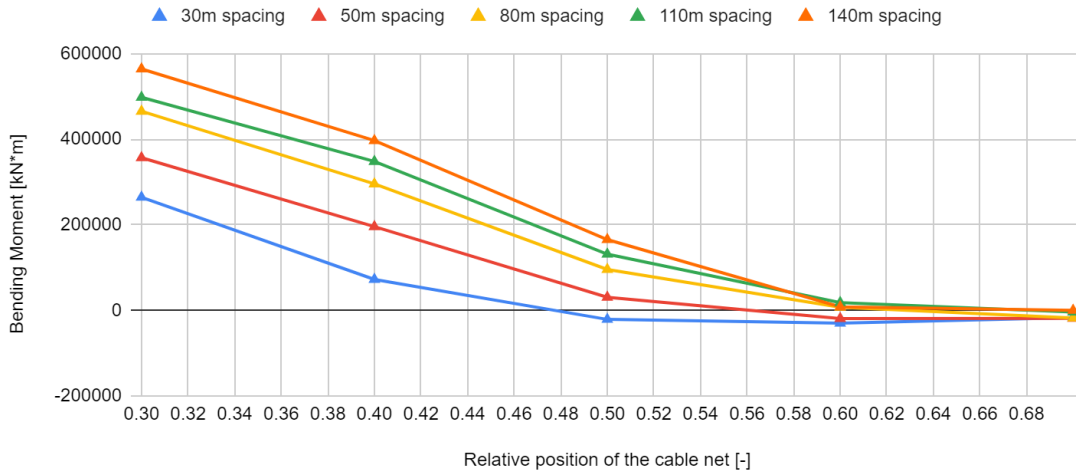


**Figure 75 Bending Moment and Relative Position of the Cable-net**

#### 7.1.3. Axial Force and Bending Moment

At the bottom of the core the tensile and compressive stresses (ULS) must be lower than the design strength of the concrete. As C45/55 concrete is used through this research, the values of the compressive and tensile design strength are 30 MPa and 1.77 respectively. The utilization of the core is checked in the both relevant load combinations, ULS 3 and ULS 4, when only mostly axial force is present (ULS 3) and when bending moment is also present (ULS 4). To account for openings in the core, the effective area of the core is considered to be equivalent to 70% of the total area.

In order to check if the core is sufficiently strong, the minimum compressive stress has to be lower than the compressive design strength and the maximum stress has to be lower than the tensile design strength, as the following equations express:

$$\sigma_{min} < f_{c,d} \quad (\text{Eq 7.1})$$

$$\sigma_{max} < f_{ct,d} \quad (\text{Eq 7.2})$$

$$\sigma_{min} = \left| \frac{-M_{bottom.core}}{W_{core}} - \frac{N_{core}}{A_{reduced}} \right| \quad (\text{Eq 7.3})$$

$$\sigma_{max} = \frac{M_{bottom.core}}{W_{core}} - \frac{N_{core}}{A_{reduced.core}} \quad (\text{Eq 7.4})$$

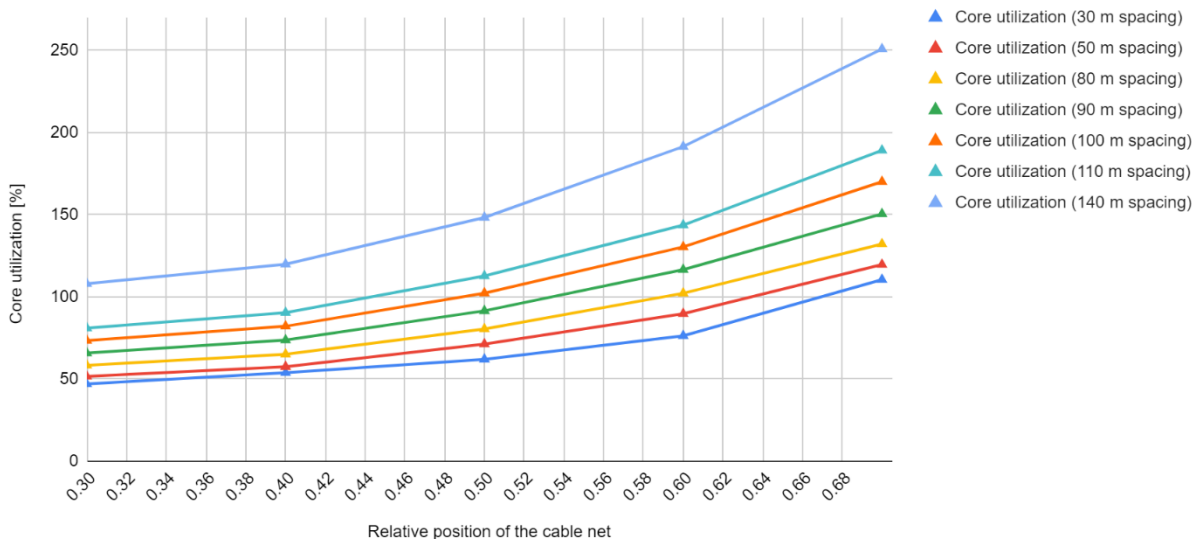
### ULS 3 check

Figure 76 shows the evolution of the utilization of the core at the bottom of the core with respect to the relative position of the cable and the spacing between towers. It is observed that the utilization of the core passes the limit of 100%, predominantly in the cases of high slenderness (high position of the connection), or in the cases of big spacing between the towers. The utilization is calculated as the ratio between the design compressive strength of the concrete and the minimum stress at the bottom of the core, using equation 7.3. As no bending moment is present, the first term on the right hand side of eq 7.3 is null, the stress being only influenced by the axial force. An example of this calculation is shown in Table 20, and the extended calculation is presented in Appendix H.

**Table 20 Outline of the bottom stress calculation in ULS 3**

Case	Core dimensions [m]	Reduced Area [m <sup>2</sup> ]	Axial Force [kN]	Bending Moment [kN x m]	Compressive stress [MPa]	Compressive strength [MPa]	Utilization [%]
RPC 0.4/ SBT 50	8.9 x 8.9 x 0.35	8.4	144609	0	17.3	30	57.5%
RPC 0.6/ SBT 110	5.7 x 5.7 x 0.35	5.2	225800	0	43.1	30	143.5%

Core utilization vs Relative Cable Position - ULS 3



**Figure 76 Core utilization in ULS 3**

### ULS 4 check

As in this load combination the bending moment at the bottom of core is present, the compressive stress is influenced by both the axial load and the bending moment. It is worth noting that due to the high axial forces, and the relatively low bending moments (especially when the relative position of the cable-net increases), under no case and system configuration do tensile forces occur. This is

visualised in Figure 77, where the maximum stresses at the bottom of the core are plotted, with respect to the RPC and SBT. As seen, all of the maximum stresses have a negative value, meaning that the compressive stresses due to the large axial force are larger than the tensile stresses induced by the bending moment under all system configurations. This is further exemplified by Figure 78 which plots the tensile stresses due to the bending moment and the compressive stresses due to the axial force for the 80 meters spacing case.

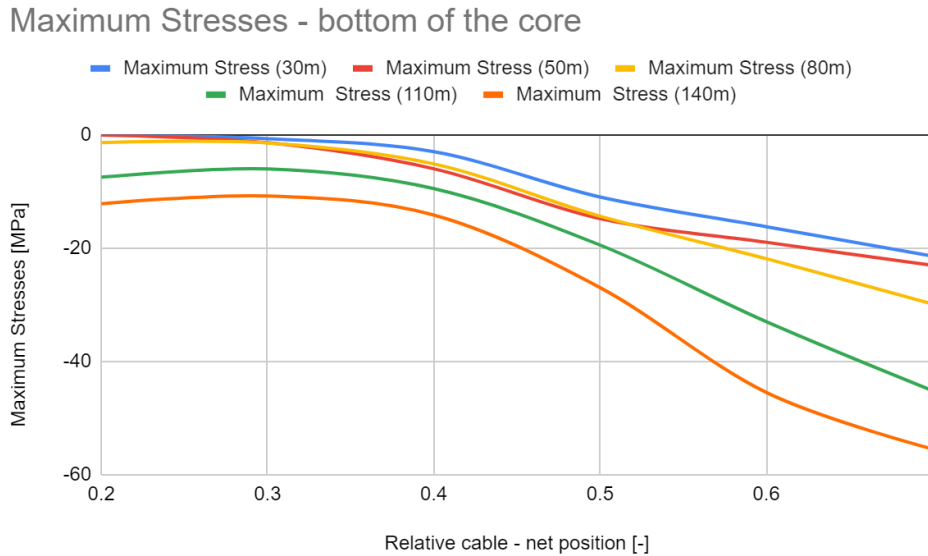


**Figure 77 Maximum tensile stresses at the bottom of the core**

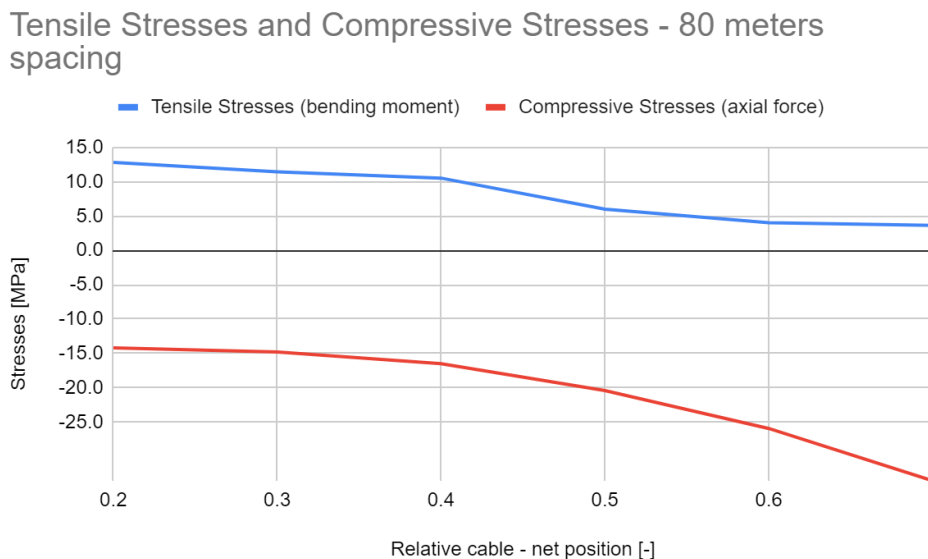


**Figure 78 Stress distribution (due to bending moment and axial force) → 80 meters spacing case**

Figure 79 shows the evolution of the utilization of the core at the bottom of the core with respect to the relative position of the cable net and the spacing between towers. It is observed that in this case, although the axial forces are slightly lower, due to the bending moment adding to the

compressive stresses, the utilization of the core is generally higher than in ULS3. An example of the stress calculation is shown in Table 21, and the extended calculation is presented in Appendix H. In ULS 4, for example, under no system configuration does the 140 meters spacing case meet the design requirements. Table 22 shows an overview of the RPC for each spacing case above which the utilization of the core is exceeded, for the two considered load combinations. To smoothen the transition from the cases of 80 to 110 meters, where big utilization differences occur, the cases of 90 and 100 meters spacing are also analyzed and plotted in Figure 76 and Figure 79.

**Table 21 Outline of the bottom stress calculation in ULS 4**

Case	Core dimensions [m]	Reduced Area [m <sup>2</sup> ]	W Core [m <sup>3</sup> ]	Axial Force [kN]	B.M. [kN x m]	Compressive stress [MPa]	Compressive strength [MPa]	Utilization [%]
RPC 0.4/ SBT 50	8.9 x 8.9 x 0.35	8.4	25.6	120455	229325	23.3	30	77.8%
RPC 0.6/ SBT 110	5.7 x 5.7 x 0.35	5.2	10	182925	39512	38.8	30	129.4%

Core utilization vs Relative Cable Position - ULS 4

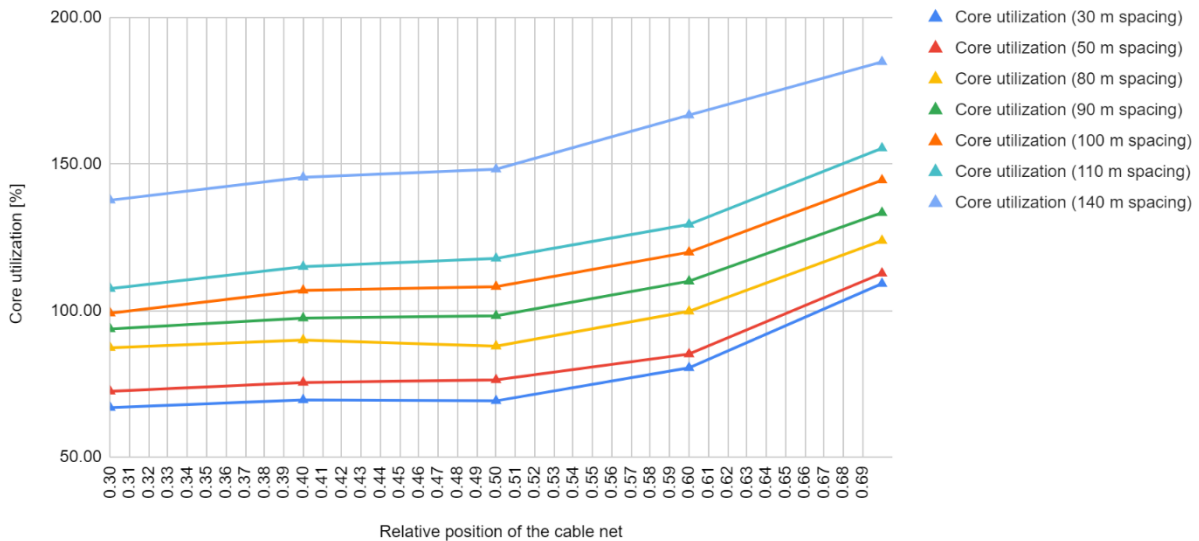


**Figure 79 Core utilization in ULS 4**

**Table 22 Maximum RPC before core design becomes governing in ULS 3 and ULS 4**

	<b>ULS 3 → maximum RPC before core maximum utilization is reached</b>	<b>ULS 4 → maximum RPC before core maximum utilization is reached</b>
30 meters	0.67	0.68
50 meters	0.65	0.65
80 meters	0.59	0.60
90 meters	0.53	0.51
100 meters	0.48	0.32
110 meters	0.44	0
140 meters	0	0

In Appedix H, the tensile stresses occuring at the relative position of the cable-net are plotted, and compared to the tensile design resistance of the concrete. It is observed that *not* under all system configuration the tensile resistance is reached, making the assumption of the reduced E-value to 9100 MPa above the RPC a conservative one.

#### **7.1.4. Buckling**

To check if buckling is a governing failure mechanism of the core, the Euler’s buckling formula is used for calculating the critical load. This is not an exact approach, but can lead to preliminary conclusions on the issue of buckling. Euler’s formula is based on the stiffness of the studied column (in this case, the EI value of the core), the critical length and the boundary conditions for the core. The following assumptions are used through the calculations:

- As the part that may be prone to buckling is located below the position of the cable-net, where the compressive forces are high and no tensile forces occur, the fictious modulus of elasticity presented in Chapter 3, of 27 000 Mpa, is used;
- The moment of inertia is calculated for each case of spacing between towers and relative position of the cable-net based on the maximum achievable slenderness for the proposed configuration (as presented in Figure 72);
- The critical length of the core is considered as the length from the base core of the to the position of the cable-net connection;
- To provide a conservative calcuation, the k factor is assumed a value of  $k = 2$ , corresponding to a column fixed at one and and free to translate and rotate at the other end.
- To provide a conservative calculation, the axial force to be compared to the critical load is considered as the maximum compressive force at the bottom of the core, under the governing load combination for axial load (ULS 3), considering the permanent loads imposed by the self weight of the core, by the floors and by the mountains weight, the live loads imposed on the floors and on the mountains surface, and the extra axial force imposed by the prestress.

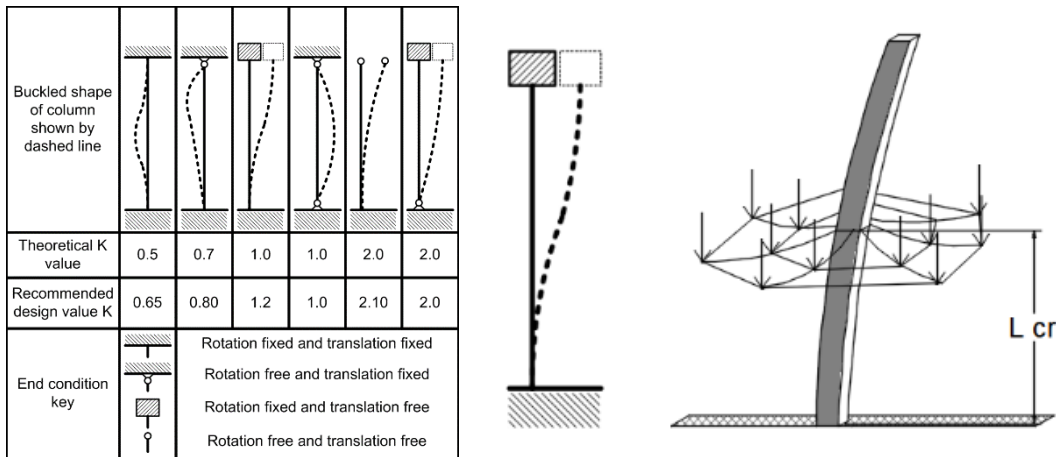


Figure 80 Buckling assumptions for Euler's Critical Load calculation (Left - Herbert, 1987)

$$F_{cr} = \frac{\pi^2 \cdot E \cdot I}{(k \cdot L_{cr})^2} \quad (\text{Eq 7.4})$$

Figure 81 shows the difference between the critical load calculated according to the Euler's formula and the axial compressive load on the core, for the spacing case 140 meters and considering the increase in the relative positions of the cable net. Table 23 shows the values used for obtaining the critical load for the 140 meters spacing case with a relative cable position of 0.6 and with a relative position of 0.7. The extended calculation is presented in Appendix H. As seen, the load on the core only exceeds the critical load in the case of 140 meters, with a high relative position of ~0.685. Such, through this preliminary calculation it is concluded that buckling is not governing in the chosen design space. However, for higher positions of the RPC than 0.7, leading to even higher slendernesses, or for higher spacings between towers leading to higher axial load, it is expected that buckling will have a more critical influence. It is worthy of noting that the slenderness of the core subject to buckling is lower than the slenderness of the full core. Due to the fact that the cable-net is connected at a relative position and the part prone to buckling is only considered up to that position, the effective slenderness decreases. For example, in the case of SBT of 80 meters with a RPC of 0.5, the achievable slenderness based on top deflection is of 1/14 (7.1 meters wide for a 100 meters high core). The actual slenderness for which the buckling calculations are considered is 1/7 (7.1 meters wide for a 50 meters high core).

Table 23 Outline of the Euler critical load check in ULS 3

Case	E-value [kN/m <sup>2</sup> ]	Core dimensions [m]	I value [m <sup>4</sup> ]	k value [-]	L critical [m]	F critical [kN]	F effective [kN]	UC [-]
RPC 0.6/ SBT 140	27000000	5.9 x 5.9 x 0.35	40.0	2	60	741106	312185	0.42
RPC 0.7/ SBT 140	27000000	4.5 x 4.5 x 0.35	16.8	2	70	228353	305935	1.3

F critical vs F compression 140 meters spacing

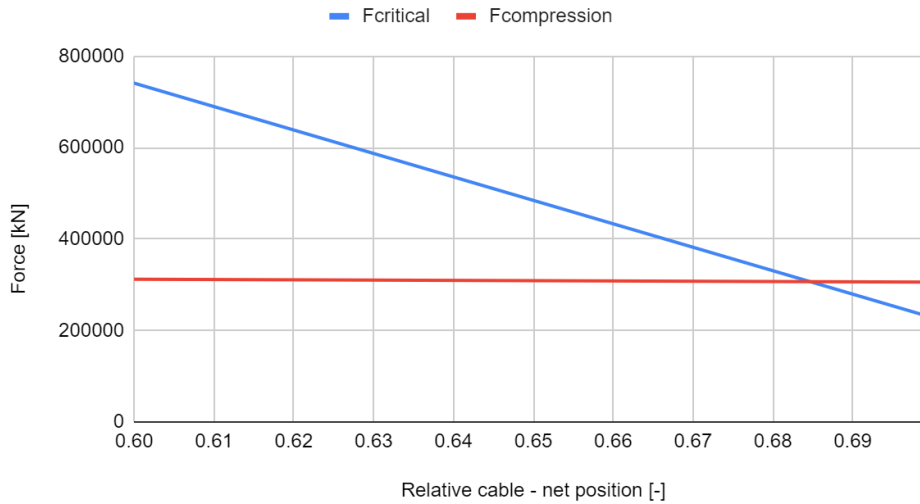


Figure 81 Buckling Critical Load and Compressive Force

### 7.1.5. Horizontal force

As the cables are connected to the core at an angle (as explained in Chapter 6.1, with an average value of 5 degrees), the occurring tensions forces can be vectorially decomposed in:

- The vertical component, transferring the load of the mountain toward the foundation, through the core (as previously addressed as the Axial Force component);
- The horizontal component, that acts horizontally on the core;

Due to the small angle of 5 degrees, this horizontal component is significantly large, especially in the case of big spacing between the towers. To address this, a simplified calculation is conducted and a preliminary solution is proposed. As the spacing between the towers is considered equal on the four sides of the core, also the horizontal forces under the governing load combination (ULS 3 for the highest occurring loads in the cables) are equal on the opposite sides of the core. The proposed solution is to place a grid of steel elements in the interior of the core, at the position of the cable connection, to withstand the large horizontal forces. The spacing between these elements is imposed to be higher than 2 meters, to account for the functionality of the core (for example, elevator placing). An example of the preliminary design of such system is presented in this chapter for an 80 meters spacing case, with the relative cable position at  $0.5 \times H$ . This leads to a core with the width of 7.1 meters ( $1/14.1$  slenderness) according to Figure 72. The extended results are presented in Appendix H.

The grid is composed of external beams (dark blue beams in Figure 82) and internal beams (light blue in Figure 82). The external beams are subjected to both axial force and bending moment and they are englobed in the concrete of the core and the internal beams are acting as supports for the external beams, being subjected only to axial force from both sides. To calculate the required dimensions of the beams, each cable force is decomposed in their three components (x, y, z) based

on the cable angle relative to the core and the cable angle relative to the external beam, as shown in Figure 83:

- $F_x$  will result in axial forces in the external beam;
- $F_y$  will result in axial force in the internal beams and external beams and bending moment in the external beams;
- $F_z$  will transfer the load of the mountain towards the foundation through the core;

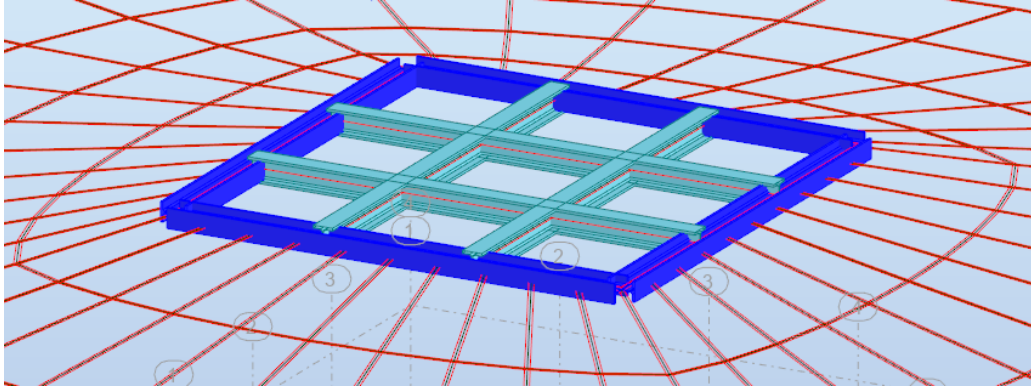


Figure 82 Steel Grid Geometry

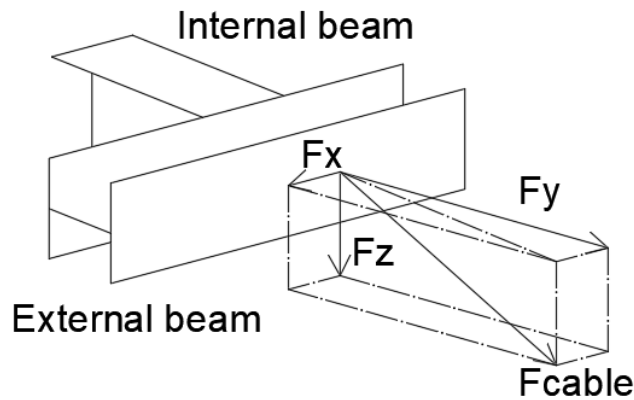


Figure 83 Cable tension distribution on the steel grid elements

As high forces occur, a steel grade of S460 is chosen. Based on the occurring internal forces in the beams, a cross section of HEM650 is chosen for the internal beams and a cross section of HEM 600 is chosen for the external beams, as presented in Table 24.

Table 24 Design of the members to account for the horizontal force on the core

Beam Type	Steel Grade	Maximum Axial Force [kN]	Maximum Bending Moment [kN x m]	Required Area $\times 10^2$ [mm <sup>2</sup> ]	Required $W_y \times 10^3$ [mm <sup>3</sup> ]	Chosen Cross Section
External Beam	S460	17273	~ 0	371	0	HEM 650
Internal Beam	S460	12900	3520	280	7609	HEM 600

## 7.2. Temporary stabilizing elements

For the construction of the cable-net + core system, the following sequence is proposed, as visualized in Figure 84.

- Phase 1: First build the core until the level of the connection to the cable-net;
- Phase 2: Build/ install the cable-net;
- Phase 3: Finish building the core until the final height of the tower;

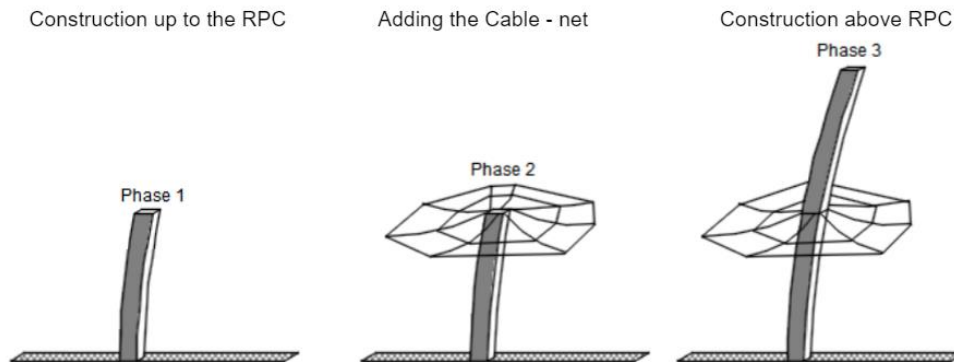


Figure 84 Construction sequence

In cases of high slenderness, the stability of the core in the construction phase is governing. In such a case, the deflection at the height at which the cable-net would be positioned is higher than the admissible limit of  $H/500$ , before the cables are in place. Such a temporary stabilizing system must be designed to withstand the lateral loads on the core until the whole system is built. Depending on the distance between the towers and the relative position of the connection of the cable-net, a limit above which temporary stabilizing elements are needed can be drawn. Figure 85 shows the limit line as a function of the SBT and RPC. As seen, if the cable-net is positioned higher than 52 – 56% of the height of the tower, then a temporary stabilizing system is needed.

The conclusions are drawn based on a highly simplified calculation of the top deflection of the core system, considered as a cantilever, where:

- The length of the cantilever is considered the length of the core, from the connection to the foundation to the position at which the cable net is applied.
- For a conservative approach, the E-value of the concrete is considered as the reduced value to account for tensile stresses in the core and for the openings in the core, with a fictitious E-value of 9100 MPa.
- The moment of inertia of the core is calculated, based on the width of the core corresponding to the maximum achievable slenderness for each configuration (based on Figure 72).
- The wind on the core is applied as a uniformly distributed load, with the maximum value calculated for the reference height corresponding to the position of the cable-net (approximately 50 meters);

- The maximum deflection limit is set to H/500, where H is equal to the length of the cantilever from the connection to the foundation to the position at which the cable-net is applied.

Table 25 shows the procedure of finding the maximum relative position for each spacing case, above which the deflection during the construction phase becomes governing. This issue can be tackled by using temporary stabilizing elements for the core during the construction phase.

$$\delta_{top} = \frac{q_{wind} \cdot L^4}{8 \cdot E \cdot I} \quad (\text{Eq 7.5})$$

Table 25 Calculation for the temporary stabilizing elements

Space case	RPC	Slenderness	Core Width [m]	q wind [kN/m]	L [m]	E [kN/m <sup>2</sup> ]	I core [m <sup>4</sup> ]	Top Disp. [mm]	Allowable Disp. [mm]
30 meters	0.52	1/16.1	6.2	48.7	52	9100000	47.1	103.7	104
50 meters	0.53	1/15.8	6.3	48.7	53	9100000	50.0	105.5	106
80 meters	0.54	1/15.55	6.4	48.7	54	9100000	52.6	107.3	107.8
110 meters	0.55	1/15.25	6.6	48.7	55	9100000	56.0	109.3	110
140 meters	0.56	1/15	6.7	48.7	56	9100000	59.0	111.5	112

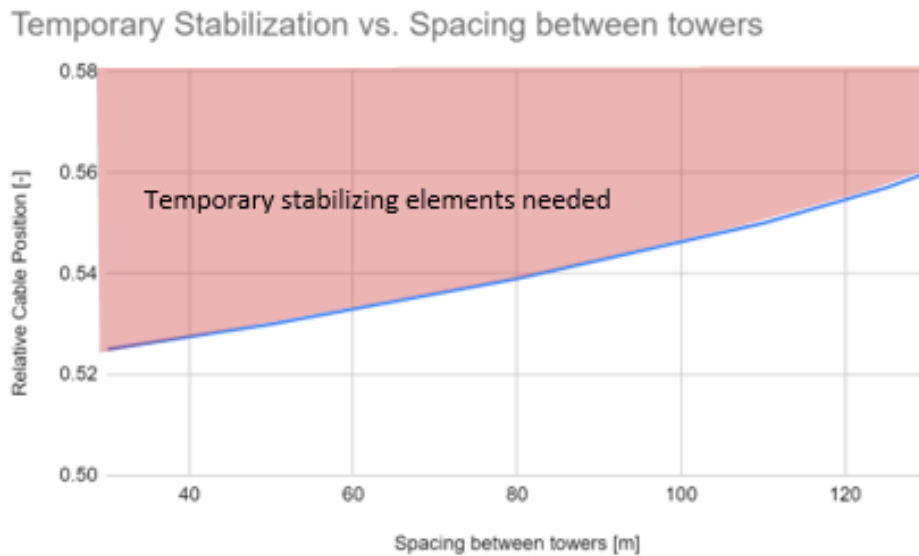


Figure 85 Temporary Stabilization minimum line

### 7.3. Lowest relevant position

As seen in Chapter 6.3, the influence of the cable-net becomes larger with the increase in RPC. Following the same logic, the lower the cable-net is applied, the smaller its influence on the design of the core. Such, the lowest position at which the cables should be applied so that they would still have a positive influence is searched for each spacing case. If the cables would be applied at a lower position, then the found one, no added value would be present, as the maximum achievable slenderness would be the same as in the case of the single core system.

The simple core system meets the deflection limit criterion when a slenderness of 1/8.1 (core width of 12.3 meters) is used. The relative cable position values for which the same core width is needed to meet the deflection limit criterion were searched for each spacing case, using an iterative process. Similar to the previous analyses, a zone, based on the RPC and SBT is plotted, to show the behavior of the system. If a system configuration corresponds below the line in Figure 86 it is concluded that the presence of the cable-net adds no additional benefit.

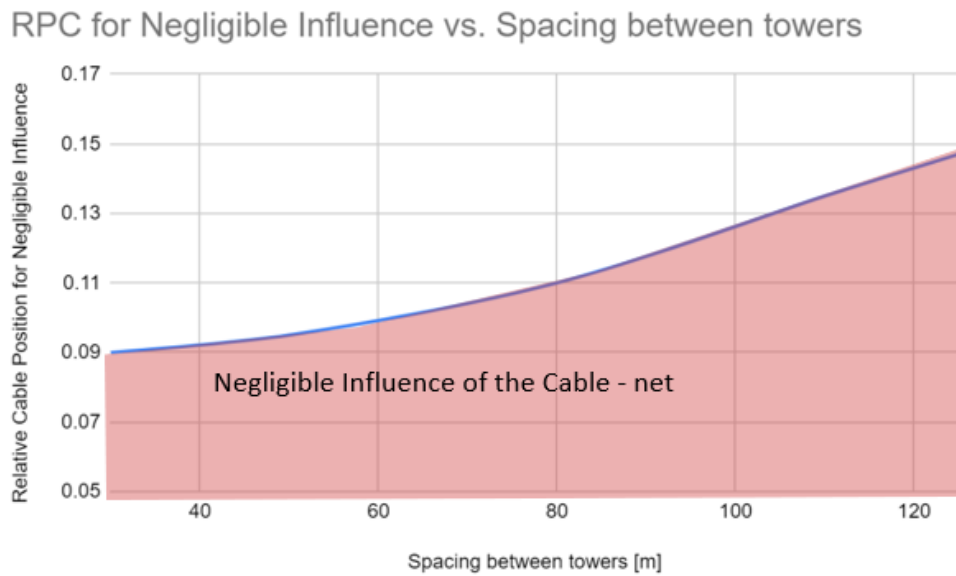


Figure 86 Negligible influence of the cable-net

## **Phase 3: Elaboration**

# 8. Results

---

## 8.1. Preliminary design of the system

---

The overall design of the system is influenced by the parameters explained in the Chapter 6 and 7. As shown, for certain configurations of the system the core design becomes governing due to the crushing of the concrete, or temporary stabilizing elements are needed, or the cable-net simply adds no added value to the stiffness of the core. Such, considering all the presented information, preliminary design guidelines with respect to the two main parameters, the spacing between towers and the relative position of the cable-net can be outlined. It has to be noted that these preliminary guidelines are based on the minimum possible stiffness of the cable-net, as the cable elements are designed to achieve an optimal cross section utilization (Chapter 6.2), and that they are obtained under the imposed initial assumptions.

Further, as presented in Chapter 6.2, the design of the cable-net for a high spacing between towers (of more than 110 meters) leads to a great number of cables, with high diameters and high steel weight. Moreover, as shown in Chapter 7.1, the load imposed by the mountain, becomes significantly high, exceeding the whole weight of the tower, when the spacing between towers exceeds 100 meters. Due to a big mountain area, it is expected that the high spacing cases will further cause significant economic implications. With these remarks in mind, it is assumed for the preliminary design of the system that a spacing between towers higher than 110 meters is inefficient.

Based on the studied parameters, and the behavior of the core under different systems configurations, the design space can be divided in multiple zones. Such, Figure 87 is produced, showing the behavior of the system under different geometrical configurations, and presenting the achievable slenderness and governing design criteria for any chosen relative position of the cable-net and spacing between towers. The figure is divided into three zones, based on the following plotted curves:

- Blue Curve (“Top Boundary”) → the curve above which, if the system configuration is placed, the design of the core becomes governing, as its utilization is higher than 100% causing its failure due to the occurring forces, as explained in Chapter 7.1;
- Red Curve (“Bottom Boundary”) → the curve below which, if the system configuration is placed, the cable-net has negligible influence, as explained in Chapter 7.3;
- Green Curve (“Temporary Stabilization”) → the curve above which, if the system configuration is placed, temporary stabilizing elements are required during the construction phase, as explained in Chapter 7.2;

- Black vertical line → corresponding to the previously explained set maximum value of the spacing between towers of 110 meters, above which the cable-net design is considered inefficient;

**Zone 1** is the zone in which the lateral stability of the system is the governing design criterion. In such a case, the maximum achievable slenderness, obtained by limiting the top deflection to  $H/500$  as presented in Chapter 6.3, can be reached. This zone can be seen as an optimum zone for the design of the cable-net + core system, as the mountain (combined with the horizontal wind load) does not add an excessive amount of load to the core, such that it would cause its failure. In this zone, the biggest economic benefit is expected due to the material reduction needed for the core, as the core does not need to be over dimensioned to account for the occurring forces. This reduction is directly influenced by the increase in slenderness, and further explained in Chapter 8.4.

The boundaries of the zone are defined as the Blue Curve (“Top Boundary”) and Red Curve (“Bottom Boundary”) in Figure 87. Zone 1 is further divided in three zones:

- Zone 1a → zone in which the design is optimal, and a significant increase in slenderness (ranging from  $1/12$  to  $1/16.5$ ) is observed, compared to the simple cores system slenderness of  $1/8.1$ ;
- Zone 1b → zone in which the design is optimal, but a more modest range of slenderness of  $1/8.3$  to  $1/12$  is obtained;
- Zone 1c → zone in which the design is semi-optimal, as solutions for a temporary stabilizing system during the construction phase must be sought;

**Zone 2** is the zone in which the design of the core becomes governing due to a utilization of the core exceeding 100%. In this zone, the core needs to be over dimensioned, and the reduced width of the core needed to reach a top deflection of  $H/500$  cannot be achieved. This further leads to a less economical design, as the material reduction is expected to be less substantial than in the cases classified in zone 1.

**Zone 3** is the zone in which the influence of the cable-net is negligible when compared to a simple core system. In these cases, the cable-net does not add benefit to the slenderness of the core.

## Design Zones based on Relative Cable Position and Spacing Between Towers

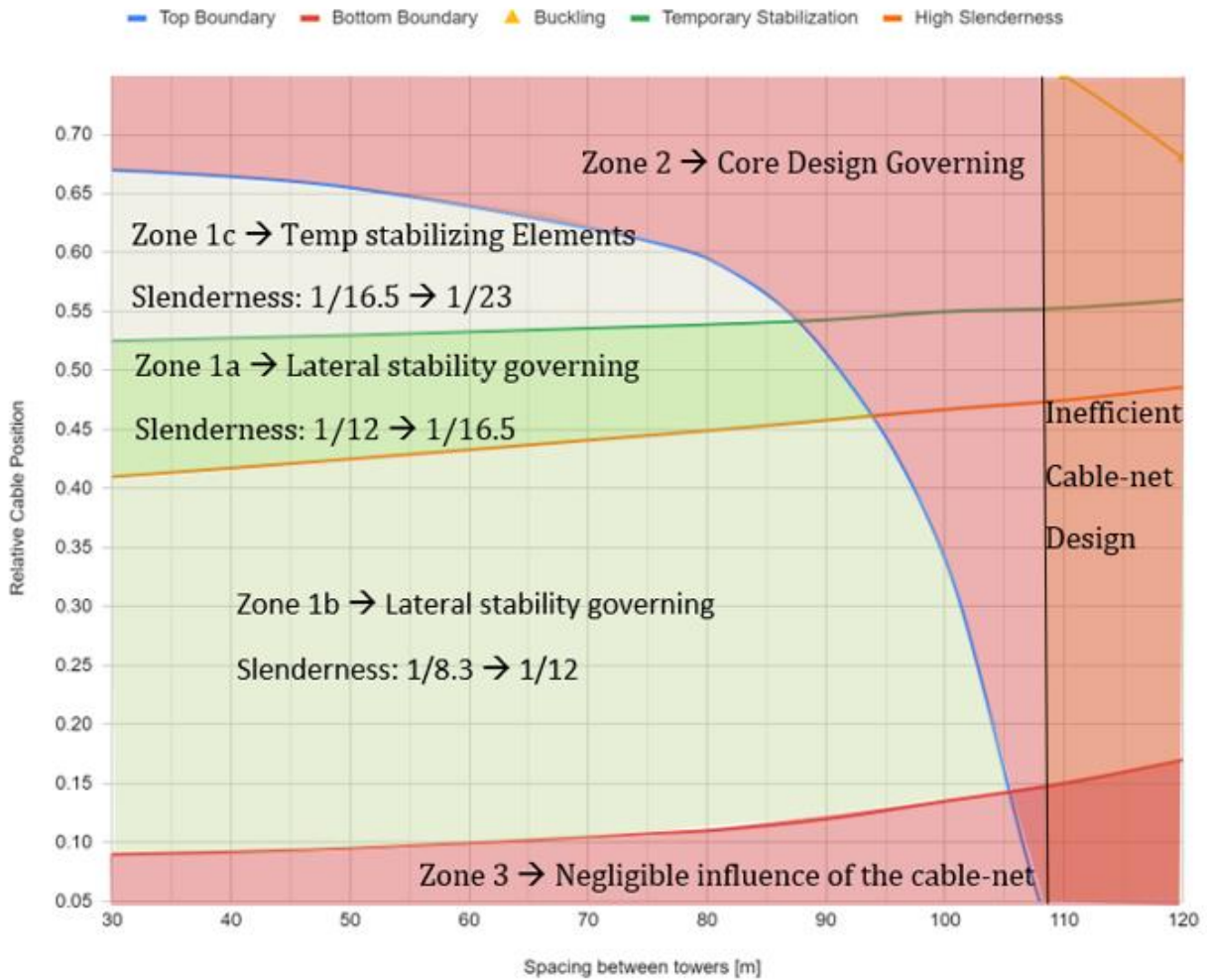


Figure 87 Design zones based on the RPC and the SBT

Based on Figure 87, the previous Figure 72 showing the increase in slenderness with respect to the relevant parameters can be revised, to account for the cases in which the design of the core is governing. Such, the slenderness curves flatten after the relative cable position for which the maximum utilization of the core is reached, for each spacing case. Such, the revised slenderness curves are plotted in Figure 88. Zone 2 is visible in the new slenderness graph, starting from the points at which the curves flatten. Compared to Figure 72, in Figure 88 the cases of 90 and 100 meters spacing are also present.

## Core Slenderness vs Relative Position of the Cable Net

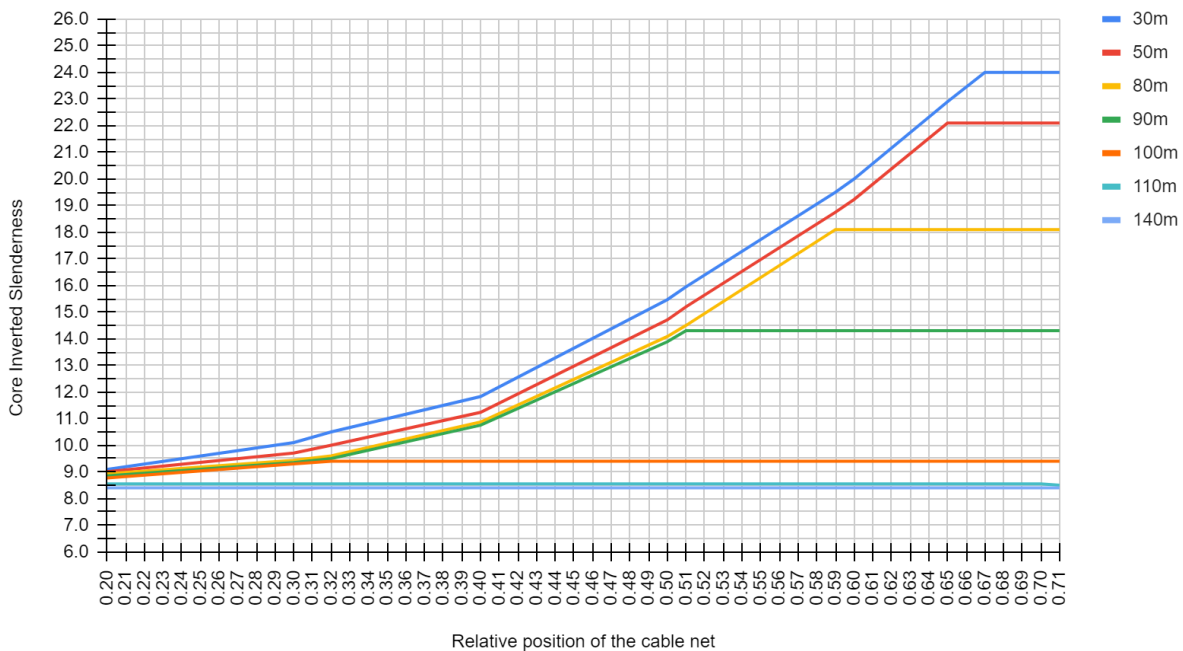


Figure 88 Core Adjusted Slenderness based on Zones

### Preliminary design of the system → Example:

Using the two graphs presented in Figure 87 and Figure 88, a structurally feasible preliminary design of the system can be obtained from an early stage, by only imposing requirements in terms of the two studied relevant parameters: the SBT and the RPC. A two-step procedure is conducted to gain information on the maximum achievable slenderness of the core, to be designed together with the cable-net. The two steps are presented below, followed by an example, to check the validity of the proposed method:

#### Step 1: Choice of the system geometry, based on the design zones.

The first step is to choose the preferred design zone, based on the desires of the designer and/ or architect. As presented above, from a structural and economical point of view, the best design zone in which the system is to be placed is zone 1 (and, specifically, zone 1a). However, more factors can come into play, such as restrictions imposed by site configurations (which may impose a minimum and maximum spacing between towers) or architectural desires. Based on the chosen design zone, the two relevant parameters (SBT and RPC), can be chosen to satisfy the boundaries of the zone or vice-versa (by imposing the two parameters, the design zone in which the system falls is obtained).

An imposed configuration in zone 1a, for example, can lead to an RPC of 0.52 and SBT of 80 meters (Example A in Figure 89), while a configuration in zone 1b can lead to an RPC of 0.37 and SBT of 50 meters (Example B in Figure 89).

## Design Zones based on Relative Cable Position and Spacing Between Towers

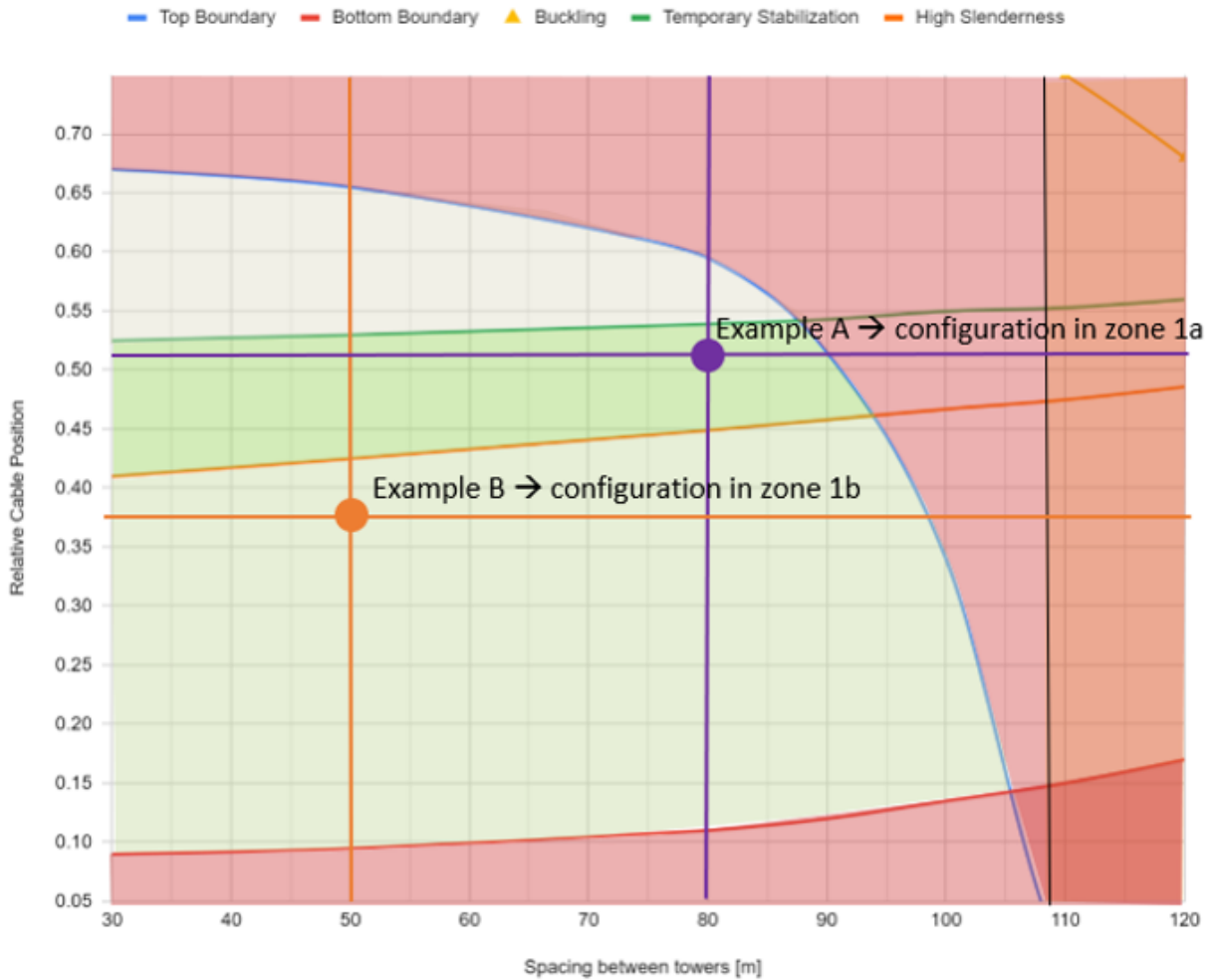


**Figure 89 Preliminary design examples A and B**

### **Step 2:** Preliminary design of the core system (maximum achievable slenderness).

Based on the chosen RPC and SBT, a maximum achievable slenderness for the core system can be determined. This is done using Figure 88 and exemplified in Figure 90, in which the maximum slenderness is plotted as a function of the RPC and SBT.

- In Example A the configuration leads to an approximate maximum achievable slenderness of  $1/14.9$ , corresponding to a core width of 6.7 meters.
- In Example B the configuration leads to an approximate maximum achievable slenderness of  $1/10.9$ , corresponding to a core width of 9.2 meters.

## Core Slenderness vs Relative Position of the Cable Net

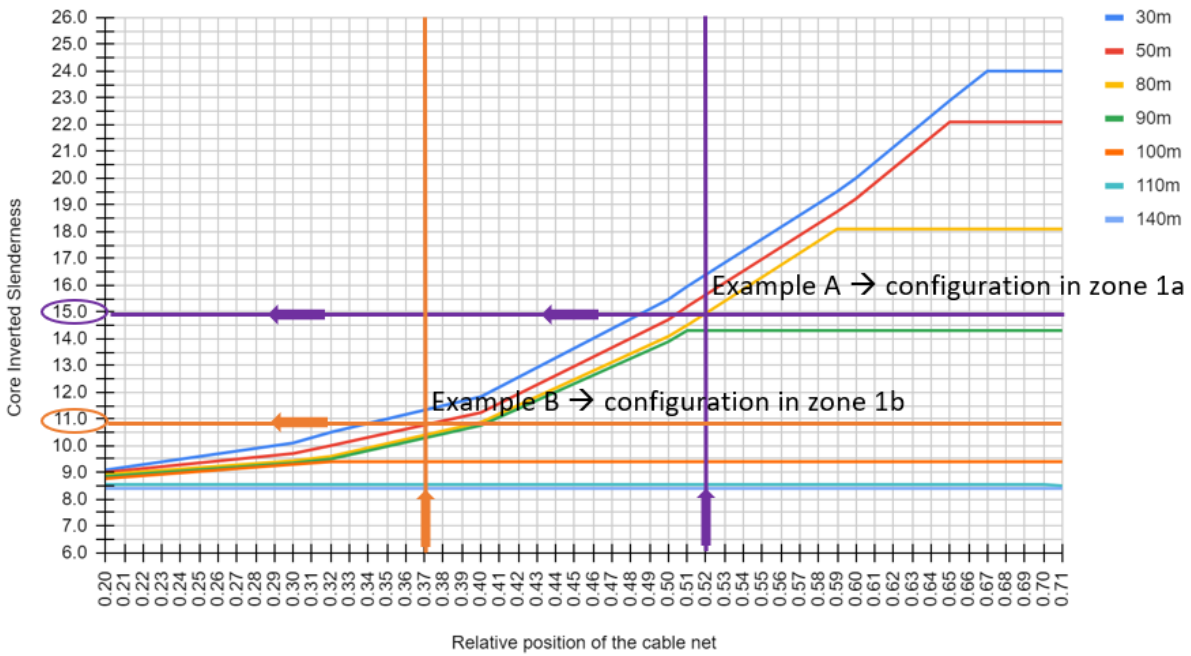


Figure 90 Preliminary design example A and B

### Example:

The proposed system configuration presented in Example A (RPC of 0.52 x H and SBT of 80 meters) is chosen to check the validity of the proposed method. The example led to the slenderness of 1/14.9, with the core dimensions of 6.7 x 6.7 x 0.35 meters. The system is analyzed with the same procedure as for the iterative analysis of the changeable parameters for the 3D study (Chapter 6, 7) as follows:

- Firstly, defining the input parameters of the system in Grasshopper, by representing the infinite rectangular grid of towers with 9 equally spaced towers (Figure 91);
- Then, performing the form finding process in Kangaroo to obtain the equilibrium geometry of the net, with a sag/ rise of approximately 4% (Figure 92);
- Then, exporting the resulting geometry as well as the boundary and loading conditions corresponding to the middle tower to Robot Structural Analysis (Figure 93);
- Then, performing the nonlinear analysis in Robot, and outputting the results (Figure 94, Figure 95);

The design of the 80 meters cable-net is according to the minimum required diameters and prestress values to satisfy the serviceability limit state and ultimate limit state, as explained in Chapter 6.2.

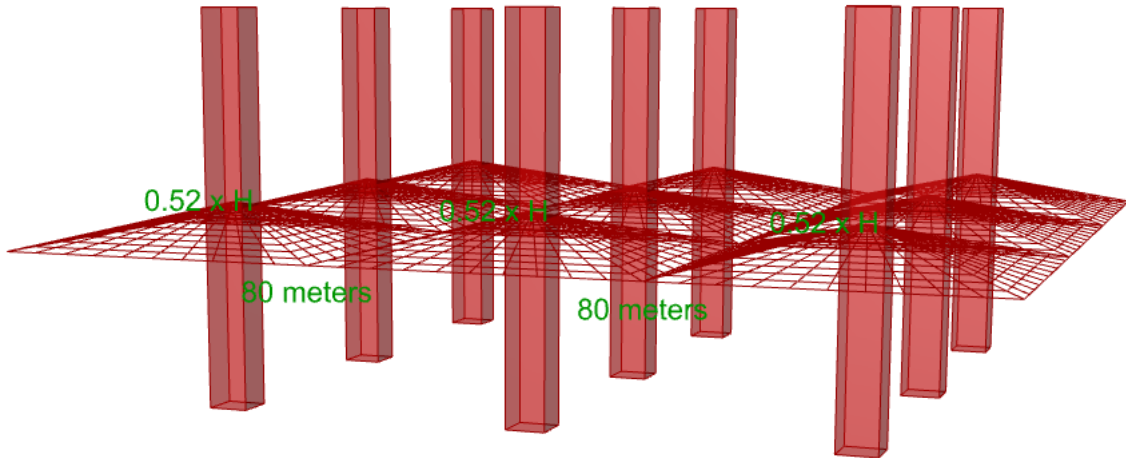


Figure 91 Initial Geometry (0.52 RPC & 80 meters SBT)

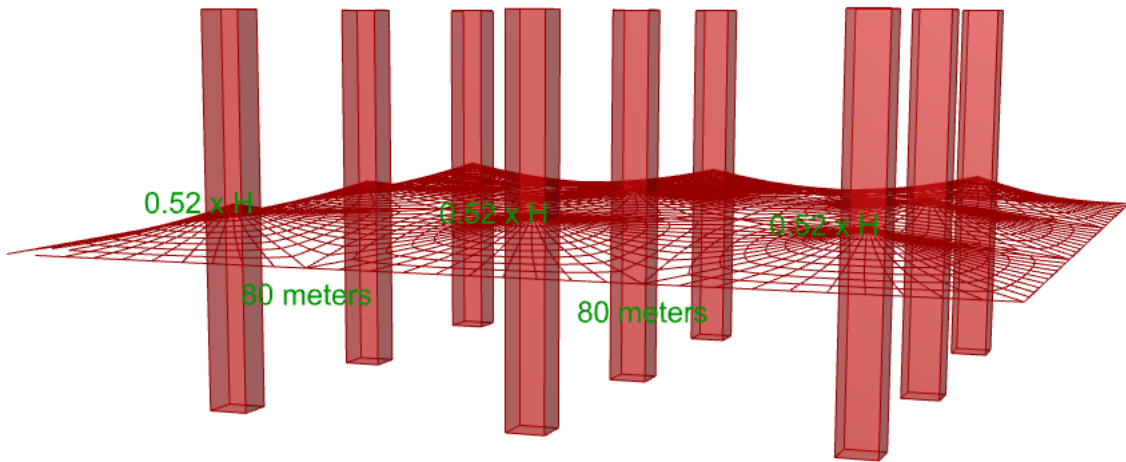


Figure 92 Form Found Geometry of the cable-net

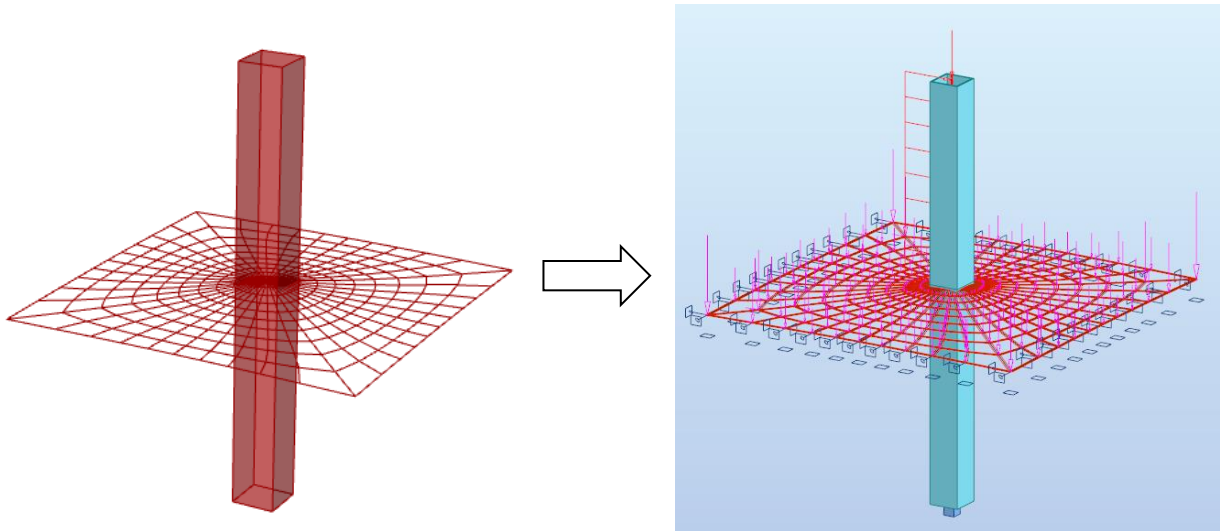


Figure 93 Middle tower export to Robot

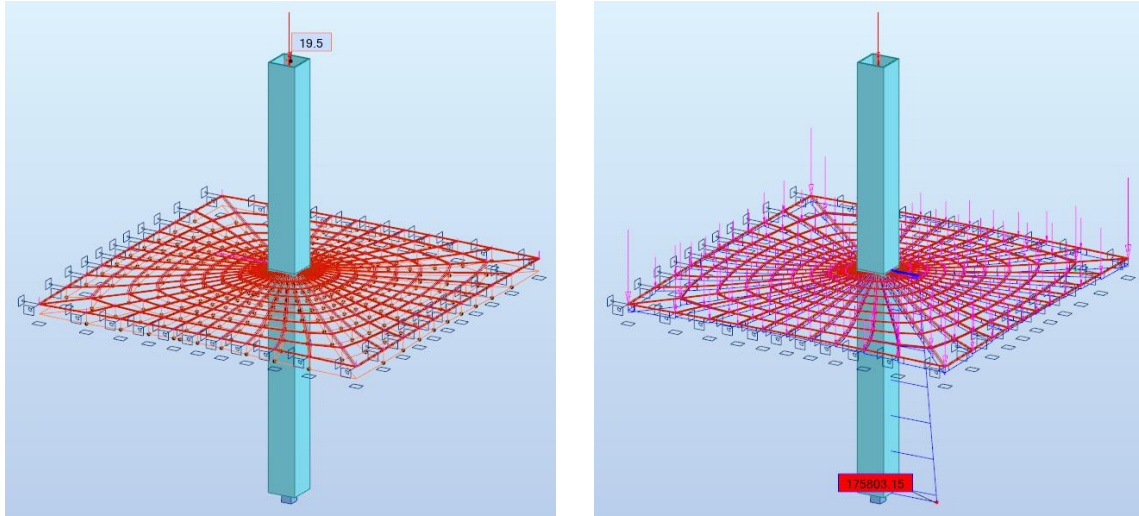


Figure 94 Results-Left: Top displacement (SLS-1); Right-Axial Force (ULS-3)

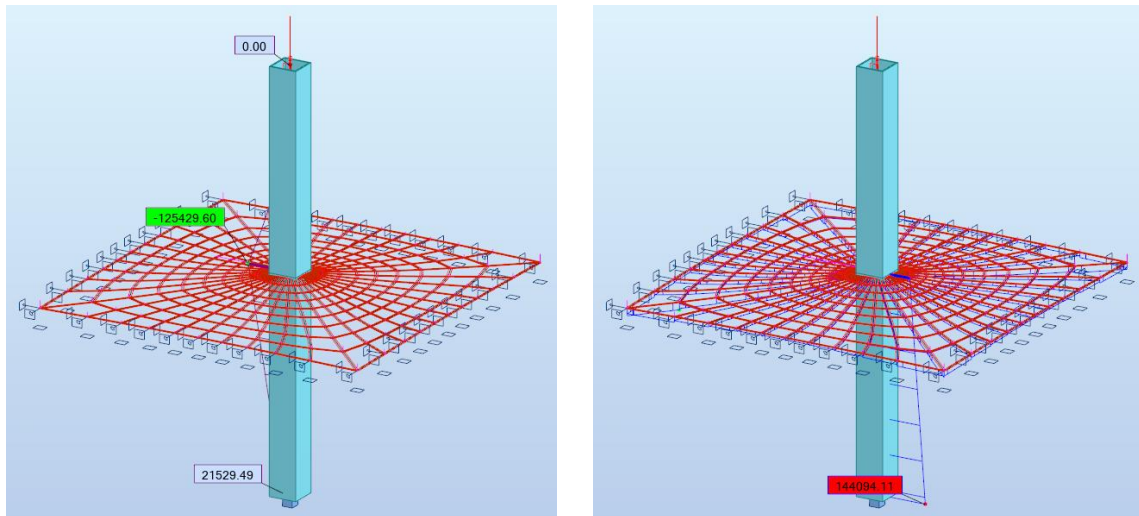


Figure 95 Results-Left: Bending Moment (ULS-4); Right-Axial Force (ULS 4)

Table 26 RSA Results → Example A study case

	Top Deflection [mm]	Axial Force ULS 3 [kN]	Axial Force ULS 4 [kN]	Bending Moment ULS 4 [kN x m]
0.52 x H RPC 80 meters spacing	195	175803	144094	21529

The results are in line with the expected behavior of the system, based on the preliminary guidelines. The calculations of the stresses, buckling critical load and top deflection in Phase 1 of the construction phase are performed as described in Chapter 7 and Appendix H.

- The top deflection at the top of the core, in the governing SLS combination (SLS 1) does not exceed the acceptable limit of  $H/500$ , with a maximum deflection of 195 mm (lower than 200 mm, corresponding to the limit of a 100 meters high tower);

- The bending moment at the bottom of the core is small, as expected from Figure 75, with a value of  $\sim 21\,500$  kN x m, and no tensile stresses occur;
- The maximum compressive stress in the core in ULS 4 has value of 24.7 MPa, lower than the design resistance of the C45/55 concrete of 30 MPa;
- The maximum compressive stress in the core in ULS 3 has a value of 26.2 MPa, lower than the design resistance of the C45/55 concrete of 30 MPa;
- No buckling issues occur, as the critical load calculated according to Euler's formula is significantly larger than the actual axial force;
- No stabilizing elements are needed, as the top deflection during Phase 1 of the construction sequence is lower than the maximum allowable deflection with a UC of 0.78;

**Table 27 Design check for the example case**

Design Check	Governing load combination	Value	Allowable Value	Unity Check
Top deflection [mm]	SLS-1	195	200	0.98
Compressive stresses bottom [MPa]	ULS-3	26.2	30	0.87
Compressive stresses bottom [MPa]	ULS-4	23	30	0.82
Buckling failure [kN]	ULS-3	175803	1852583	0.09
Top deflection Phase 1 [mm]	SLS-1	82	104	0.78

As all the proposed design checks are met, it is validated that Figure 87 does indeed provide a strong preliminary design guideline for the system, with respect to the spacing between towers and the relative position of the cable-net, under the imposed initial assumptions of the research.

## 8.2. Comparison to the 2D case

A comparison to the 2D case is further proposed, to check the reliability of a simplified, linear, 2D analysis in Karamba, as it was proposed in the early steps of the thesis (Chapter 4 and 5). To do a fair comparison, the actual used dimensions of the cable-net, as calculated in Chapter 6.2, are modelled as an equivalent diameter, to be applied to the 2D model. It must be noted that this is a reverse process, as the diameters used for the net were calculated based on the output of the 3D model. It is virtually impossible to determine the actual dimensions of the cable elements in a 2D case, but engineering judgement and justified assumptions can be imposed. By calculating the effective area of each cable contributing towards the windward side, an equivalent single cable diameter of 360 mm is obtained.

The comparison case is the one previously presented in Example A, with an RPC of 0.52 and a SBT of 80 meters, and a concrete core of 6.7 x 6.7 x 6.7 meters. The same material properties are used, and the same loading values and combinations are imposed on both models, based on the assumptions in Chapter 3. The mountain load is calculated by means of tributary area and linearly distributed on the equivalent cable.

Table 28 Equivalent single cable diameter calculation

Spacing case [-]	Cable Diameter // Number of cables [mm // -]	Angle factor for windward side [-]	Equivalent Area [cm <sup>2</sup> ]	Equivalent Single Cable Diameter [mm]
80 meters	Edge cable 150 mm / 2 cables Internal Diagonal Cable 110 mm / 18 cables	0.55	1032	360

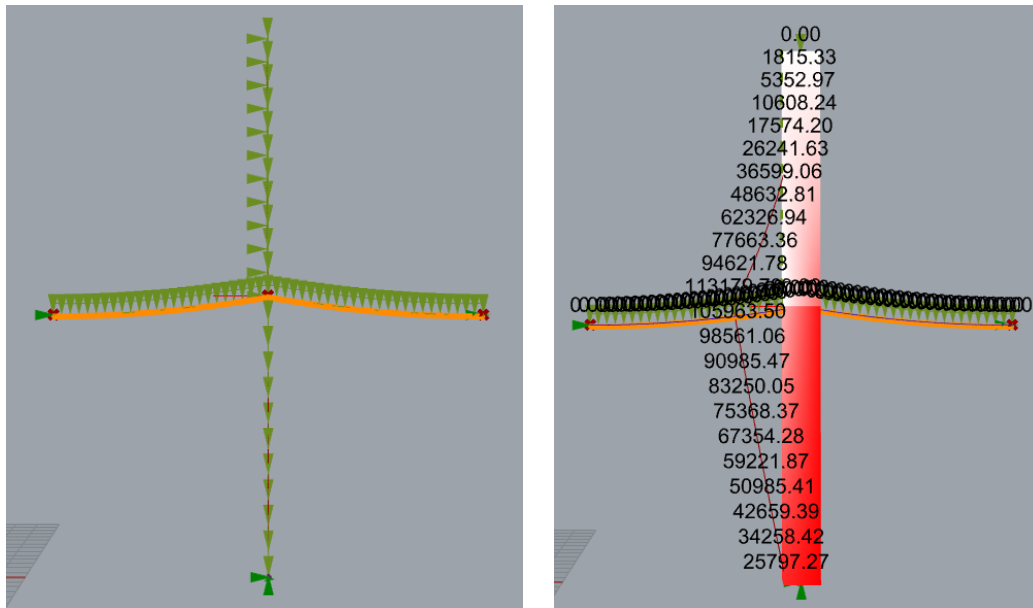


Figure 96 2D model (Karamba3D)

Table 29 Comparison between 2D and 3D study results

Result	2D study	3D study	Difference
Top Deflection SLS 1 [mm]	241	195	18.3%
Bottom Bending Moment ULS 4 [kN x m]	25797	21529	19.1%
Bottom Axial Force ULS 3[kN]	176532	175803	0.9%

A difference of 18.3% is observed in the results regarding the top displacement, showing a slight underestimation of the stiffness of the system in the 2D case. This is backed up by the difference of 19.1% in the bottom bending moment, the 2D case overestimating the results. However, the results are of the same magnitude order, showing that for early calculations and preliminary design situations, a 2D approach can provide a rough understanding on the behavior of the system.

### 8.3. Comparison to existing systems

---

The system is further compared to other conventionally used lateral load resisting systems for high-rise towers. Such, the performance of the previously studied case (Example A), configured in zone 1a with the RPC of 0.52 and SBT of 80 meters is compared to a simple core system and an outrigger system. A simplified analysis is performed for the two conventional systems, presented in the following subchapters, the goal being to observe the difference in terms of material usage and bottom bending moment for configurations that lead to the same performance, using the top deflection as comparison parameter.

The top deflection is obtained in the governing SLS load combination (SLS 1), and the bottom bending moment in the ULS combination where lateral forces are also included (ULS 4). For the cable-net + core system, the results are obtained from Chapter 8.1, as follows:

- Top deflection = 195 mm;
- Bottom bending moment = 21 529 kN x m;

This configuration leads to a concrete weight for the core of approximately 2200 tons and a total steel weight for the cable-net of approximately 268 tons.

#### 8.3.1. Simple Core System

The simple core system acts as a fixed cantilever that laterally deflects under the lateral loads. The modulus of elasticity of the concrete is reduced over the height of the core to the value of 9100 MPa, as described in Chapter 3. To obtain the admissible top deflection of  $H/500$ , the core needs to be 12.3 meters wide (slenderness of 1/8.1), as already seen in Chapters 4, 5 and 6.

This configuration leads to a concrete weight for the core of approximately 4200 tons. The results in terms of the top deflection and of the bottom bending moment are as follows:

- Top deflection = 198 mm ;
- Bottom Bending Moment = 434 863 kN x m;

#### 8.3.2. Outrigger System

A simplified analysis is also performed for an outrigger system with a conventional configuration. The core dimensions are maintained the same as for the cable-net + core system (6.7 x 6.7 x 0.35 meters), the modulus of elasticity is reduced over the height of the core, with a value of 9100 MPa, and the stiffness of the outrigger is chosen based on the recommendations of Terwel et al. (2017) to limit the top deflection, as follows:

- Outrigger on two levels, with the middle position at  $0.61 \times H$ , with the configuration:
  - Four columns: HEM 900;
  - Horizontal Beams of the Outrigger: HEM 550;
  - Diagonals Hollow Cross Section 300 x 40 mm;

This configuration leads to a concrete weight for the core of approximately 2200 tons and an approximate steel total weight of the outrigger system of 284 tons. The results in terms of the top deflection and of the bottom bending moment are as follows:

- Top deflection = 198 mm;
- Bottom Bending Moment = 230 723 kN x m;

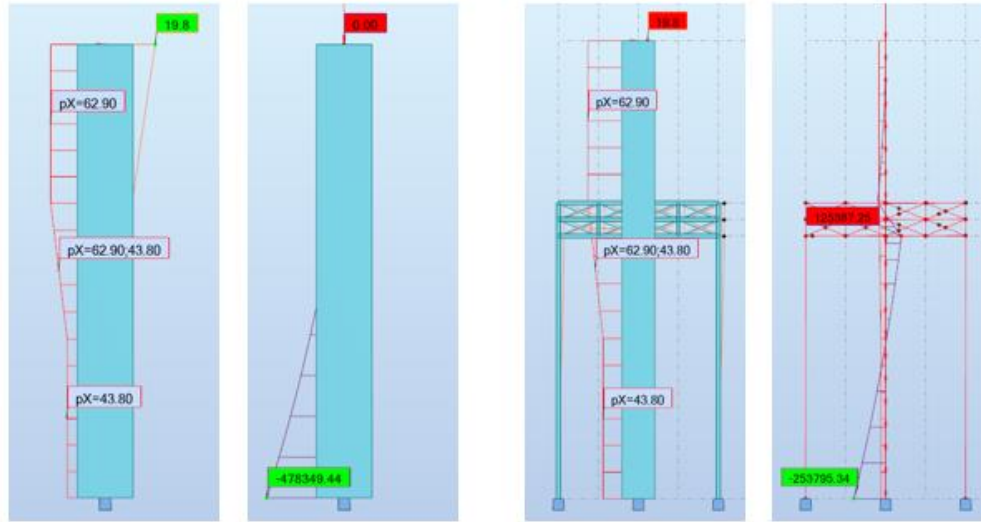


Figure 97 Left: Single Core System Results; Right: Outrigger System Results

### 8.3.3. Simplified comparison

Through this simplified comparison, the core + cable-net system shows to be a feasible alternative to the existing lateral load resisting systems commonly used for high-rise towers. With the reference height set to 100 meters, systems as the tube or mega frame were not included in the comparison, as they are typical solutions for higher buildings. From Table 30 the clear reduction of the bending moment at the foundation level, compared to the simple core system is observed. This reduction is significantly larger than the reduction that the outrigger provides. More importantly, the weight calculation shows a reduction of the concrete required to almost half, when compared to the single core system - this is further discussed in Chapter 8.4, where preliminary economic evaluations are presented. Further, the weight of the steel necessary for the used cable-net is comparable (in this case slightly lower), to the total weight needed for the outrigger system. However, an economic comparison is difficult to produce in this regard, as the steel of the outrigger is a common steel grade of S355, while the cable-net is produced of high strength steel wires. Overall, it can be concluded that the proposed system offers an alternative to other stability systems, as its performance and weight is comparable or slightly better in certain regards.

Table 30 Comparison for similar configuration

System [-]	System Description [-]	Top Deflection [mm]	Bottom B.M. [kN x m]	Concrete Weight [ton]	Steel Weight [ton]
Core System	12.3 x 12.3 x 0.35 m core	198	478 394	4182.5	-
Outrigger System	6.7 x 6.7 x 0.35 m core	198	253 795	2222.5	284.4
Core + Cable-net	6.7 x 6.7 x 0.35 m core	195	21 529	2222.5	268.3

## 8.4. Simplified economic evaluation

---

Based on the outcome of the study with respect to the behavior of the system, finding a suitable range of slenderness in which the system falls based on the relevant parameters, preliminary economic evaluations can be obtained. The evaluation is performed for zone 1a of Figure 87, where the achievable slenderness is highest, without having the need of adding temporary stabilizing elements during construction phase. As show, the slenderness in this zone ranges between  $1/12$  and  $1/16.5$ . These system configurations are compared to the simple core system, which requires a slenderness of  $1/8.1$ . Appendix I shows the procedure used for the simplified economic evaluation, presenting the background of the information in this chapter.

The simplified evaluation is performed using as comparison parameter the weight of the structure. Such, by calculating the total weight of the towers structure in the case where a simple core stability system is used, and comparing it to the total weight of the towers structure when the cable-net adds to the stiffness of the system, a simplified comparison can be obtained. In this case, only the weight of the tower is included in the calculations, without adding the weight of the cable-net and the weight of the mountain.

The weight is calculated using a conventional floor plan for a typical rectangular tower, with the in-plane dimensions of 30 meters by 30 meters used throughout this thesis. In order to simplify the economic implications, the tower is fully built out of cast in situ reinforced concrete, using the presented elements dimensions (beams, columns, slab) found in Appendix I. For the 100 meters tall tower, 27 floors are assumed. This leads to an approximate concrete volume of 198 cubic meters / floor, or approximately 490 tons of concrete / floor.

Similarly, the weight of the core is calculated for the case of the simple core system, and for the cases of cable-net stabilized core systems. As the width of the core is significantly larger in the case of the simple core, its weight is consequently higher. By differencing the weight of the core in the two cases, a volume reduction can be found when the cable-net is added. Further, this volume reduction can be used to calculate the number of extra floors that can be built with the same amount of material. Table 31 shows the difference in the concrete volume for the two cases, of the simple core and of the cable-net stabilized core, and the equivalent constructable number of floors with the corresponding reduction.

**Table 31 Equivalent number of extra floors based on volume reduction**

Simple Core			Cable-net Stabilized Core			Volume Reduction [m <sup>3</sup> ]	Equivalent number of extra floors
Core Width [m]	Slenderness	Core Volume [m <sup>3</sup> ]	Core Width [m]	Slenderness	Core Volume [m <sup>3</sup> ]		
12.3	1/8.1	1673	8.3	1/12	1118	555	~3
			7.7	1/13	1028	645	~3
			7.1	1/14	951	722	~4
			6.7	1/15	884	789	~4
			6.3	1/16	826	847	~4
			5.9	1/17	775	898	~5

Further, a comparison can also be made not by considering the equivalent numbers of extra floors, but by representing the volume reduction as percentage of the total volume, for a tower of the same height. This total volume, for the simple core system adds up to approximately 7200 cubic meters. Such, a reduction of 7.8% up to 12.8% is observed when increasing the slenderness of the core, due to the stiffening effect of the cable structure, as Figure 98 presents.

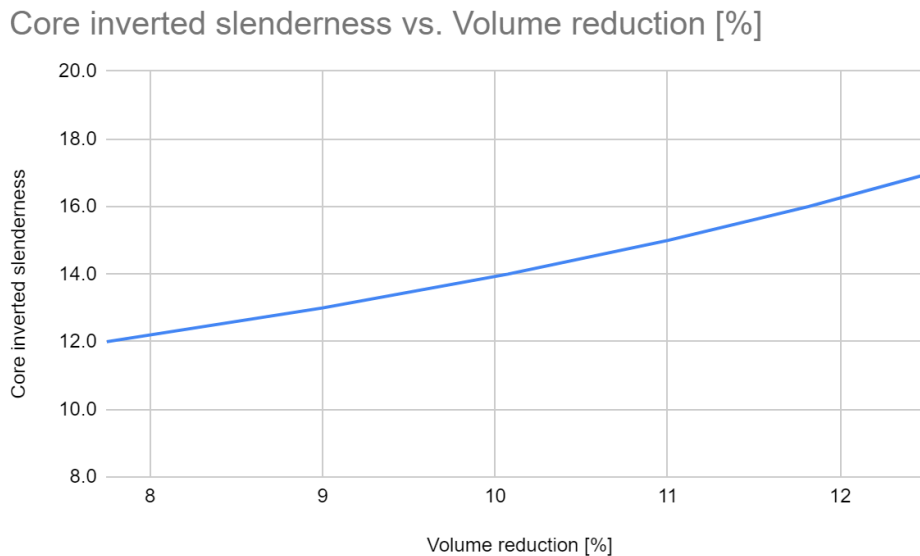


**Figure 98 Core inverted slenderness and volume reduction**

# 9. The Rotterdam Mountain Project

---

The secondary objective of the thesis is to provide a feasible design alternative for the Rotterdam Mountain, to respect the site configuration of the Terbregseplein in Rotterdam. To do so, the used parametric script is developed to create a pattern of tower placement to respect with a set of requirements. The goal is to design each tower, representing a core + cable-net system, in the proposed optimal design zone 1a, as explained in Chapter 8. Such, the following requirements are set for the output of the parametric script:

- Provide a system configuration such that every core is placed in the buildable area of the Terbregseplein intersection (Figure 99);
- Provide a system configuration in which the spacing between towers is between the set limits of zone 1a (30 and 110 meters), but in which the spacing between towers is equalized to obtain, as much as possible a rectangular grid;
- Provide a system configuration in which the relative position of the cable-net is between the set limits of zone 1a (0.4 to 0.55) → an RPC of 0.5 is chosen for all towers.
- Limit the height of the towers up to 110 meters.

The following remarks are addressed with respect to the placing of the towers:

- The towers use a height ranging from 30 to 110 meters, to respect the mountain orography (at the middle, big heights are used, while at the perimeter low heights are used).
- Areas where the spacing between the cores needs to be larger than 110 meters are identified, where the cable-net needs to pass the highway. These zones shall require further attention in a possible later study.

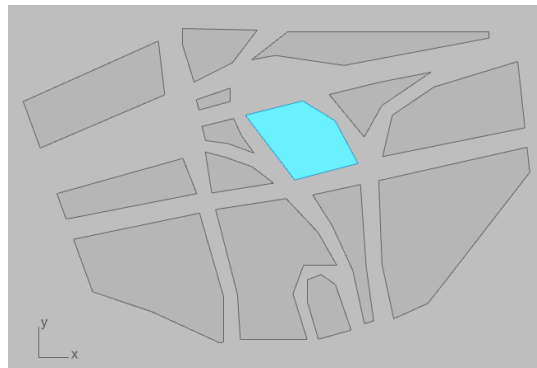


**Figure 99 Buildable Area of the Terbregseplein highway node**

A full analysis of the system was desired for the Rotterdam Mountain. However, due to the extremely large number of cable elements (58 000 individual cable elements for the whole configuration), a bigger computational power than the one available for this research would have been needed. Such, a simplified analysis, considering only one buildable area (highlighted zone in Figure 99) was performed. Nine cores have been modeled to populate the proposed area, with an average spacing between towers of 50 meters, and analyzed by the same method used for the 3D study (Chapter 6 and Chapter 7):

- First modelling the initial geometry of the system;
- Then performing the form finding process to obtain the final geometry of the cable-net to be analyzed with the towers;
- Finally exporting the geometry to RSA and performing the nonlinear analysis;

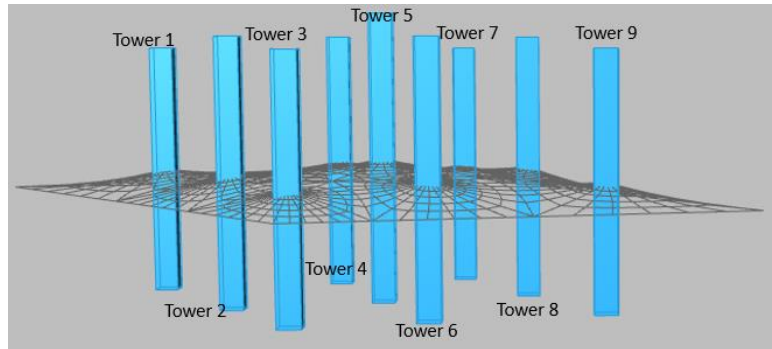


**Figure 100 Geometry of the system for the Rotterdam Mountain Proposal**

The geometrical properties of the system and the outlined results are presented below. Appendix J provides the background of the results, as well as the description of the steps taken in the preliminary design of the Rotterdam Mountain, and figures from the analysis model.

**Table 32 Geometrical properties and results of the Rotterdam Mountain preliminary design**

Tower	RPC [-]	SBT [m]	Max achievable Slenderness [-]	Core width [m]	Top Deflection [mm]	Unity Check [-]	Minimum Stress [MPa]	Utilization core [%]
Tower 1				6.1	210	<b>1.19</b>	34.8	<b>116.1</b>
Tower 2				6.3	143	0.77	26.2	88.4
Tower 3				6.1	126	0.72	24.4	85.8
Tower 4				6.3	134	0.73	22.9	81.4
Tower 5	0.5	~50	1/14.5	6.9	174	0.87	25.4	88.1
Tower 6				6.3	183	0.99	29.1	97.0
Tower 7				6.1	137	0.78	24.2	85.7
Tower 8				6.3	109	0.60	22.3	87.3
Tower 9				6.1	68	0.39	26.5	90.3

The chosen dimensions of the core are based on Figure 88, by designing the core in zone 1a (Figure 87) – for the chosen RPC of 0.5 and SBT of 50 meters, this translates to a maximum achievable slenderness of 1/14.5. The results are in line with the expected behavior of the system, as presented throughout this research. For towers 2-9 the unity check and utilization of the core are within the satisfactory margins. For tower 1, the unity checks are not satisfactory, so the width of the core needs to be increased. This is due to the fact that 50 meters spacing between towers was assumed. In reality, for Tower 1, the spacing is larger towards the towers that were not modelled, leading to a less stiff cable-net and a bigger tributary area loading the core than assumed in the predesign. Overall, the obtained results are adequate, further showing the validity of Figure 87.

# 10. Discussion

---

As the title of this thesis suggested, the goal of the research has been to provide *preliminary* guidelines on the design of cable-net stabilized towers. Such, a significant number of assumptions and simplifications have been imposed to reduce the big design space towards a more manageable problem. In this chapter, the starting assumptions and their influence on the final results is discussed. Further, the chosen methodology, software and analysis method and the sensibility of the results is addressed.

## 10.1. Discussion on the high-rise tower system

---

Throughout the research, a tower with unchangeable dimensions, as presented in Chapter 3, has been used. Further, a simple core lateral load resisting system has been imposed as the stability system for the towers, to be combined with the cable-net system. This has been assumed so that the influence of the cable-net becomes apparent, when comparing different cases, in terms of the studied variable relevant parameters. These assumptions further translate to:

1. A constant peak velocity pressure, leading to the same wind load value to be applied on the core above the position of the cable-net connection for all studied cases.
  - A tower with rather wide in-plane dimensions has been considered for the study (30 x 30 meters), to lead to conservative results for the range maximum achievable slenderness for the system. Naturally, if a tower with lower in-plane dimensions is proposed by the designer or architect, the total wind load to be transferred to the core decreases, leading to a higher maximum achievable slenderness based on the top deflection criterion.
  - Further, the studied tower was assumed to have a height of 100 meters. This can be seen as a reasonable assumption for the Netherlands, as most tall towers are in this height range. However, if the height of the tower changes, so does the peak velocity pressure, leading to slightly different wind loads on the tower. This will further lead to a slightly lower or higher range of achievable slenderness, based on the increase or decrease in the tower's height.
2. Only results based on the concrete core system for the tower, with the assumed fictitious E-value and a concrete class of C45/55.
  - The results only treat the case where the towers use a core stability system. The core enabled a rapid modelling process, as not many elements need to be inputted in the analysis software (compared to, for example, an outrigger system). Results in terms of the overall behavior of the system are expected to differ if a different lateral load resisting system is used for the tower (for example an outrigger + cable-net system, tube + cable-net system, etc.), and stiffer configurations may be obtained.

- The results only treat the case where the core is built of concrete. The fictitious E-modulus above the cable-net connection of 9100 MPa (reduced to account for tensile stresses and openings in the core) can be seen as a conservative assumption, as not in all systems configuration the tensile stresses exceed the tensile strength of the used concrete (see Appendix H). Such, the system may behave stiffer than the assumed design, under certain system configurations. The fictitious E-modulus below the cable-net connection (only reduced due to openings in the core) is considered as a fair assumption, as under no cases do tensile stresses occur at the bottom of the core (Chapter 7.1).
- If a different concrete class is chosen, the behavior in terms of the utilization of the core, as described in Chapter 7.1 also changes due to a different compressive resistance. Although higher than the typical concrete used for towers, C45/55 is considered a fair assumption, that can be used in practice. A higher concrete class is expected to increase the total costs, and a lower class leads to a more rapid reach of the maximum utilization, decreasing the range of achievable slenderness. Naturally, if the core is designed using a different material, such as a timber core or a braced steel core, the behavior of the system is expected to change significantly.

## 10.2. Discussion on the cables and cable-net

---

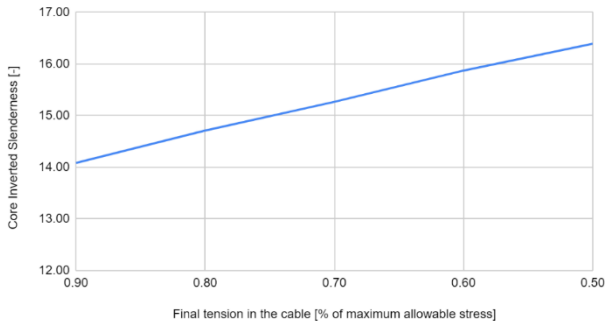
Throughout the research, the cables used are spiral strands, made of wires with the strength of 1570 MPa and with an E-modulus of 160 GPa, as presented in Chapter 3.2, in accordance with the EN 12385 recommendations. The typology of the cable-net is defined as a double-curved mast supported (with the cores acting as masts) with radial cables, with the average cable sag/ rise of 5% and average spacing between cables of 4 meters, respecting the guidelines proposed by Buchholdt (1999) and Krishna (2013) on the preliminary design of prestressed cable nets. These assumptions further translate to:

1. The design of the cable elements and stiffness of the cable-net
  - As explained in Chapter 6.2, and further developed in Appendix G, the cable elements are designed to an optimal unity check, both in terms of strength requirements (influencing area of the cable elements) and deflection requirements (influencing the final prestress). This translates to the fact that, the cable-net is designed to its minimum possible stiffness for each case. If the designer chooses to over dimension the cable elements or apply more initial prestress, this will further translate to an increase in the stiffness of the cable-net, and, consequently, an increase of the stiffness of the whole system. Such the found results in terms of range of slenderness, presented in Chapter 6.3 change, adding a third dimension to Figure 87. If a stiffer cable-net is used, naturally, a higher range of slenderness will be achievable. On the other hand, due to higher cable forces and a lower area of the core, the design of the core will become governing faster.

To further explain this concept, a simplified analysis is conducted for the case of an RPC of  $0.5 \times H$  and a SBT of 80 meters. Figure 101 shows the increase in the maximum achievable slenderness as a function of the increase in the stiffness of the cable-net. The cable-net is stiffened by using larger diameters of the cable than the needed ones, resulting in a lower unity check for the cable design

(horizontal axis of Figure 101), and further leading to an increase in the maximum achievable slenderness of up to 20%. On the other hand, the core utilization as defined in Chapter 7.1 also increases with the increase of the cable-net stiffness, as seen in Figure 102. This concept is visualized in Figure 103, that presents the increase in achievable slenderness in Zone 1, while the top boundary decreases.

Core Inverted Slenderness vs Cable Stiffness



Core utilization vs Cable Stiffness

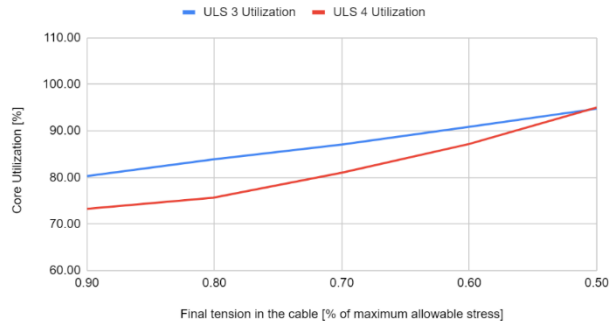


**Figure 101 Increase in core slenderness due to cable stiffness (Left)**

**Figure 102 Increase in core utilization due to cable stiffness (Right)**

Design Zones based on Relative Cable Position and Spacing Between Towers

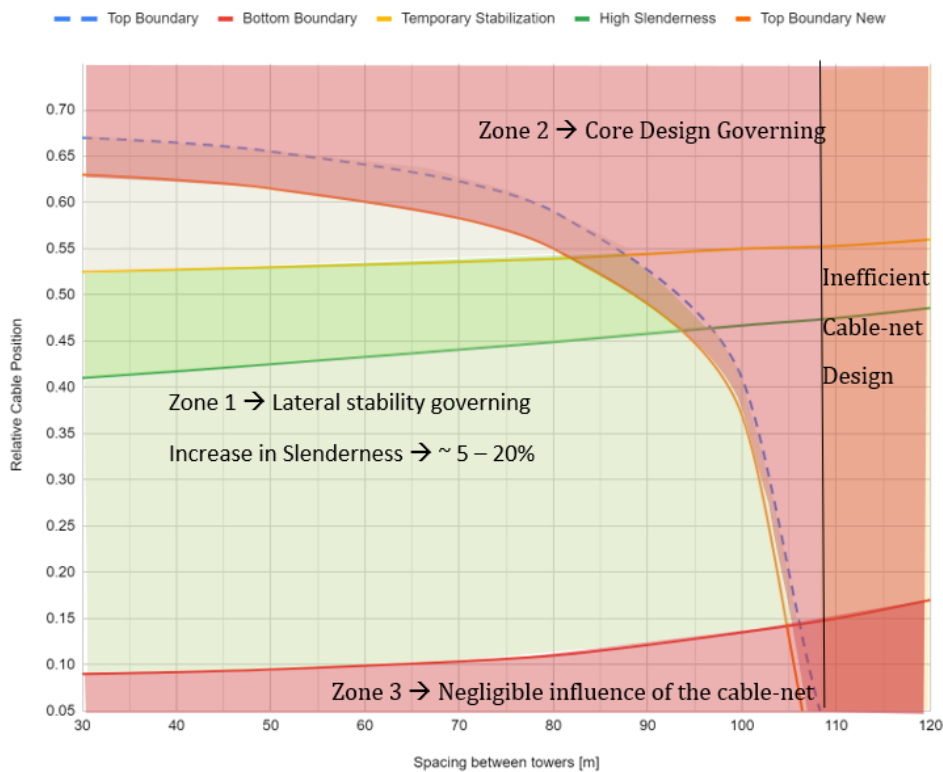


**Figure 103 Variability of the design zones graph based on the cable stiffness**

- Spiral strands are considered to be a reasonable starting assumption for the design of such system, due to their good strength/ weight ratio, availability in a great number of sizes, and due to their use in similar projects.

## 2. Typology of the cable-net

- The most supported typology for the cable-net has proven to be a suitable alternative for the design of the mountain. Using the imposed set requirements in terms of the sag / rise of the cable-net has led, as Buchholdt described, to a sound design of the net, as the deflections under the governing SLS combination were maintained under the admissible limit, while limiting the prestress in the cables to a maximum of 40% of their ultimate strength capacity, according to the recommendations of Gabriel. Naturally, for a more thorough design of the system, different typologies of the net can be studied together with the tower. For example, as explained in Chapter 3.3, a cable-net using stronger edge cables or edge beams, together with a regular cable grid will lead to more sagged cables and higher local forces on the core, which will lead to a different overall behavior of the system.

## 3. Not included in the *preliminary* design of the cable-net

- Dynamic analysis → a dynamic analysis was not included as part of the research. The justification is that, due to the big load imposed by the mountain surface, much higher than the occurring variable loads, the cable-net will not be subject to dynamic problems.
- Constructability → the constructability of the cable-net has not been addressed. Due to the used typology of radial cables, the connections between different cable elements need to be designed individually, which may impose challenges both from a constructability and economical point of view.

## 10.3. Discussion on the imposed loads

---

At the start of the research a thorough analysis of the loads acting on the structure was desired. However, as the Rotterdam Project is still in the very early design stages, a number of variables had to be assumed to define the loads. The principal assumptions regarding the loads, and their influence is as follows:

- Permanent mountain loads → the mountain load has been a central parameter of the Overall Design of the System (Chapter 7), as it has a high influence on the axial load on the core. As no information was provided on the actual stratification of the green roof, a conventional intensive green roof system was imposed, supported by a concrete slab on top of the cables. Based on the final desires of the designer, the actual loads may differ, thus influencing the design of the core. However, a conservative approach is used, as an intensive green roof system (heavier than commonly used extensive green roof systems), is used for the design of the mountain surface. An optimization of the used materials for the mountain can lead to lower axial loads on the core, thus increasing the range of achievable slenderness before the core design becomes governing.
- Wind load on the mountain → determining the actual wind loads acting on the mountain requires a thorough analysis and, preferably, a wind tunnel test. As such test has not been a part of the research, an assumption was made that the mountain's surface acts as a duo-pitch roof. Moreover, the horizontal component of the wind acting on the mountain is

imposed as a point load on the tower, at the position of the cable connection. It is expected that this is an overestimation of the wind loads, as the wind is imposed both on the tower as an equivalent point load, and at the cable-net joints as a vectorial sum of the normal forces (pressure/ suction) and the friction.

- Permanent loads imposed by the tower floors → throughout the research, the tower was assumed to be constructed of cast in-situ concrete, in order to allow for the ease of a simplified economic evaluation. Lighter solutions can be sought, such as composite floor systems typical for the design of high-rise towers, which can reduce the final axial load on the core. This can, as for the discussion on the mountain load, lead to the increase in the range of achievable slenderness before the core design becomes governing, due to the reduction in the axial load.

#### **10.4. Discussion on the proposed methodology**

---

The used methodology proposed a systematic approach, to gradually increase the level of complexity of the system, from a highly simplified 2D representation of the system using a linear analysis, to a more complex 3D representation of the system using a nonlinear analysis.

The benefits of the proposed methodology are retrospectively identified as follows:

- It allowed for an organized work process, by dividing the research into steps.
- It allowed for the understanding of individual parameters in the simplified 2D case, as the parameters were gradually added to the model (first the changeable parameters with respect to the geometric configuration - Chapter 4, then the prestress - Chapter 5.2, then the force density and load on the cables - Chapter 5.3).
- It allowed for a full analysis of the system in the 3D case, once the basis of the system behavior was understood, based on which the main conclusions of the thesis were drawn.

The drawbacks of the proposed methodology are as follows:

- The 2D case only offered preliminary results and conclusions, as it is difficult to represent the behavior of the whole 3D net using a 2D approach.
- The main results are based on the final step of the proposed methodology (Chapter 7), which can be seen as a slight inequality between the work load of the first steps and final step.

The methodology proposed the use of a parametric script throughout the research, to allow for the rapid change of the parameters. This approach allowed for the analysis of multiple iterations, that would have only been possible with a significant amount of time spent in modelling if a different approach was used. However, for the 3D cases, the export of the geometry from the Grasshopper environment to the Robot Structural Analyses software has been a time-consuming process. A better approach would have been to analyze the whole system within the Grasshopper environment with plug-ins such as Kiwi3D, that allow for tension only members and non-linear analysis. RSA has been finally chosen due to the larger community surrounding the software (including a fast support group and a big number of users) compared to the relatively new Kiwi 3D, as well as the authors expertise in the software.

## **10.5. Discussion on the 2D and 3D representation of the cable-net**

---

As presented in Chapter 8.2, a 2D representation of the cable-net was provided for a particular system configuration case and compared in terms of results to the 3D representation. Based on the results, the following comments can be addressed:

- A simplified linear 2D analysis can provide a good first estimation on the behavior of the system, as the results in terms of top deflection and bending moment are ~19% higher than in the 3D case, slightly underestimating the stiffness of the system. This can be seen as an acceptable margin for first conclusions in terms of the influence on the cable-net in an early design stage.
- To provide an accurate estimation on the equivalent cable diameter to be used in the 2D case, sound engineering assumptions need to be imposed. For this research, the process was reversed, by firstly finding the needed cable diameters in the 3D study, and further transposing them to an equivalent 2D cable.

## **10.6. Discussion on the economic evaluation and comparison to existing systems**

---

A rough economic evaluation and comparison to other existing systems was conducted, to form a preliminary idea on the benefit that the cable-net adds. With respect to these two evaluations, the following comments can be addressed:

- It is difficult to provide an estimation on the cost of the cable-net, as little information is found in literature on the cost spiral strands. A preliminary steel weight evaluation has been presented in Chapter 6.2, and a preliminary discussion on the total weight of the mountain has been presented in Chapter 7.1. Construction, material and manufacturing costs, maintenance and any other additional costs have been disregarded.
- The core + cable-net system was evaluated by estimating the total weight of the concrete used for the tower, and comparing it to the total weight of a tower when a simple core is used. This was explained in Chapter 8.4, where rough estimates on the total weight reduction have been presented. A full comparison, where the core + cable-net system is treated as a whole was not produced, based on the previous comment
- The comparison to other existing systems has been performed comparing the total material usage for systems with a similar performance, as presented in Chapter 8.3. Only one design case was treated. A more in-depth study, comparing multiple system configurations for both the proposed system, and the existing systems can lead to a better understanding of the comparison in terms of economic implications and performance.

# 11. Conclusion

---

In this chapter an overview of the thesis objectives and main research questions, as defined in Chapter 1.2 is presented. These questions are addressed based on the results of the research (Chapter 8) with respect to the imposed (Chapter 3) and discussed (Chapter 10) initial assumptions. The main research questions are reiterated below:

**Question 1:** *“What are the most relevant parameters that influence the design of the cable-net stabilized high-rise towers and what is their influence on the overall performance of the system?”*

**Question 2:** *“Are cable-net stabilized high-rise towers feasible design alternatives to the existing stability systems for high-rise towers?”*

To answer the research questions, three main objectives were set for the thesis:

The first thesis objective proposed a thorough study on the starting assumptions to be used throughout the thesis, based on a literature review focusing on the design and analysis of high-rise towers and the design and analysis of cables and cable-nets. By completing this objective, the large initial design space was drastically reduced, in order to achieve a manageable number of variable parameters. The initial assumptions, which relate to the dimensions and structural system of the core, to the typology of the cable-net, to the imposed loads on the structure and to the analysis procedure have a significant influence on the final results of this thesis.

The second thesis objective proposed a study on the influence of cables connected to the ground on the stability of a single high-rise tower. To understand the influence of the cables, the complexity of the system was gradually increased, from a configuration in which only the windward cable side stiffens the system, to a configuration where the cables are gravitationally loaded by the weight of the mountain. The second objective allowed for a continuous understanding of the different parameters, as the influence of different connections of the core to the foundation, the influence of the form density value used through the form finding process or the influence of the geometrical properties of the system (as the relative cable position or the angle of connection to the core). The conclusions of the second objectives, found in Chapter 4.4 and 5.4 enabled the restriction of the variability of the changeable parameters to sensible values.

The third thesis objective proposed the study on the influence on the overall design of a high-rise, when multiple towers are placed in a rectangular grid, interconnected by a network of cables. The third objective was achieved by studying the influence of the two set main parameters, the relative position of the cable net and the spacing between the towers in an iterative way as described in Chapter 6 and 7.

Completing the three proposed objectives, the main research questions were addressed, and are answered below:

### **Addressing question 1: most relevant design parameters**

By studying the behavior of the system under multiple configurations, the following conclusions with respect to the design parameters can be addressed:

- The relative position of the cable-net is the parameter with the highest influence on the stiffness of the system (lateral stability, measured with the top deflection as comparison parameter). As the relative position increases, so does the maximum achievable slenderness of the system, forming a range between  $1/8$  and  $1/23$ , under the imposed initial assumptions.
- The spacing between towers has a low influence on the stiffness of the system, as only a slight decrease in the stiffness is observed when the spacing between the tower increases. On the other hand, this parameter has a high influence on the design of the strength of core, primarily due to the high axial loads imposed by the mountain (Chapter 7.1)
- The influence of the cable-net on the design of the system is negligible when the cable net is placed lower than  $\sim 0.1$  of the height of the tower, as the same achievable slenderness can be obtained using a simple core system.
- Above the relative cable position of  $\sim 0.55$  of the height of the tower, temporary stabilizing elements are needed during the construction phase, as the core is not sufficiently stiff by itself before the cable-net is applied.
- The increase in the stiffness of the cable-net leads to an increase in the maximum achievable slenderness (observed to up to 20% when using practical dimensions), but on the other hand leads to a faster reach of the maximum core utilization, as discussed in Chapter 10.2.

### **Addressing question 1: influence of the design parameters on the overall performance**

Following these conclusions, a preliminary design chart has been proposed for the system, as presented in Figure 104. This chart identifies a number of design zones based on the relative position of the cable-net and spacing between towers. An optimal design zone, in which the maximum achievable slenderness based on the stability requirements can be reached, as the core does not need to be over dimensioned to withstand the large axial forces imposed by the mountain, and temporary stability issues do not occur during the construction phase is found. In this zone, high slenderness values can be reached, ranging between  $1/12$  to  $1/16.5$ , leading to a significant reduction in the weight of the core. The proposed optimal design zones and its boundaries is observed in zone 1a of Figure 104. An optimal design zone with lower achievable slenderness (zone 1b), a semi-optima design zone where temporary stabilizing elements are needed (zone 1c), a zone where the design of the core is governing (zone 2) and a zone where the influence of the cable-net is negligible (zone 3) are also identified, as Figure 104 shows.

Further, a two-step approach is proposed for the design of the system, as described in Chapter 8. By firstly choosing the system configuration (RPC and SBT) based on Figure 104, and translating it to the maximum achievable slenderness graph (Figure 88), a required core dimension can be obtained for any system configuration. It is concluded that the two-step approach (verified in Chapter 8), provides a good first insight in the behavior of the system and is used to propose and analyze a feasible design configuration for the Rotterdam Mountain to cover the Terbregseplein highway node in Rotterdam (Chapter 9). This further leads to the conclusion that, under the assumptions of this *preliminary* study, if designed accordingly, the project envisioned by the Rotterdam Dreamers is feasible from a technical point of view.

Design Zones based on Relative Cable Position and Spacing Between Towers

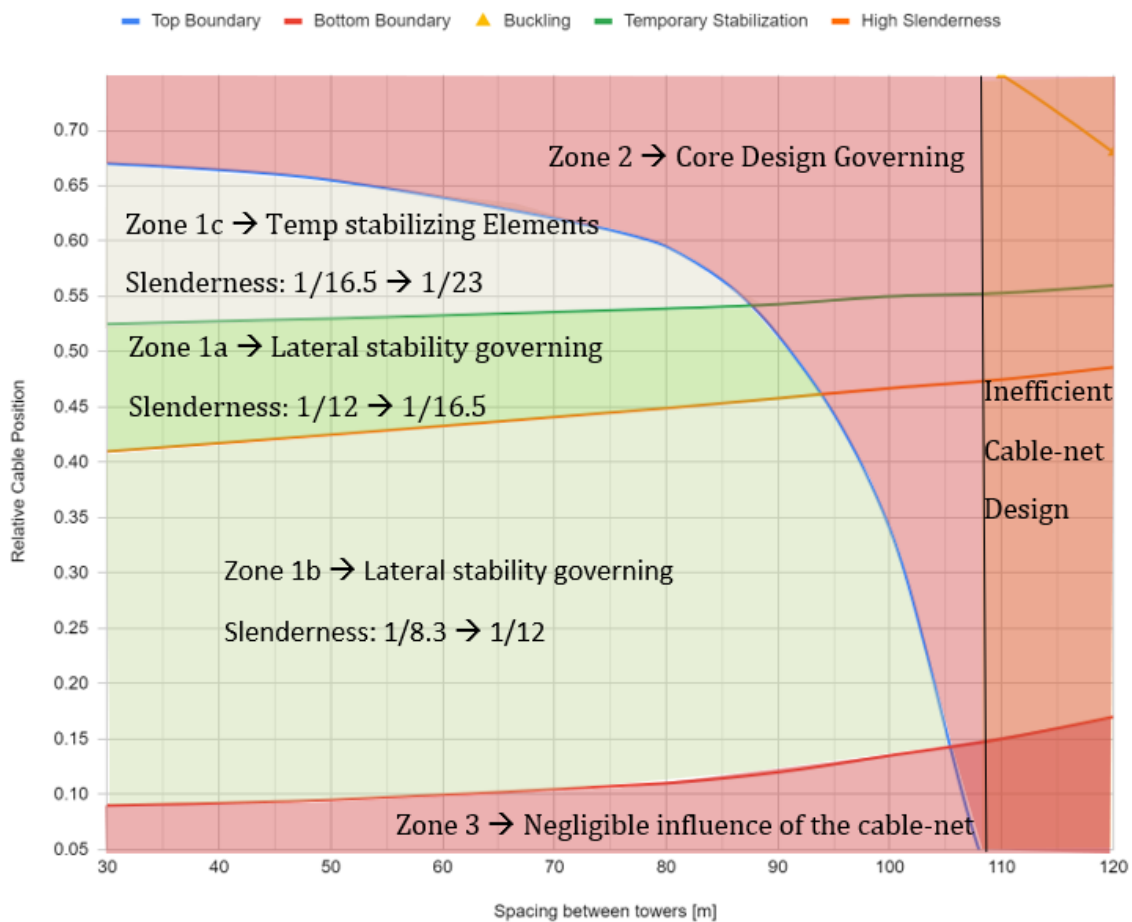


Figure 104 Design zones based on the relevant parameters

Three further remarks can be addressed with respect to the design of the system, as follows:

- For cases of high slenderness, the design of the core becomes governing (Zone 2), as its maximum utilization with respect to the compressive stresses is reached. In such cases, the slenderness corresponding to the stability criterion cannot be reached

- The bending moment at the base connection of the core decreases significantly with the increase in the relative position of the cable net resulting in no occurring tensile stresses in the core below the position of the cable-net connection, under any system configuration (Chapter 7.1).
- Based on the preliminary studies on the design of the cable-net, a conclusion is drawn that above 110 meters spacing between the towers, the design of the cable-net becomes impractical, due to uncommonly large needed spiral strand diameters and excessive axial loads transferred to the core (Chapter 6.2).

### **Addressing question 2: from a technical point of view**

Based on the obtained results in terms of performance of the system, that are presented in Chapter 8, it is concluded that from a technical point of view, the proposed system *is* a feasible design alternative to existing systems used for high-rise towers. However, it needs to be noted that the proposed research is a *preliminary* study, the results being obtained under a number of simplifications and initial assumptions.

Such, in Chapter 8.3 the proposed core + cable-net system has been compared to the simple core and outrigger system. It has been observed that the proposed system performs (at least) as good in terms of stability and strength as the conventional systems with less material usage. A concrete weight reduction of the core of up to 50% is observed when compared to the simple core system and a steel weight reduction of up to 20% is observed when compared to the outrigger system.

### **Addressing question 2: from an economic point of view**

From an economic point of view, the preliminary calculations have shown a reduction of the total weight of the structure of 8-13% (Chapter 8.4), due to the increase in slenderness when the cable-net is placed. This reduction can be further translated to an equivalent number of 3 to 5 extra floors on the tower, with the same final material usage. This can lead to the preliminary conclusion that, also from an economic perspective, the system does provide advantages. However, to gain a comprehensive evaluation on the overall feasibility of the system, a proper economic evaluation should be conducted for the cable-net and mountain as well. As this could not have been done during this research, the question of economic feasibility is still to be addressed.

# 12. Recommendations for future research

---

In this chapter, recommendations with respect to further research opportunities on the design of cable-net stabilized high-rise towers are outlined.

## 12.1. Weight optimization of the system components

---

Chapter 7.1 presented the influence of the large axial load transferred by the mountain and by the floors of the tower towards the core. This large force has a governing influence on the design of the core, limiting the range of achievable slenderness. By optimizing the weight of the system's elements, a higher range of achievable slenderness is expected, as lower forces are transferred to the cores. In this regard, the main research opportunities are:

- A thorough study on the design of the mountain (considering the cladding system, the green roof system and the overall mountain surface) → can lead to a lower mountain load to be transferred to the core by considering lightweight materials for the cladding instead of concrete, an optimized green roof system instead of the intensive green system used, and searching for solutions for weight reduction where large spans are present (for example, using glass or polycarbonate domes instead of the green roof in certain areas).
- A thorough study on the design of the tower → considering different flooring systems (such as a composite flooring system instead of the cast-in-situ reinforced concrete system) or different materials (as timber).

## 12.2. Typology of the towers

---

Throughout the research, the towers were designed using the core typology as the lateral load resisting system (LLRS), and a tower built fully of concrete is considered.

- To gain a more comprehensive view on the influence of the cable-net, a more comprehensive study, where different LLRS for the tower are used can be performed. Such, an outrigger + cable-net system, tube + cable-net system, mega frame + cable-net system, etc. can be studied, which may lead to stiffer overall behaviour.
- Further, a study with respect to different materials used for the tower system, as timber or steel is advised. This will have influence both on the overall stiffness of the system, as well as economic implications.
- Lastly, through the exploration phase, the width and height of the tower have been set to unchangeable dimensions. Adding them as changeable parameters will further extend the result spectrum, due to their influence on the peak velocity pressure and value of the wind load to be transferred to the core, as well as economic implications.

### **12.3. In depth study of the cable-net**

---

The cable-net supporting the mountain load has been *preliminary* designed to withstand the occurring forces. However, further research opportunities can be identified with respect to a more in-depth analysis of the cable-net, as follows:

- An accurate modelling of the wind-load on the mountain surface is advised if a thorough design is desired. This can be done, for example, by a wind tunnel testing.
- A dynamic analysis of the cable-net when the wind load fluctuations are considered or when the live loads are imposed in cycles is advised, as this research only covered a static analysis of the system.
- A study on the constructability of the mast-supported cable-net with radial cables, including detailed drawings of the connections, construction sequences and construction techniques.

### **12.4. Other research opportunities**

---

Lastly, a number of other further research opportunities are identified, as follows:

- A thorough economic evaluation of the system, including a study on the economic implications of the mountain, as well as a study on the economic implications of the tower is advised, to reach strong conclusions on the feasibility of the system.
- A study on the design of the temporary stabilizing elements needed during the construction Phase 1, as addressed in Chapter 7.2.
- A study on the influence of the proposed system on the foundation design, both for the connection of the towers to the foundation, as well as for the connection of the edge cables to the foundation.
- An in-plane shape optimization of the core (or tower) based on the different occurring tensile forces in the different cable elements (stronger diagonal cables and less strong internal cables).

# References

---

- Bradshaw R., Campbell D., Gargari M., Mirmiran A., Tripeny P. (2002), *Special Structures: Past, Present and Future*. American Society of Civil Engineers, 150<sup>th</sup> Anniversary Paper
- Primos (2020), *Population Forecast*, <https://www.abfresearch.nl/producten/prognoses/primos-bevolkingsprognose/> (Accessed 24.08.2021)
- De Groot C., Vreiselaar N. (2021), *Dutch Housing Market Quarterly*, <https://economics.rabobank.com/publications/2021/march/housing-shortage-and-low-interest-rates-are-driving-up-house-prices/> (Accessed 22.08.2021)
- Rotterdam Dreamers (2020), *Not plodering, but stacking in the Rotterdamse Berg*, <https://rotterdamsedromers.nl/2020/02/13/rotterdamse-berg-dutch-mountain/> (Accessed 14.02.2021)
- Summum Engineering (2020), *Rotterdam Mountain, 2020*, <https://www.summum.engineering/portfolio/mountain/> (Accessed 11.11.2020)
- Santiago Calatrava Architects & Engineers (2016), *Dubai Creek Tower* <https://calatrava.com/projects/> (Accessed 10.10.2021)
- SMITH, B. S., & COULL, A. (1991), *Tall building structures: Analysis and design*, New York, N.Y. Wiley
- P.P. Hoogendoorn (2009), *Lateral Load Design of Tall Buildings*, Delft, Civil Engineering and Geosciences-Building Engineering Department, TU Delft.
- Christian Sandelin, Evgenij Budajev (2013), *The Stabilization of High-rise Buildings*, Department of Engineering Science, Applied Mechanics, Civil Engineering, Uppsala University
- Terwel K. C., Ham P. H. (2017), *Structural Calculations of High-Rise Towers*, Delft, Civil Engineering and Geosciences, TU Delft
- Ching, F., (2014), *Building construction illustrated*, Hoboken, New Jersey, N.J: Wiley.
- Stottrup-Andersen Ulrik (2014), *Masts and Towers*, Journal of the International Association for Shell and Spatial Structures, vol 55, no 1 March n. 179
- Gantes C., Khoury R., Connor J., Pouangare C. (1993), *Modeling, loading and preliminary design considerations for tall guyed towers*. Computers & Structures, Vol. 49, no. 5, Pages 797-805
- Nielsen Mogens G. (2014), *Analysis and Design of Masts and Towers*, Journal of the International Association for Shell and Spatial Structures, vol 55, no 2 June n. 180
- Foster & Partners, *Torre de Collserola*, <https://www.fosterandpartners.com/projects/torre-de-collserola/> (Accessed 20.05.2021)
- Wikipedia, *Sydney Tower*, [https://en.wikipedia.org/wiki/Sydney\\_Tower](https://en.wikipedia.org/wiki/Sydney_Tower) (Accessed 20.05.2021)

- Wise C.M. (1993), *Design of the Torre de Collserola, Barcelona*, The Structural Engineer, vol 71, no 20, Institution of Structural Engineers
- Krishna, P., 1978. *Cable- suspended roofs*. New York: McGraw-Hill.
- Ossman Mohammad Mohie Eldin Mohammad (2003), *Static and dynamic analysis of circular cable roof*, Mansoura, Civil Engineering Department, Alexandria University
- J. Llorens (2015), *-Detailing for fabric architectural structures*, In Woodhead Publishing Series in Textiles, Fabric Structures in Architecture, Woodhead Publishing, Pages 283-387
- E. Pipinato (2016), *Innovative Bridge Design Handbook*, Elsevier, Butterworth-Heinemann, Pages 555-596
- EN 12385 (2002), *Steel Wire Ropes*, European Committee for Standardization
- EN 1993-1-11 (2006), *Design of Steel Structures*, European Committee for Standardization
- Buchholdt H. A. (1999), *An Introduction to Cable Roof Structures*, Cambridge University Press
- Krishna, P. and Godbole, P. (2013), *Cable-Suspended Roofs, Second Edition*, McGraw Hill Education (India) Private Limited.
- Gabriel, K. (1974), *Structural Design of Cable-suspended Structures*, International Conference on Tension Roof Structures, Polytechnic of Central London
- Veenendaal D. (2017), *Design and form finding of flexibly formed concrete shell structures*, Doctoral Thesis, Zurich, ETH Zurich.
- Adriaenssens, S., Bock P., Veenendaal D., Williams C., (2014) *Shell structures for architecture: form finding and optimization*. Abingdon, Oxon: Routledge
- Lewis, W. J. (2003), *Tension structures. Form and Behavior*, Thomas Telford, London.
- Li, J.-J., Chan, S.-L. (2004), *An integrated analysis of membrane structures with flexible supporting frames*, Finite Elements in Analysis and Design.
- Buchholdt H. A., Davies M., Hussey M. J. L. (1968), *The analysis of cable-nets*, Journal of the Institute of Mathematics and its Applications 4.
- Harding J., Shepherd P. (2011), *Structural form finding using zero-length springs with dynamic mass*, Proceedings of the International Association of Shells and Spatial Structures, London.
- H.-J. Schek (1974), *The force density method for form finding and computation of general networks*, Computer Methods in Applied Mechanics and Engineering, Volume 3.
- Malerba, Pier & Patelli, Matteo & Quagliaroli, Manuel. (2012). *An Extended Force Density Method for the form finding of cable systems with new forms*. Structural Engineering & Mechanics, vol 42, Milan.
- Van Ingen (2021), *Stabiliteitskern met tweede-orde-effecten*, <https://www.cementonline.nl/stabiliteitskern-met-tweede-orde-effecten> (Accessed 10.04.2021).
- Cascone S. (2019), *Green Roof Design: State of the Art on Technology and Material*, Department of Civil Engineering and Architecture, University of Catania, Catania.

SIG Technology 2020, *Green Roofs*, <https://www.singleply.co.uk/green-roofs/> (Accessed 11.03.2021).

EN 1991-1-4 (2004), *Actions on structures-Part 1-4: General Actions-Wind actions*, European Committee for Standardization.

NEN-EN 1990+A1:2006+A1:2006/C2:2019 (2019), *Eurocode: Basis of structural design*, The Royal Netherlands Standardization Institute.

NEN-EN 1990-1-1+A1+A1/C2/NB (2019), *National Annex to NEN-EN 1990+A1:2006+A1:2006/C2:2019*, The Royal Netherlands Standardization Institute.

Soons F.A.M., Wagemans L.A.G., Pasterkamp S. (2014), *Quick Reference*, Section Structural and building Engineering, Delft, TU Delft.

Vrouwenvelder T., Steenberg H. (2005) *Implementation of eurocodes: Handbook 3 — actions effects for buildings*, Chapter 3: Wind actions. Leonardo Da Vinci Pilot Project, Aachen.

Robot Structural Analysis Support and Learning (2020), *User's Guide*, <https://autode.sk/3kuF8kY> (Accessed 15.05.2021)

Herbert W. G. (1987), *Steel Constructions Manual*, American Institute of Steel Constructions

W. Lewis, M. Jones, K. Rushton (1984) *Dynamic relaxation analysis of the non-linear static response of pretensioned cable roofs*, Computers and Structures 18

Thai H-T., Kim S-E. (2010), *Nonlinear static and dynamic analysis of cable structures*, Department of Civil Engineering and Geosciences, Sejong University, Sejong.

J. Michalos, C. Birnstiel (1962), *Movements of a cable due to changes in loading*, Journal of Structural Division ASCE 127 267–303.

G. Tibert, (1998), *Numerical analyses of cable roof structures*: Royal Institute of Technology, Dept. of Structural Engineering, 1998.

W. O'Brien, A. Francis (1964), *Cable movements under two-dimensional loads*, Journal of the Structural Division, ASCE 90 (3) 89–123.

# Appendix A

## Structural elements of the tower

As presented in the main report, Chapter 3, the structural elements of the tower are dimensioned by rules of thumb to conventional values based on their span. The structural plan of a common floor of the tower is presented below, in Figure 105.

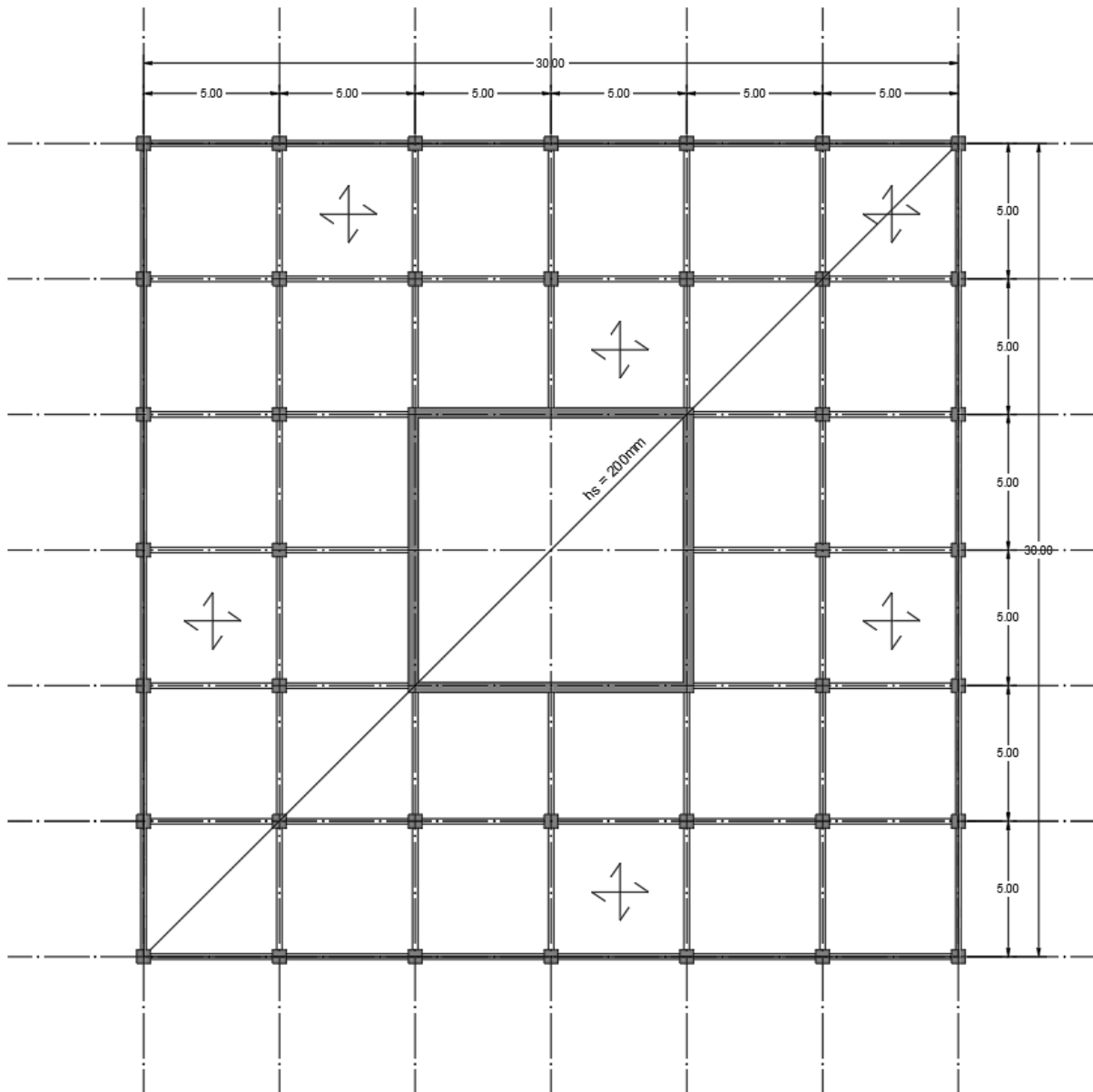


Figure 105 Structural Plan

## 1. Columns

The columns are assumed to be placed every 5 meters, to allow for the flexibility of the usable space. This translates to a 25 square meters area loading each column. Based on the loads imposed on the tower, a required area for the columns can be calculated:

**Table 33 Column Dimensioning**

ULS Load [kN/m <sup>2</sup> ]	Unloading Area [m <sup>2</sup> ]	Force / 1 level [kN]	Nr of Levels [-]	Force/ 1 column [kN]	Compressive Strength [MPa]	Required Area [mm <sup>2</sup> ]	Required width [mm]
11.91	25	297.75	27	8039.25	30	267975	518

A required width of the columns of ~520 millimeters is found, to withstand the total load at the bottom of the tower. However, the columns on the façade are loaded with only half of the load, as the tributary area loading them is half. Moreover, an optimization of the area of the column can be performed over the height of the building, as the loads are lower as the reference height is increased. Such, an assumption is made that the *average* column width, considering an optimization over the height and a lower loading on the façade columns, is of 400 millimeters.

## 2. Beams

The beams are conventionally dimensioned based on the rule of thumb, to have a height of ~1/12 of the span, and a width of ~1/2 of their height. This results in a beam with the height of 417 millimeters (400 millimeters is chosen) and a width of 208 millimeters (200 millimeters is chosen).

**Table 34 Rule of thumb dimensioning for beams**

Span [mm]	Height Rule of thumb [-]	Height [mm]	Width Rule of thumb [-]	Width [mm]
5000	1/12	417	1/2	208

## 3. Floors

The two-way spanning concrete slab is dimensions based on the rule of thumb, to have a height of at least 1/30 of the maximum span. A minimum thickness of 167 millimeters is required by the rule of thumb, but a 200-millimeter thickness is chosen to account for fire safety requirements.

**Table 35 Rule of thumb dimensioning for slab**

Span [mm]	Thickness rule of thumb [-]	Minimum Thickness [mm]	Chosen thickness [mm]
5000	1/30	167	200

# Appendix B

## Loads on the structure

### Loads on the Core

The permanent loads on the core are imposed by the tributary area loading the core, as also explained in Chapter 3.6. The tributary area is considered of approximately 15.5 x 15.5 meters (0.5 meters for the thickness of the core), as the core has an approximate dimension of 10 meters (and slightly lower throughout the study, so this is considered a conservative approach), and the spacing between columns is 5 meters. A 15 square meters area is considered for the elevator shaft. This leads to a total area of 225 square meters loading the core. As presented in Chapter 3.6, the floor system imposes a load of 6.8 kN / m<sup>2</sup>.

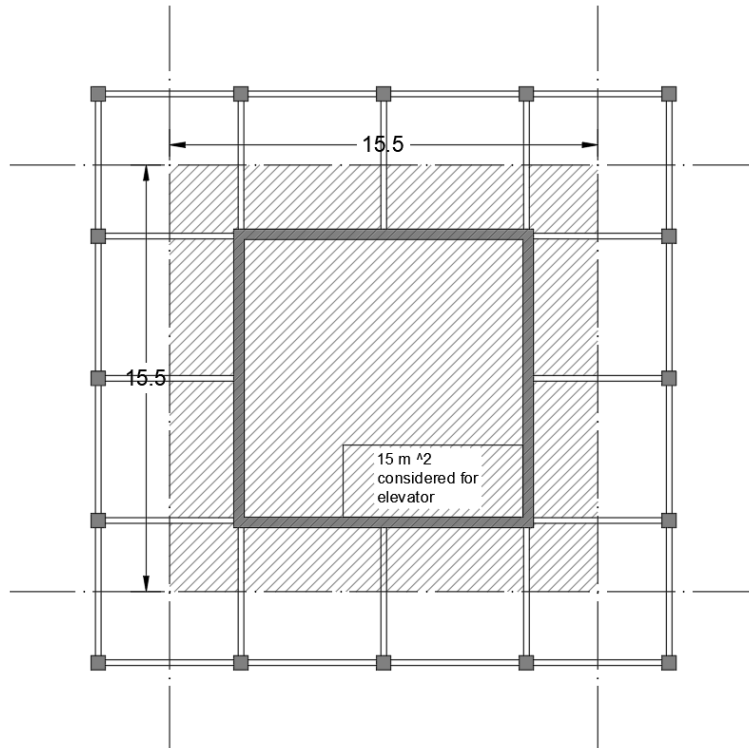


Figure 106 Tributary area of the core

The live loads on the core are imposed by the Eurocode requirements, and have a value of 2.5 kN/m<sup>2</sup>. The equivalent distributed vertical load on the core, implemented in the analysis models, is obtained by calculating the whole load on the core (considering the tributary area and 27 floors), and dividing it by the height of the core (100 meters), considering the partial factors for each load combination.

Table 36 Equivalent vertical line load calculation

Load Combination [-]	Tributary Area [m <sup>2</sup> ]	Nr of Floors [-]	Height [m]	LL [kn/m <sup>2</sup> ]	DL [kN/m <sup>2</sup> ]	LL factor [-]	DL factor [-]	Equivalent Vertical Load [kN/m]
ULS1	225	27	100	2.5	6.8	0	1.5	620
ULS2	225	27	100	2.5	6.8	0.825	1.5	745
ULS3	225	27	100	2.5	6.8	1.65	1.3	788
ULS4	225	27	100	2.5	6.8	0.825	1.3	662
SLS1	225	27	100	2.5	6.8	0.5	1	489
SLS2	225	27	100	2.5	6.8	1	1	565

## Wind Load

### Wind load on the Tower

As presented in Chapter 3.6, the wind load on the tower is calculated using the simplified formula for regular in-plane shape buildings.

$$F_i = c_s c_d \cdot c_f \cdot q_p(z_e) \cdot A_{ref} \quad (\text{Eq B.1})$$

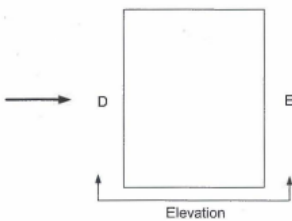


Table 37  $c_f$  value for zones

Façades h/d	A	B	$c_f$ for zone		
			C	D	E
5	-1,2	-0,8	-0,5	+0,8	-0,7
1	-1,2	-0,8	-0,5	+0,8	-0,5
≤ 0,25	-1,2	-0,8	-0,5	+0,7	-0,3

The factor  $c_f$  is obtained from Table 37, for zones D and E, corresponding to pressure zone and suction zone respectively. As the h/d ratio is 3.33, for zone D a factor +0.8 is used and for zone E, a factor of -0.62 is calculated by interpolation.

Table 38 Calculation of  $c_f$  factor

Height [m]	Width [m]	h/d [-]	$C_{f,D}$ [-]	$C_{f,E}$ [-]
100	30	3.33	0.8	-0.62

The peak velocity pressure value is obtained from the Dutch National Annex, based on the zone and reference height, according to Figure 108 shown below and Table 40 shown below. According to EN 1991-1-4 the wind value can be reduced for buildings with the height larger than twice the width, according to Figure 107 Wind reduction over the height of the building (EN 1991-1-4) Such, two reference heights are set, at 30 meters (equivalent to the width of the building), at 100 meters (top height).

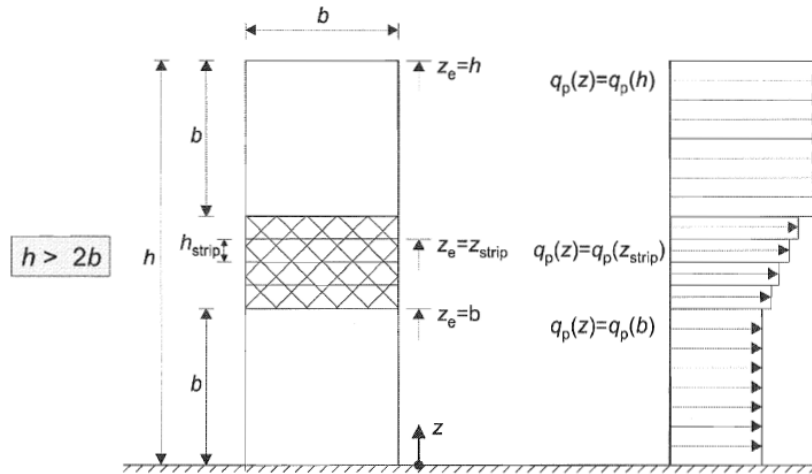


Figure 107 Wind reduction over the height of the building (EN 1991-1-4)

Table 39 Wind on tower calculation

	Reference height [m]	Peak velocity pressure [kN/m <sup>2</sup> ]	Width of the structure [m]	Q wind [kN/m <sup>2</sup> ]	Q wind [kN/m]	Total Line Load Wind [kN/m]
Bottom pressure	30	1.03	30	0.82	24.7	43.8
Bottom suction	30	1.03		-0.64	19.1	
Top pressure	100	1.48		1.18	35.5	62.9
Top suction	100	1.48		-0.91	27.4	

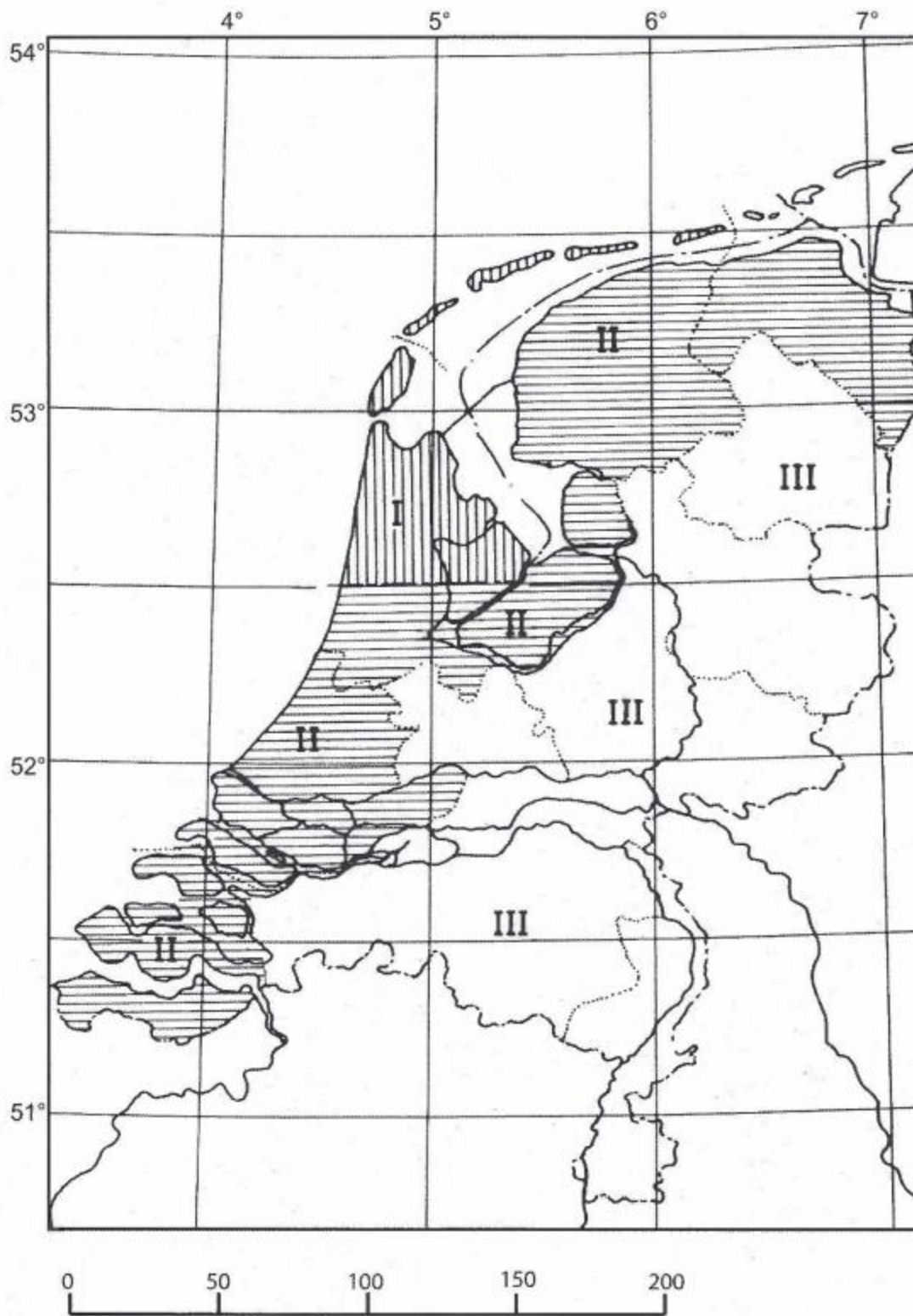


Figure 108 Wind Zones in the Netherlands

**Table 40 Peak velocity pressure according to zones**

$z_e$ [m]	$q_s(z_e)$ [kN/m <sup>2</sup> ]							
	Area I Coastal	Rural	Urban	Area II Coastal	Rural	Urban	Area III Rural	Urban
1	0,93	0,71	0,69	0,78	0,60	0,58	0,49	0,48
2	1,11	0,71	0,69	0,93	0,60	0,58	0,49	0,48
3	1,22	0,71	0,69	1,02	0,60	0,58	0,49	0,48
4	1,30	0,71	0,69	1,09	0,60	0,58	0,49	0,48
5	1,37	0,78	0,69	1,14	0,66	0,58	0,54	0,48
6	1,42	0,84	0,69	1,19	0,71	0,58	0,58	0,48
7	1,47	0,89	0,69	1,23	0,75	0,58	0,62	0,48
8	1,51	0,94	0,73	1,26	0,79	0,62	0,65	0,51
9	1,55	0,98	0,77	1,29	0,82	0,65	0,68	0,53
10	1,58	1,02	0,81	1,32	0,85	0,68	0,70	0,56
15	1,71	1,16	0,96	1,43	0,98	0,80	0,80	0,66
20	1,80	1,27	1,07	1,51	1,07	0,90	0,88	0,74
25	1,88	1,36	1,16	1,57	1,14	0,97	0,94	0,80
30	1,94	1,43	1,23	1,63	1,20	1,03	0,99	0,85
35	2,00	1,50	1,30	1,67	1,25	1,09	1,03	0,89
40	2,04	1,55	1,35	1,71	1,30	1,13	1,07	0,93
45	2,09	1,60	1,40	1,75	1,34	1,17	1,11	0,97
50	2,12	1,65	1,45	1,78	1,38	1,21	1,14	1,00
55	2,16	1,69	1,49	1,81	1,42	1,25	1,17	1,03
60	2,19	1,73	1,53	1,83	1,45	1,28	1,19	1,05
65	2,22	1,76	1,57	1,86	1,48	1,31	1,22	1,08
70	2,25	1,80	1,60	1,88	1,50	1,34	1,24	1,10
75	2,27	1,83	1,63	1,90	1,53	1,37	1,26	1,13
80	2,30	1,86	1,66	1,92	1,55	1,39	1,28	1,15
85	2,32	1,88	1,69	1,94	1,58	1,42	1,30	1,17
90	2,34	1,91	1,72	1,96	1,60	1,44	1,32	1,18
95	2,36	1,93	1,74	1,98	1,62	1,46	1,33	1,20
100	2,38	1,96	1,77	1,99	1,64	1,48	1,35	1,22
110	2,42	2,00	1,81	2,03	1,68	1,52	1,38	1,25
120	2,45	2,04	1,85	2,05	1,71	1,55	1,41	1,28
130	2,48	2,08	1,89	2,08	1,74	1,59	1,44	1,31
140	2,51	2,12	1,93	2,10	1,77	1,62	1,46	1,33
150	2,54	2,15	1,96	2,13	1,80	1,65	1,48	1,35
160	2,56	2,18	2,00	2,15	1,83	1,67	1,50	1,38
170	2,59	2,21	2,03	2,17	1,85	1,70	1,52	1,40
180	2,61	2,24	2,06	2,19	1,88	1,72	1,54	1,42
190	2,63	2,27	2,08	2,20	1,90	1,75	1,56	1,44
200	2,65	2,29	2,11	2,22	1,92	1,77	1,58	1,46

**Wind load on the mountain**

As presented in Chapter 3.6, the wind load on the mountain is calculated by finding the peak velocity pressure at the reference height according to the EN 1991-1-4 formulas, to account for terrain orography and roughness. Below, the calculation is exemplified for a reference height of 50 meters (relative cable position of 0.5 x H), and a cable-net obtained from a spacing between towers of 50 meters.

Table 41 Basic wind speed calculation

Reference height z [m]	Directional factor $c_{dir}$ [-]	Seasonal factor $c_{season}$ [-]	Fundamental value $v_{b,0}$ [m/s]	Basic wind speed $v_b$ [m/s]
50	1	1	27	27

Table 42 Roughness factor calculation

Reference height z [m]	$z_0$ terrain category [-]	$z_{min}$ terrain category [-]	Terrain factor $k_r$ [-]	Roughness factor $c_r(z)$ [-]
50	0.5	7	0.223	1.03

Table 43 Orography factor calculation

Reference height z [m]	Mountain angle [degrees]	Orographic location factor s [-]	Upstream slope $\Phi$ [-]	Orography factor $c_0$ [-]
50	5	0.5	0.12	1.12

Table 44 Mean wind velocity calculation

Reference height z [m]	Roughness factor $c_r(z)$ [-]	Orography factor $c_0$ [-]	Basic wind speed $v_b$ [m/s]	Mean wind velocity $v_m(z)$ [m/s]
50	1.03	1.12	27	31.1

Table 45 Turbulence intensity calculation

Reference height z [m]	$z_0$ terrain category [-]	Turbulence factor $k_l$ [-]	Orography factor $c_0$ [-]	Turbulence intensity $I_{vz}$ [-]
50	0.5	1	1.12	0.194

Table 46 Peak velocity pressure calculation

Reference height z [m]	Turbulence intensity $I_{vz}$ [-]	Air density $\rho$ [kg/m <sup>3</sup> ]	Mean wind velocity $v_m(z)$ [m/s]	Peak velocity pressure $q_p(z)$ [kN/m <sup>2</sup> ]
50	0.194	1.25	31.1	1.42

Table 47 Wind forces normal to the mountain surface

Reference height z [m]	$c_s c_d$ [-]	Peak velocity pressure [kN/m <sup>2</sup> ]	Zone F $c_{f,i}$	Zone G $c_{f,g}$	Zone H $c_{f,h}$	Zone I $c_{f,i}$	Zone J $c_{f,j}$
50	1	1.42	-1.7	-1.2	-0.6	-0.6	0.2
			zone F [kN/m <sup>2</sup> ]	zone G [kN/m <sup>2</sup> ]	zone H [kN/m <sup>2</sup> ]	zone I [kN/m <sup>2</sup> ]	zone J [kN/m <sup>2</sup> ]
			-2.41	-1.70	-0.85	-0.85	0.28

**Table 48 Friction forces on the mountain surface, parallel to the wind direction**

Reference height $z$ [m]	Friction coefficient $c_{fr}$ [-]	Peak velocity pressure [kN/m <sup>2</sup> ]	Friction force on all zones [kN/m <sup>2</sup> ]
50	0.02	1.42	<b>0.03</b>

These calculations are automatically generated in the parametric script, and were numerically presented in this Appendix to be exemplified.

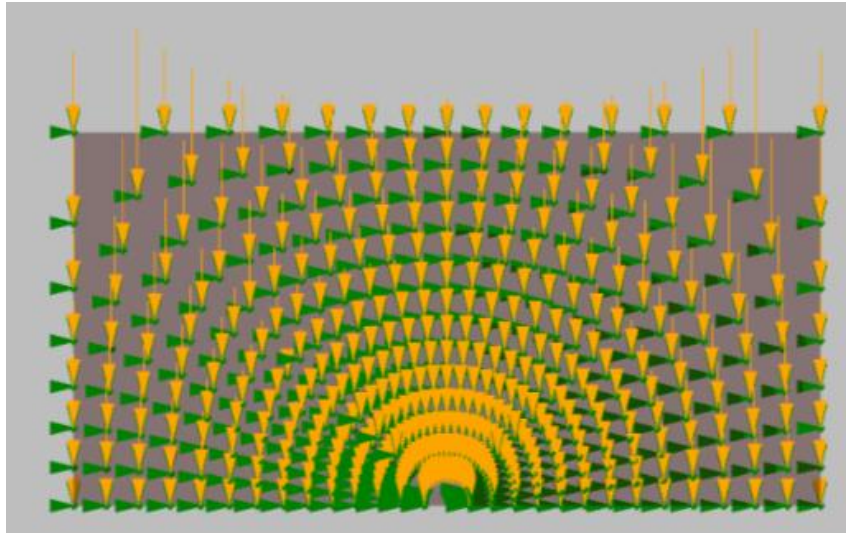


**Figure 109 Top view of the vectorial sum of forces acting on the nodes of the cable-net, calculated by parametric script**

As explained in Chapter 3.6, an equivalent point load acting above the relative position of the cable-net is calculated for each spacing case. This is done automatically in the parametric script, and explained below for a spacing case of 50, 80 and 110 meters and a relative position of  $0.5 \times H$ . Such the peak velocity pressure used has a value of  $1.42 \text{ kN/m}^2$ , as presented previously in this Appendix, for a reference height of 50 meters. The reference area of the cable-net that is considered to transfer wind load on the tower is calculated as a trapezoidal area, with the large base being the width of the cable-net and the small base being the width of the tower (30 meters).

Reference height [m]	Cable-net width [m]	Cable-net area [m <sup>2</sup> ]	Peak velocity pressure [kN/m <sup>2</sup> ]	Equivalent Wind force [kN]
50	50	1000	1.42	1420
50	80	2200	1.42	3124
50	110	3850	1.42	5467

# Appendix C

## Trial Models

As explained in Chapter 3.8, to verify the proposed nonlinear analysis performed in Robot Structural Analysis, a few trial models were created and the results were compared to similar studies. The chosen configurations of the trial models are standard geometries used in the development of analysis methods of cable systems - Michalos et al. (1962), O'Brien et al. (1964), Tibert (1998), Thai et al. (2010) and Lewis (1984) analyzed the same systems based on each of their proposed method. A comparison is made to Thai's and Lewis's results.

Thai et al propose an incremental-iterative solution based on the Newmark integration to solve the nonlinear equation of motion.

Lewis analyses the non-linear static response of the pretensioned cable-net using the minimum potential energy principle.

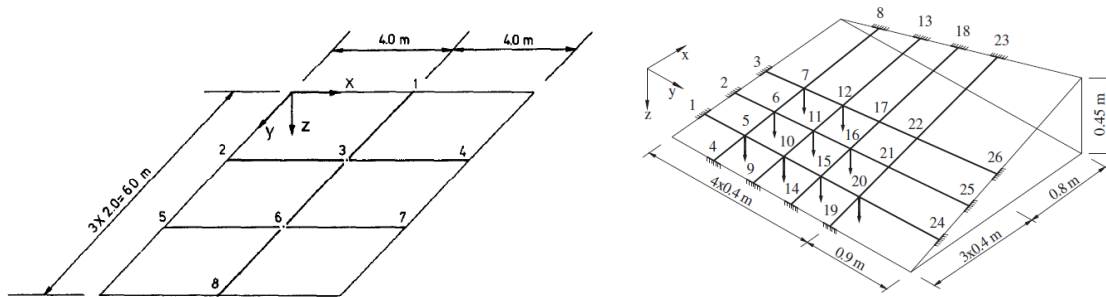


Figure 110 Geometry of the trial models (Thai et al., 2010)

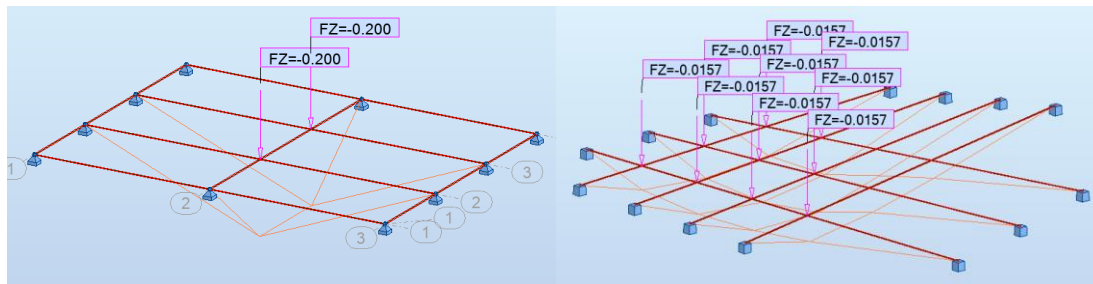


Figure 111 Trial Models (RSA)

### Trial model 1. 2x1 cable-net

The structure is a flat-net with six degrees of freedom. The pretension force in all cables is 0.5 kN and the cross-section area of all elements is 2.0 mm<sup>2</sup>. The Young's modulus is 110 kN/m<sup>3</sup>. A point load of 0.2 kN acts at nodes 3 and 6.

## Trial model 2. Hypar net

The geometry of the hypar is obtained by a set of two straight lines, forming a structure with 36 degrees of freedom. The pretensions force in all cables is 0.2 kN and the cross-section area of all elements is 0.785 mm<sup>2</sup>. The Young's modulus is 128.3 kN/m<sup>3</sup>. Point loads of 0.0157 kN are applied at each internal node, except for the nodes 17, 21, 22.

**Table 49 Results for the trial models**

Structure	Cable diameter [mm <sup>2</sup> ]	Pretension [kN]	Applied Force [kN]	Youngs Modulus [kN/mm <sup>2</sup> ]	Node	Deflection (Lewis) [mm]	Deflection (Thai) [mm]	Deflection (Robot) [mm]	Max Difference [%]
2x1 grid	2	0.5	0.2	110	6	199.7	201.31	200.28	0.51
					5	195	195.6	195.1	0.26
					6	253	257	256.6	1.42
Hypar	0.785	0.2	0.0157	128.3	7	228	233.7	233.9	2.59
					11	336	341.6	341.7	1.70
					12	288	296	296.6	2.99

A divergence between the results obtained from Robot and the studies between 0.26% to 2.99% is observed. These divergences are considered to fall in acceptable limits, confirming that the nonlinear analysis is correct and can be used for the analysis of the full cable-net.

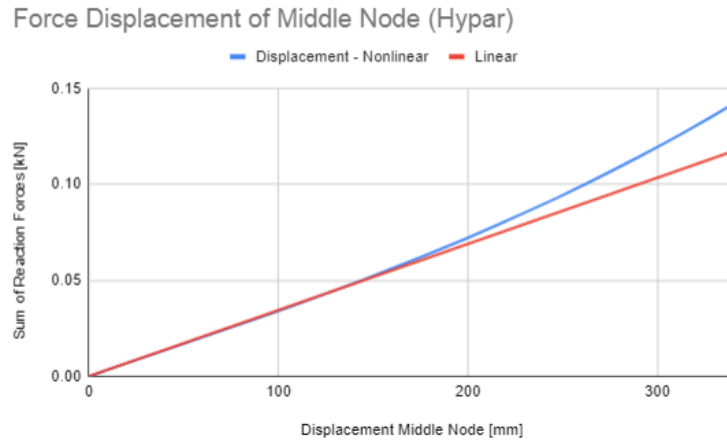


**Figure 112 Force vs Displacement for Middle Node of the Hypar Trial model**

The effects of the geometric non-linearity of the cable-net are shown in Figure 112. As expected, a stiffening behavior is present, when compared to a linear distribution of the deflection of the nodes.

# Appendix D

## Linear and Nonlinear analysis for the 2D Cases

As explained in Chapter 4, at first a comparison between the linear analysis in Karamba and the nonlinear analysis in Robot Structural Analysis is performed, to check if, for the 2D cases, the linear analysis suffices. The check is performed for the same geometric configuration and for the same load in both software, as follows:

- Using a core dimensions of 10 x 10 x 0.35 meters, a concrete class of C45/55 with a reduced E-modulus of 9100 MPa;
- Using a cable diameter of 350 millimeters, using spiral strands with a wire strength of 1570 MPa, and a E-modulus of 160 GPa;
- Considering the core fixed to the base;
- Considering the cables pinned to the core connection and to their base connection;
- Considering an angle between the tower and the core of 55 degrees and a relative cable position of 0.5 x H;
- Considering a UDL of 43.8 kN/m below 0.5 x H and 62.9 kN/m above 0.5 x H, as Karamba does not allow for trapezoidal loads;

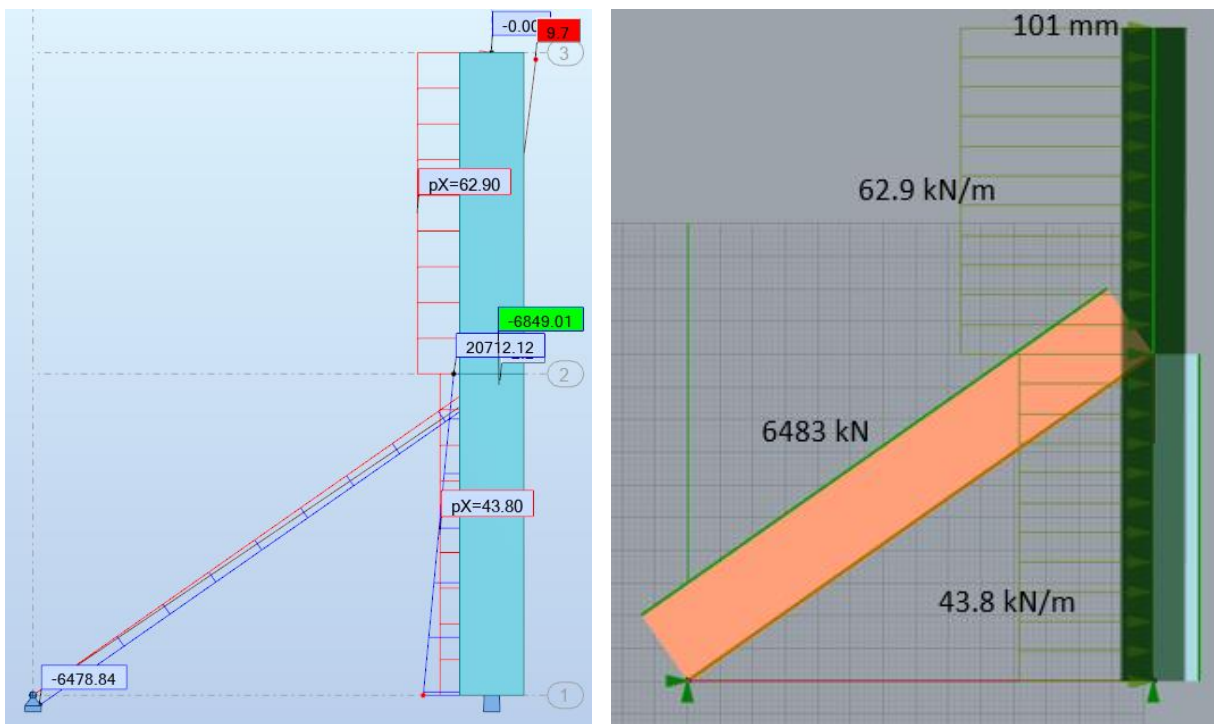


Figure 113 RSA (Left) and Karamba (Right) output

As expected from the remarks of Krishna (1978), the linear analysis overestimates the displacements. However, for this simplified analysis the displacement is only overestimated with

4% (101 millimeters compared to 97 millimeters), concluding that the results are sufficiently accurate to perform the 2D analysis using the linear method.

**Table 50 Karamba Model Results vs RSA Model Results**

	<b>Tension in the cable [kN]</b>	<b>Top Displacement [mm]</b>	<b>Displacement at the cable connection [mm]</b>
Karamba Model	6483	101	2.3
RSA Model	6478	97	2.2

For a simple core system with the same dimensions, that is not stiffened by the cable, the top deflection results in a value of 302 millimeters.

**Table 51 Top deflection-simple core stability system**

<b>Core dimensions [m]</b>	<b>E core [MPa]</b>	<b>I core [m4]</b>	<b>Top Deflection [mm]</b>
Core 10 x 10 x 0.35	9100	209.95	302.15

# Appendix E

## Parametric Study

In this appendix the procedure used for the parametric study, as described in Chapter 4 is further explained. The parametric study is conducted using the following assumptions for the model:

- The core has unchangeable dimensions of 10 x 10 x 0.35 meters;
- The core is considered fixed to the foundation;
- The cables are considered pinned to their foundation and to their connection to the core;
- The loads on the system are described in Chapter 3.6 → as the top deflection is the comparison parameters, only the load combination SLS-1 is considered; the load that the mountain imposes on the cables, is, however, for this case, not considered;
- The used material properties are described in Chapter 3 (tower) and Chapter 3.2 (cables);

### Top deflection based on the Cable stiffness

As the diameter of the cable element is increased, the top deflection decreases. The results for the range of diameters from 100 to 500 millimeters are exported to Excel for graphing, and presented in the two figures below, for a diameter of 100 and a diameter of 300 millimeters, under the above-mentioned assumptions.

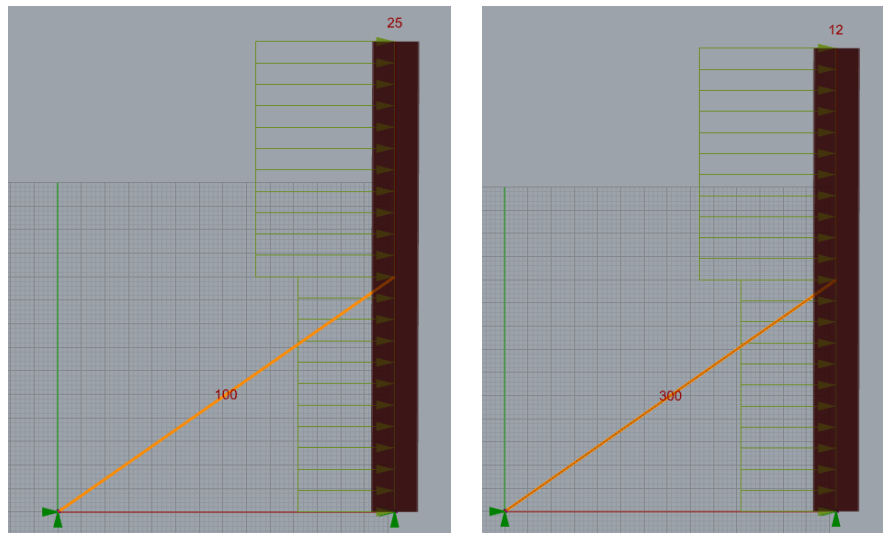


Figure 114 Top deflection based on Cable Diameter (Left-Diameter = 100 millimeters; Right-Diameter = 300 millimeters), under the geometric assumptions, for a cable angle of 55 degrees and an RPC of 0.5 x H;

### Top deflection based on relative position of the cable-net

As the relative position of the cable increases, the top deflection decreases. The results for the range of RPC of 0.3 to 0.75 x H are exported to Excel for graphing and presented in the two figures below, for an RPC of 0.3 x H and an RPC of 0.5 x H, under the above mentioned assumptions.

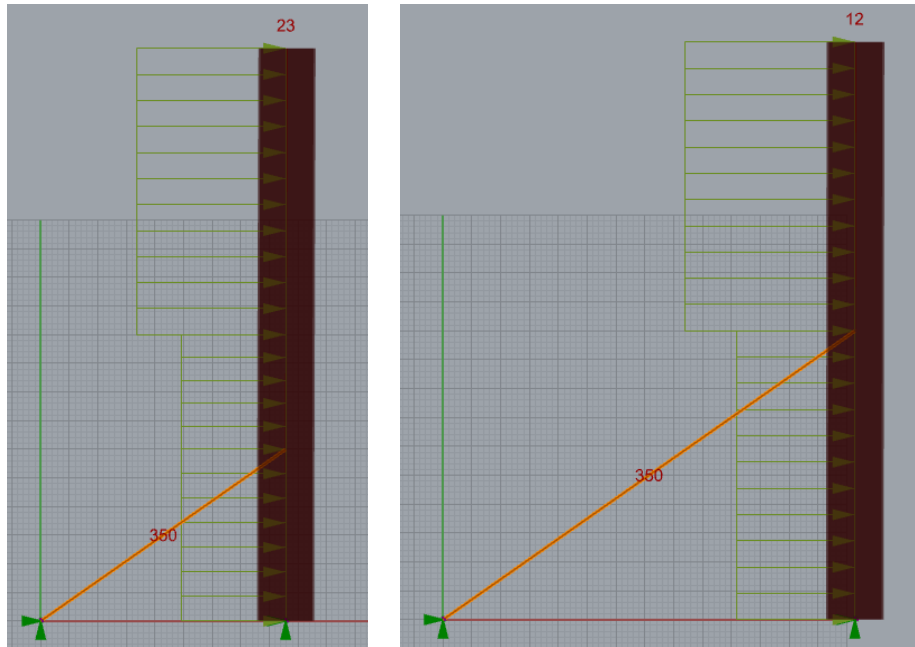


Figure 115 Top deflection based on RPC (Left-RPC = 0.3 x H; Right-RPC = 0.5 x H) under the geometric assumptions, for a cable angle of 55 degrees and cable diameter of 350 millimeters;

**Top deflection based on the angle.**

The influence of the cable angle was shown in Figure 38, with the optimum of 55 degrees. The cable angle is increased from an angle of 30 degrees to an angle of 75 degrees, and the results are exported to Excel for graphing. In the two figures below the results are presented for an angle of 35 degrees and 55 degrees, under the above-mentioned assumptions.

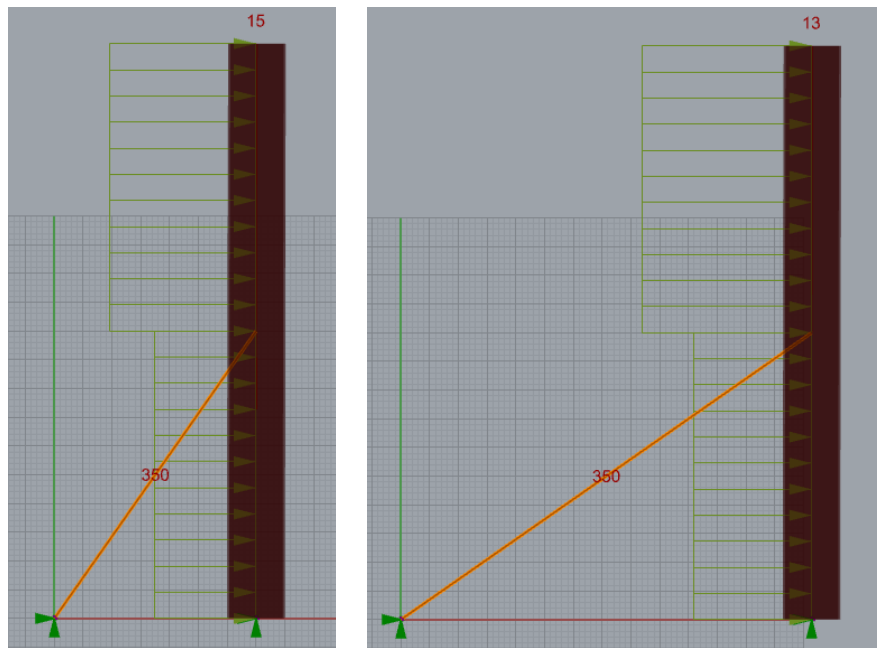


Figure 116 Top deflection based on cable angle (Left-angle = 35 degrees; Right-angle = 55 degrees) under the geometric assumptions, for a RPC of 0.5 x H and cable diameter of 350 millimeters;

### Explanation on the 55 degrees optimum angle

As seen in Figure 38, the biggest influence on the top deflection when the cables are connected to the ground was found for the angle of 55 degrees. This minimum value for the cable angle can be explained as follows:

- The moment and total deflection are influenced by the horizontal component of the tension in the cable.
- The question is to find a relation that expresses the tension in the cable as a function of the stiffnesses, load and cable angle.

The tension in the cable  $N$  is assumed unknown. By doubly integrating the  $-M(x)/EI$ , the displacement field formula of the core can be found. The elongation of the cable is assumed to  $N \cdot L_c / EA$ . By equalizing the elongation of the cable transposed to horizontal direction with the displacement of the core at the position of the cable connection, an equation for  $N$  can be found, and, consequently, an equation for  $N_{\text{horiz}} = N \cdot \sin(\alpha)$ . By derivation the formula of  $N_{\text{horiz}}$  with the angle  $\alpha$  and equalizing to 0, the angle  $\alpha$  for which  $N_{\text{horiz}}$  is maximum can be found. This angle is 54.73 degrees, explaining the graphs above. Below, the Maple script used for the calculation is presented, and finally, the graph showing the evolution of  $N_{\text{horiz}}$ , which has a maximum value of 54.73 degrees is shown.

$$N = \frac{A}{1 + \gamma * \frac{EI}{EA}}$$

$$A = \frac{q * (6 * L^2 - 4 * L * a + a^2)}{8 * \sin \alpha}$$

$$\gamma = \frac{3}{a^2 * \cos \alpha * (\sin \alpha)^2}$$

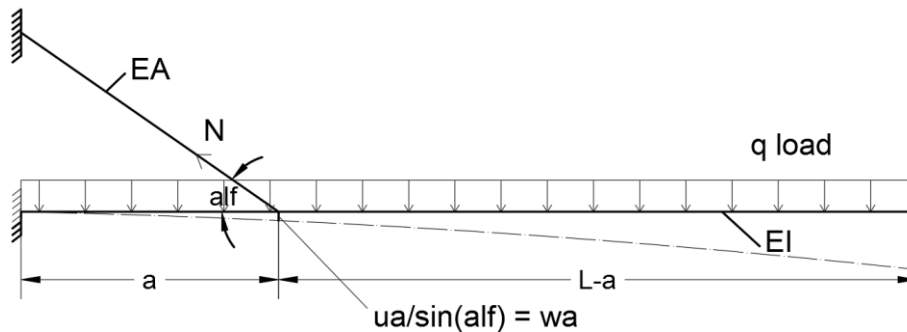
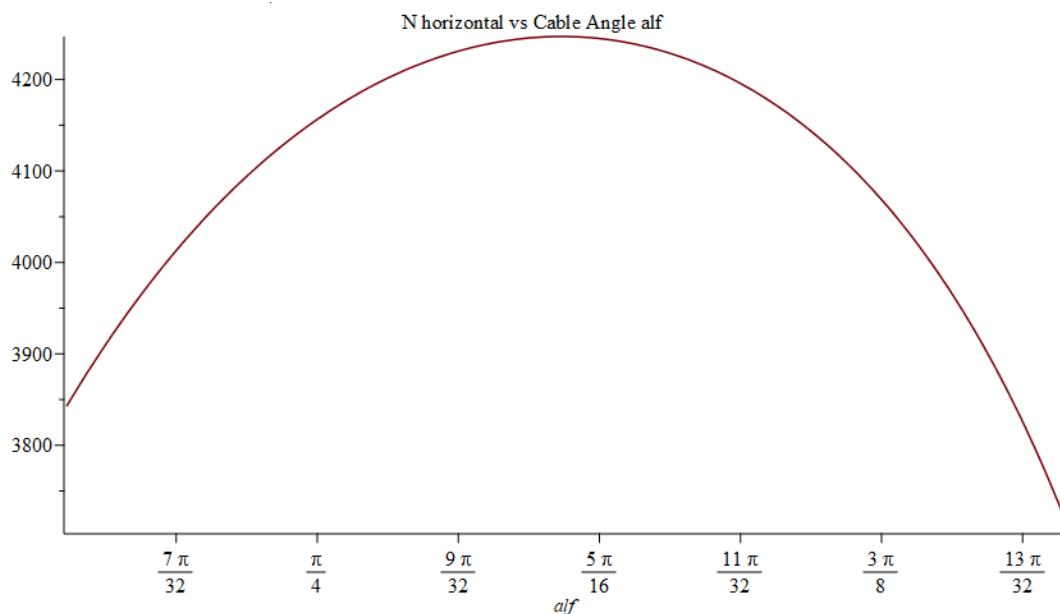


Figure 117 Sketch of analytical calculation

```

> restart;
> with(plots) :
>
> M1 := -  $\frac{q \cdot L \cdot L}{2}$  + N · sin(alf) · a + (q · L - N · sin(alf)) · x -  $\frac{q \cdot x^2}{2}$  :
> simplify(M1) :
> M2 := -  $\frac{q \cdot L \cdot L}{2}$  + N · sin(alf) · a + (q · L - N · sin(alf)) · x -  $\frac{q \cdot x^2}{2}$  + N · sin(alf) · (x - a) :
> simplify(M2) :
>
> phi1 := int( $\frac{M1}{EI}$ , x = 0 .. x) : phi2 := int( $\frac{M2}{EI}$ , x = 0 .. x) :
> wa := int(-phi1, x = 0 .. x) :
> wtop := (int(-phi1, x = 0 .. x) + int(-phi2, x = x .. L)) · 100 :
> w2 :=  $\frac{N}{EA} \cdot \frac{x^2}{\sin(alf)}$  :
> x := a : eq := wa = w2 :
> N := solve(eq, N) : assign(sol) : N1 := N : simplify(N) :
> Nhoriz := N · sin(alf) :
> L := 100 : a := 50 : EI := 1.911 · 109 : EA := 1.828 · 107 : x := a : q := 53 : x2 :=  $\frac{a}{\cos(alf)}$  : alf :=  $\frac{55 \cdot \text{Pi}}{180}$  :
> N := evalf(N) :
>
> x := a : wa := evalf(wa) · 100 :
> wtop := evalf(wtop) :
> x := 0 : M1 := evalf(M1) :
> alf := 'alf':
>
> plot(Nhoriz, alf =  $\frac{35 \cdot \text{Pi}}{180}$  ..  $\frac{75 \cdot \text{Pi}}{180}$ , title = "N horizontal vs Cable Angle alf");

```



# Appendix F

## 2D analysis of a single tower

---

The modelling assumptions for the 2D analysis of a single tower were presented in Chapter 5. In this chapter, the goal was to find a range a slenderness under which the system falls based on these assumptions, by changing the relative position of the cable-net. The cable angle was set to 55 degrees and the cable diameter to 350 millimeters.

### **Not prestressed and not loaded gravitationally cables**

---

The procedure for finding the range of slenderness in the 2D analysis, for not prestressed and not loaded gravitationally cables is as follows:

- Set the initial geometry of the system, based on the proposed relative position of the cable;
- Analyze the system using the 2D linear analysis in Karamba;
- Verify if the top deflection limit of  $H/500$  (200 millimeters for the 100 meters high tower) is respected → search for a unity check above 0.95 and below 0.99;
- If the unity check is lower than 0.95 → decrease the width of the core and rerun the analysis until the UC is satisfactory;
- If the unity check is higher than 0.99 → increase the width of the core and rerun the analysis until the UC is satisfactory;

For example, for the  $0.5 \times H$  RPC case:

- If a 10 meters wide core is used → a 11.7 cm top deflection is obtained → UC = 0.585;
- The width of the core is reduced until a top deflection of 19.9 cm is obtained → UC = 0.99;
- The 19.9 cm top deflection corresponds to a core width of 7.4 meters;
- This result in a slenderness of  $1/13.5$  for the 100-meter-high core;

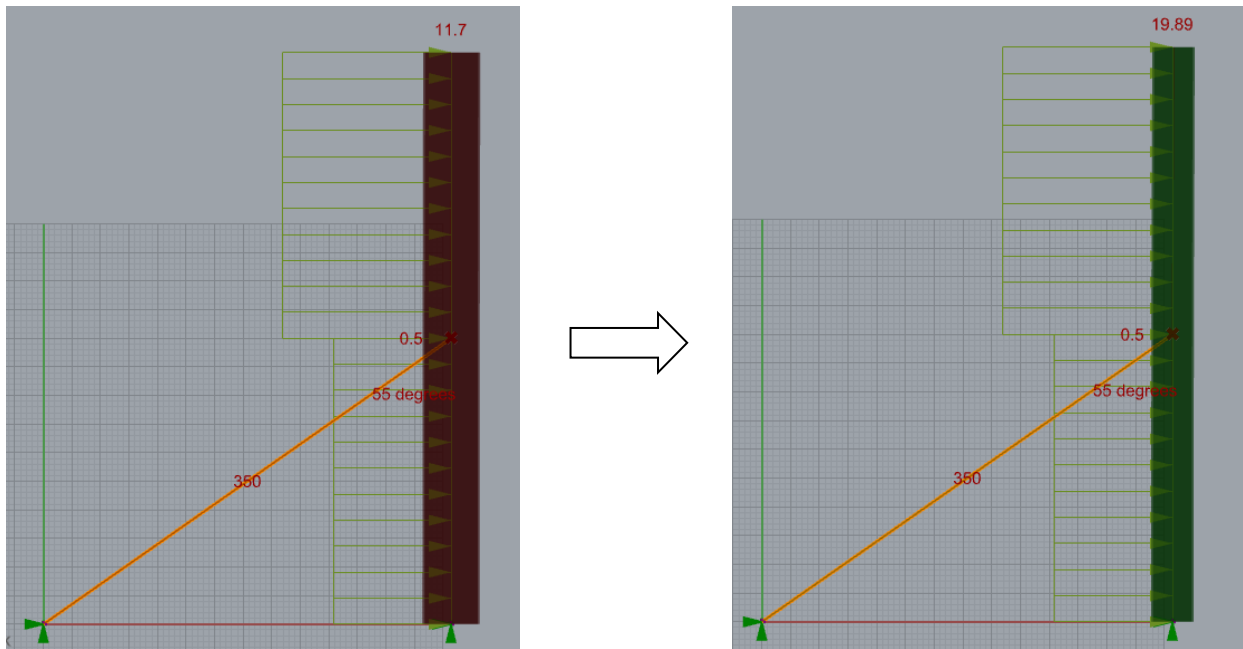


Figure 118 Core width reduction → unprestressed cables

The same procedure is used for the range of studied relative cable position, from 0.3 to 0.7, considering both the pinned and fixed connection, resulting in the following descriptive table, based on which Figure 43 is produced.

Table 52 Range of slenderness for the unprestressed cables

Range of slenderness based on RPC for a cable angle of 55 degrees → unprestressed cables					
Nr. Crt [-]	Connection type [-]	Prestress force [% of strength]	Connection Position [-]	Core dimension [cm]	Slenderness no prestress [-]
1	fixed		no cable	1230	8.1
2	fixed	0	0.3 x H	1050	9.5
	pinned			1350	7.4
3	fixed	0	0.4 x H	910	11.0
	pinned			950	10.5
4	fixed	0	0.5 x H	730	13.7
	pinned			740	13.5
5	fixed	0	0.6 x H	540	18.5
	pinned			540	18.5
6	fixed	0	0.7 x H	350	28.6
	pinned			350	28.6

## Prestressed and not loaded gravitationally cables

The procedure for the prestressed cables case is exactly the same as for the unprestressed case, to find a range of slenderness. As shown in Figure 45, the cables are prestressed to the level at which the leeward side cable does not sag under the lateral loads, thus adding stiffness to the system. Such, before finding the range of slenderness the prestress value for each RPC under which the leeward cable does not go slack is found, as shown in Figure 119, for an RPC of  $0.5 \times H$ :

- For a prestress value of 5.7 % of the strength of the spiral strand, the leeward cable goes slack;
- For a prestress value of 12.3 % of the strength of the spiral strand, the leeward cable does not go slack anymore;

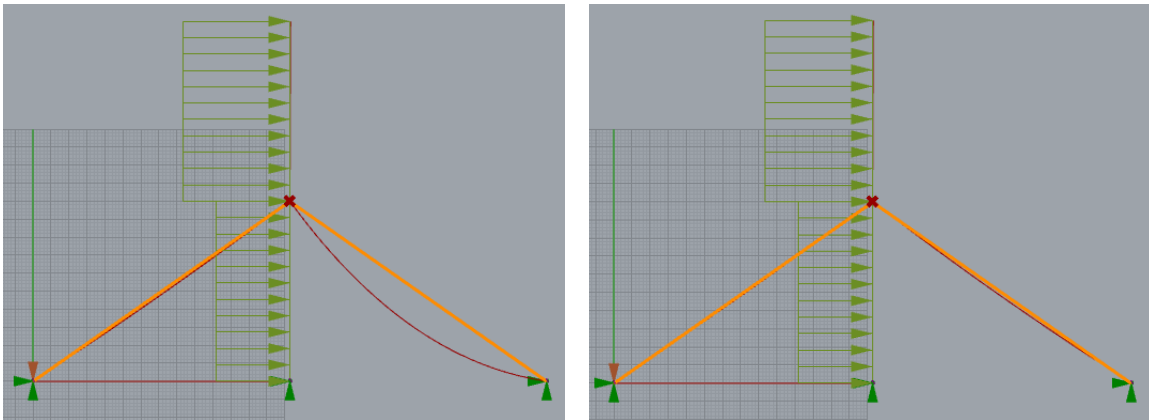


Figure 119 Prestressed leeward cable for no sag

The same example, for the  $0.5 \times H$  RPC case is presented:

- If a 10 meters wide core is used  $\rightarrow$  an 8.43 cm top deflection is obtained  $\rightarrow$  UC = 0.42
- The width of the core is reduced until a top deflection of 19.7 cm is obtained  $\rightarrow$  UC = 0.98
- The 19.8 cm top deflection corresponds to a core width of 6.5 meters
- This result in a slenderness of  $1/15.4$  for the 100-meter-high core

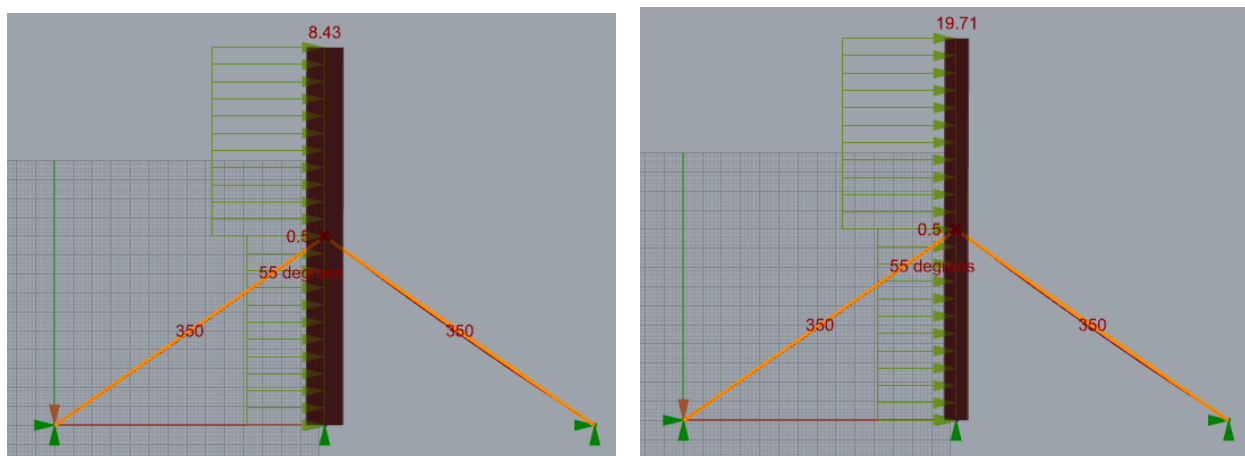


Figure 120 Core width reduction  $\rightarrow$  prestressed cables

The same procedure is used for the range of studied relative cable position, from 0.3 to 0.7, considering both the pinned and fixed connection, resulting in the following descriptive table, based on which Figure 46 is produced.

**Table 53 Range of slenderness for the prestressed cables**

<b>Range of slenderness based on RPC for a cable angle of 55 degrees → prestressed cables</b>					
<b>Nr. Crt</b>	<b>Connection type</b>	<b>Prestress force</b>	<b>Connection Position</b>	<b>Core dimension</b>	<b>Slenderness</b>
<b>[-]</b>	<b>[-]</b>	<b>[% of strength]</b>	<b>[-]</b>	<b>[cm]</b>	<b>no prestress</b>
					<b>[-]</b>
1	fixed		no cable	1230	8.1
2	fixed	9.88%	0.3 x H	960	10.4
	pinned			980	10.2
3	fixed	11.40%	0.4 x H	810	12.3
	pinned			820	12.2
4	fixed	12.30%	0.5 x H	650	15.4
	pinned			650	15.4
5	fixed	13.30%	0.6 x H	460	21.7
	pinned			460	21.7
6	fixed	14.25%	0.7 x H	325	30.8
	pinned			325	30.8

## **Prestressed and loaded cables**

The procedure to find the range of slenderness for the prestress and loaded cables is similar to the previous cases. In this case, however, the form finding process of finding the initial geometry of the cable under the applied loads is of relevance. The procedure thus becomes:

- Set the initial geometry of the system, based on the proposed relative position of the cable;
- Form find the geometry of the cable under the applied loads;
- Analyze the system using the 2D linear analysis in Karamba;
- Verify if the top deflection limit of  $H/500$  (200 millimeters for the 100 meters high tower) is respected → search for a unity check above 0.95 and below 0.99
- If the unity check is lower than 0.95 → decrease the width of the core and rerun the analysis until the UC is satisfactory;
- If the unity check is higher than 0.99 → increase the width of the core and rerun the analysis until the UC is satisfactory;

An example of the procedure is presented, for the case of a RPC of 0.5, using the explained “medium” force density value:

1. Setting up the geometry of the system:

- By choosing an arbitrary dimension for the core, to be later optimized for according to the top deflection requirement;
- First creating the straight geometry of the cables;
- Inputting the wind load on the core;
- Dividing the cable element in 25 segments;
- Calculating the corresponding load imposed by the mountain on each node:

Table 54 Equivalent point load calculation

Dead Load [kN/m]	Live Load [kN/m]	Span [m]	Equivalent Line Load [kN/m]	Cable Length [m]	Number of points [-]	Equivalent Point Load [kN]
3.7	2.5	50	310	86.8	25	1076

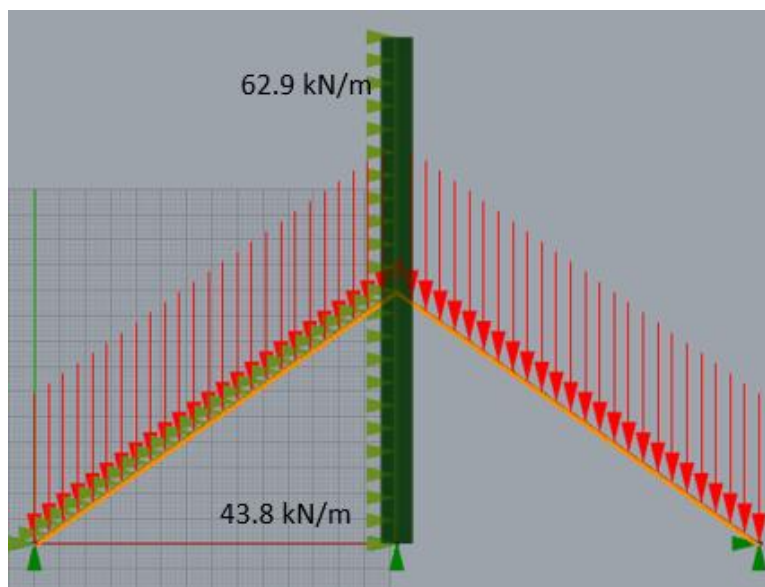


Figure 121 Initial configuration → straight loaded cables

2. Performing the form finding process using the medium force density value. This results in the geometry to be analyzed together with the core and to the initial strains in each of the 25 cable elements.

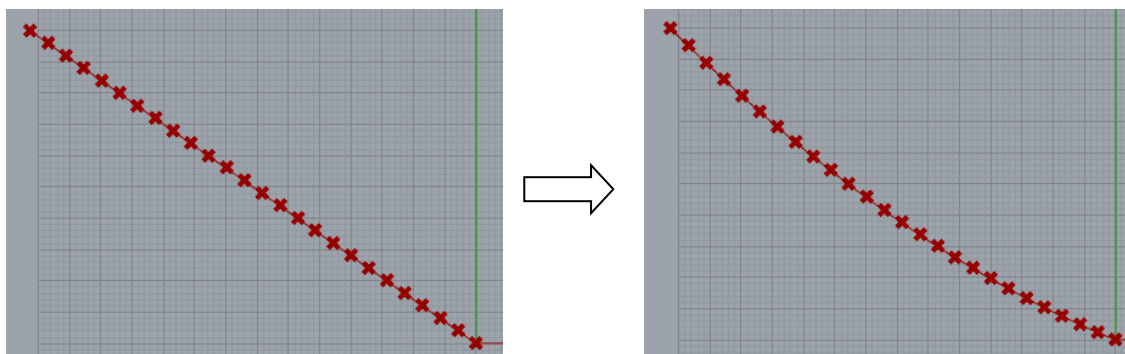


Figure 122 Form finding output with medium FD value

- Results of the form finding process → geometry of the cable with the sag of 4.9;

- Initial strain in the cable, calculated as per the definition of the FDM, in Chapter 2.5.3. This is calculated for each of the 25 segments of the cable, and presented in Table 55 as average:
  - Final lengths of the form found cable multiplied by FD value → Forces in the cable
  - Forces in the cables divided by the stiffness of the cable → Initial Strain in the cable

Table 55 Prestress calculation based on form finding process

FD Value [-]	Average Final Length [m]	Average Force [kN]	Cable Stiffness EA	Average Initial Strain [-]	Prestress as % of ultimate strength [%]
8800	3.52	31274	18200000	0.0017	31.80%

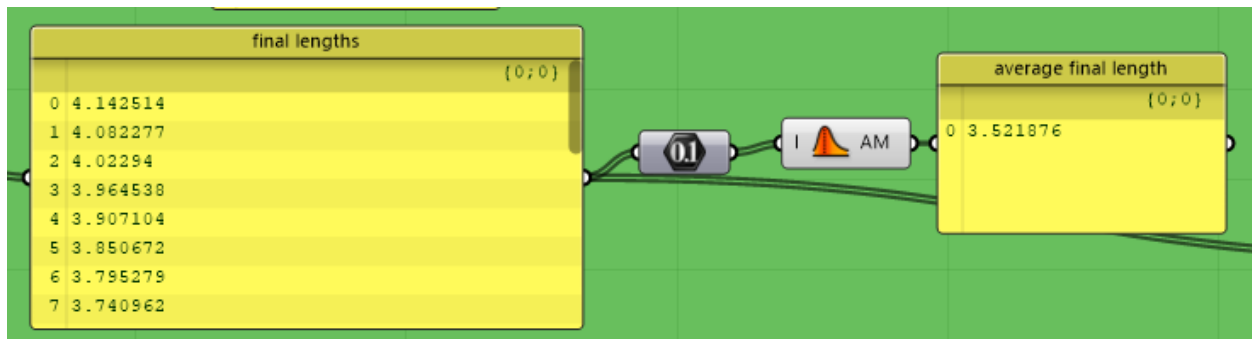


Figure 123 Final lengths output → Grasshopper

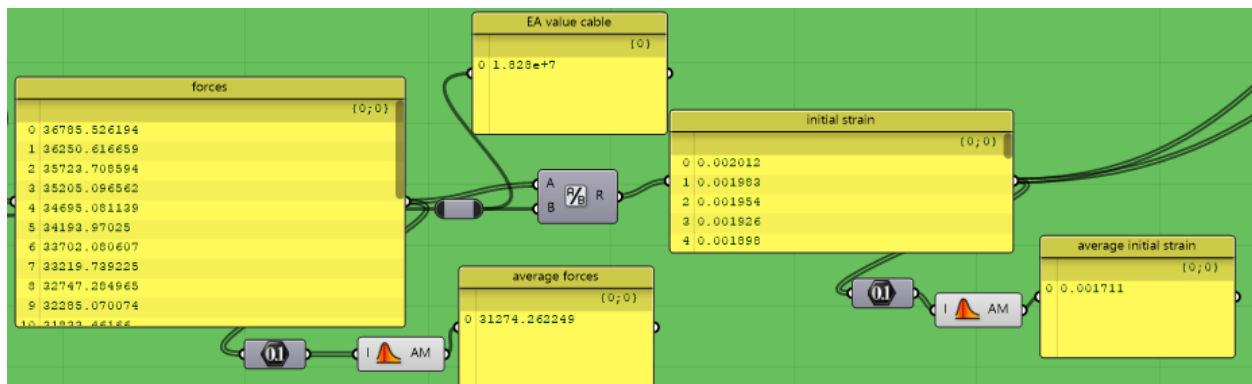


Figure 124 Average initial strain calculation → Grasshopper

- Performing the static analysis in Karamba, to check the top displacement requirement and to obtain, as for the previous cases, the range of slenderness.
  - If an 8 meters wide core is used → a 25.84 cm top deflection is obtained → UC = 1.3;
  - The width of the core is increased until a top deflection of 19.5 cm is obtained → UC = 0.98;
  - The 19.5 cm top deflection corresponds to a core width of 9 meters;
  - This result in a slenderness of 1/11.1 for the 100-meter-high core;

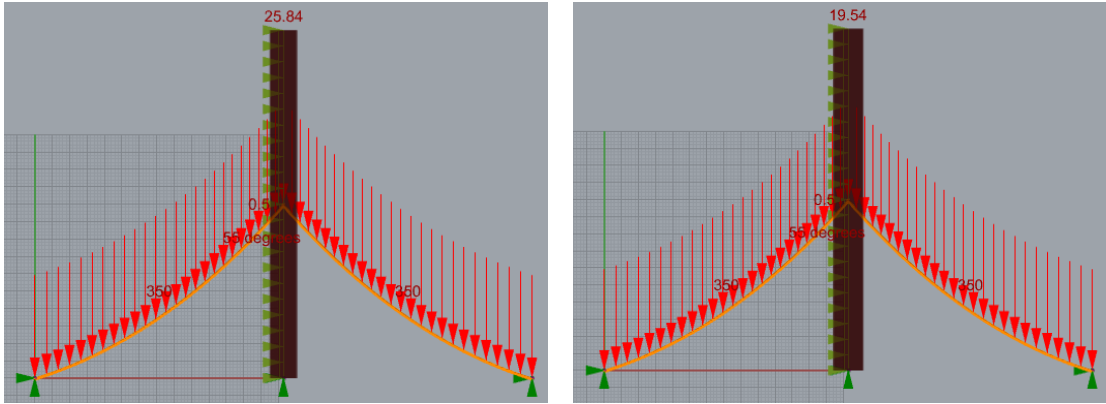


Figure 125 Core width reduction → loaded cables

Results in terms of the bending moment diagram, or the axial force on the tower can be also obtained. The following figures are presented. It should be noted that the results are from the load combination SLS-1, as the ULS combination was not part of the 2D study.

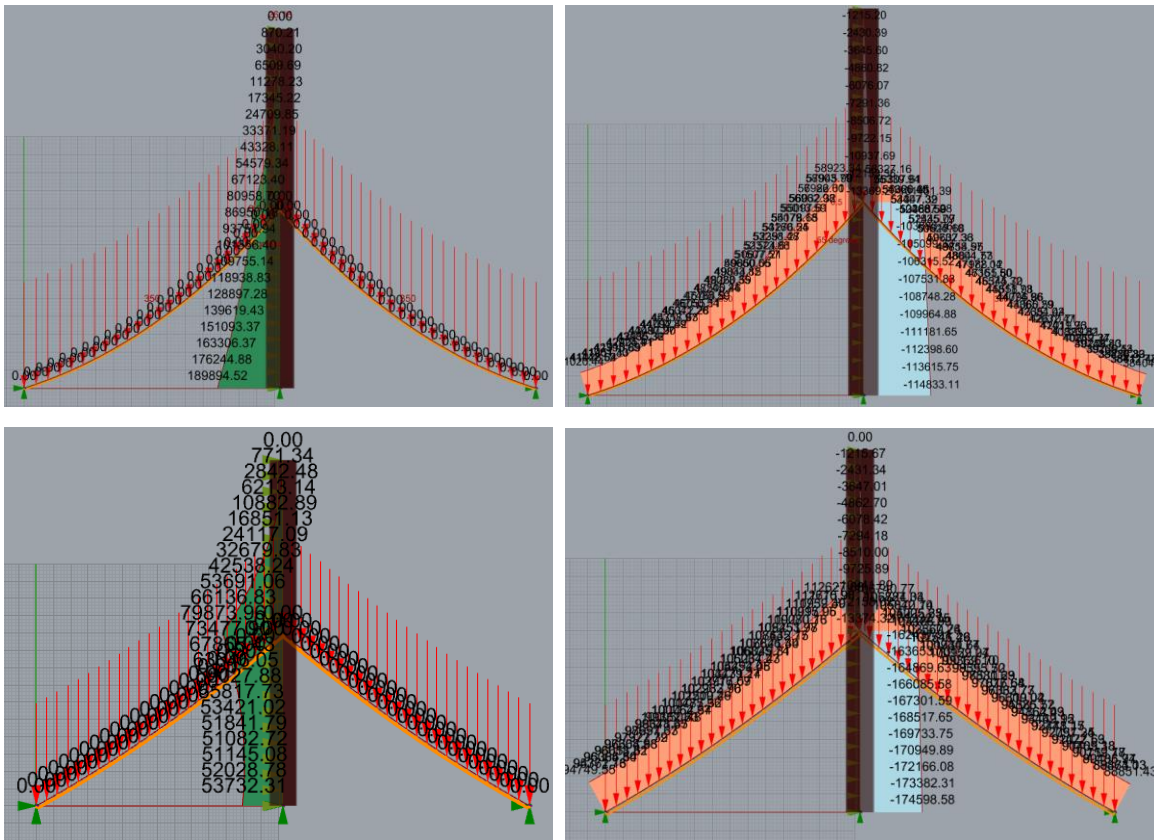


Figure 126 Karamba output → loaded cables; Medium FD (top); High FD (bottom)

Table 56 shows the initial prestress in the cable as a function of the relative position of the cable and of the force density. As expected, if a high FD is used and the cable tends to be straight, high values of the initial prestress are required, higher than the admissible values presented by Gabriel (1974).

**Table 56 Initial prestress based on force density and relative position of the cable**

<b>Initial Prestress based on FD and RPC as % of ultimate strength of the cable</b>					
<b>Force Density</b>	<b>0.3 x H RPC</b>	<b>0.4 x H RPC</b>	<b>0.5 x H RPC</b>	<b>0.6 x H RPC</b>	<b>0.7 x H RPC</b>
low	14.8%	19.7%	24.5%	29.4%	34.3%
medium	19.5%	26.1%	31.8%	39.1%	45.5%
high	38.7%	51.6%	64.5%	77.4%	90.3%

Table 57 shows the final tension in the cables as a function of the relative position of the cable and the force density. Naturally, an increase in the utilization of the cable is observed when compared to Table 56, which showed the initial tension due to prestress. On average, this increase is in the range of 10 – 30% of the ultimate strength of the cable, which is in line with the guidelines of Gabriel (1974). In cases of high loading (high RPC), and high FD, the ultimate strength of the proposed cable is exceeded. The tension in the cables and further design of the cable-net is later addressed in Chapter 6.2.

**Table 57 Final tension based on force density and relative position of the cable**

<b>Final Tension based on FD and RPC as % of ultimate strength of the cable</b>					
<b>Force Density</b>	<b>0.3 x H RPC</b>	<b>0.4 x H RPC</b>	<b>0.5 x H RPC</b>	<b>0.6 x H RPC</b>	<b>0.7 x H RPC</b>
low	23.6%	31.8%	38.8%	47.2%	54.9%
medium	31.5%	40.7%	51.5%	60.7%	69.6%
high	55.1%	71.5%	86.1%	101.1%	115.2%

The same procedure is used for the range of studied relative cable position, from 0.3 to 0.7, considering both the pinned and fixed connection, resulting in the following descriptive tables, from which Figure 54 is produced

**Table 58 Range of slenderness → loaded cables, low FD value**

<b>Range of slenderness based on RPC for a cable angle of 55 degrees-Low FD value</b>					
<b>Nr. Crt [-]</b>	<b>Connection type [-]</b>	<b>Connection Position [-]</b>	<b>Core dimension [cm]</b>	<b>Cable Diameter [mm]</b>	<b>Slenderness no prestress [-]</b>
1	fixed	no cable	1230	no cable	8.1
2	fixed	0.3 x H	1140	350	8.8
	pinned		-	350	not enough stiffness provided
3	fixed	0.4 x H	1120	350	8.9
	pinned		-	350	not enough stiffness provided
4	fixed	0.5 x H	1090	350	9.2
	pinned		-	350	not enough stiffness provided
5	fixed	0.6 x H	1040	350	9.6
	pinned		-	350	not enough stiffness provided

6	fixed	0.7 x H	980	350	10.2
	pinned		-	350	not enough stiffness provided

Table 59 Range of slenderness → loaded cables, medium FD value

Range of slenderness based on RPC for a cable angle of 55 degrees-Medium FD value					
Nr. Crt [-]	Connection type [-]	Connection Position [-]	Core dimension [cm]	Cable Diameter [mm]	Slenderness no prestress [-]
1	fixed	no cable	1230	no cable	8.1
2	fixed	0.3 x H	1110	350	9.0
	pinned		-	350	not enough stiffness provided
3	fixed	0.4 x H	1040	350	9.6
	pinned		-	350	not enough stiffness provided
4	fixed	0.5 x H	900	350	11.1
	pinned		-	350	not enough stiffness provided
5	fixed	0.6 x H	750	350	13.3
	pinned		800	350	12.5
6	fixed	0.7 x H	550	350	18.2
	pinned		630	350	15.9

Table 60 Range of slenderness → loaded cables, high FD value

Range of slenderness based on RPC for a cable angle of 55 degrees-High FD value					
Nr. Crt [-]	Connection type [-]	Connection Position [-]	Core dimension [cm]	Cable Diameter [mm]	Slenderness no prestress [-]
1	fixed	no cable	1230	no cable	8.1
2	fixed	0.3 x H	1040	350	9.6
	pinned		-	350	not enough stiffness provided
3	fixed	0.4 x H	880	350	11.4
	pinned		910	350	11.0
4	fixed	0.5 x H	690	350	14.5
	pinned		690	350	14.5
5	fixed	0.6 x H	520	350	19.2
	pinned		520	350	19.2
6	fixed	0.7 x H	390	350	25.6
	pinned		400	350	25.0

# Appendix G

## 3D study of a rectangular grid of towers

### Form finding 3D cable-net

In this Appendix the procedure used for the form finding of the 3D net, as presented in Chapter 6.1 is further developed. A case of 80 meters spacing with a relative position of the cable-net of  $0.5 \times H$  is presented:

Step 1: Initial Geometry of the system

- Setting up the initial geometry of the system, by spacing the towers accordingly and by positioning the cable-net at the set RPC

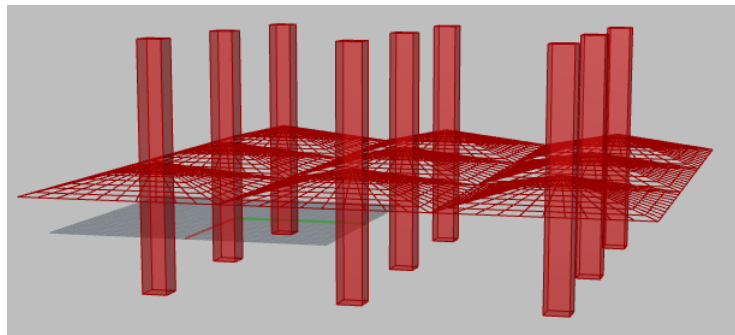


Figure 127 Initial Geometry

- Choosing a grid of elements (divisions of the cable elements in horizontal and vertical direction), to obtain a final average cable length of 4 meters (this is an iterative process)
  - For the 5x5 grid the average final length is 6.2 meters
  - For the 10x10 grid the average final length is 4.1 meters → 10x10 is chosen

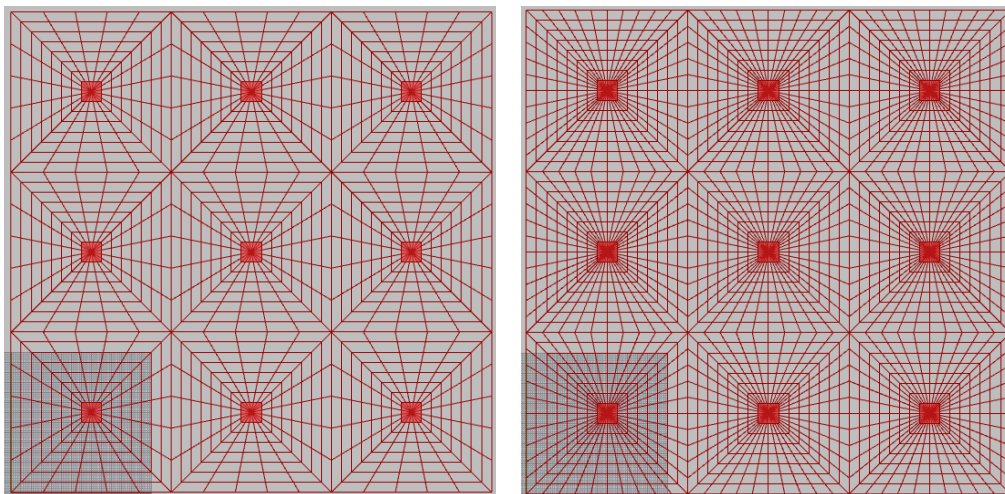


Figure 128 Left: 5x5 Grid (Avg Final Length = ); Right: 10x10 Grid

Step 2: Form finding analysis

- Iteratively conduct the form finding process to obtain a cable net with the sag/ rise of ~4 %, by changing the FD value → a FD value of 6000 is found suitable to reach a sag/ rise of ~4%.

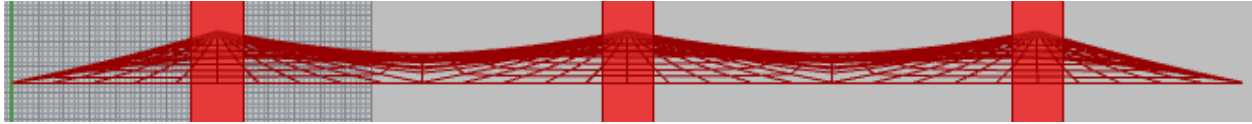


Figure 129 FD too low → sag/ rise of 7%

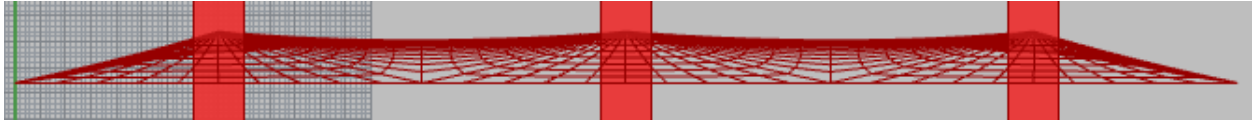


Figure 130 FD too high → sag/ rise of 2%

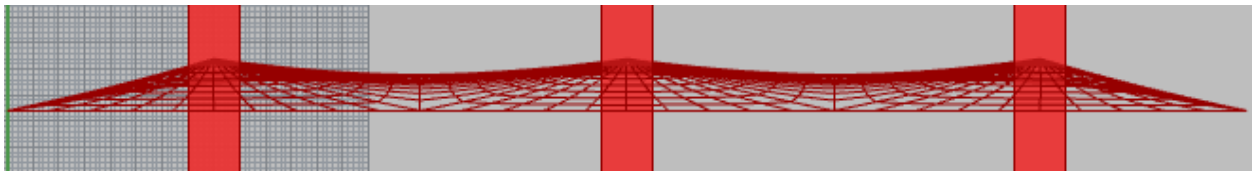


Figure 131 Good value for FD under initial assumptions → sag/ rise of 4.1%

Step 3: Calculate the initial strain, prestress and relative elongation / cable element type

- This process is done automatically in Grasshopper, using the K2 Engineer component, and further analytical expressions of the equations in Chapter 2.5
- The process is conducted for all cable types (diagonal, edge, internal vertical and internal horizontal). Below, the script for the diagonal cable is shown:

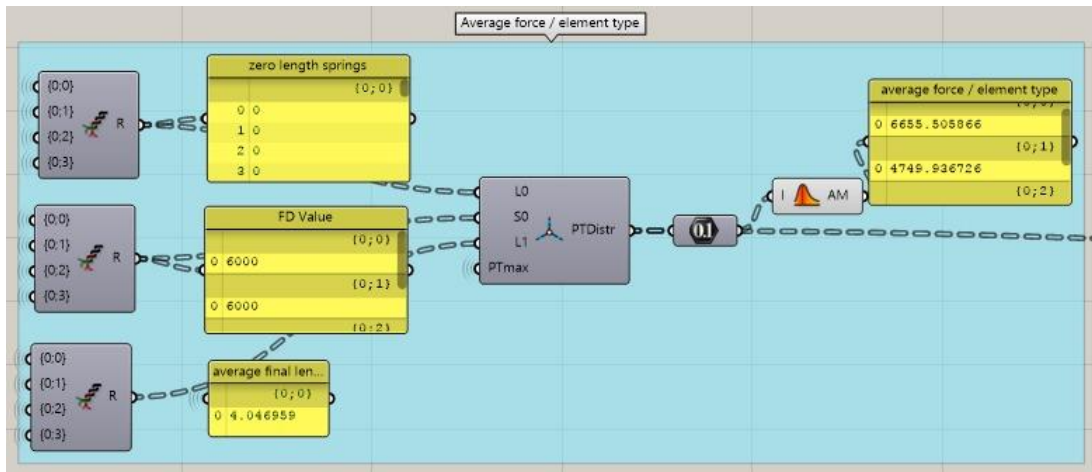


Figure 132 Forces based on FD and Final Length

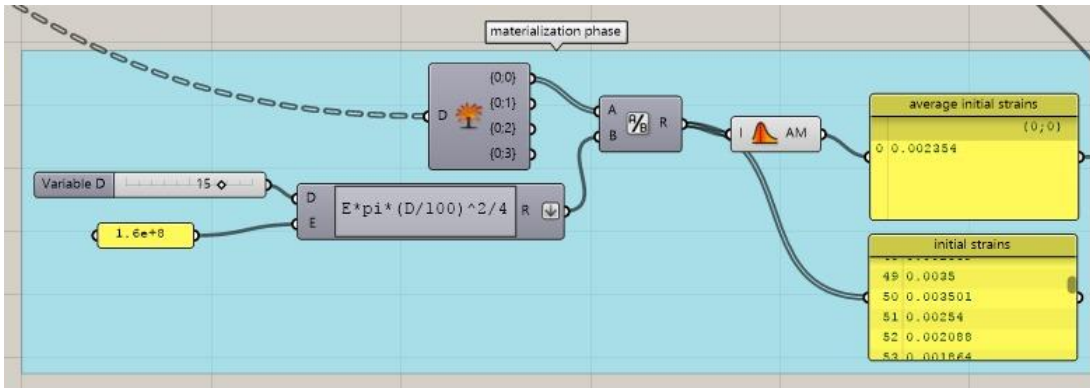


Figure 133 Materialization Phase

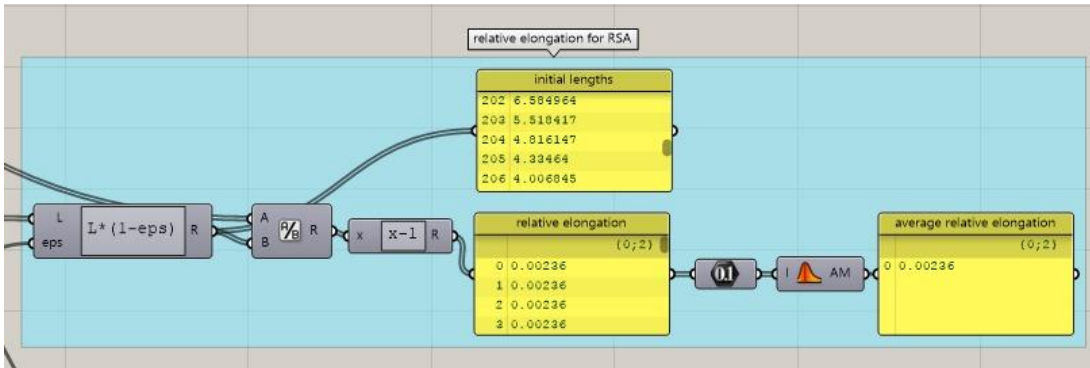


Figure 134 Average relative elongation to be applied as prestress in RSA

Table 61 Prestress in the Diagonal Cable as % of strength → SBT of 80 meters

Force Density Value [-]	Average Final Length [m]	Cable Stiffness EA [kN/m <sup>2</sup> ]	Average Initial Strain [-]	Prestress as % of ultimate strength [%]
6000	4.04	2.83 x 10 <sup>6</sup>	0.00235	30.3%

Table 62 Prestress in all cables as % of strength

	Edge Cable	Diagonal Cable	Internal Cable - Vertical	Internal Cable - Horizontal
30 meters	29.2%	27.3%	32.2%	17.1%
50 meters	30.1%	28.7%	34.1%	18.2%
80 meters	32.9%	30.3%	36.9%	19.1%
110 meters	36.1%	34.2%	38.8%	21.3%
140 meters	39.2%	38.9%	43.1%	24.8%

Table 62 shows the prestress as % of the maximum strength of the cables for all analyzed cases (SBT between 30 and 140 meters) and for all cable types. These values are obtained directly in the Grasshopper script, after the form finding process and materialization phase are conducted.

## Full Analysis (9 towers) vs Simplified Analysis (Single Tower)

As explained in Chapter 6.1, a comparison is made between the analysis of a single tower and the analysis of 9 towers. The properties of the model are maintained the same for the two cases:

- The core(s) has the dimension of 6.9 x 6.9 x 0.35 meters (this is, to reach a deflection with a 0.95-0.99 unity check in the single tower case)
- The core(s) is considered fixed to the foundation;
- The cables are considered pinned to the edges for the 9 towers case;
- The cables are considered pinned in their direction (X for node in X-direction, Y for node in y-direction, XY for corner node) for the single tower analysis;
- The core has an E-value of 9100 above the cable-net connection, and an E-value of 27000 MPa below the cable-net connection;
- The wind load acts only on the middle tower for the 9-tower analysis;

**Results:** A divergence in the results of up to 8% is observed. This is considered acceptable as the time for a single iteration is reduced significantly (up to 10 times)

- Single tower iteration → approximately 1.5 minutes
- Full 9 tower iteration → approximately 15 minutes
- **Table 63 Comparison between full and simplified model**

	Simplified Model	Full Model	Divergence
Top Deflection (SLS-1) [mm]	194	211	8.1
Cable Net (Max) Deflection (SLS-1) [mm]	482	464	-3.9
Bending Moment (ULS-4) [kN x m]	16651	17323	3.9
Axial Force (ULS-4) [kN]	141984	142300	0.2

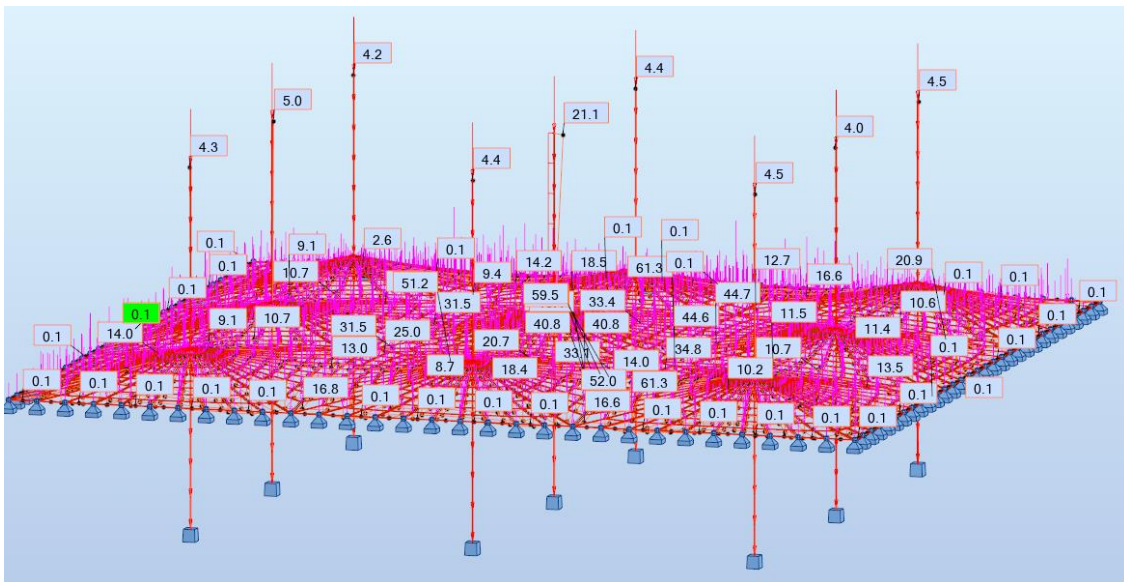


Figure 135 Displacement simplified model

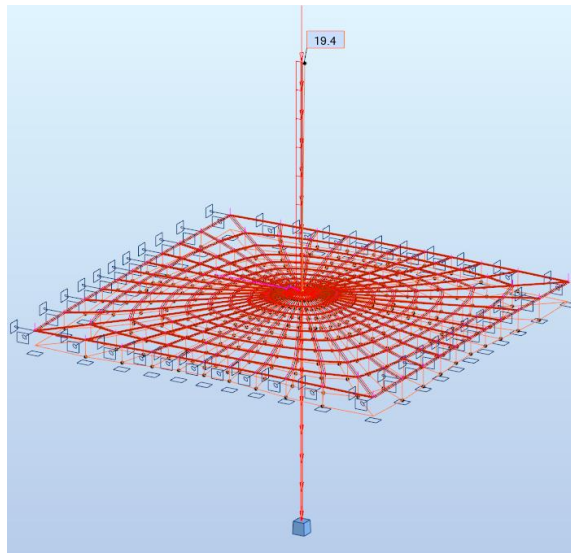


Figure 136 Displacement full model

## Design of the cable-net

The cable elements are designed as described in Chapter 6.2, to account for both the ULS and SLS requirements. In Chapter 6.2 a design example was presented for the 80 meters spacing case. In this appendix, the required dimensions of the cables based on the occurring tensile force, and prestress required to limit the deflection to span/200 for each spacing case is presented.

### 30 meters spacing

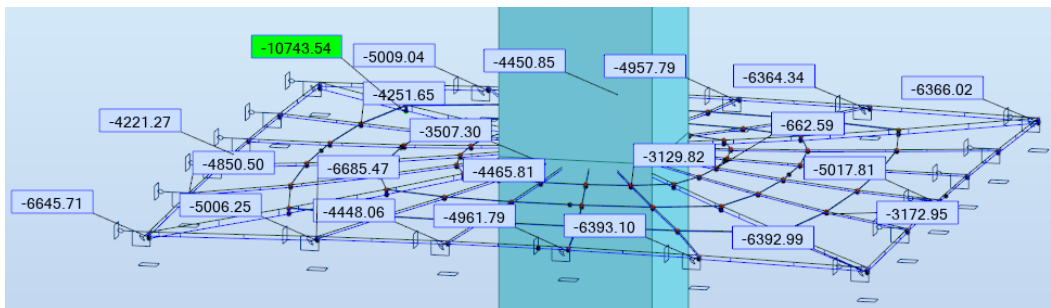


Figure 137 Axial force cables 30 meters spacing case

Table 64 Cables design for 30 meters spacing case

Case	Cable Type	Maximum Axial Force [kN]	Required Diameter [mm]	Chosen Diameter [mm]	Maximum Stress Cable [MPa]	Admissible Stress [MPa]	Unity Check [-]
30 meters spacing	Edge Cable	6645	91	100	846.1	1020	0.83
	Diagonal Cable	10743	116	120	949.9	1020	0.93
	Internal - Vertical	5017	79	80	998.1	1020	0.98
	Internal - Horizontal	662	29	70	172.0	1020	0.17

## 50 meters spacing

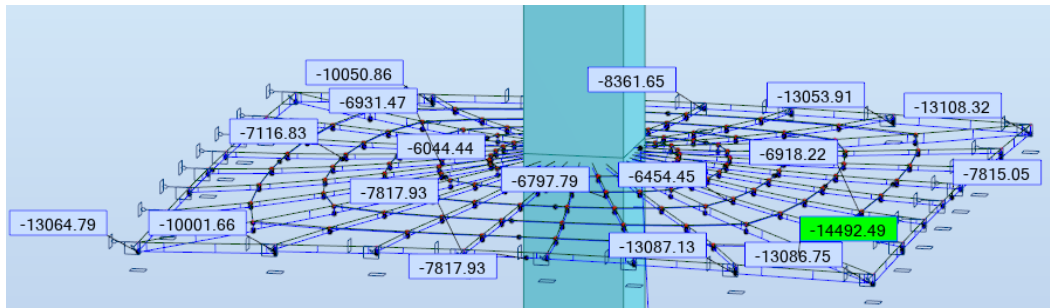


Figure 138 Axial force cables 50 meters spacing case

Table 65 Cables design for 50 meters spacing case

Case	Cable Type	Maximum Axial Force [kN]	Required Diameter [mm]	Chosen Diameter [mm]	Maximum Stress Cable [MPa]	Admissible Stress [MPa]	Unity Check [-]
50 meters spacing	Edge Cable	13108	128	130	987.6	1020	0.97
	Diagonal Cable	14492	134	135	1012.4	1020	0.99
	Internal - Vertical	7815	99	100	995.0	1020	0.98
	Internal - Horizontal	1040	36	80	206.9	1020	0.20

## 80 meters spacing

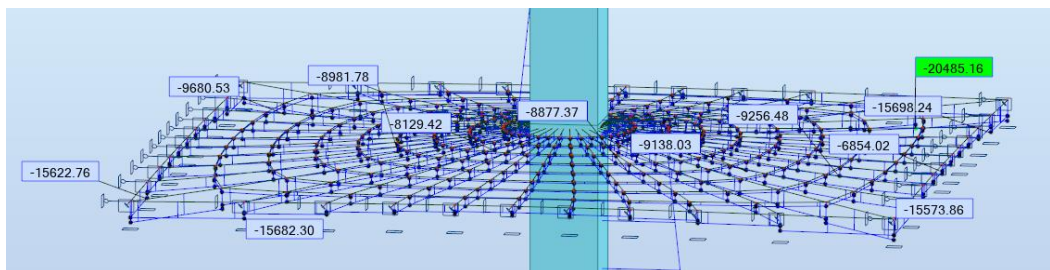


Figure 139 Axial force cables 80 meters spacing case

Table 66 Cables design for 80 meters spacing case

Case	Cable Type	Maximum Axial Force [kN]	Required Diameter [mm]	Chosen Diameter [mm]	Maximum Stress Cable [MPa]	Admissible Stress [MPa]	Unity Check [-]
80 meters spacing	Edge Cable	15896	141	145	962.6	1020	0.94
	Diagonal Cable	20485	160	165	958.0	1020	0.94
	Internal - Vertical	9680	110	115	931.9	1020	0.91
	Internal - Horizontal	2714	58	90	539.9	1020	0.53

### 110 meters spacing

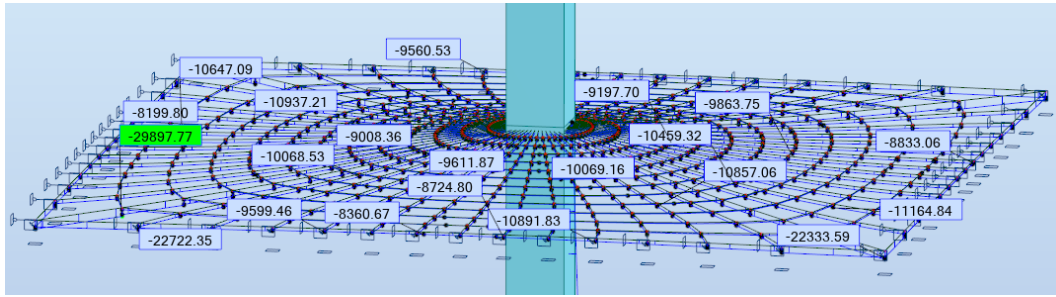


Figure 140 Axial force cables 110 meters spacing case

Table 67 Cables design for 110 meters spacing case

Case	Cable Type	Maximum Axial Force [kN]	Required Diameter [mm]	Chosen Diameter [mm]	Maximum Stress Cable [MPa]	Admissible Stress [MPa]	Unity Check [-]
110 meters spacing	Edge Cable	22897	169	170	1008.8	1020	0.99
	Diagonal Cable	29827	193	195	998.7	1020	0.98
	Internal - Vertical	11164	118	125	909.7	1020	0.89
	Internal - Horizontal	3812	69	90	599.2	1020	0.59

### 140 meters spacing

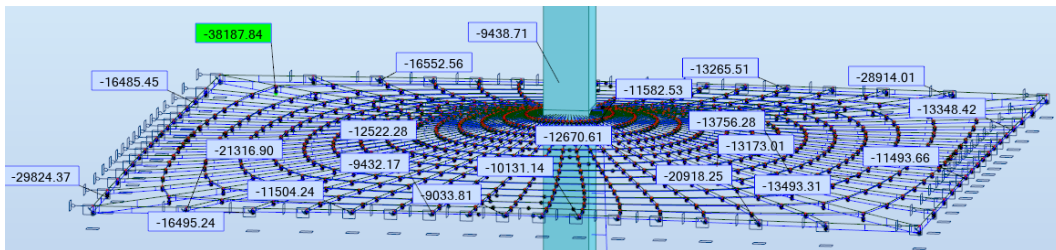


Figure 141 Axial force cables 140 meters spacing case

Table 68 Cables design for 140 meters spacing case

Case	Cable Type	Maximum Axial Force [kN]	Required Diameter [mm]	Chosen Diameter [mm]	Maximum Stress Cable [MPa]	Admissible Stress [MPa]	Unity Check [-]
140 meters spacing	Edge Cable	29824	193	195	998.6	1020	0.98
	Diagonal Cable	38187	218	220	1004.6	1020	0.98
	Internal - Vertical	16552	144	150	936.7	1020	0.92
	Internal - Horizontal	5523	83	100	703.2	1020	0.69

## Range of Slenderness

The procedure to obtain the range of slenderness for the 3D case is the same as the one used for the 2D case, with the difference that in this case the analysis is conducted in RSA. The procedure is as follows:

- Set the initial geometry of the system, based on the proposed relative position of the cable;
- Form-find the geometry of the cable-net under the applied loads
- Export the system to the RSA software
- Analyze the system using the 3D nonlinear analysis in RSA;
- Verify if the top deflection limit of  $H/500$  (200 millimeters for the 100 meters high tower) is respected → search for a unity check above 0.95 and below 0.99
- If the unity check is lower than 0.95 → decrease the width of the core and rerun the analysis until the UC is satisfactory;
- If the unity check is higher than 0.99 → increase the width of the core and rerun the analysis until the UC is satisfactory;

For example, for a configuration with RPC of 0.5 and SBT of 80 meters:

- If a 7.4 meters wide core is used → a 16.8 cm top deflection is obtained → UC = 0.84
- The width of the core is reduced until a top deflection of 19.9 cm is obtained → UC = 0.97
- The 19.7 cm top deflection corresponds to a core width of 6.7 meters
- This result in a slenderness of  $1/14.9$  for the 100-meter-high core

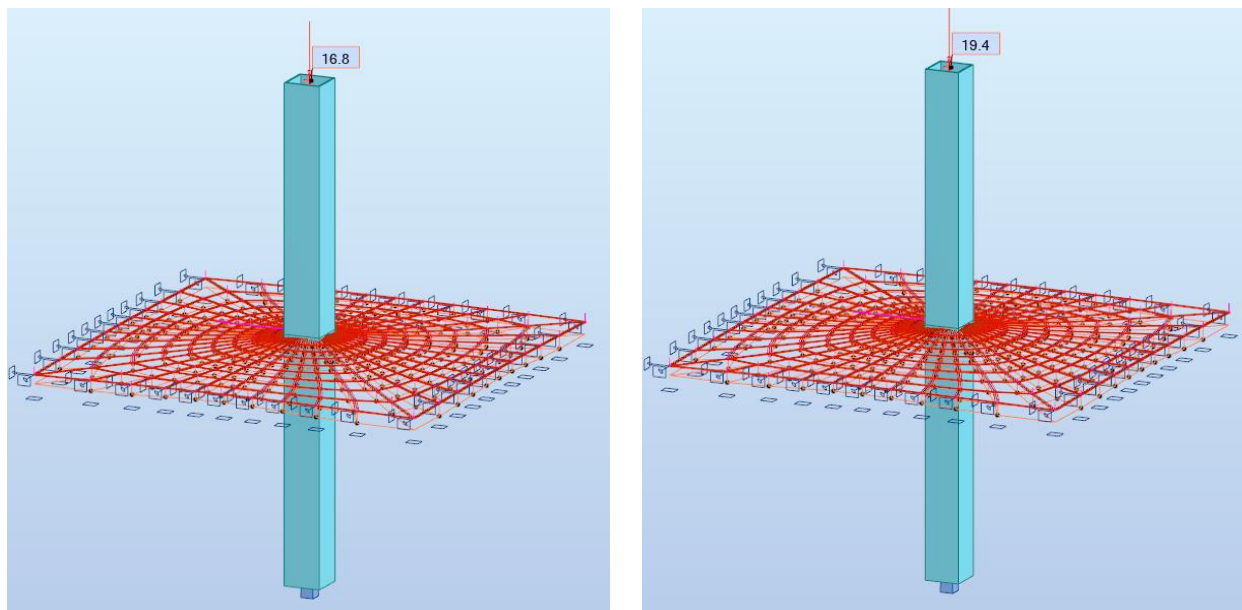


**Figure 142 Core width reduction → 3D model**

By conducting this procedure for all the analyzed geometries (with the RPC from 0.2 to 0.7 and the SBT from 30 to 140 meters) the following table is produced, with respect to the core widths to achieve the desired UC for top displacement.

**Table 69 Core widths for the studied cases**

Relative Position [-]	Height [m]	Spacing between towers [m]	Core width [m]	Core thickness [m]	Slenderness
0.2	100	30	11	0.35	9.09
0.3			9.9	0.35	10.10
0.4			8.2	0.35	12.20
0.5			6.4	0.35	15.63
0.6			5	0.35	20.00
0.7			3.9	0.35	25.64
0.2			100	50	11.1
0.3	10.3	0.35			9.71
0.4	8.9	0.35			11.24
0.5	6.8	0.35			14.71
0.6	5.2	0.35			19.23
0.7	4	0.35			25.00
0.2	100	80			11.2
0.3			10.6	0.35	9.43
0.4			9.2	0.35	10.87
0.5			7.1	0.35	14.08
0.6			5.4	0.35	18.52
0.7			4.1	0.35	24.39
0.2			100	110	11.3
0.3	10.8	0.35			9.26
0.4	9.5	0.35			10.53
0.5	7.4	0.35			13.51
0.6	5.7	0.35			17.54
0.7	4.3	0.35			23.26
0.2	100	140			11.4
0.3			10.9	0.35	9.17
0.4			9.7	0.35	10.31
0.5			7.7	0.35	12.99
0.6			5.9	0.35	16.95
0.7			4.5	0.35	22.22

# Appendix H

## Design of the core

### Forces on the Core

In this appendix, the tables that provide the information presented in Chapter 7 are presented. Based on these tables, the axial force and bending moment graphs can be computed, and the stresses occurring in the core can be calculated. The results of Chapter 7.1 were presented in terms of the two governing ULS combinations (ULS 3 and ULS 4). In ULS 3 the full live loads were considered, but the wind load was not considered, while in ULS 4 the live load values were reduced and the full wind load was considered.

**Table 70 Results → bottom stresses and forces ULS 3**

Model Properties		Bottom Forces		Sectional properties			Stresses				
RPC [-]	SBT [-]	Width [m]	Thickness [m]	Slenderness [-]	Axial Force [kN]	Bending Moment [kN x m]	Core area [m <sup>2</sup> ]	Wy core [m <sup>3</sup> ]	Iy core [m <sup>4</sup> ]	Maximum stresses bot [MPa]	Minimum stresses bot [MPa]
0.2		11	0.35	9.09	136430	0	10.4	39.7	282.2	-13.1	-13.1
0.3		9.9	0.35	10.10	131519	0	9.4	31.9	203.5	-14.1	-14.1
0.4	30	8.2	0.35	12.20	123930	0	7.7	21.6	113.1	-16.1	-16.1
0.5		6.4	0.35	15.63	115894	0	5.9	12.8	51.8	-19.5	-19.5
0.6		5	0.35	20.00	109643	0	4.6	7.6	23.6	-24.1	-24.1
0.7		3.9	0.35	25.64	104723	0	3.5	4.4	10.5	-30.1	-30.1
0.2			11.1	0.35	9.01	154431	0	10.5	40.5	290.2	-13.9
0.3		10.3	0.35	9.71	150859	0	9.8	34.7	230.1	-14.7	-14.7
0.4	50	8.9	0.35	11.24	144609	0	8.4	25.6	146.1	-16.4	-16.4
0.5		6.8	0.35	14.71	135234	0	6.3	14.6	62.8	-20.3	-20.3
0.6		5.2	0.35	19.23	128090	0	4.8	8.2	26.8	-25.6	-25.6
0.7		4	0.35	25.00	122733	0	3.6	4.7	11.5	-32.6	-32.6
0.2			11.2	0.35	8.93	178203	0	10.6	41.2	298.3	-16.8
0.3		10.6	0.35	9.43	175445	0	10.0	36.8	251.6	-17.5	-17.5
0.4	80	9.2	0.35	10.87	168969	0	8.7	27.4	162.0	-19.5	-19.5
0.5		7.1	0.35	14.08	159350	0	6.6	16.0	72.0	-24.1	-24.1
0.6		5.4	0.35	18.52	151533	0	4.9	8.9	30.2	-30.6	-30.6
0.7		4.1	0.35	24.39	145555	0	3.7	4.9	12.4	-39.6	-39.6

0.2	11.3	0.35	8.85	202403	0	10.7	42.0	306.7	-18.9	-18.9	
0.3	10.7	0.35	9.35	199820	0	10.1	37.5	259.0	-19.7	-19.7	
0.4	90	9.3	0.35	10.75	193568	0	8.8	28.1	167.5	-22.1	-22.1
0.5		7.2	0.35	13.89	184030	0	6.7	16.4	75.2	-27.4	-27.4
0.6		5.5	0.35	18.18	176288	0	5.0	9.3	32.0	-34.9	-34.9
0.7		4.2	0.35	23.81	170220	0	3.8	5.2	13.4	-45.1	-45.1
0.2		11.4	0.35	8.77	226602	0	10.8	42.8	315.1	-20.9	-20.9
0.3	10.75	0.35	9.30	224194	0	10.2	37.9	262.8	-22.0	-22.0	
0.4	100	9.4	0.35	10.64	218166	0	8.9	28.7	173.2	-24.6	-24.6
0.5		7.3	0.35	13.70	208709	0	6.8	16.9	78.5	-30.6	-30.6
0.6		5.6	0.35	17.86	201044	0	5.1	9.7	33.9	-39.1	-39.1
0.7		4.25	0.35	23.53	194885	0	3.8	5.3	14.0	-51.0	-51.0
0.2	11.4	0.35	8.77	250801	0	10.8	42.8	315.1	-23.2	-23.2	
0.3	10.8	0.35	9.26	248569	0	10.2	38.2	266.6	-24.3	-24.3	
0.4	110	9.5	0.35	10.53	242765	0	9.0	29.3	179.0	-27.1	-27.1
0.5		7.4	0.35	13.51	233389	0	6.9	17.4	82.0	-33.8	-33.8
0.6		5.7	0.35	17.54	225800	0	5.2	10.0	35.9	-43.1	-43.1
0.7		4.3	0.35	23.26	219550	0	3.9	5.5	14.5	-56.7	-56.7
0.2	11.2	0.35	8.93	336740	0	10.6	41.2	298.3	-31.7	-31.7	
0.3	10.9	0.35	9.17	334508	0	10.3	39.0	274.3	-32.4	-32.4	
0.4	140	9.7	0.35	10.31	329150	0	9.2	30.6	191.0	-35.9	-35.9
0.5		7.7	0.35	12.99	320221	0	7.2	18.9	92.9	-44.5	-44.5
0.6		5.9	0.35	16.95	312185	0	5.4	10.8	40.0	-57.4	-57.4
0.7		4.5	0.35	22.22	305935	0	4.1	6.0	16.8	-75.2	-75.2

Table 71 Results → bottom stresses and forces ULS 4

Model Properties					Bottom Forces		Sectional properties			Stresses	
RPC [-]	SBT [-]	Width [m]	Thickness [m]	Slenderness [-]	Axial Force [kN]	Bending Moment [kN x m]	Core area [m <sup>2</sup> ]	Wy core [m <sup>3</sup> ]	Iy core [m <sup>4</sup> ]	Maximum stresses bot [MPa]	Minimum stresses bot [MPa]
0.2		11	0.35	9.09	114703	438496	10.4	39.7	282.2	0.1	-22.0
0.3		9.9	0.35	10.10	110551	264341	9.4	31.9	203.5	-3.5	-20.1
0.4	30	8.2	0.35	12.20	104132	158190	7.7	21.6	113.1	-6.2	-20.9
0.5		6.4	0.35	15.63	97332	55921	5.9	12.8	51.8	-12.1	-20.8
0.6		5	0.35	20.00	92042	-30034	4.6	7.6	23.6	-24.2	-16.2
0.7		3.9	0.35	25.64	87866	-33220	3.5	4.4	10.5	-32.8	-17.7
0.2	50	11.1	0.35	9.01	128760	472719	10.5	40.5	290.2	0.1	-23.3
0.3		10.3	0.35	9.71	125740	329453	9.8	34.7	230.1	-2.7	-21.8

0.4	8.9	0.35	11.24	120455	229325	8.4	25.6	146.1	-4.7	-22.7
0.5	6.8	0.35	14.71	112523	87526	6.3	14.6	62.8	-10.9	-22.9
0.6	5.2	0.35	19.23	106477	-35336	4.8	8.2	26.8	-25.6	-17.0
0.7	4	0.35	25.00	101944	-31532	3.6	4.7	11.5	-33.8	-20.3
0.2	11.2	0.35	8.93	150780	527124	10.6	41.2	298.3	-1.4	-27.0
0.3	10.6	0.35	9.43	148448	420532	10.0	36.8	251.6	-3.3	-26.2
0.4	9.2	0.35	10.87	143006	288315	8.7	27.4	162.0	-6.0	-27.0
0.5	7.1	0.35	14.08	134837	95650	6.6	16.0	72.0	-14.4	-26.4
0.6	5.4	0.35	18.52	128221	35993	4.9	8.9	30.2	-21.9	-29.9
0.7	4.1	0.35	24.39	123162	-17993	3.7	4.9	12.4	-37.2	-29.9
0.2	11.3	0.35	8.85	168540	510399	10.7	42.0	306.7	-3.5	-27.9
0.3	10.7	0.35	9.35	166350	439821	10.1	37.5	259.0	-4.7	-28.1
0.4	9.3	0.35	10.75	161095	304885	8.8	28.1	167.5	-7.5	-29.2
0.5	7.2	0.35	13.89	153007	109829	6.7	16.4	75.2	-16.1	-29.5
0.6	5.5	0.35	18.18	146456	37166	5.0	9.3	32.0	-25.0	-33.0
0.7	4.2	0.35	23.81	141320	-13324	3.8	5.2	13.4	-40.0	-34.9
0.2	11.4	0.35	8.77	186300	518476	10.8	42.8	315.1	-5.1	-29.3
0.3	10.75	0.35	9.30	184252	441922	10.2	37.9	262.8	-6.4	-29.7
0.4	9.4	0.35	10.64	179184	340314	8.9	28.7	173.2	-8.3	-32.1
0.5	7.3	0.35	13.70	171177	124007	6.8	16.9	78.5	-17.8	-32.5
0.6	5.6	0.35	17.86	164690	38339	5.1	9.7	33.9	-28.0	-36.0
0.7	4.25	0.35	23.53	159478	-8656	3.8	5.3	14.0	-43.3	-40.1
0.2	11.4	0.35	8.77	204061	514152	10.8	42.8	315.1	-11.1	-35.2
0.3	10.8	0.35	9.26	202154	478399	10.2	38.2	266.6	-7.2	-32.3
0.4	9.5	0.35	10.53	197274	366313	9.0	29.3	179.0	-9.5	-34.5
0.5	7.4	0.35	13.51	189348	138186	6.9	17.4	82.0	-19.5	-35.3
0.6	5.7	0.35	17.54	182925	39512	5.2	10.0	35.9	-31.0	-38.8
0.7	4.3	0.35	23.26	177636	-3987	3.9	5.5	14.5	-46.6	-45.2
0.2	11.4	0.35	8.77	271272	550049	10.8	42.8	315.1	-12.2	-37.9
0.3	10.9	0.35	9.17	269385	593944	10.3	39.0	274.3	-10.8	-41.3
0.4	9.7	0.35	10.31	264859	450858	9.2	30.6	191.0	-14.2	-43.6
0.5	7.7	0.35	12.99	257309	165403	7.2	18.9	92.9	-27.0	-44.5
0.6	5.9	0.35	16.95	250508	42552	5.4	10.8	40.0	-42.1	-50.0
0.7	4.5	0.35	22.22	225505	0	4.1	6.0	16.8	-55.4	-55.4

Two stress calculations were outlined in Chapter 7.1, for two cases (one case with an RPC of 0.4 and SBT of 50 meters, and one case with an RPC of 0.6 and SBT of 110 meters). The full calculation for the RPC of 0.4 and SBT of 50 meters is presented below. The same stress calculation applies for all analyzed cases.

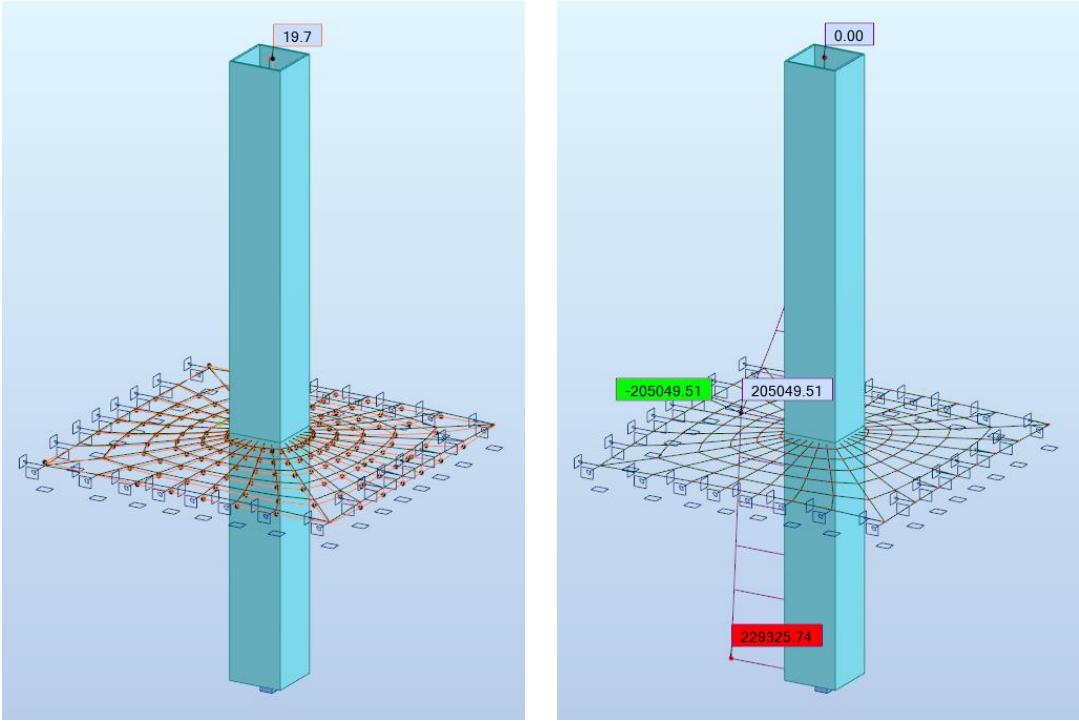


Figure 143 RSA results → Top Displacement SLS 1 (Left); Bending Moment ULS 4 (Right)

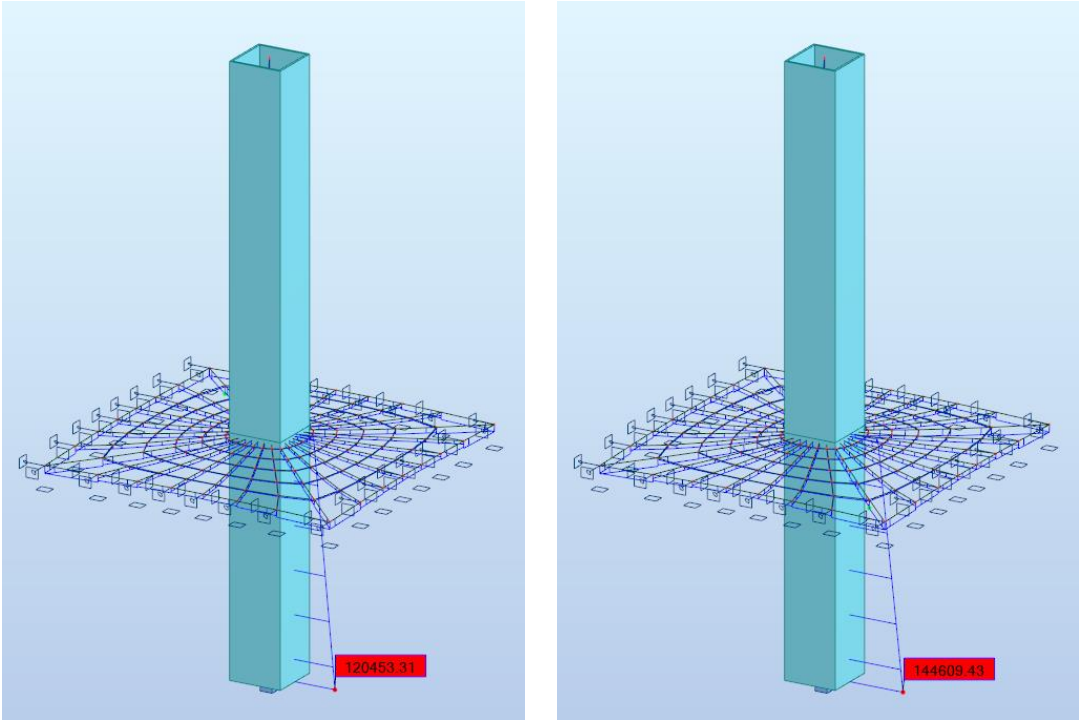
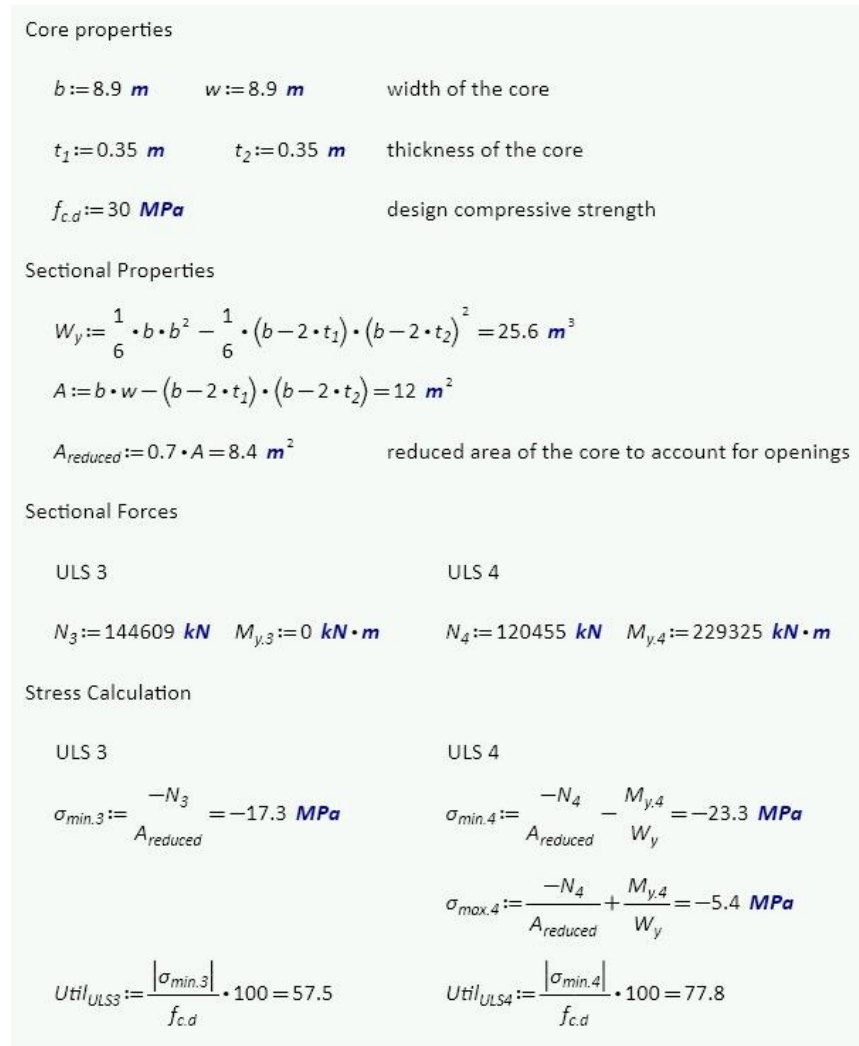


Figure 144 RSA results → Axial Force ULS 3 (Left); Axial Force ULS 4 (Right)

- The axial force in ULS 3 has a value of 144609 kN;
- The bending moment in ULS 3 is null;
- The axial force in ULS 4 has a slightly lower value, of 120453 kN;
- The bending moment in ULS 4 has a value of 229325 kN x m;



**Figure 145 Core Utilization Calculation**

Additionally, the tensile stresses are checked at the position of the cable connection in ULS 4, according to equation 7.4. Tensile stresses occur due to the bending moment at the RPC, and compressive stresses occur due to the axial force at that position. In this case, the axial force is significantly lower, as the mountain load is not considered, and is similar in all spacing cases as differences occur only due to the increase in slenderness for lower SBT (Figure 147). The bending moment at this position is only a function of the RPC, and, naturally, decreases with the increase in RPC, as the wind force value becomes lower (because the length of the core above RPC is smaller with the increase in RPC-see Figure 146. Figure 148 shows the evolution of the stresses with respect to the RPC and spacing between towers, plotting them against the design tensile resistance of C45/55. It is observed that not in all system configuration do the tensile stresses at the PRC exceed the design limit.

Bending Moment at Connection Position vs. RPC

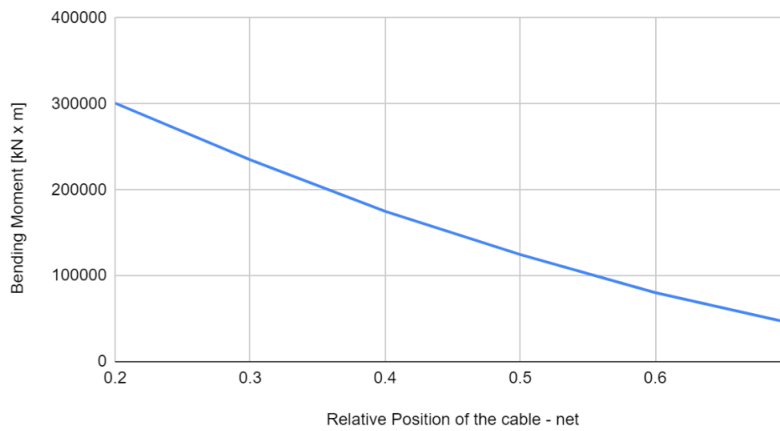


Figure 146 Bending moment at RPC vs RPC

Axial Force at Connection Position vs RPC

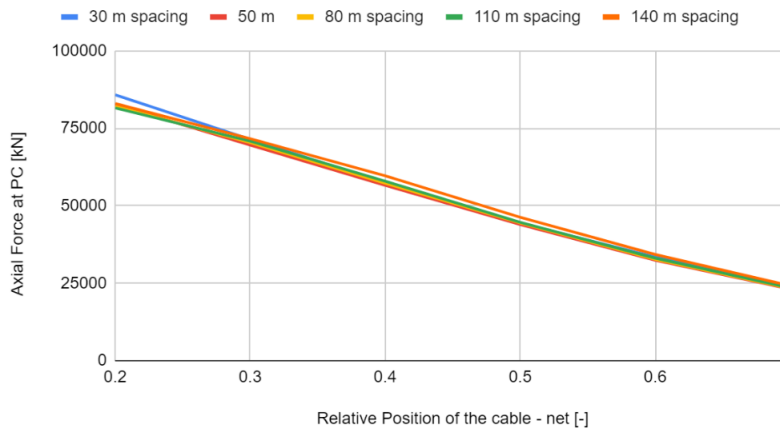


Figure 147 Axial Force at RPC vs RPC

Maximum Stresses Connection Position

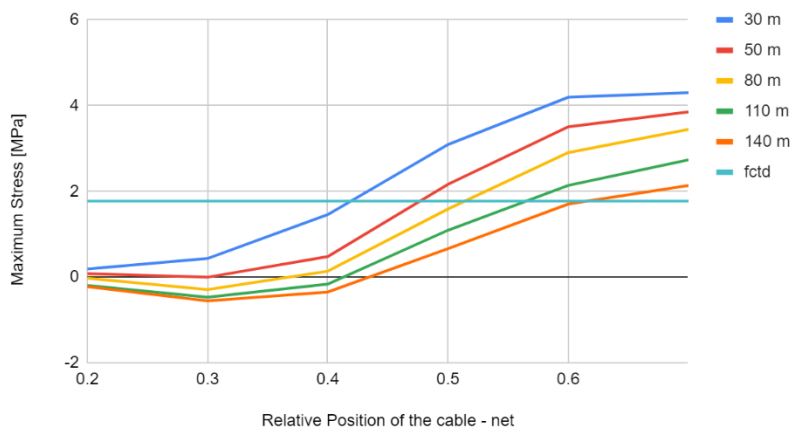


Figure 148 Maximum stresses at connection position

Table 72 shows the results in terms of stresses at the RPC connection. These stresses are calculated using the same formulas as for the stresses at the bottom of the core, that were presented earlier in this appendix (Figure 145)

**Table 72 Tensile stresses at the RPC**

RPC [-]	SBT [-]	Core width [m]	Core thickness [m]	Slenderness [-]	Axial Force connection [kN]	B.M. Connection [kN x m]	Core area [m <sup>2</sup> ]	Wy core [m <sup>3</sup> ]	Stresses connection [MPa]
0.2		11	0.35	9.09	84968	330707	10.4	39.7	0.2
0.3		9.9	0.35	10.10	71438	257600	9.4	31.9	0.4
0.4	30	8.2	0.35	12.20	57376	192400	7.7	21.6	1.5
0.5		6.4	0.35	15.63	44411	135700	5.9	12.8	3.1
0.6		5	0.35	20.00	33411	87400	4.6	7.6	4.2
0.7		3.9	0.35	25.64	23811	49300	3.5	4.4	4.3
0.2			11.1	0.35	9.01	85272	330707	10.5	40.5
0.3		10.3	0.35	9.71	72497	257600	9.8	34.7	0.0
0.4	50	8.9	0.35	11.24	58965	192400	8.4	25.6	0.5
0.5		6.8	0.35	14.71	45168	135700	6.3	14.6	2.2
0.6		5.2	0.35	19.23	33714	87400	4.8	8.2	3.5
0.7		4	0.35	25.00	23924	49300	3.6	4.7	3.9
0.2		11.2	0.35	8.93	85574	330707	10.6	41.2	0.0
0.3		10.6	0.35	9.43	73291	257600	10.0	36.8	-0.3
0.4	80	9.2	0.35	10.87	59646	192400	8.7	27.4	0.1
0.5		7.1	0.35	14.08	45736	135700	6.6	16.0	1.6
0.6		5.4	0.35	18.52	34018	87400	4.9	8.9	2.9
0.7		4.1	0.35	24.39	24039	49300	3.7	4.9	3.4
0.2		11.4	0.35	8.77	85876	330707	10.8	42.8	-0.2
0.3		10.8	0.35	9.26	73818	257600	10.2	38.2	-0.5
0.4	110	9.5	0.35	10.53	60325	192400	9.0	29.3	-0.2
0.5		7.4	0.35	13.51	46304	135700	6.9	17.4	1.1
0.6		5.7	0.35	17.54	34472	87400	5.2	10.0	2.1
0.7		4.3	0.35	23.26	24266	49300	3.9	5.5	2.7
0.2		11.4	0.35	8.77	86179	330707	10.8	42.8	-0.2
0.3		10.9	0.35	9.17	74084	257600	10.3	39.0	-0.6
0.4	140	9.7	0.35	10.31	60780	192400	9.2	30.6	-0.3
0.5		7.7	0.35	12.99	46873	135700	7.2	18.9	0.7
0.6		5.9	0.35	16.95	34777	87400	5.4	10.8	1.7
0.7		4.5	0.35	22.22	24495	49300	4.1	6.0	2.1

## Buckling

In this appendix, the tables that provide the information presented in Chapter 7.1 are presented. Based on these graphs, the buckling failure can be checked for each spacing case. This issue is treated in the governing combination for axial load, ULS 4, when the full live loads are applied.

**Table 73 Results → calculation of Euler's critical load**

Model Properties						Euler Critical Load Calculation					
Relative Position [-]	Height [m]	Spacing [m]	Core width [m]	Core thickness [m]	Slenderness [-]	Axial Force [kN]	K [-]	Critical Length [m]	Concrete E value [kN/m <sup>2</sup> ]	Iy core [m <sup>4</sup> ]	Fcr [kN]
0.2	100	30	11	0.35	9.09	136430	2.0	40.0	2.7	282.2	46993515
0.3			9.9	0.35	10.10	131519	2.0	60.0	2.7	203.5	15063672
0.4			8.2	0.35	12.20	123930	2.0	80.0	2.7	113.1	4709033
0.5			6.4	0.35	15.63	115894	2.0	100.0	2.7	51.8	1381521
0.6			5	0.35	20.00	109643	2.0	120.0	2.7	23.6	436606
0.7			3.9	0.35	25.64	104723	2.0	140.0	2.7	10.5	143308
0.2			100	50	11.1	0.35	9.01	154431	2.0	40.0	2.7
0.3	10.3	0.35			9.71	150859	2.0	60.0	2.7	230.1	17035076
0.4	8.9	0.35			11.24	144609	2.0	80.0	2.7	146.1	6082552
0.5	6.8	0.35			14.71	135234	2.0	100.0	2.7	62.8	1673387
0.6	5.2	0.35			19.23	128090	2.0	120.0	2.7	26.8	495175
0.7	4	0.35			25.00	122733	2.0	140.0	2.7	11.5	155682
0.2	100	80			11.2	0.35	8.93	178203	2.0	40.0	2.7
0.3			10.6	0.35	9.43	175445	2.0	60.0	2.7	251.6	18621535
0.4			9.2	0.35	10.87	168969	2.0	80.0	2.7	162.0	6744797
0.5			7.1	0.35	14.08	159350	2.0	100.0	2.7	72.0	1917422
0.6			5.4	0.35	18.52	151533	2.0	120.0	2.7	30.2	558770
0.7			4.1	0.35	24.39	145555	2.0	140.0	2.7	12.4	168750
0.2			100	110	11	0.35	9.09	250801	2.0	40.0	2.7
0.3	10.8	0.35			9.26	248569	2.0	60.0	2.7	266.6	19732112
0.4	9.5	0.35			10.53	242765	2.0	80.0	2.7	179.0	7453471
0.5	7.4	0.35			13.51	233389	2.0	100.0	2.7	82.0	2184121
0.6	5.7	0.35			17.54	225800	2.0	120.0	2.7	35.9	664039
0.7	4.3	0.35			23.26	219550	2.0	140.0	2.7	14.5	197048
0.2	100	140			11.2	0.35	8.93	336740	2.0	40.0	2.7
0.3			10.9	0.35	9.17	334508	2.0	60.0	2.7	274.3	20303593
0.4			9.7	0.35	10.31	329150	2.0	80.0	2.7	191.0	7952493
0.5			7.7	0.35	12.99	320221	2.0	100.0	2.7	92.9	2474492
0.6			5.9	0.35	16.95	312185	2.0	120.0	2.7	40.0	741106
0.7			4.5	0.35	22.22	305935	2.0	140.0	2.7	16.8	228353

Two examples of the calculation were outlined in Chapter 7.1 (for an RPC of 0.6 and SBT of 140 meters and for an RPC of 0.7 and SBT of 140 meters). The full calculation for the RPC of 0.7 and SBT of 140 meters is presented below. The same calculation applies for all analyzed cases.

Core properties

$b := 4.5 \text{ m}$        $w := 4.5 \text{ m}$       width of the core

$t_1 := 0.35 \text{ m}$        $t_2 := 0.35 \text{ m}$       thickness of the core

Concrete properties

$E := 2.7 \cdot 10^7 \frac{\text{kN}}{\text{m}^2}$       concrete modulus of elasticity

Sectional properties

$I := \frac{1}{12} \cdot b \cdot b^3 - \frac{1}{12} \cdot (b - 2 \cdot t_1) \cdot (b - 2 \cdot t_2)^3 = 16.796 \text{ m}^4$

Buckling check

$k := 2$       factor for critical length

$RPC := 0.7$       relative position of cable net

$H := 100 \text{ m}$       core total height

$L := RPC \cdot H = 70 \text{ m}$        $L_{cr} := k \cdot L = 140 \text{ m}$       critical length calculation

$F_{cr} := \pi^2 \cdot E \cdot \frac{I}{L_{cr}^2} = 228352.949 \text{ kN}$

$N_{core} := 305935 \text{ kN}$        $UC := \frac{N_{core}}{F_{cr}} = 1.34$

The following figures present the axial force with respect to the Euler's critical load for the 30 meters, 50 meters 80 meters spacing and 110 meters spacing as they were not included in Chapter 7.1. For the 140 meters spacing, the graphs are found in the chapter.

### F critical vs F compression 30 m spacing

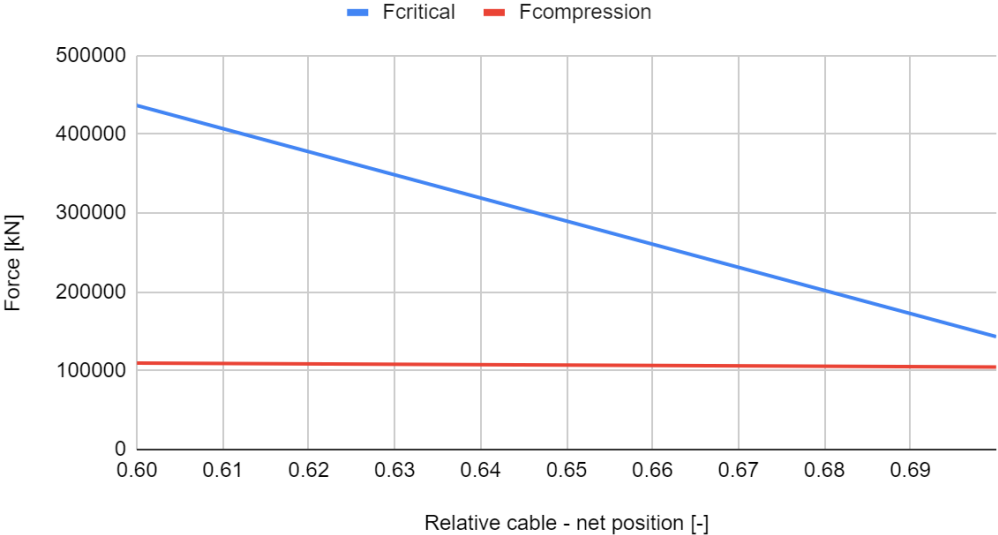


**Figure 149 Axial force and Euler’s critical load 30 meters spacing**

### F critical vs F compression 50 m spacing

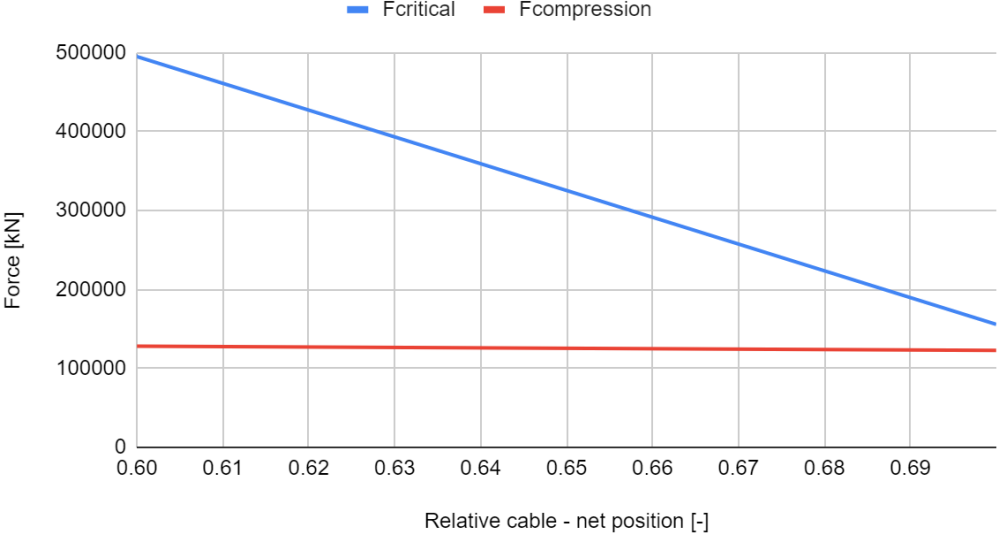


**Figure 150 Axial force and Euler’s critical load 50 meters spacing**

### F critical vs F compression 80 m spacing

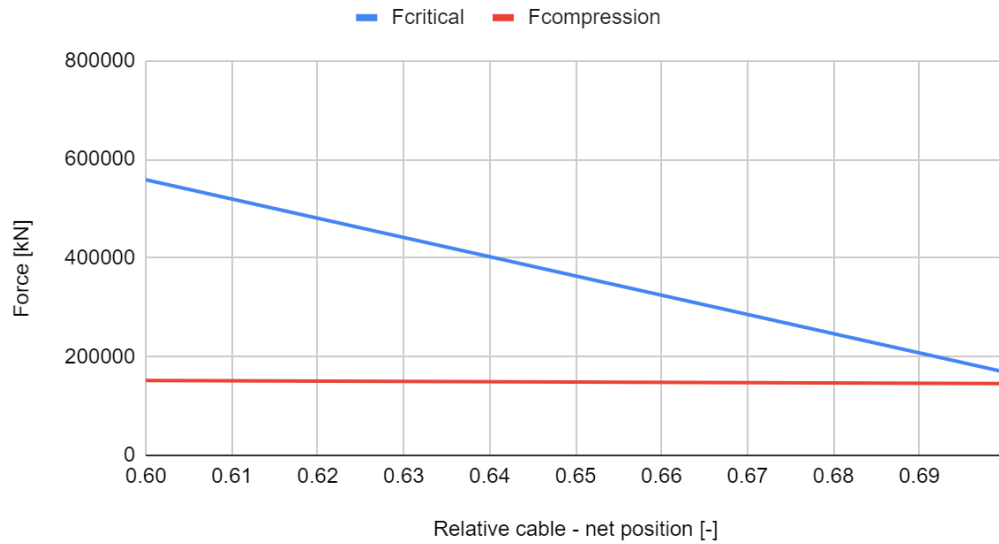


**Figure 151 Axial force and Euler's critical load 80 meters spacing**

### F critical vs F compression 110 m spacing

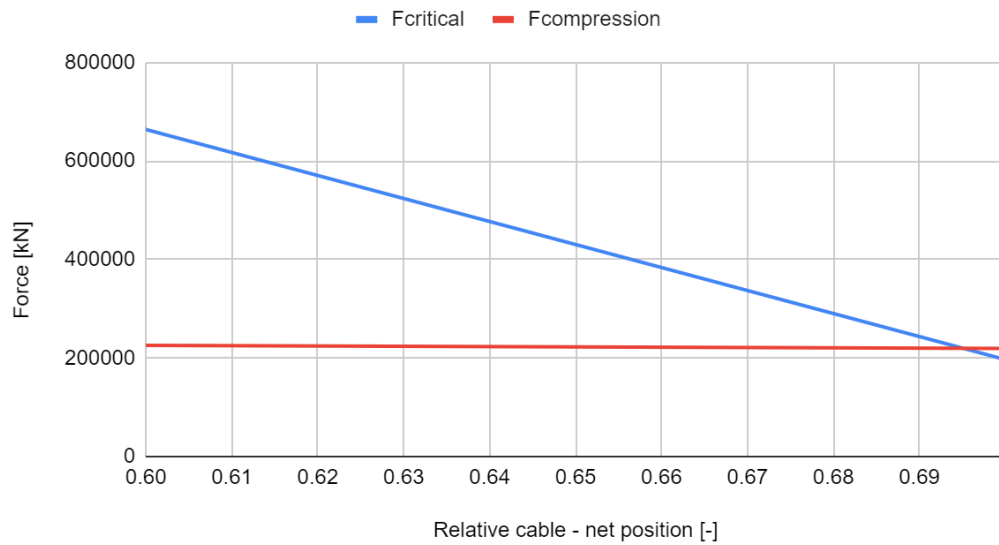


**Figure 152 Axial force and Euler's critical load 110 meters spacing**

## F critical vs F compression 140 meters spacing

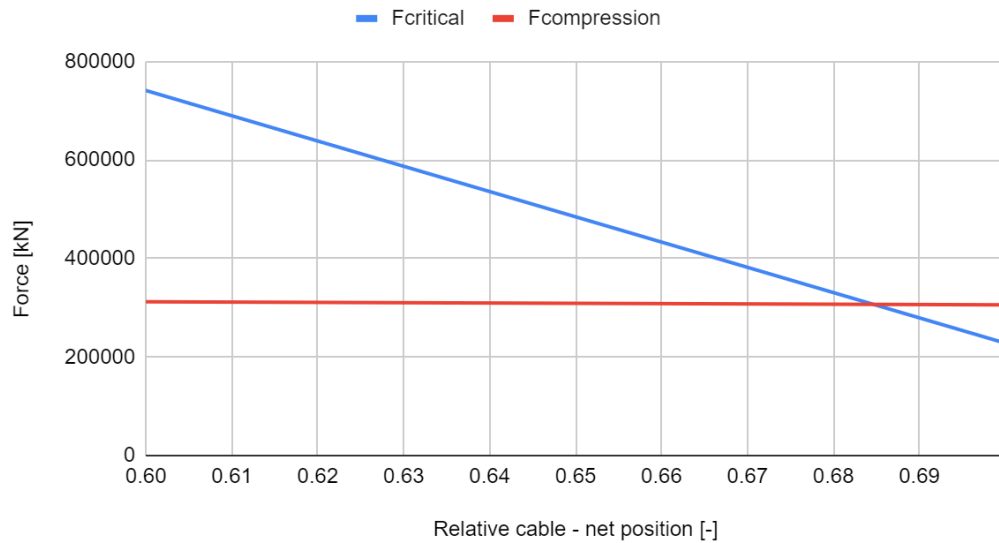


Figure 153 Axial force and Euler's critical load 140 meters spacing

## Horizontal Force

The calculation of the steel grid to withstand the horizontal forces, as explained in Chapter 7.1 is presented for the 80 meters spacing case. The analysis is performed in Robot, considering the ULS 3 load combination, resulting in the highest load on the cables. This further leads to the highest tensile stresses in the cables and, consequently, highest forces to be resisted by the steel grid.

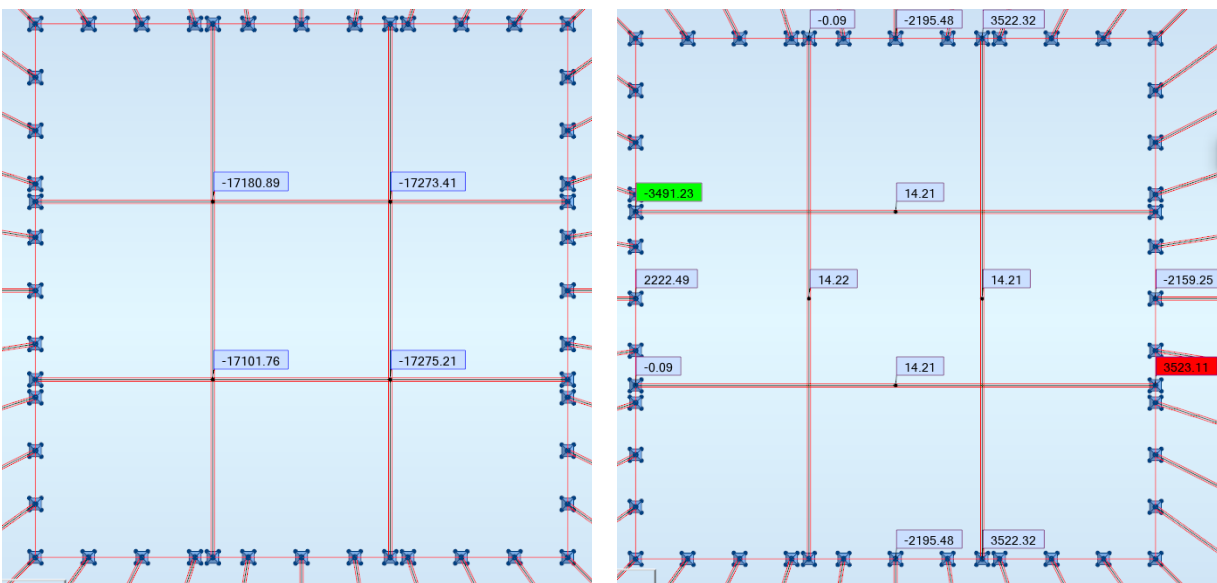


Figure 154 Forces on the steel grid

Table 74 Horizontal Beams properties

Beam Type	Steel Grade	Maximum Axial Force [kN]	Maximum Bending Moment [kN x m]	Required Area x10 <sup>2</sup> [mm <sup>2</sup> ]	Required Wy x10 <sup>3</sup> [mm <sup>3</sup> ]	Chosen Cross Section
External Beam	S460	17273	~ 0	371	0	HEM 650
Internal Beam	S460	12900	3520	280	7609	HEM 600

	profile type						section properties						
	G	h	b	tw	tf	A <sub>ax</sub>	I <sub>y</sub>	I <sub>x</sub>	W <sub>y,rel</sub>	W <sub>x,rel</sub>	i <sub>y</sub>	i <sub>x</sub>	
	[kg/m]	[mm]	[mm]	[mm]	[mm]	x 10 <sup>2</sup> [mm <sup>2</sup> ]	x 10 <sup>4</sup> [mm <sup>4</sup> ]	x 10 <sup>4</sup> [mm <sup>4</sup> ]	x 10 <sup>2</sup> [mm <sup>3</sup> ]	x 10 <sup>3</sup> [mm <sup>3</sup> ]	[mm]	[mm]	
	HE 550 AA	120.0	522.0	300.0	11.5	15.0	153	72870	6767	2792	451	218.0	66.5
	HE 550 A	166.2	540.0	300.0	12.5	24.0	212	111900	10820	4146	721	230.0	71.5
	HE 550 B	199.4	550.0	300.0	15.0	29.0	254	136700	13080	4971	872	232.0	71.7
	HE 550 M	278.2	572.0	306.0	21.0	40.0	354	198000	19160	6923	1252	236.0	73.5
	HE 600 AA	128.8	571.0	300.0	12.0	15.5	164	91870	6993	3218	466	237.0	65.3
	HE 600 x 137	137.4	575.0	300.0	11.8	17.5	175	101500	7893	3529	526	241.0	67.2
	HE 600 x 151	151.2	582.0	300.0	11.6	20.6	193	117100	9287	4024	619	247.0	69.4
	HE 600 x 175	175.2	588.0	300.0	13.6	23.9	223	136400	10780	4639	719	247.0	69.5
	HE 600 A	177.8	590.0	300.0	13.0	25.0	226	141200	11270	4787	751	250.0	70.5
	HE 600 B	211.9	600.0	300.0	15.5	30.0	270	171000	13530	5701	902	252.0	70.8
	HE 600 M	285.5	620.0	305.0	21.0	40.0	364	237400	18980	7660	1244	256.0	72.2
	HE 650 AA	138.0	620.0	300.0	12.5	16.0	176	113900	7221	3676	481	255.0	64.1
	HE 650 A	189.7	640.0	300.0	13.5	28.0	242	175200	11720	5474	782	269.0	69.7
	HE 650 B	224.8	650.0	300.0	16.0	31.0	286	210600	13980	6480	932	271.0	69.9
HE 650 M	293.4	668.0	305.0	21.0	40.0	374	281700	18980	8433	1245	275.0	71.3	

Figure 155 Sectional properties (Soons et al., 2014)

Internal beam		External beam	
$\sigma_{max} := 460 \text{ MPa}$		$\sigma_{max} := 460 \text{ MPa}$	
$M_{max} := 0 \text{ kN} \cdot \text{m}$	$W_{y,nec} := \frac{M_{max}}{\sigma_{max}} = 0 \text{ mm}^3$	$M_{max} := 3500 \text{ kN} \cdot \text{m}$	$W_{y,nec} := \frac{M_{max}}{\sigma_{max}} = (7.609 \cdot 10^6) \text{ mm}^3$
$F_{max} := 17273 \text{ kN}$	$A_{nec} := \frac{F_{max}}{\sigma_{max}} = 375.5 \text{ cm}^2$	$F_{max} := 12700 \text{ kN}$	$A_{nec} := \frac{F_{max}}{\sigma_{max}} = 276.087 \text{ cm}^2$

Figure 156 Explicit calculation for the horizontal beams

Obtaining the required sectional properties, a HEM 650 beam is selected for the internal beams, and a HEM 600 is selected for the external beams, obtaining the sectional properties from Figure 155 (Soons et al., 2014).

# Appendix I

## Simplified Economic Evaluation

In this Appendix, the simplified economic evaluation, as described in Chapter 8.4 is further addressed.

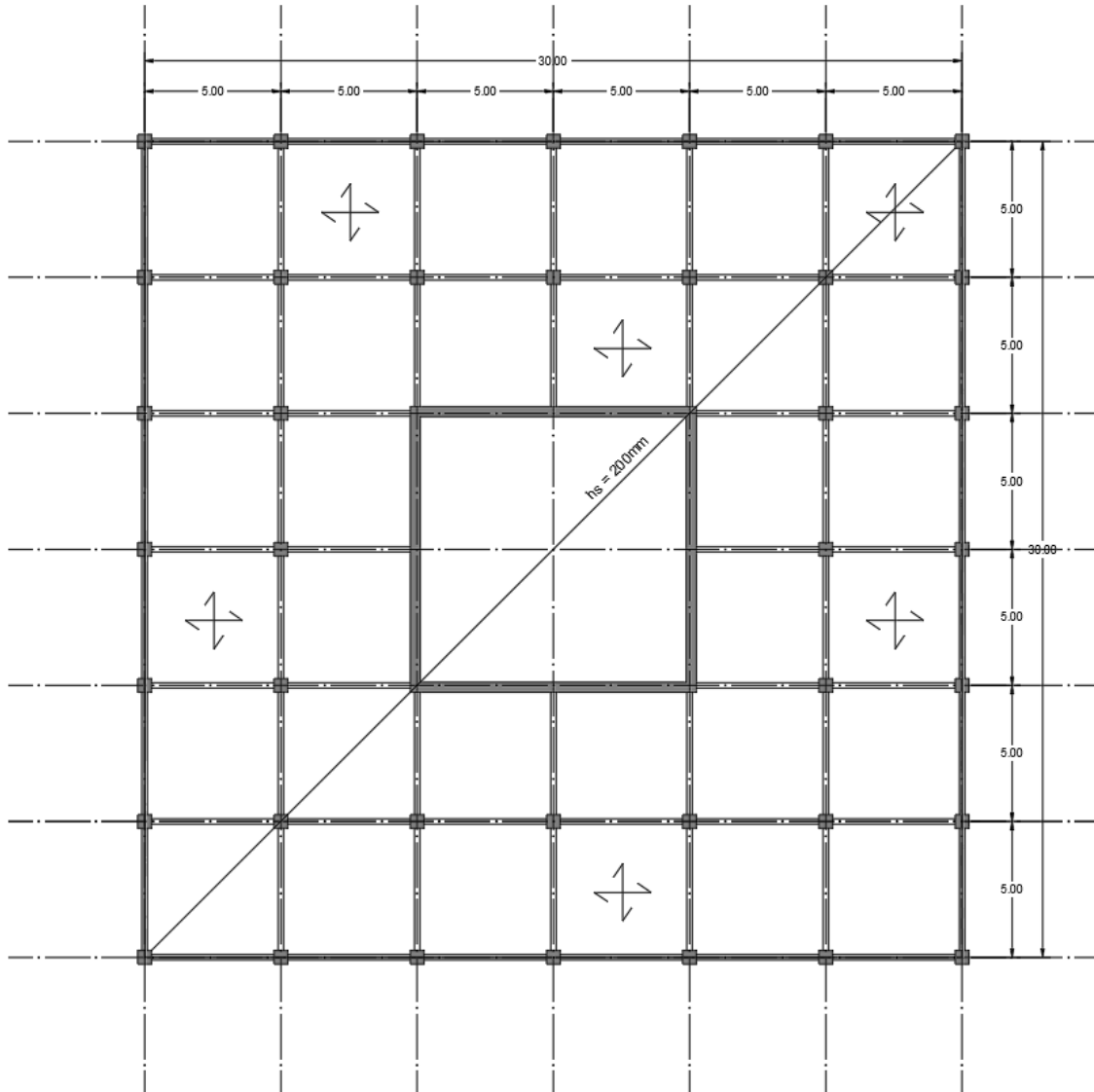


Figure 157 Typical floor plan

The total concrete volume per each floor is calculated by using the proposed dimensions of the structural elements, described in Appendix A, by calculating their total volume on each floor. This is shown in Table 75 to Table 78.

Table 75 Slab volume / floor

Tower width [m]	Tower depth [m]	Slab thickness [m]	Tower GFA/ floor [m <sup>2</sup> ]	Concrete Volume/ floor [m <sup>3</sup> ]
30	30	0.2	900	180

Table 76 Column volume / floor

Column width [m]	Column dept [m]	Column height [m]	Nr of columns [-]	Concrete Volume / floor [m <sup>3</sup> ]
0.4	0.4	3.6	24	13.8

Table 77 Beam volume / floor

Beam height [m]	Beam width [m]	Beam length [m]	Nr. of beams [-]	Concrete Volume / floor [m <sup>3</sup> ]
0.4	0.2	5	12	4.8

Table 78 Total volume / floor

Slab volume / floor [m <sup>3</sup> ]	Column volume / floor [m <sup>3</sup> ]	Beam volume / floor [m <sup>3</sup> ]	Total volume / floor [m <sup>3</sup> ]
180	13.8	4.8	198.6

In Table 79, the volume reduction that is obtained by increasing the slenderness of the core when the cable-net adds stiffness to the system (with a more slender core, a smaller width of the core is needed, translating to a lesser weight of the core) is presented. This volume reduction is further translated to either a number of extra achievable floors with the same amount of material, or to a total weight reduction for the same height of the tower, as presented in Chapter 8.4

Table 79 Volume reduction extended calculation

Slenderness [-]	Core width [m]	Core depth [m]	Core thickness [m]	Core Area [m <sup>2</sup> ]	Height [m]	Concrete Volume [m <sup>3</sup> ]	Concrete Weight [ton/m <sup>3</sup> ]	Volume Reduction [m <sup>3</sup> ]
8.1	12.3	12.3	0.35	16.7	100	1673	25	0
12.0	8.3	8.3	0.35	11.2	100	1118	25	555
13.0	7.7	7.7	0.35	10.3	100	1028	25	645
14.0	7.1	7.1	0.35	9.5	100	951	25	722
15.0	6.7	6.7	0.35	8.8	100	884	25	789
16.0	6.3	6.3	0.35	8.3	100	826	25	847
17.0	5.9	5.9	0.35	7.7	100	775	25	898
18.0	5.6	5.6	0.35	7.3	100	729	25	944

# Appendix J

## The Rotterdam Mountain

In this appendix, the procedure used for the proposed design for the Rotterdam Mountain is presented. The design of the Rotterdam Mountain, according to the proposed method, is a step wise approach, and presented below.

Step 1. Obtaining the Buildable Area for the Terbregseplein (buildable area received from Summum Engineering based on the first sketches of the Rotterdam Dreamers).

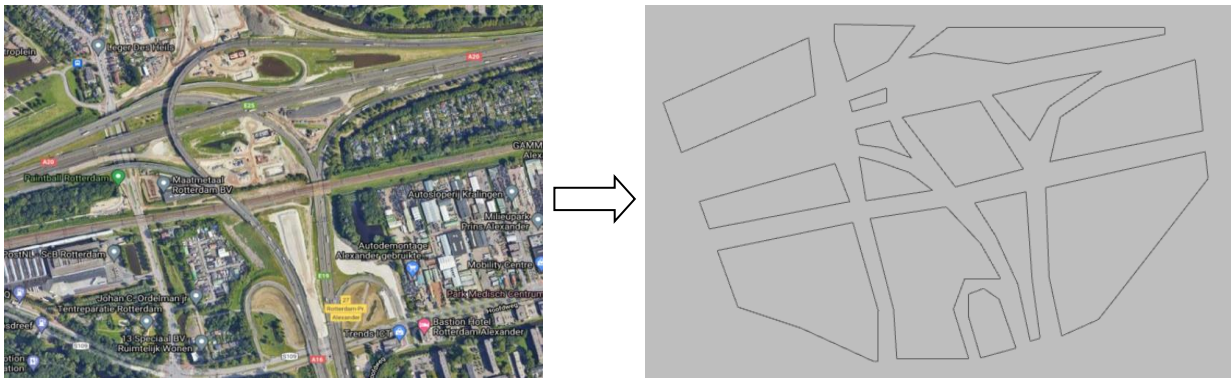


Figure 158 Buildable area

Step 2. Populating the area with towers based on the set recommendations of zone 1a. This translates to a spacing between towers between 30 and ~90 meters. To maintain a grid that is as rectangular as possible, an average spacing of 50 meters is used, and each parcel is populated by tower by proposing a rectangular grid.

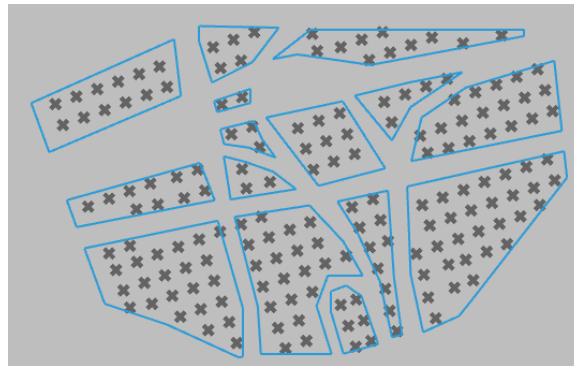
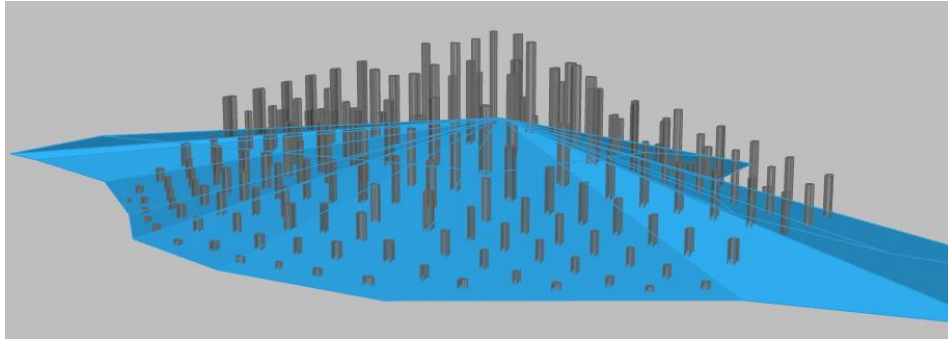


Figure 159 Point distribution in buildable area

Step 3. Proposing the geometry of the system of towers, according to the initial orography proposed by the Rotterdam Dreamers, so that the relative connection of the cable-net is placed at  $\sim 0.5 \times H$ . Such, each tower has a different height, to respect both the mountain orography and the set relative position of the cable-net. The heights of these towers range from low-rise with the height of up to

25 meters (at the perimeter of the mountain) to high-rise with the height of up to 110 meters (at the middle of the mountain).



**Figure 160 Heights based on initial mountain orography**

Step 4. Choose one buildable area to analyze, due to the large number of elements in the system. Due to a high computational power needed to analyze the whole system (including all towers and the cable-net between them), a single reference area (buildable parcel) is chosen to be analyzed.

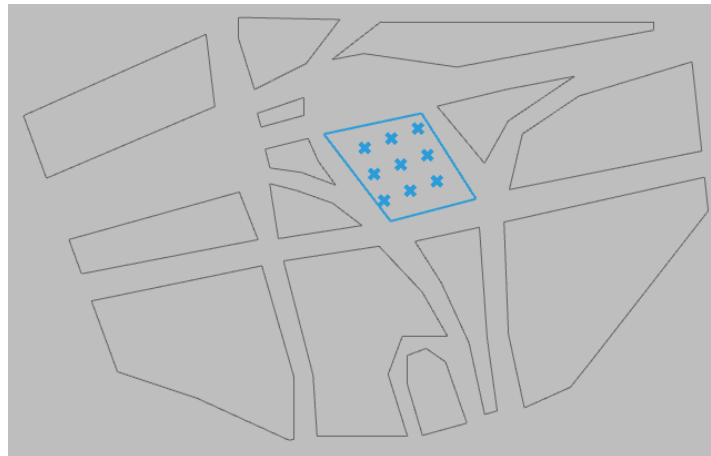


**Figure 161 Chosen analyzed parcel**

Step 5. To analyze the chosen parcel, the same procedure as the one used during the iterative study of the relevant parameters for the 3D case (Chapters 6 and 7) is used, as follows:

- Firstly, obtaining the initial geometry of the system
- Performing the form finding process to find the final geometry of the cable-net
- Exporting the geometry together with the prestress values for the cable elements to RSA for analysis.
- Performing the analysis in RSA and evaluating the results.

The height of the towers differs with respect to their position, due to the orography of the mountain, as explained in Step 3. The tower heights range between 88 and 100 meters. Based on the maximum achievable slenderness for the 0.5 RPC and 50 meters spacing case, described in Figure 88, the core widths are obtained for each tower.

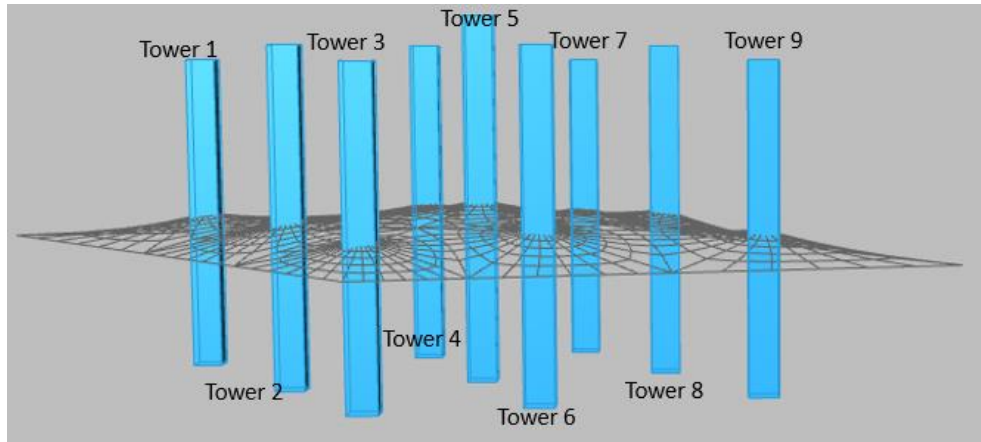


Figure 162 Geometry of the analyzed case

Table 80 Geometrical Properties

Tower	Relative Cable Position [-]	Spacing Between Towers [m]	Height [m]	Max achievable Slenderness [m]	Core width [m]
Tower 1			88		6.1
Tower 2			92		6.3
Tower 3			88		6.1
Tower 4			92		6.3
Tower 5	0.5	~50	100	1/14.5	6.9
Tower 6			92		6.3
Tower 7			88		6.1
Tower 8			92		6.3
Tower 9			88		6.1

The results are obtained from the RSA software, and presented below, in terms of Top deflection in SLS 1, Bending Moment in ULS 4 and Axial Force in ULS 3.

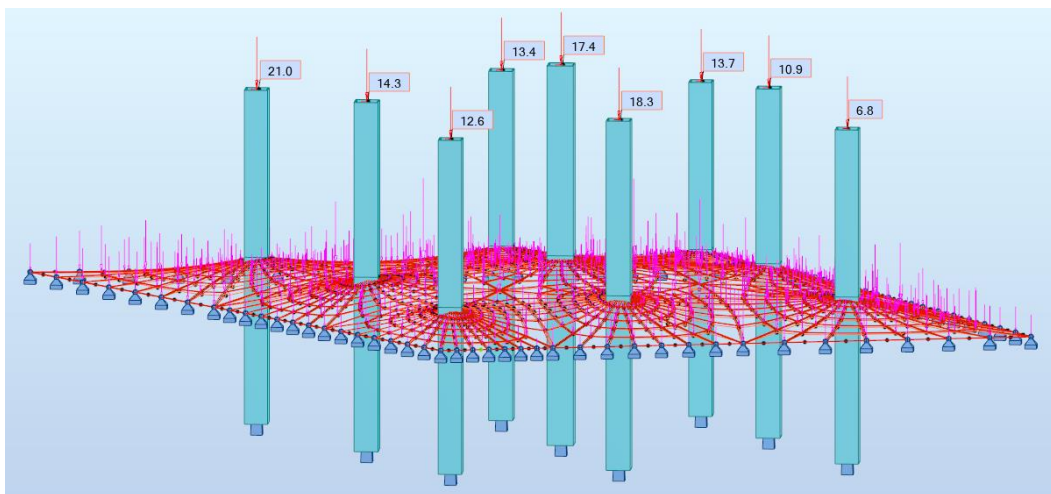


Figure 163 Top Deflection SLS 1

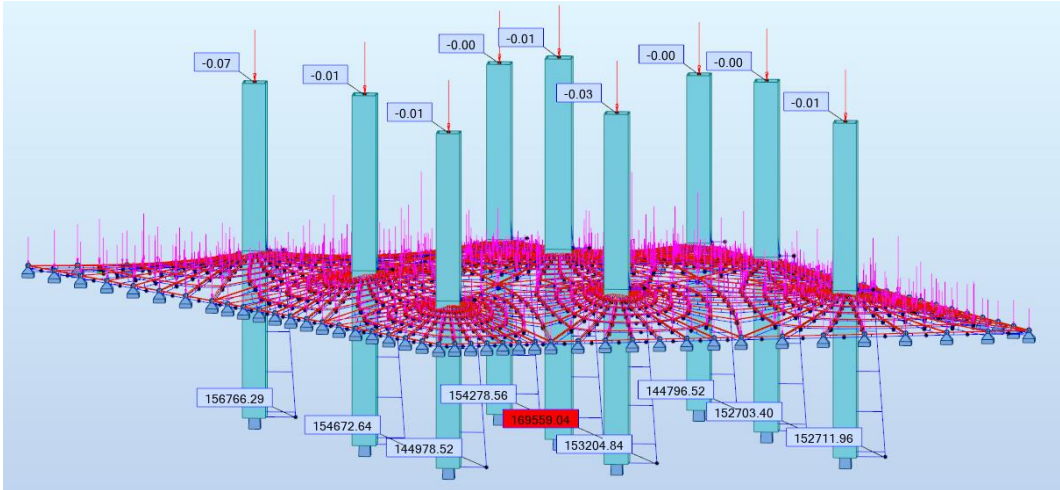


Figure 164 Axial Force ULS 3

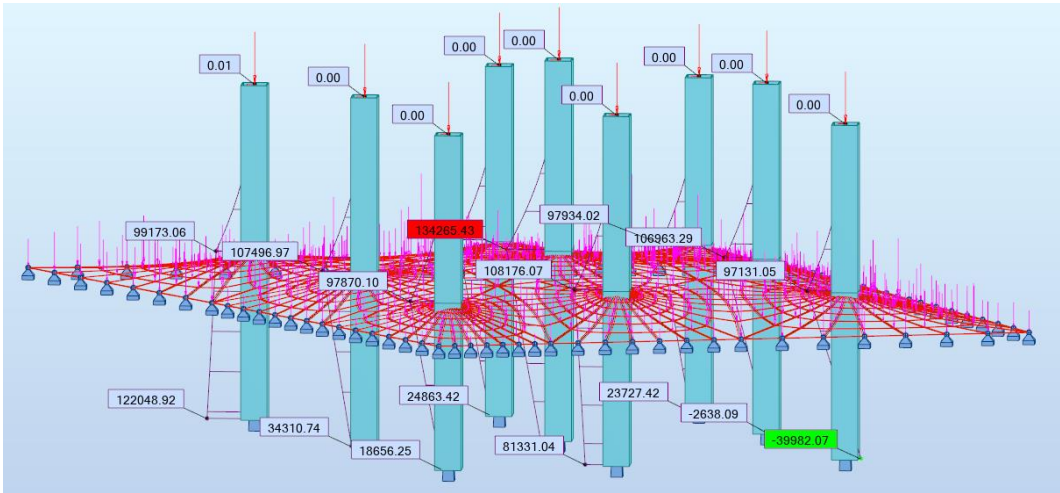


Figure 165 Bottom Bending Moment ULS 4

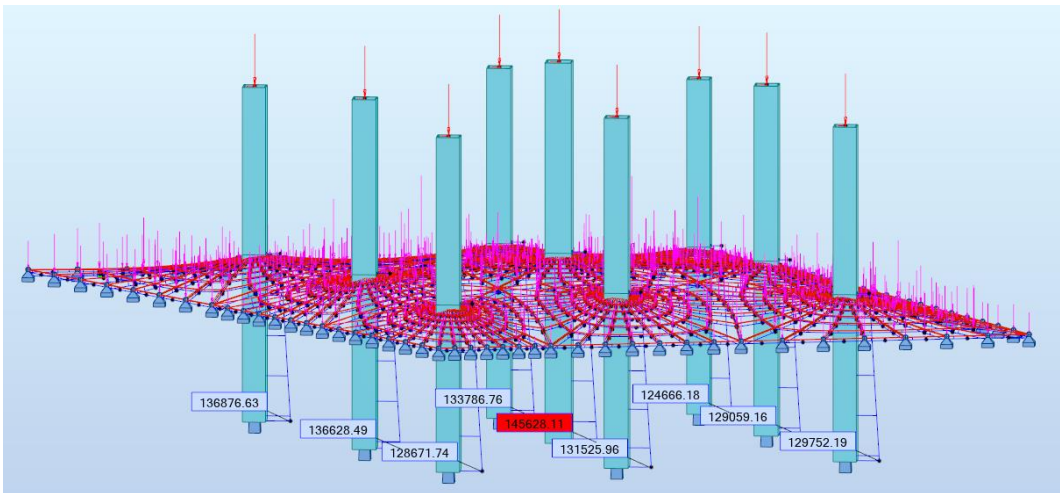


Figure 166 Axial Force ULS 4

Table 81 shows the results in terms of the top deflection, compared to the set limit of H/500. It can be seen that towers 2-9 are in line with the expected behavior, with a unity check of 0.6 to 0.97. Tower 1, on the other hand, fails to meet the deflection criterion. This is due to the fact that the spacing towards the towers that were not modeled is approximately 80 meters, thus the cable-net acts slightly less stiff than assumed.

Table 82 shows the results in terms of forces and stresses. Again, the results are in line with the expectations for towers 2-9, with a core utilization of 70-80%. For tower 1, due to the increased dimensions of the cable-net, the utilization of the core is exceeded with 10%.

The obtained results are satisfying, as only one tower needs to be reevaluated, thus proving that the proposed preliminary design method is a suitable one.

**Table 81 Top Deflection Results**

<b>Tower</b>	<b>Top Deflection [mm]</b>	<b>Height [m]</b>	<b>Top Deflection Limit [mm]</b>	<b>Unity Check</b>
Tower 1	210	88	176	<b>1.19</b>
Tower 2	143	92	184	0.77
Tower 3	126	88	176	0.72
Tower 4	134	92	184	0.73
Tower 5	174	100	200	0.87
Tower 6	183	92	184	0.99
Tower 7	137	88	176	0.78
Tower 8	109	92	184	0.60
Tower 9	68	88	176	0.39

**Table 82 Forces & Stresses Results**

<b>Tower</b>	<b>Core width [m]</b>	<b>Core thickness [m]</b>	<b>Axial Force [ULS 3] [kN]</b>	<b>Axial Force [ULS 4] [kN]</b>	<b>Bending Moment Bot [kN x m]</b>	<b>Core area [m<sup>2</sup>]</b>	<b>Wy core [m<sup>3</sup>]</b>	<b>Absolute minimum [MPa]</b>	<b>Utilization core [%]</b>
Tower 1	6.1	0.35	156766	136876	122048	5.6	11.6	34.8	116.1
Tower 2	6.3	0.35	154672	136628	34310	5.8	12.4	26.5	88.4
Tower 3	6.1	0.35	144978	128671	18656	5.6	11.6	25.7	85.8
Tower 4	6.8	0.35	154278	133786	24863	6.3	14.6	24.4	81.4
Tower 5	6.9	0.35	169559	145628	40332	6.4	15.0	26.4	88.1
Tower 6	6.3	0.35	153204	131525	81331	5.8	12.4	29.1	97.0
Tower 7	6.1	0.35	144796	124666	23727	5.6	11.6	25.7	85.7
Tower 8	6.3	0.35	152703	129059	-2638	5.8	12.4	26.2	87.3
Tower 9	6.1	0.35	152711	129752	-39982	5.6	11.6	27.1	90.3

# Appendix K

## Parametric Script

In this Appendix the parametric scripts used throughout this research are further explained. The scripts are rather extensive, and explaining and showing each component in this report would extend drastically the length of this Appendix. For a full description of the script, you can contact the author. Such, in this Appendix only a part of the relevant used components is described.

### Parametric Script for the 2D Model

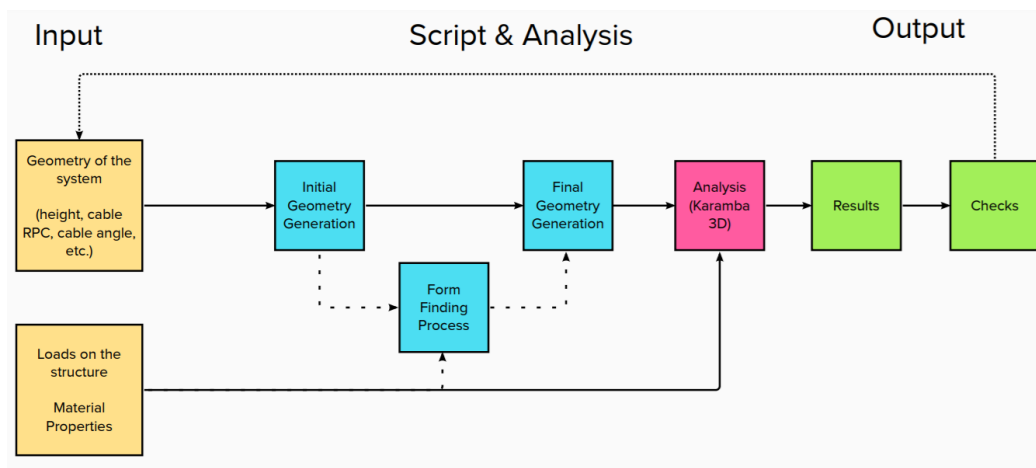


Figure 167 Script Logic 2D model

### Input Parameters

The 2D model allows for the change of multiple relevant input parameters, to provide a fast iterative process for the generation and analysis of the system. These parameters are:

- The cable type, based on the proposed research steps: straight unprestressed cable, straight prestressed cable or loaded prestressed cable (form – found) – as used in Chapter 5;
- The height of the tower: set for the models to the unchangeable value of 100 meters;
- The relative position of the cable-net’s connection;
- The cable (equivalent) diameter;
- The division of the cable element for the curve refinement;
- The cable angle with respect to the tower;
- The “scaled” force – density value for the form finding phase – as used in Chapter 5.3;
- The in – plane dimension of the core (core considered of rectangular shape);
- The prestress value imposed on the straight cables (for Step 2 of the Exploration Phase – as described in Chapter 5.2), inputted as initial strain value;
- The loads on the system (dead load and live load acting as gravitational load on the single equivalent cable, and live loads acting on the core);

- The material properties and cross-sectional properties of the core;
- The material properties and cross-sectional properties of the cables;

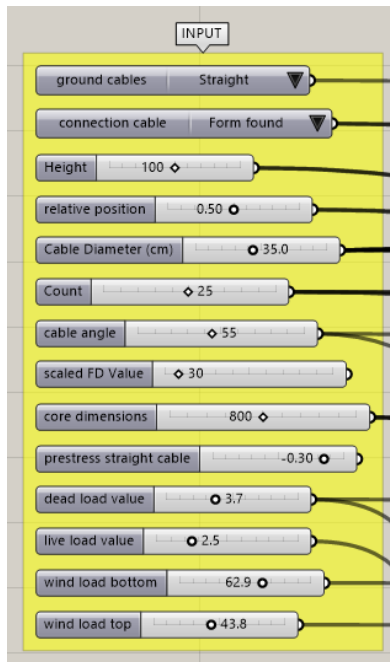


Figure 168 Input variables 2D Model

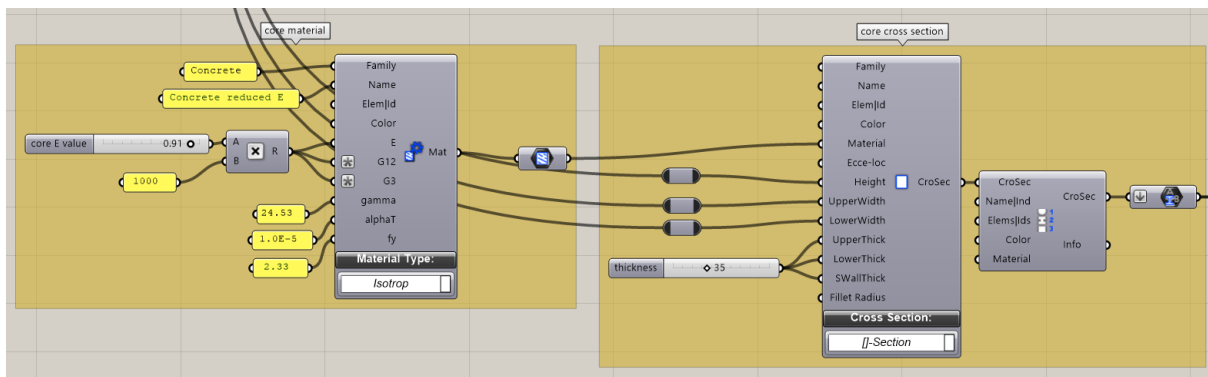


Figure 169 Input properties: material & cross-sectional properties core

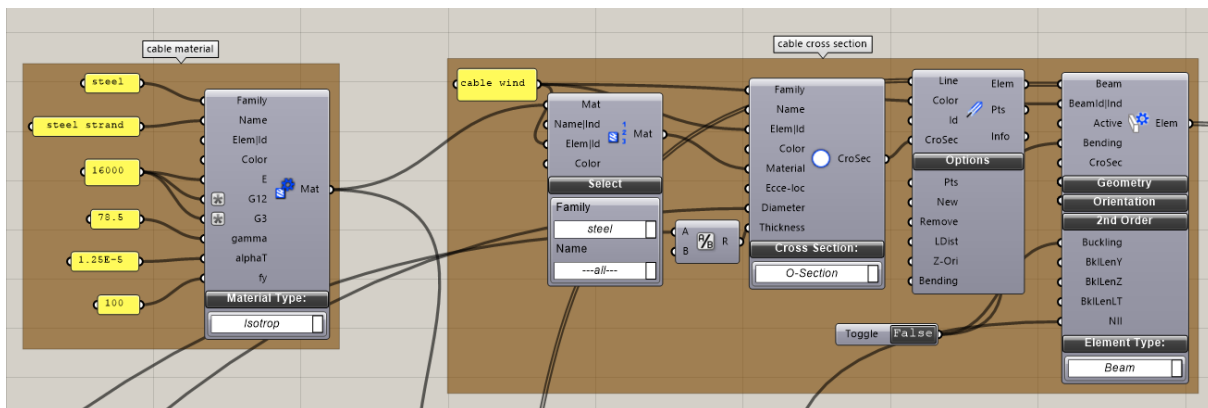


Figure 170 Input properties: material & cross-sectional properties cables

## Geometry Generation

Based on these input parameters, a large design space is created, which allows the rapid reconfiguration of the system based on the desired initial conditions. Below, a few figures of different geometrical configurations of the system are shown. Depending on the types of cables used, the geometry of the system is either generated directly after the definition of the input parameters or a form – finding process precedes the final geometry generation:

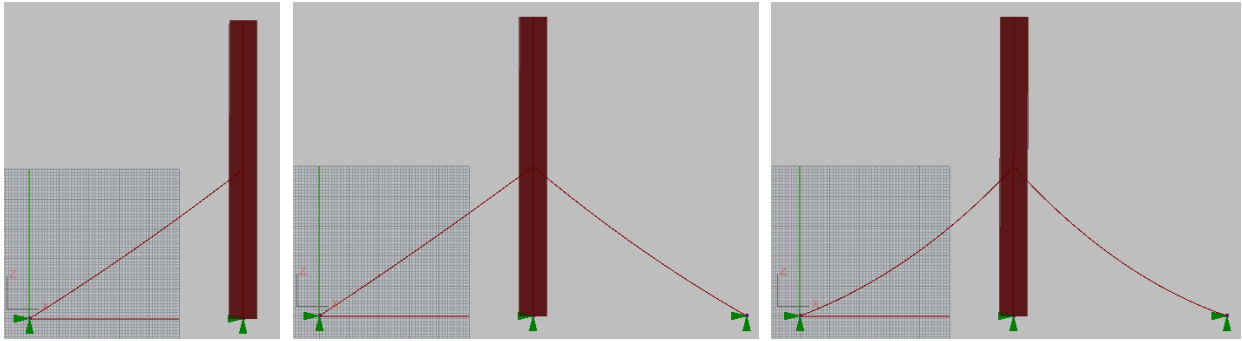


Figure 171 Different cable types (Left - unloaded + unstressed; Middle - unloaded + prestressed; Right - load + prestress)

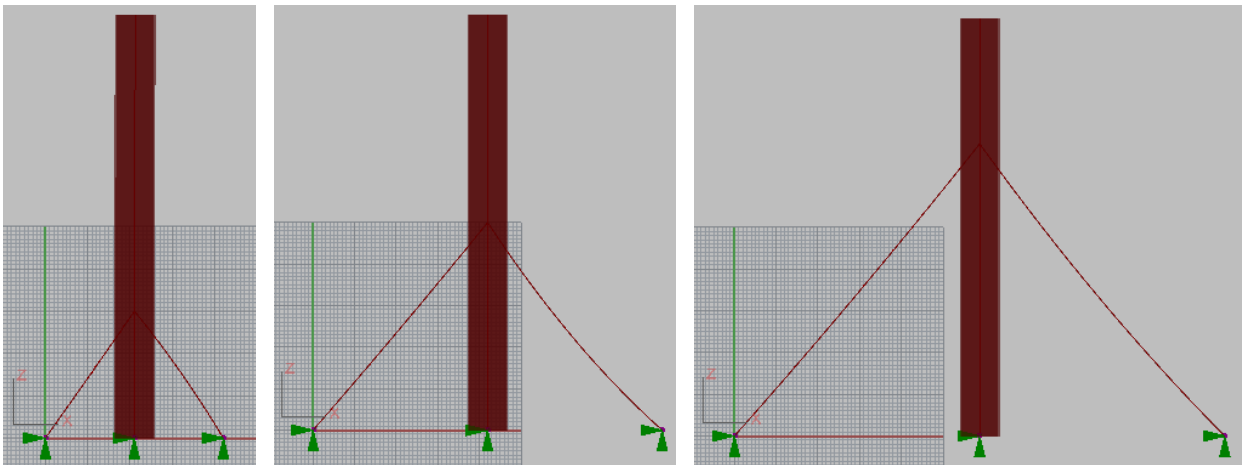


Figure 172 Different Relative Position of the Connection

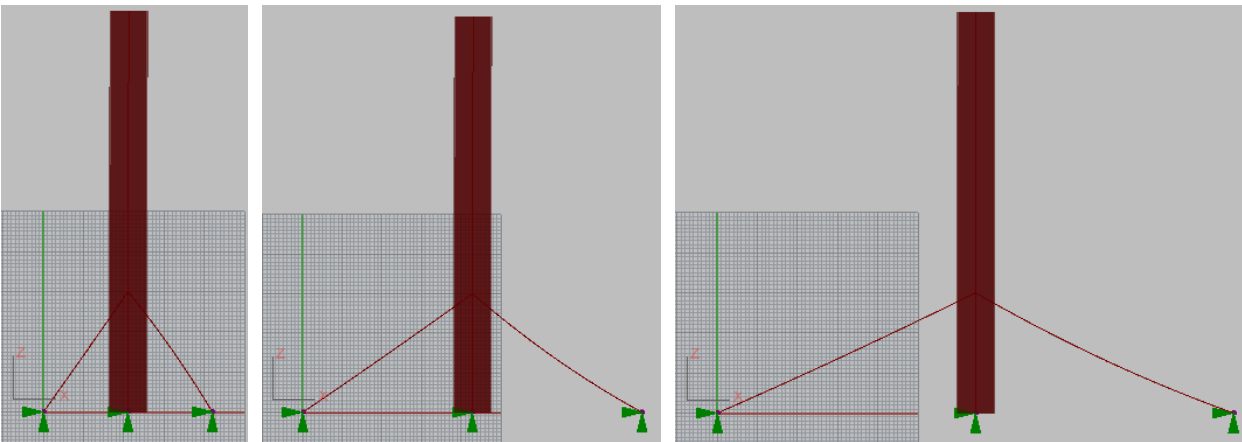


Figure 173 Different angle of the cable with respect to the tower

## Form finding process for the 2D case

As explained in Chapter 5.3, the form finding process is conducted in the Grasshopper environment, using the Kangaroo plug-in. This process is relevant in the case of loaded cables, where the equilibrium shape of the cable under the given loading and boundary conditions is of interest. The cable is divided in 25 segments.

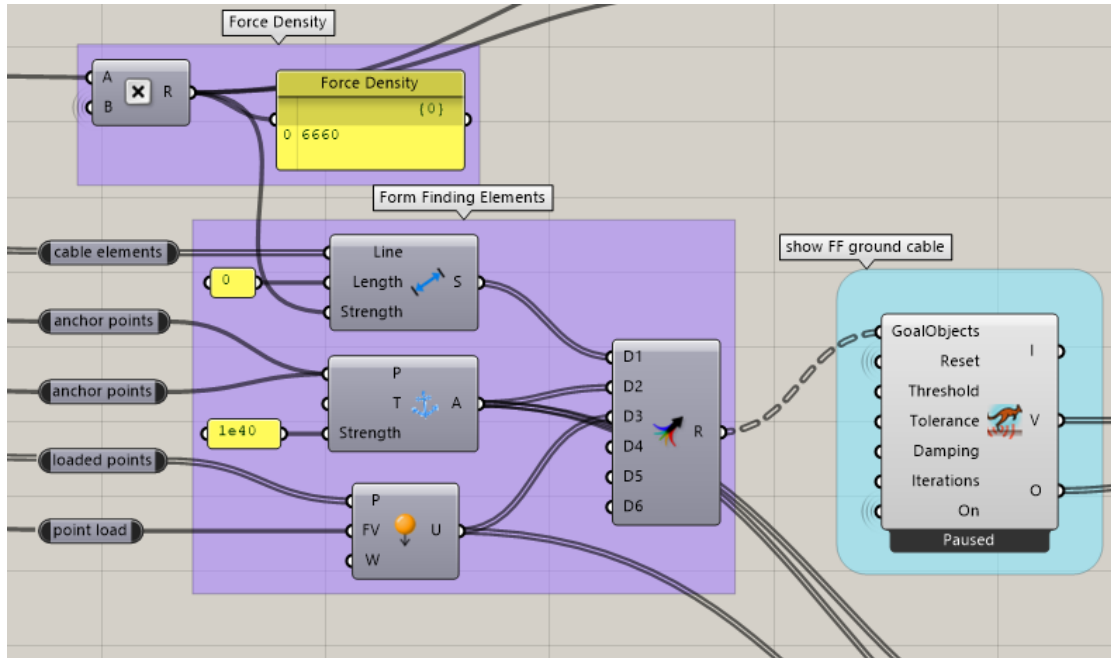


Figure 174 Kangaroo Form Finding

For the 2D case, 3 components are used to define the input of the Kangaroo solver:

- The “Length to Line” component → defining the cable elements as ‘zero-length’ springs, by setting their length to 0, and inputting the chosen Force Density value as their strength;
- The “Anchor” component → defining the anchor points as pinned connections of the cable elements to the ground and to the core;
- The “Load” component → defining the line load on the cables (imposed by the gravitational load of the mountain) as equivalent point loads at the joint between adjacent cable segments;

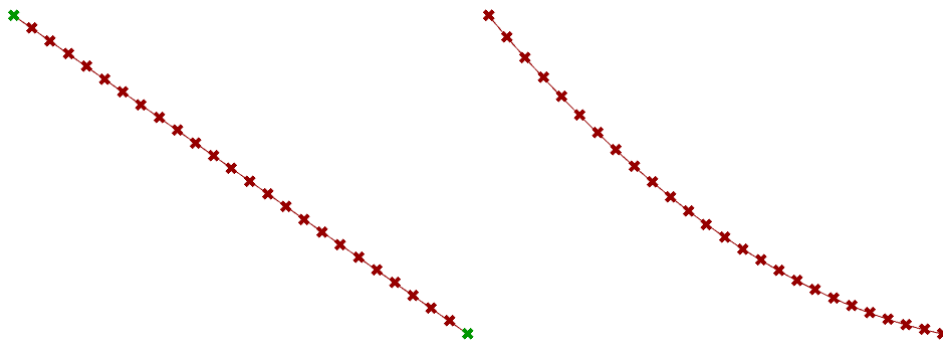


Figure 175 Initial Geometry (Left) – green points (anchor points); Final form found geometry (Right)

After the Form Finding process, the geometric shape of the cable is found, as well as the initial strain (prestress) in the form found cable. As presented in Appendix F, this initial prestress is calculated using the final lengths of the FF cables, the assumed FD value and the EA values of the cable, as reiterated bellow.

Table 83 Prestress calculation based on form finding process

FD Value [-]	Average Final Length [m]	Average Force [kN]	Cable Stiffness EA	Average Initial Strain [-]	Prestress as % of ultimate strength [%]
8800	3.52	31274	18200000	0.0017	31.80%

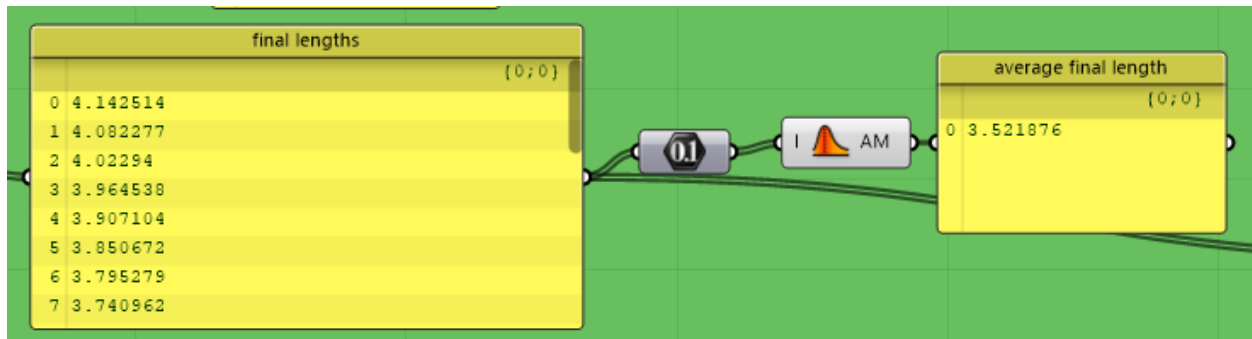


Figure 176 Final lengths output → Grasshopper

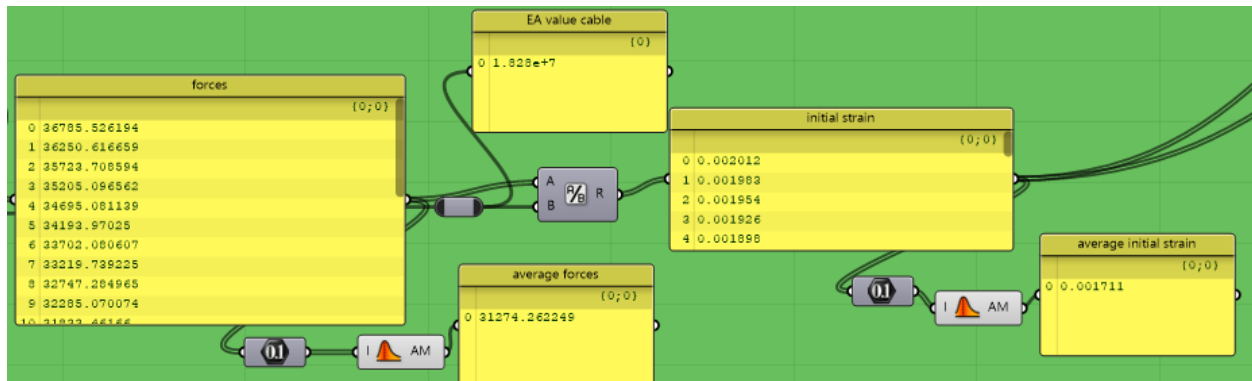


Figure 177 Average initial strain calculation → Grasshopper

## Analysis (Karamba)

After the final geometry generation (which includes the core and the straight or form found cables), the system is analyzed using the Karamba plug-in. A linear analysis is considered. The cables are defined so that no bending moment can occur, by using the 'ModifyElem' component of Karamba.

- The supports are defined at the position of the core connection to the foundation and at the position of the cable connections to the foundation;
- The model is assembled using the 'Assemble Model' component, by defining all elements (cross section + material) as described in the *Input Parameters* subchapter of this Appendix;
- The loads are defined with the assumed values (Chapter 3.6), using the 'Load' component of Karamba;

- The model is analyzed using the Analyze Theory II (second order theory) component in Karamba, to account for the imposed initial strain (prestress values)

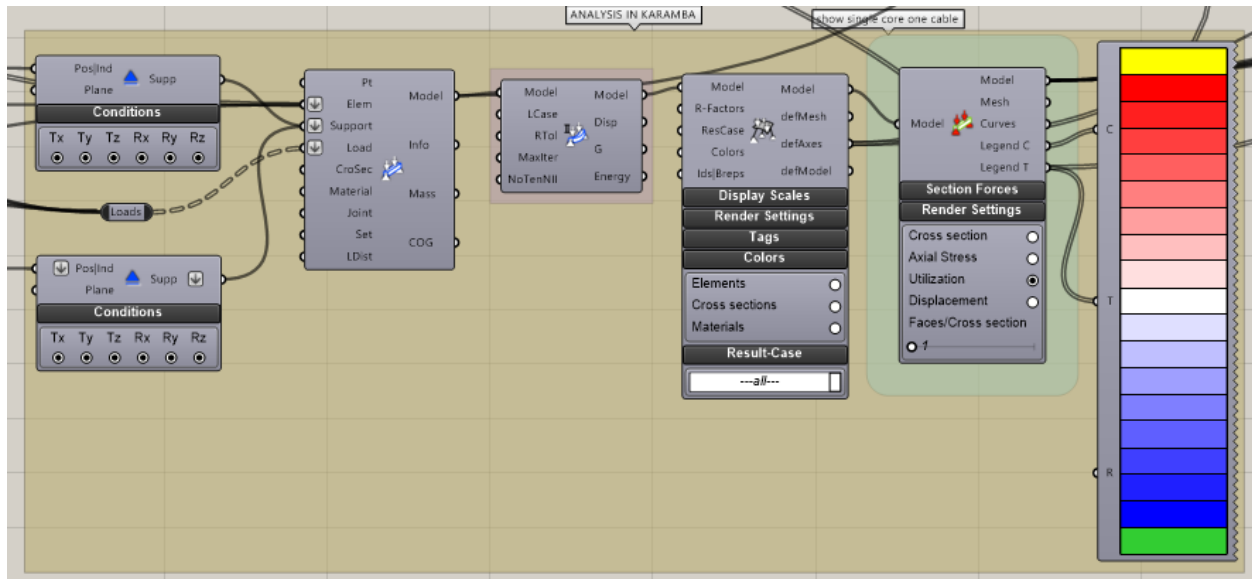


Figure 178 Karamba Analysis Component

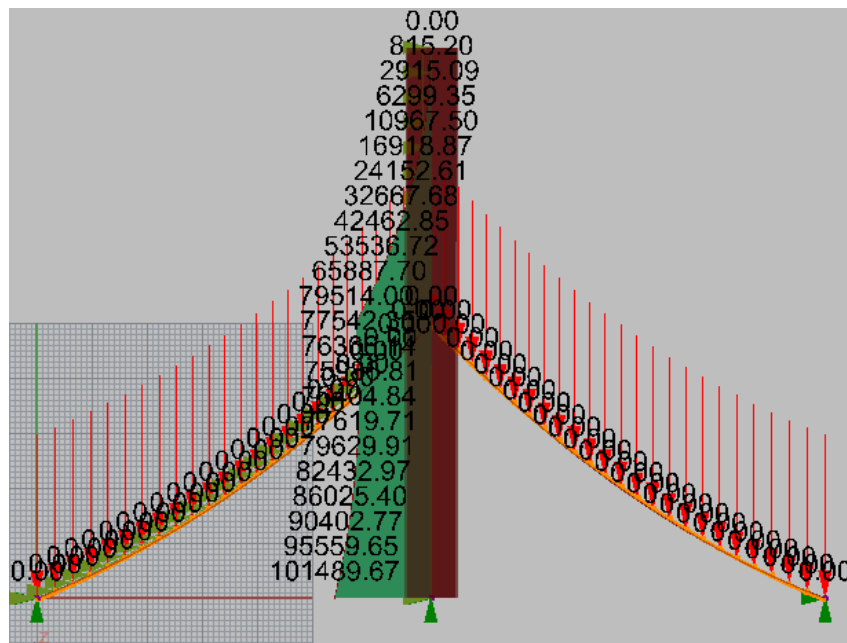


Figure 179 Example of Karamba Output

## Results

The linear analysis provides results in terms of the displacement at the top of the core or at the connection of the cable position, tension forces in the cable, axial and bending moment forces on the core and the respective utilizations of the cross sections. These results are used when studying the influence on the different parameters on the design of the system in later chapters of this

research. The script allows for a rapid visualization of these results, making the iterations of changing parameters a fast process.

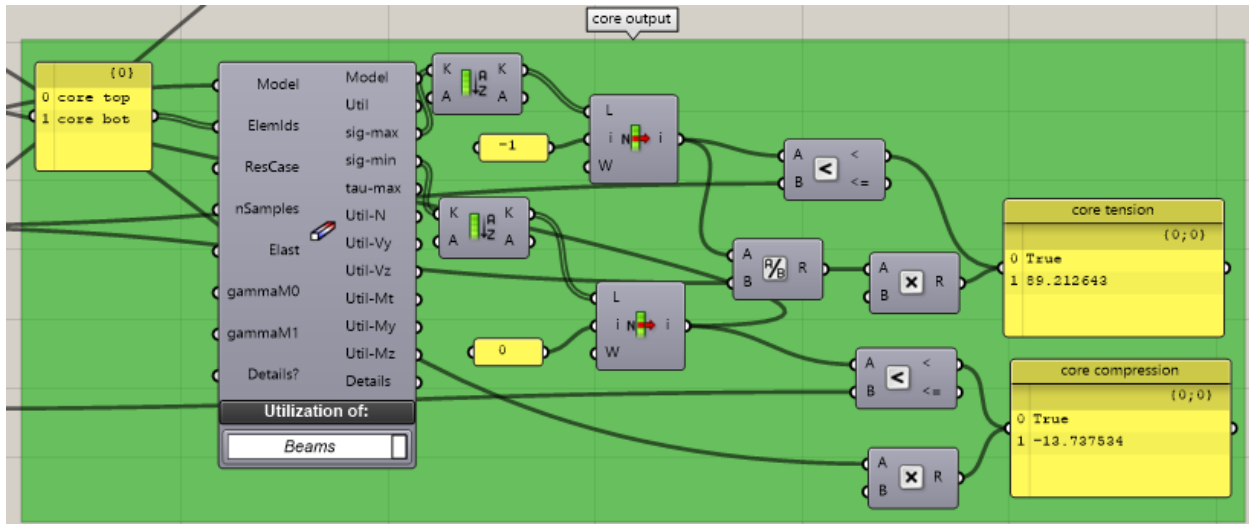


Figure 180 Core output

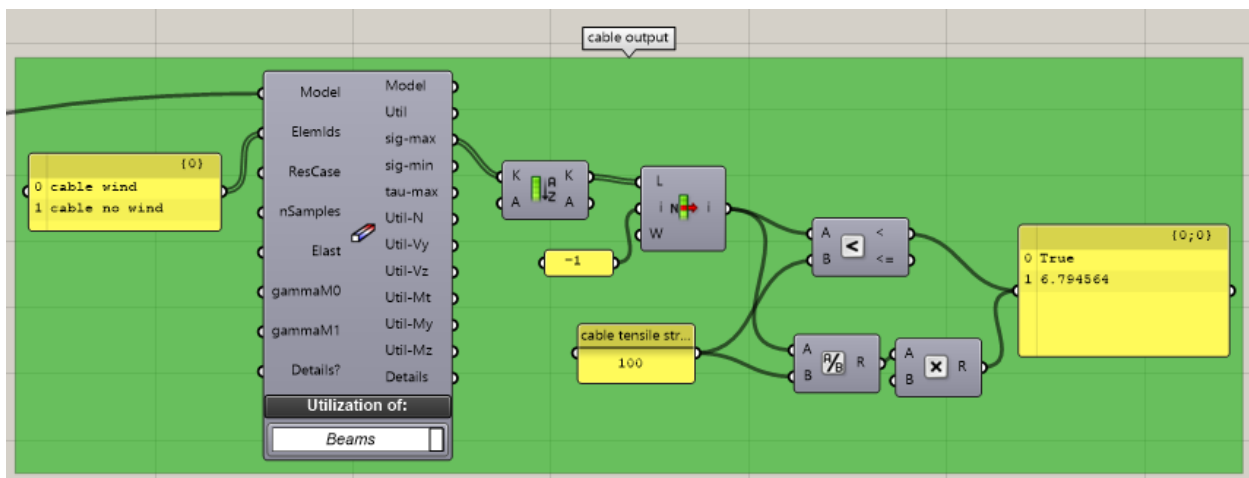


Figure 181 Cable output

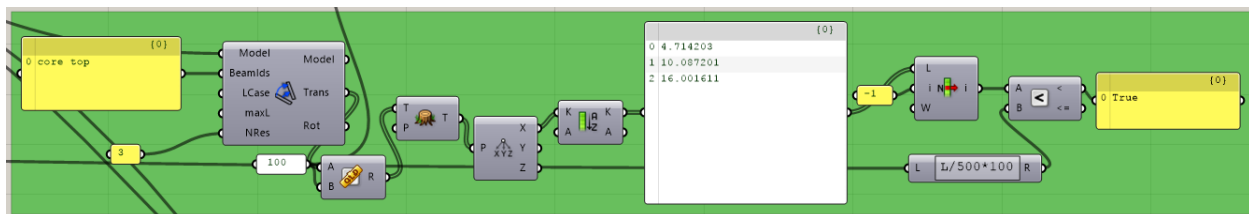


Figure 182 Displacement results

## Parametric Script for the 3D Model

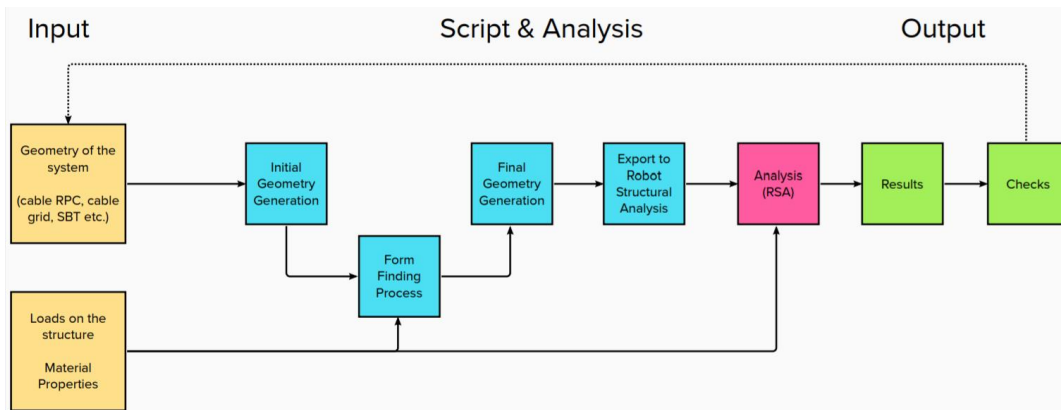


Figure 183 Script Logic for the 3D Model

### Input Parameters

The 3D model also allows for the change of multiple relevant input parameters. The same parameters are used as for the 2D model, with the following exceptions:

- The cable type, is no longer a changeable parameter;
- The cable angle is no longer a changeable parameter;
- The spacing between towers becomes a changeable parameter;
- The cable diameters are defined individually for each cable type;
- The divisions of the cable elements (in x and y) direction become a changeable parameter.

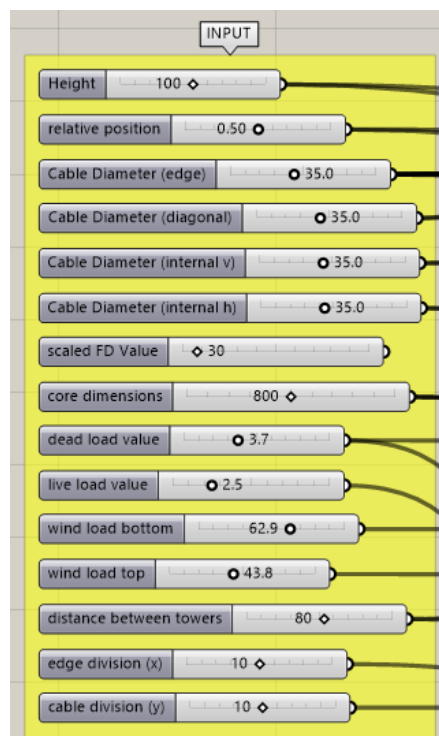


Figure 184 Input variables 3D model

# Geometry Generation

Based on the input parameters a big design space is generated. With the variability of the spacing between towers and the relative cable positions, multiple system geometries can be obtained. Bellow, a few examples of such geometries are presented.

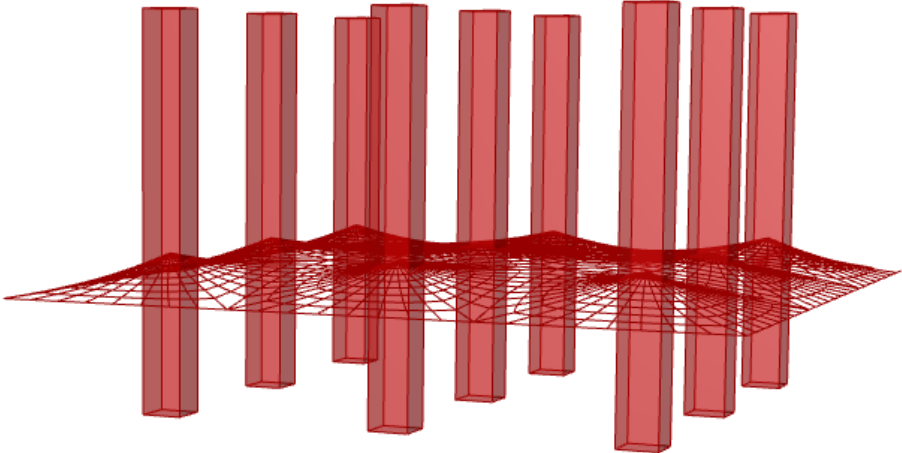


Figure 185 RPC 0.4 and SBT 50 meters

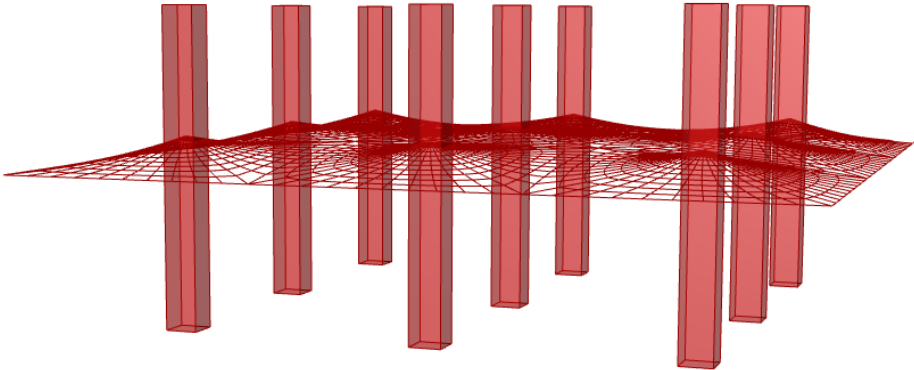


Figure 186 RPC 0.6 and SBT 80 meters

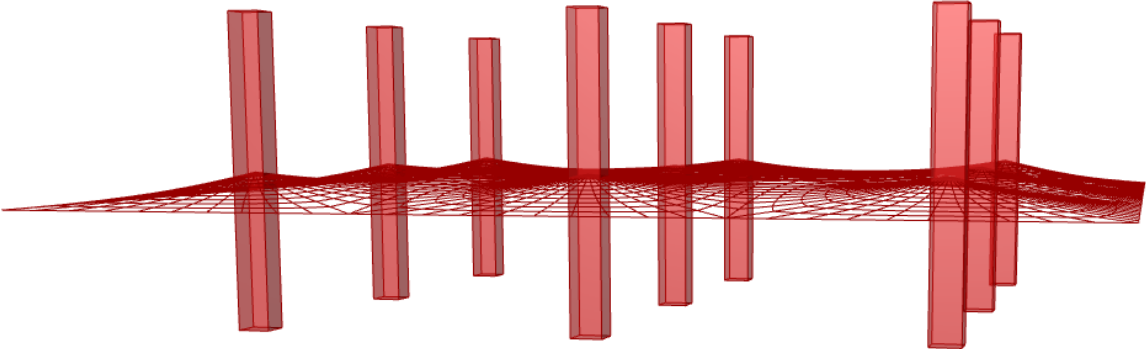


Figure 187 RPC 0.5 and SBT 140 meters



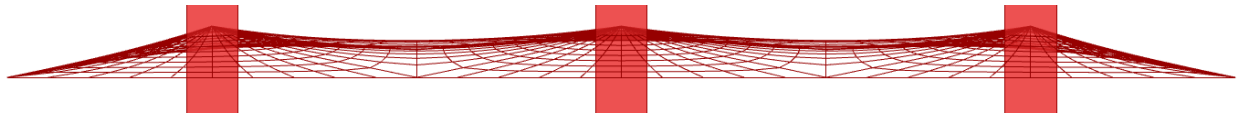


Figure 190 Final Geometry FF

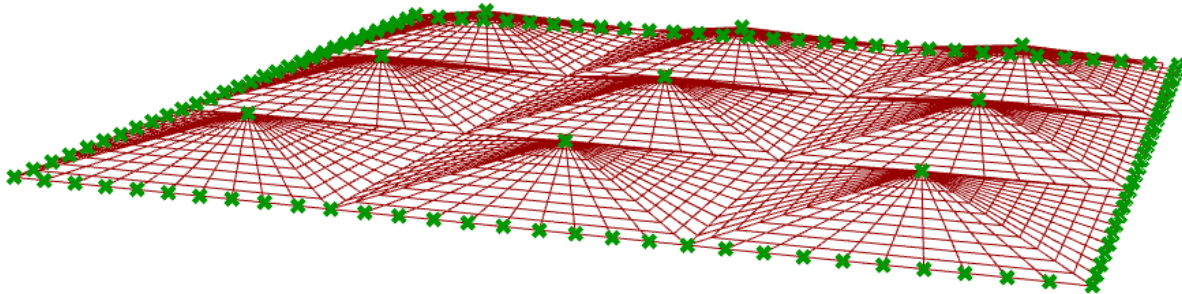


Figure 191 Anchor Points FF 3D model

After the Form Finding process, the geometric shape of the cable is found, as well as the initial strain (prestress) in the form found cable. As presented in Appendix G, this initial prestress is calculated using the final lengths of the FF cables, the assumed FD value and the EA values of the cable, as reiterated bellow.

Table 84 Diagonal Cable

Force Density Value [-]	Average Final Length [m]	Cable Stiffness EA [kN/m <sup>2</sup> ]	Average Initial Strain [-]	Prestress as % of ultimate strength [%]
6000	4.04	2.83 x 10 <sup>6</sup>	0.00235	30.3%

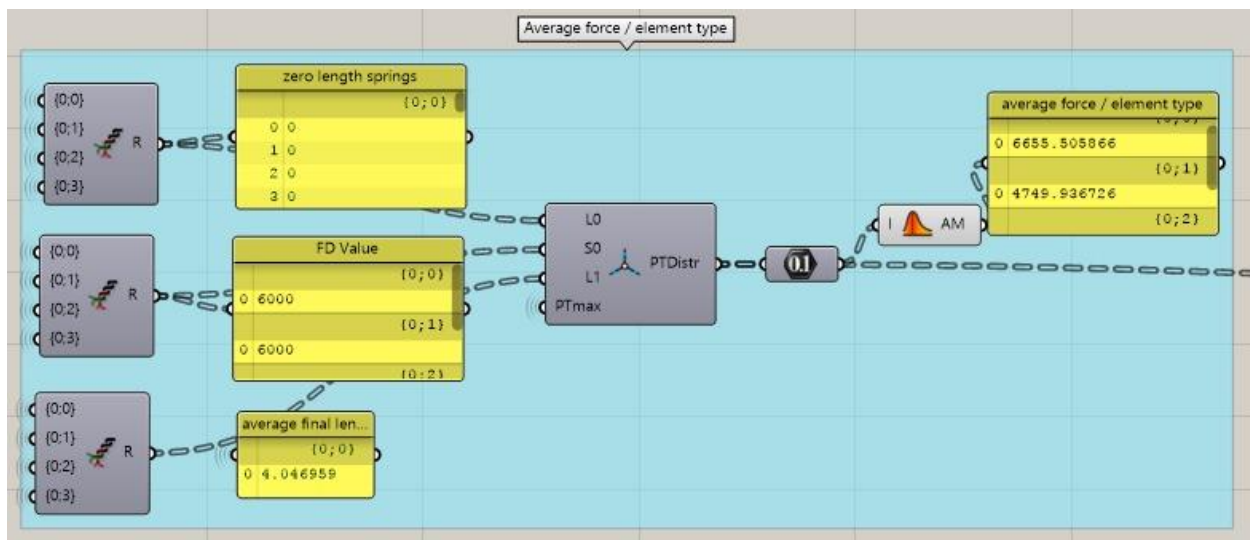


Figure 192 Forces based on FD and Final Length

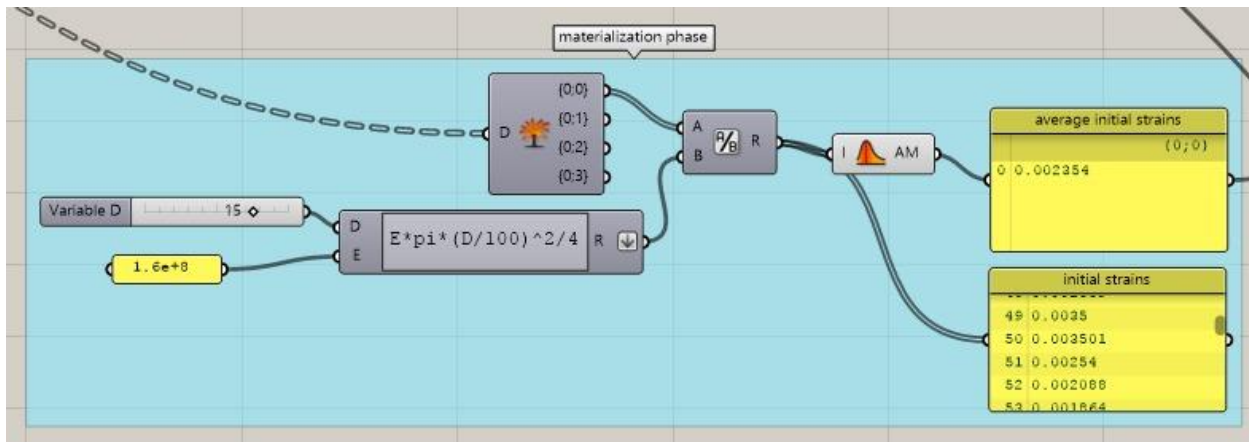


Figure 193 Materialization Phase

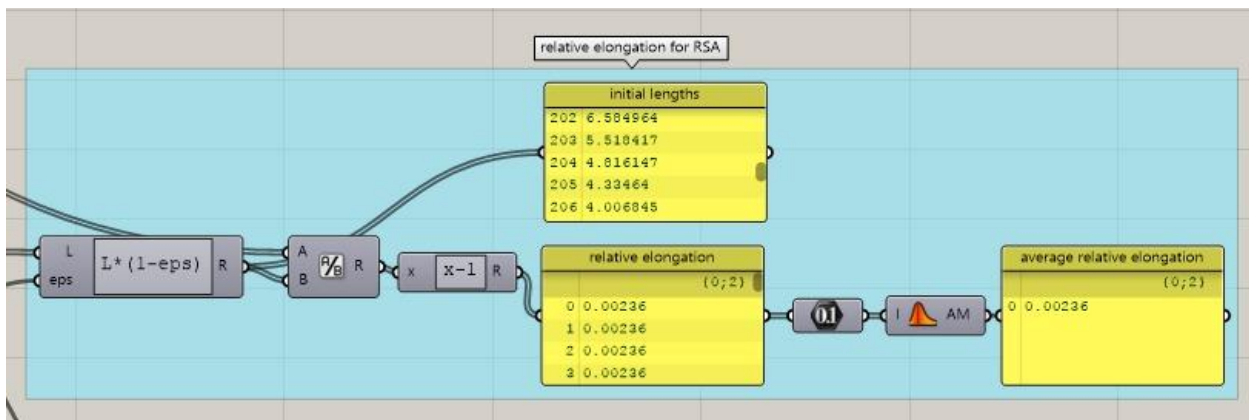


Figure 194 Average relative elongation to be applied as prestress in RSA

## Export to Robot Structural Analysis

As the analysis of the system is, in the case of the 3D study, performed in Robot Structural Analysis, the geometry is exported using the plug – in for Rhino, Geometry Gym. This allows for a reasonably rapid interaction between the Grasshopper environment and the RSA software.

All the sectional properties of the elements, loading cases and combinations, and boundary conditions are defined within the Grasshopper environment. The prestress of each cable element is computed after the form finding process and attributed to the exported cable elements. Such, RSA directly runs the analysis after the information is transferred, without any additional steps being performed.

The loads acting on the net are assumed to act at the intersection nodes of the cable elements, as explained in Chapter 3.3. Using Karamba’s component “Disassemble Mesh Load”, the tributary area corresponding to each of the nodes is calculated, directly attributing the respective mountain load force to each node. This again allows for the rapid reconfiguration of the system, as no manual work in computing the tributary area must be conducted. Similarly, the wind load on the nodes, as explained in Chapter 3.6, is evaluated with respect to the area corresponding to each joint.

